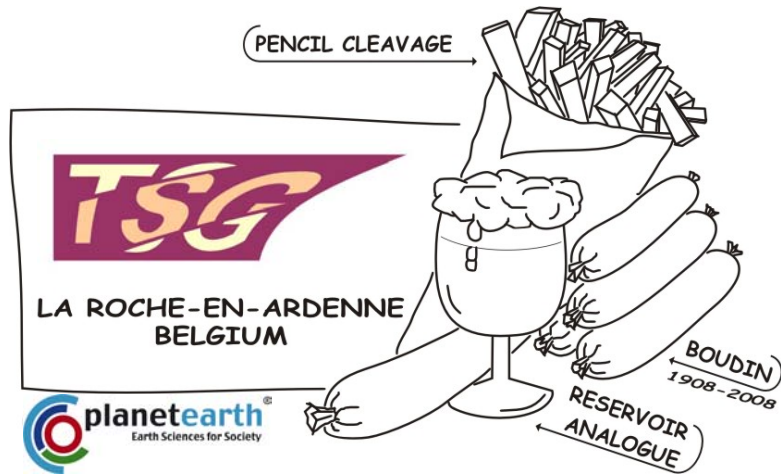


KATHOLIEKE UNIVERSITEIT
LEUVEN



Tectonic Studies Group Annual Meeting

La Roche-en-Ardenne, Belgium
8th - 11th January 2008

Programme
Abstracts
Field trip guide





Tectonic Studies Group

Annual Meeting 2008

La Roche-en-Ardenne, Belgium

8 - 10 January 2008



Organisers

Manuel Sintubin, Sara Vandycke & Timothy Debacker

With special thanks to the following people:

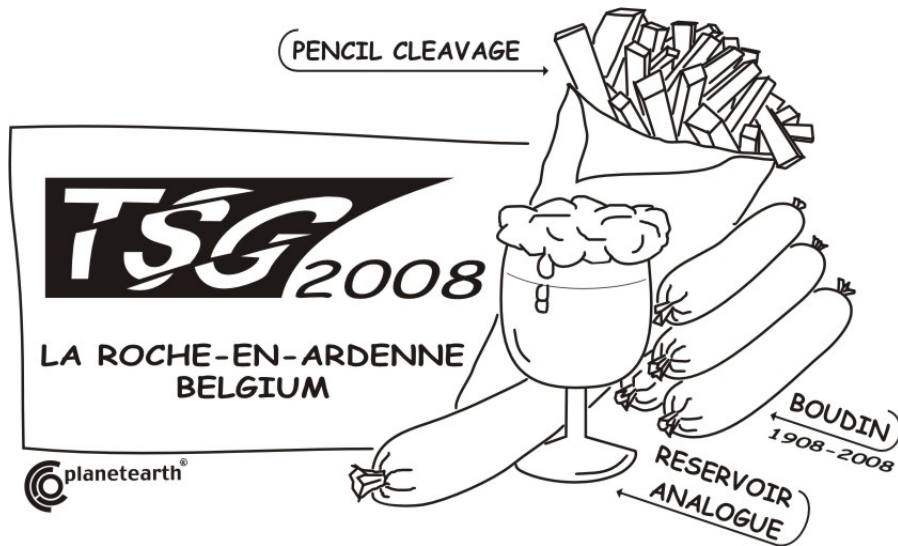
Isaac Berwouts, Johan Boon, Bérenice Deletter, Cécile Havron, Ghislaine Huberland, Barbara Ledoux (a.s.b.l. GREEN FPMS), Katrien Smeets, Yves Quinif, Hervé Van Baelen, Koen Van Noten, Hilde Vandenhoeck, Greet Willems

Sponsors



Contents

Part I Conference programme	v
Part II Conference abstracts	1
Plenary lecture	5
Oral presentations	9
Poster presentations	89
Author index	129
Part III List of participants	135
Part IV Field trip guide	139
Safety information	141
Introduction	143
The geology of the Ardennes in a nutshell	145
STOP A – Bastongne – Mardasson quarry	149
STOP B – Wellin – Fond des Vaulx quarry	170
STOP C – Namur – Chemin de Ronde	181
References	188
Acknowledgements	191




PART I

Conference programme

Tectonic Studies Group Annual Meeting 2008

January 8th - 10th, 2008

Monday 07 January 2008

19h00 – 20h00	Ice breaker – sponsored by <i>GF Consult</i>	
---------------	---	---

Tuesday 08 January 2008

Session 1 – 9h00 – 10h30 – Faults and fault rocks – chairperson: Richard Lisle

9h00 – 9h15	<u>Woodcock Nigel</u> & <u>Mort Kate</u>	<i>Fault breccia classification: proposals</i>
9h15 – 9h30	<u>Balsamo Fabrizio</u> , <u>Storti Fabrizio</u> & <u>Nestola Yago</u>	<i>The influence of ultrasonic mobilisation in laser-aided analytical procedures on particle size distributions in fault core rocks</i>
9h30 – 9h45	<u>Tueckmantel Christian</u> , <u>Fisher Quentin</u> & <u>Knipe Rob</u>	<i>Microstructural comparison of major faults and minor damage zone faults, eastern Gulf of Suez rift</i>
9h45 – 10h00	<u>Walker Richard J.</u> , <u>Imber Jonathan</u> , <u>Holdsworth Robert E.</u> & <u>Moy David J.</u>	<i>Faults, fault rocks and fractures in basalts: the Faroe Islands, NE Atlantic margin</i>
10h00 – 10h15	<u>Moy David J.</u> , <u>Imber Jonathan</u> , <u>Holdsworth Robert E.</u> & <u>Walker Richard J.</u>	<i>The nature and significance of transfer zones on the NE Atlantic margin: three case studies from the Faroe-Shetland Basin</i>
10h15 – 10h30	Discussion	

10h30 – 11h00	Coffee break
---------------	--------------

Session 2 – 11h00 – 12h30 – Faults and fault rocks – chairperson: Julia Gale

11h00 – 11h15	<u>Imber Jonathan</u> , <u>Holdsworth Robert E.</u> , <u>Smith Steven</u> & <u>Colletini Cristiano</u>	<i>Seismicity of weak faults?</i>
11h15 – 11h30	<u>Tondi Emanuele</u> & <u>Agosta Fabrizio</u>	<i>Fault growth in porous carbonate grainstones: examples from western Sicily, Italy</i>
11h30 – 11h45	<u>Giba Marc</u> , <u>Walsh John J.</u> , <u>Nicol Andrew</u> & <u>Childs Conrad</u>	<i>Evolution and stability of relay zones on a normal fault in the Taranaki Basin, New Zealand</i>
11h45 – 12h00	<u>Long Jonathan</u> , <u>Imber Jonathan</u> , <u>Wightman Ruth</u> , <u>Jones Richard</u>	<i>Using geological rules and terrestrial laser scanning datasets to constrain uncertainty in three-dimensional</i>

	McCaffrey Kenneth, Holdsworth Robert E., Holliman Nick & De Paola Nicola	<i>structural models of sub-seismic scale fault networks</i>
12h00 – 12h15	<u>Bistacchi Andrea</u> , Massironi Matteo, Menegon Luca & Pellegrini Claudio	<i>3D modelling of the Pusteria and Sprechenstein-Mules fault system. Part 2: implications for the mechanical evolution of crustal-scale strike-slip faults</i>
12h15 – 12h30	Discussion	

12h30 – 14h00	Lunch	
---------------	-------	--

Session 3 – 14h00 – 15h30 – Faults and fault rocks – chairperson: John Walsh

14h00 – 14h15	<u>Leslie Graham</u> & Krabbendam Maarten	<i>Reactivated steep basement shear zones as a locus for generation of brittle and ductile lateral thrust ramps and culmination walls in the Caledonian Moine Thrust Zone, NW Scotland</i>
14h15 – 14h30	<u>Wilson Paul</u> , Hodgetts David, Gawthorpe Robert L. & Rarity Franklin	<i>Reactivated versus newly initiated faults: modelling of a normal fault system from the Suez rift using digital outcrop data</i>
14h30 – 14h45	<u>Agosta Fabrizio</u> & Tondi Emanuele	<i>Hydrocarbon flow and accumulation in carbonate-hosted normal faults of the Majella Mountain, central Italy</i>
14h45 – 15h00	<u>Faulkner Daniel</u> & Mitchell Thomas	<i>The structure and fluid flow properties of fault zones: inferences from combined field and laboratory studies</i>
15h00 – 15h15	<u>Smith Steven</u> , Collettini Cristiano & Holdsworth Robert E.	<i>Signatures of the seismic cycle along ancient faults: CO₂-induced fluidization of brittle cataclasites in the footwall of a sealing low-angle normal fault</i>
15h15 – 15h30	Discussion	

15h30 – 16h00	Coffee break	
---------------	--------------	--

Session 4 – 16h00 – 17h30 – Deformation mechanisms & rheology – chairperson: John Ramsay


16h00 – 16h15	<u>Rutter Ernest</u> , Llana-Funez Sergio & Brodie Katharine	<i>Dehydration and deformation of intact serpentinite under controlled pore pressure with pore volumetry</i>
---------------	--	--

16h15 – 16h30	<u>Barrie Craig</u> , Boyle Alan, Cox Stephen & Prior David	<i>An analysis of micro-structural development in experimentally deformed polycrystalline pyrite using electron backscatter diffraction (EBSD)</i>
16h30 – 16h45	<u>ten Grotenhuis Saskia</u> , Spiers Chris & de Bresser Hans	<i>Behaviour of two-phase shear zones in high strain deformation experiments</i>
16h45 – 17h00	<u>Van Brabant Yves</u> & Dejonghe Léon	<i>Boudins vs. mullions in the Ardenne Allochthonous: a century of academic debates in the “Terra Ardennensis Incognita”</i>
17h00 – 17h15	<u>Urai Janos L.</u> & Sintubin Manuel	<i>Crustal rheology of fine-grained siliciclastic rocks deforming by solution-precipitation processes</i>
17h15 – 17h30	Discussion	

17h30 – 18h00	Poster presentation 1
---------------	-----------------------

18h00 – 19h00	Poster session 1
---------------	------------------

1. Taylor Rochelle. *Towards an understanding of the seismic properties of major fault zones*
2. Bistacchi Andrea, Massironi Matteo & Menegon Luca. *3D modelling of the Pusteria and Sprechenstein-Mules fault system. Part 1: geomodelling as applied to fault-zone architecture studies*
3. Debacker Timothy N., Piessens Kris, Herbosch Alain, De Vos Walter & Sintubin Manuel. *The Asquempont Detachment System, Anglo-Brabant Deformation Belt, Belgium: state-of-the-art*
4. Wu Shimin, Lu Huafu & Wang Shengli. *Geometry and evolution of the Nansha trough foreland thrust and fold belt of South China Sea, China*
5. Bergman Helena & Piazzolo Sandra. *Grain boundary migration in quartz: not a simple story*
6. Edwards Alexander, Covey-Crump Stephen & Rutter Ernest. *The effect of grain size sensitive flow on synthetic calcite 'conglomerates'*
7. Hildyard Rebecca, Faulkner Daniel, Prior David, De Paolo Nicola & Colletini Cristiano. *The fabric and kinematics of anhydrite rocks from central Italy*
8. Llana-Funez Sergio, Faulkner Daniel & Wheeler John. *Experimental dehydration and deformation of Volterra Gypsum: preliminary experiments and overview*
9. Schmatz Joyce & Urai Janos L. *The role of fluid-filled grain boundaries in substructure development: new insights from see-through deformation experiments*
10. Sintubin Manuel. *The centennial of the terms 'boudin' and 'boudinage': a historical retrospect*
11. van Gent Heijn, Holland Marc & Urai Janos L. *The compaction dependent cohesion and tensile strength of gypsum powder - the effect on scaled analogue models*

19h00 – 23h00	Belgian beer party – sponsored by <i>Geologica Belgica</i>	
---------------	---	---

Wednesday 09 January 2008

Session 5 – 9h00 – 10h30 – Folding – chairperson: Timothy Debacker

9h00 – 9h15	<u>Lisle Richard</u> & Shan Yehua	<i>A 3D view of folds</i>
9h15 – 9h30	<u>Hubert-Ferrari Aurelia</u> & Suppe John	<i>Surface effects of active folding, illustrated with examples from the Tian Shan intracontinental mountain belt (China)</i>
9h30 – 9h45	<u>Burliga Stanislaw</u> & Koyi Hemin A.	<i>Analogue modelling of material supply to a diapiric structure rising above an active basement fault</i>
9h45 – 10h00	<u>Eggenhuisen Joris</u> , Butler Rob, McCaffrey Bill & Haughton Peter	<i>Syn-depositional formation of shear fabrics and folded laminations in turbidite sandstones: an example of deformation of granular media</i>
10h00 – 10h15	<u>McCaffrey Kenneth</u> & Jolly Richard	<i>Sediment loading drives folding in the South Caspian</i>
10h15 – 10h30	Discussion	

10h30 – 11h00	Coffee break	
---------------	--------------	--

Session 6 – 11h00 – 12h30 - Tectonics – chairperson: Maarten Krabbendam

11h00 – 11h15	<u>Butler Rob</u> & Paton Douglas	<i>Tectonic evolution of the Caribbean-South America plate boundary at Columbia: implications for ocean-continent interactions</i>
11h15 – 11h30	<u>Richardson Steve</u>	<i>A structural transect through an accretionary complex, North West Colombia</i>
11h30 – 11h45	<u>Watkinson Ian</u> , Elders Chris & Hall Robert	<i>The role of strike-slip faulting in Peninsular Thailand</i>
11h45 – 12h00	<u>Adiotomre Emmanuel</u> & Gawthorpe Robert L.	<i>Evolution of growth faults in a salt dominated slope, offshore Angola, West African margin</i>
12h00 – 12h15	<u>Festa Andrea</u> & Dela Pierre Francesco	<i>Interaction of tectonic, sedimentary and diapiric processes in the origin of mélanges: examples from the Messinian of NW Italy (Tertiary Piedmont Basin)</i>
12h15 – 12h30	Discussion	

12h30 – 14h00	Lunch	
---------------	-------	--


Session 7 – 14h00 – 15h30 – Geological structures – chairperson: Rob Butler

14h00 – 14h15	<u>Krabbendam Maarten</u> , Bradwell Tom & Clarke Stuart	<i>Effect of bedrock structures upon formation of glacial megagrooves by Pleistocene ice streams in NW Scotland: implications for structural interpretation of remote sensing images in formerly glaciated terrains</i>
14h15 – 14h30	Clarke Stuart, Austin Linda, Egan Stuart & Leslie Graham	<i>The analysis and mapping of geological structures using high-resolution Digital Elevation Models</i>
14h30 – 14h45	<u>Baudouy Lucie</u> , Haughton Peter & Walsh John J.	<i>Syn-depositional tectonics in a deep-water "mini-basin" setting, Tabernas, SE Spain</i>
14h45 – 15h00	<u>Vinnels Jamie</u> , Butler Rob, McCaffrey Bill, Lickorish Henry, Apps Gillian & Peel Frank	<i>Sediment distribution and architecture around early Alpine intra-basinal structures, Champsaur Basins, SE Ecrins, France</i>
15h00 – 15h15	<u>Osmaston, Miles</u>	<i>Structural and tectonic basis for some far-reaching new insights on the dynamics of the Earth's mantle</i>
15h15 – 15h30	Discussion	

15h30 – 16h00	Poster presentation 2
---------------	-----------------------

16h00 – 17h00	Poster session 2
---------------	------------------

12. Hubert-Ferrari Aurelia, Garcia David, Moernaut Jasper, Van Daele Maarten, Damci Emre, Boes Xavier, Fraser Jeff, Cagatay Namik & De Batist Marc. *The Hazar pull-apart along the East Anatolian Fault: structure and active deformation*
13. Drews Michael & Deckert Hagen. *3D joint density mapping*
14. Berwouts Isaac, Muechez Philippe & Sintubin Manuel. *Deformation-controlled fluid migration in a middle to upper-crustal level. A research strategy for the western part of Armorica (Brittany, France)*
15. Haest Maarten, Muechez Philippe & Vandycke Sara. *Structural control on the Dikulushi Cu-Ag deposit, Katanga, Democratic Republic of Congo*
16. Roberts Katie, Davies Richard, Stewart Simon & McCaffrey Kenneth. *Global search for intrusive mud systems: analogues for the subsurface*
17. Austin Linda, Egan Stuart & Clarke Stuart. *The geological and geodynamic evolution of the Northumberland Trough Region, Northern England: insights from the numerical modelling of lithosphere deformation and basin formation*
18. Debacker Timothy N. & Sintubin Manuel. *The Quenast plug: a mega-porphycroclast during the Brabantian Orogeny (Senne valley, Brabant Massif, Belgium)*
19. Kelly John E. & Turner Jonathan P. *The post-Triassic uplift and erosion history of the southwest UK*
20. Martin Jennifer, Holdsworth Robert E., McCaffrey Kenneth, Conway Andy & Clarke Stuart. *Characterising fractured basement using the Lewisian Complex: implications for petroleum potential in the Clair Field*

17h00 – 18h00	Tectonic Studies Group Annual General Meeting	
18h00 – 19h30	Plenary Lecture <u>Murphy J. Brendan</u> & Nance R. Damian PANGEA: A GEODYNAMIC CONUNDRUM	
20h30 – 23h00	Conference dinner – sponsored by <i>Tractebel Engineering</i>	

Thursday 10 January 2008

Session 8 – 9h00 – 10h30 – Active tectonics – chairperson: Iain Stewart

9h00 – 9h15	<u>Walsh John J.</u>	<i>Displacement-length scaling relations of normal faults and paleoearthquakes in the active Taupo Rift, New Zealand</i>
9h15 – 9h30	<u>Verbeeck Koen</u> , Colbeaux Jean-Pierre, Vandycke Sara, Bergerat Françoise, Vanneste Kris, Tesnière Christophe, Sébrier Michel, Petermans Toon & Camelbeeck Thierry	<i>Active tectonics in northern France</i>
9h30 – 9h45	<u>Vanneste Kris</u> , Verbeeck Koen, Mees Florias & Vandenberghe Dimitri	<i>New paleoseismic evidence for prehistoric surface rupturing in the intraplate Lower Rhine graben area</i>
9h45 – 10h00	<u>Lafuente Paloma</u> , Simón José Luis, Arlegui Luis Eduardo, Liesa Carlos Luis & Rodríguez-Pascua Miguel Ángel	<i>A multidisciplinary approach to paleoseismic behaviour of the Conclud fault (Iberian Chain, Spain)</i>
10h00 – 10h15	<u>Yerli Baris</u> , ten Veen Johan H. & Sintubin Manuel	<i>Geological and archaeoseismological evidence of Neotectonic activity in the Fethiye-Burdur Fault Zone (Eşen Basin, SW Turkey)</i>
10h15 – 10h30	Discussion	

Session 9 – 11h00 – 12h30 – Paleostress, fractures and veins – chairperson: Daniel Faulkner

11h00 – 11h15	<u>Duperret Anne</u> , Vandycke Sara, Genter Albert & Mortimore Rory N.	<i>Is present-day coastal recession of the eastern English Channel guided by the tectonic state of stress of NW Europe?</i>
11h15 – 11h30	<u>van Gent Heijn</u> , Back Stefan, Urai Janos L., Kukla Peter A. & Reicherter Klaus	<i>Paleostress based on seismic data - examples from the NW Groningen and Dutch offshore gas fields</i>
11h30 – 11h45	<u>Gale Julia</u> & Holder Jon	<i>Natural fractures in shales and their importance for gas production</i>
11h45 – 12h00	<u>Van Noten Koen</u> , Hilgers Christoph, Urai Janos L. & Sintubin Manuel	<i>The record of a tectonic inversion in the Lower Devonian Ardenne-Eifel basin (Belgium, Germany): a switch from bedding-normal to bedding parallel quartz veins</i>
12h00 – 12h15	<u>Van Baelen Hervé</u> , Muchez Philippe & Sintubin Manuel	<i>Vein-cleavage fabrics associated to a late-orogenic destabilisation of the Variscan cleavage in the High-Ardenne slate belt (Belgium)</i>
12h15 – 12h30	Discussion	

12h30 – 13h30	Lunch	
---------------	-------	--

Session 10 – 13h30 – 15h00 - Petrophysics – chairperson: Janos Urai

13h30 – 13h45	<u>Raynaud Suzanne</u> , Richard Olivier, Bergerat Françoise & Vandycke Sara	<i>Natural alteration of chalk in contact with air versus transformation due to shearing: examples in the Mons Basin (Belgium)</i>
13h45 – 14h00	<u>Desbois Guillaume</u> & Urai Janos L.	<i>In-situ observation of fluid-filled-pores in Boom Clay (Belgium) using cryo-FIB-SEM technology: first results</i>
14h00 – 14h15	<u>Saillet Elodie</u> & Wibberley Christopher	<i>Evolution of brittle deformation and fault growth in a high porosity sandstone analogue from the Cretaceous of the Bassin du Sud-Est, Provence, France</i>
14h15 – 14h30	<u>Abe Steffen</u> , Schmatz Joyce & Urai Janos L.	<i>DEM simulation of shear induced mixing in layered sand-clay sequences - initial results</i>
14h30 – 14h45	<u>Schöpfer Martin</u> , Abe Steffen, Childs Conrad & Walsh John J.	<i>Elasticity, strength, friction and porosity relations in Discrete Element Method (DEM) models of cohesive granular materials</i>

14h45 – 15h00	Discussion
---------------	------------

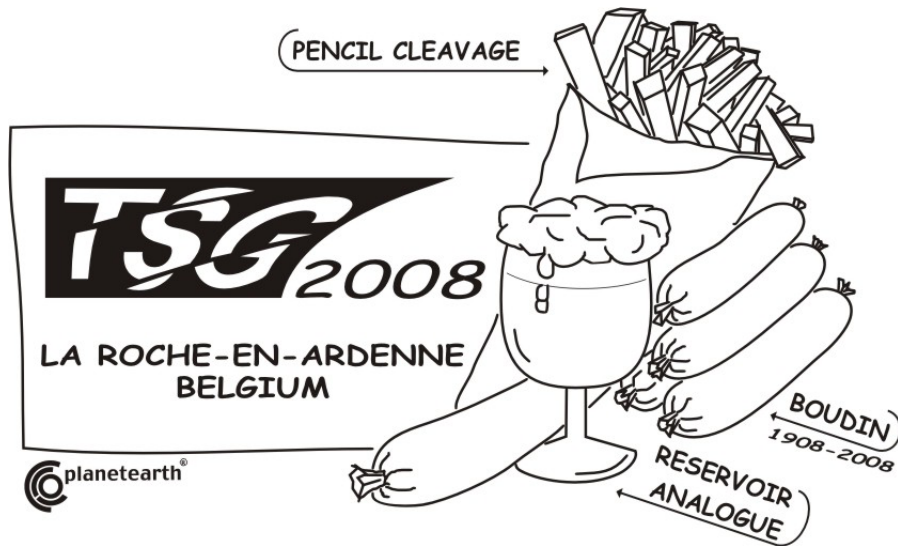
15h00 – 15h15	Closing of meeting
---------------	--------------------

Friday 11 January 2008

Field trip

“A taste of the Ardennes”

Manuel Sintubin, Sara Vandycke & Timothy Debacker



PART II

Conference abstracts

Tectonic Studies Group Annual Meeting 2008

January 8th - 10th, 2008



Plenary lecture

Pangea: a geodynamic conundrum

Brendan J. Murphy¹ & Damian R. Nance²

1. *St. Francis Xavier University, Department of Earth Sciences, Antigonish, Nova Scotia Canada*

2. *Ohio University, Department of Geological Sciences, Athens, Ohio, USA*

Presenting author: bmurphy@stfx.ca

Although the existence of Pangea is one of the cornerstones of geology, the mechanisms responsible for its amalgamation are poorly understood. To a first order, we know where and when, but not why. The formation of Pangea is primarily recorded in the origin and evolution of the Paleozoic oceans (Iapetus, Rheic, Paleotethys) between Laurentia (ancestral North America), Baltica (northwestern Europe) and northern Gondwana (South America-West Africa), whose closure resulted in its amalgamation. Although well documented, this record runs counter to many widely accepted geodynamic models for the forces that drive plate tectonics. Recent theoretical and geodynamic models debate whether plate tectonics is primarily driven by the top-down cooling affects of subduction, which stimulates convection in the mantle, or whether plate motions are the surface manifestation of mantle convection. At the heart of this debate is a lack of understanding of the forces that initiate the subduction process. Likewise, the documented evolution of Pangea highlights fundamental gaps in our understanding of the processes responsible for its amalgamation. Between ca. 600 and 545 Ma, Laurentia, Baltica and Gondwana broke up to form the Iapetus Ocean, and at ca. 500 Ma, the Rheic Ocean opened. At the same time, subduction zones in the oceanic domains at the leading edges of the dispersing continents (e.g. Terra Australis ocean) were well established. According to conventional geodynamic models, slab pull forces associated with this subduction should have resulted in the migration of the dispersing continents towards these subduction zones. However, this motion reversed when subduction commenced in the relatively newly formed Iapetus and Rheic oceans between Laurentia, Baltica and Gondwana. Subduction in the modern world preferentially removes the oldest, coldest and most negatively buoyant oceanic lithosphere, a selectivity generally considered fundamental to plate tectonics and applicable to plate geodynamics in the past. However, is not applicable to the formation of Pangea. Opening of the Rheic Ocean at ca. 500 Ma coincided with the onset of subduction in the Iapetus Ocean and the convergence of Laurentia and Baltica. At ca. 460 Ma, the Rheic Ocean began to subduct, initiating the convergence of Gondwana with Laurentia and Baltica that would ultimately give rise to Pangea. During the assembly of Pangea, therefore, subduction was not only initiated within the new Paleozoic oceans, but the rates of subduction of this relatively young lithosphere must also have overpowered those of the already well established subduction zones within the exterior ocean.

To understand the processes leading to the formation of Pangea, we need to investigate the geodynamic linkages between the evolution of the Rheic Ocean and the penecontemporaneous evolution of the exterior (Paleopacific) ocean. Oceanic domains at the leading edges of the dispersing continents in the exterior ocean are recorded in the 18,000 km Terra Australis orogen which preserves a record of subduction until 230 Ma.



Oral presentations

(in order of presentation)

Oral presentations: table of contents

1. Fault breccia classification: proposals.....	12
Nigel Woodcock & Kate Mort	12
2. The influence of ultrasonic mobilisation in laser-aided analytical procedures on particle size distributions in fault core rocks	13
Fabrizio Balsamo, Fabrizio Storti & Yago Nestola	13
3. Microstructural comparison of major faults and minor damage zone faults, eastern Gulf of Suez rift	14
Christian Tueckmantel, Quentin Fisher & Rob Knipe	14
4. Faults, fault rocks and fractures in basalts: the Faroe Islands, NE Atlantic Margin	16
Richard J. Walker, Jonathan Imber, Robert E. Holdsworth & David J. Moy	16
5. The nature and significance of transfer zones on the NE Atlantic margin: three case studies from the Faroe-Shetland Basin.....	17
David J. Moy, Jonathan Imber, Robert E. Holdsworth & Richard J. Walker	17
6. Seismicity of weak faults?	18
Jonathan Imber, Robert E. Holdsworth, Steven Smith & Cristiano Collettini.....	18
7. Fault growth in porous carbonate grainstones: examples from western Sicily, Italy	19
Emanuele Tondi & Fabrizio Agosta	19
8. Evolution and stability of relay zones on a normal fault in the Taranaki Basin, New Zealand.....	20
Marc Giba, John J. Walsh, Andrew Nicol & Conrad Childs	20
9. Using geological rules and terrestrial laser scanning datasets to constrain uncertainty in three-dimensional structural models of sub-seismic scale fault networks	21
Jonathan Long, Jonathan Imber, Ruth Wightman, Richard Jones, Kenneth McCaffrey, Robert E. Holdsworth, Nick Holliman & Nicola De Paola	21
10. 3D modelling of the Pusteria and Sprechenstein-Mules fault system. Part 2: implications for the mechanical evolution of crustal-scale strike-slip faults.....	22
Andrea Bistacchi, Matteo Massironi, Luca Menegon & Claudio Pellegrini	22
11. Reactivated steep basement shear zones as a locus for generation of brittle and ductile lateral thrust ramps and culmination walls in the Caledonian Moine Thrust Zone, NW Scotland	24
Graham Leslie & Maarten Krabbendam	24
12. Reactivated versus newly initiated faults: modelling of a normal fault system from the Suez rift using digital outcrop data.....	25
Paul Wilson, David Hodgetts, Robert L. Gawthorpe & Franklin Rarity	25
13. Hydrocarbon flow and accumulation in carbonate-hosted normal faults of the Majella Mountain, central Italy	27
Fabrizio Agosta & Emanuele Tondi	27
14. The structure and fluid flow properties of fault zones: inferences from combined field and laboratory studies	28
Daniel Faulkner & Thomas Mitchell	28
15. Signatures of the seismic cycle along ancient faults: CO ₂ -induced fluidization of brittle cataclasites in the footwall of a sealing low-angle normal fault.....	29
Steven Smith, Cristiano Collettini & Robert E. Holdsworth	29
16. Dehydration and deformation of intact serpentinite under controlled pore pressure with pore volumetry	30
Ernest Rutter, Sergio Llana-Funez & Katharine Brodie	30
17. An analysis of micro-structural development in experimentally deformed polycrystalline pyrite using electron backscatter diffraction (EBSD)	32
Craig Barrie, Alan Boyle, Stephen Cox & David Prior	32
18. Behaviour of two-phase shear zones in high strain deformation experiments.....	34
Saskia ten Grotenhuis, Hans de Bresser & Chris Spiers.....	34
19. Boudins vs. mullions in the Ardenne Allochthonous: a century of academic debates in the “Terra Ardennensis Incognita”	35
Yves Vanbrabant & Léon Dejonghe.....	35
20. Crustal rheology of fine-grained siliciclastic rocks deforming by solution-precipitation processes	37
Janos L. Urai & Manuel Sintubin.....	37
21. A 3D view of folds.....	38
Richard Lisle & Yehua Shan	38

22. Surface effects of active folding, illustrated with examples from the TianShan intracontinental mountain belt (China)	39
Aurelia Hubert-Ferrari & John Suppe	39
23. Analogue modelling of material supply to a diapiric structure rising above an active basement fault	41
Stanislaw Burliga & Hemin A. Koyi	41
24. Syn-depositional formation of shear fabrics and folded laminations in turbidite sandstones: an example of deformation of granular media	43
Joris Eggenhuisen, Rob Butler, Bill McCaffrey & Peter Haughton	43
25. Sediment loading drives folding in the South Caspian	44
Kenneth McCaffrey & Richard Jolly	44
26. Tectonic evolution of the Caribbean-South America plate boundary at Colombia: implications for ocean-continent interactions	45
Rob Butler & Douglas Paton	45
27. A structural transect through an accretionary complex, North-West Colombia	46
Steve Richardson	46
28. The role of strike-slip faulting in Peninsular Thailand	47
Ian Watkinson, Chris Elders & Robert Hall	47
29. Evolution of growth faults in a salt dominated slope, offshore Angola, West African margin	48
Emmanuel Adiotomre & Robert L. Gawthorpe	48
30. Interaction of tectonic, sedimentary and diapiric processes in the origin of mélanges: examples from the Messinian of NW Italy (Tertiary Piedmont Basin)	50
Andrea Festa & Francesco Dela Pierre	50
31. Effect of bedrock structures upon formation of glacial megagrooves by Pleistocene ice streams in NW Scotland: implications for structural interpretation of remote sensing images in formerly glaciated terrains	52
Maarten Krabbendam, Tom Bradwell & Stuart Clarke	52
32. The analysis and mapping of geological structures using high-resolution Digital Elevation Models	54
Stuart Clarke, Linda Austin, Stuart Egan & Graham Leslie	54
33. Syn-depositional tectonics in a deep-water “mini-basin” setting, Tabernas, SE Spain	55
Lucie Baudouy, Peter Haughton & John J. Walsh	55
34. Sediment distribution and architecture around early Alpine intra-basinal structures, Champsaur Basins, SE Ecrins, France	56
Jamie Vinnels, Rob Butler, Bill McCaffrey, Henry Lickorish, Gillian Apps & Frank Peel	56
35. Structural and tectonic basis for some far-reaching new insights on the dynamics of the Earth’s mantle	57
Miles Osmaston	57
36. Displacement-length scaling relations of normal faults and paleoearthquakes in the active Taupo Rift, New Zealand	59
John J. Walsh	59
37. Active tectonics in northern France	60
Koen Verbeek, Jean-Pierre Colbeaux, Sara Vandycke, Françoise Bergerat, Kris Vanneste, Christophe Tesnière, Michel Sébrier, Toon Petermans & Thierry Camelbeek	60
38. New paleoseismic evidence for prehistoric surface rupturing in the intraplate Lower Rhine graben area	62
Kris Vanneste, Koen Verbeek, Florias Mees & Dimitri Vandenberghe	62
39. A multidisciplinary approach to paleoseismic behaviour of the Conclud fault (Iberian Chain, Spain)	63
Paloma Lafuente, José Luis Simón, Luis Eduardo Arlegui, Carlos Luis Liesa & Miguel Ángel Rodríguez-Pascua	63
40. Geological and archaeoseismological evidence of neotectonic activity in the Fethiye-Burdur Fault Zone (Eşen Basin, SW Turkey)	65
Baris Yerli, Johan H. ten Veen & Manuel Sintubin	65
41. Is present-day coastal recession of the eastern English Channel guided by the tectonic state of stress of NW Europe?	66
Anne Duperret, Sara Vandycke, Albert Genter & Rory N. Mortimore	66
42. Paleostress based on seismic data – examples from the NW Groningen and Dutch offshore gas fields	68
Heijn van Gent, Stefan Back, Janos L. Urai, Peter A. Kukla & Klaus Reicherter	68

43. Natural fractures in shales and their importance for gas production.....	71
Julia Gale & Jon Holder	71
44. The record of a tectonic inversion in the Lower Devonian Ardenne-Eifel basin (Belgium, Germany): a switch from bedding-normal to bedding-parallel quartz veins	72
Koen Van Noten, Christoph Hilgers, Janos L. Urai & Manuel Sintubin	72
45. Vein-cleavage fabrics associated to a late-orogenic destabilisation of the Variscan cleavage in the High-Ardenne slate belt (Belgium)	74
Hervé Van Baelen, Philippe Muchez & Manuel Sintubin	74
46. Natural alteration of chalk in contact with air versus transformation due to shearing: examples in the Mons Basin (Belgium)	76
Suzanne Raynaud, Olivier Richard, Françoise Bergerat & Sara Vandycke	76
47. In-situ observation of fluid-filled-pores in Boom Clay (Belgium) using cryo-FIB-SEM technology: first results	79
Guillaume Desbois & Janos L. Urai	79
48. Evolution of brittle deformation and fault growth in a high porosity sandstone analogue from the Cretaceous of the Bassin du Sud-Est, Provence, France	80
Elodie Sallet & Christopher Wibberley	80
49. DEM simulation of shear induced mixing in layered sand-clay sequences – initial results	82
Steffen Abe, Joyce Schmatz & Janos L. Urai	82
50. Elasticity, strength, friction and porosity relations in Discrete Element Method (DEM) models of cohesive granular materials.....	84
Martin Schöpfer, Steffen Abe, Conrad Childs & John J. Walsh.....	84

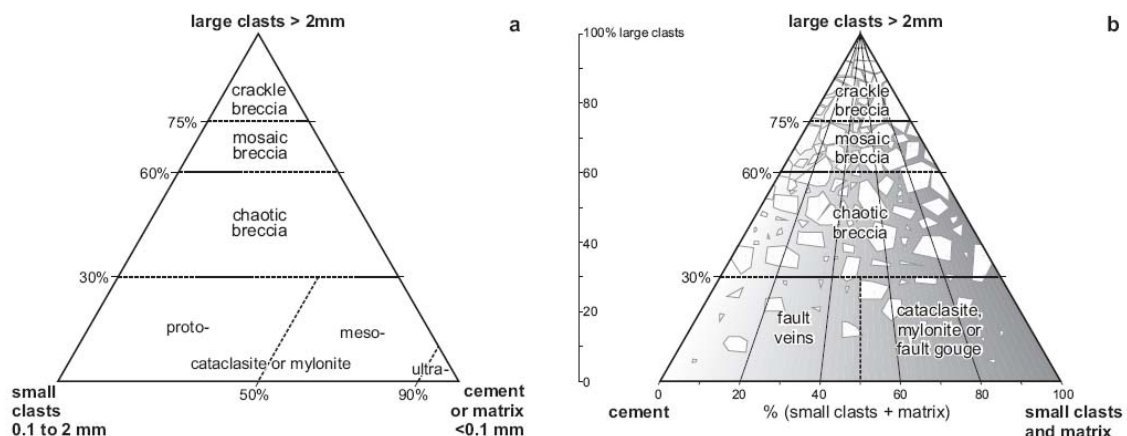
1. Fault breccia classification: proposals

Nigel Woodcock¹ & Kate Mort¹

*1. University of Cambridge, Department of Earth Sciences, U.K.
Presenting author: nhw1@esc.cam.ac.uk*

Keyword(s): fault rock, breccia

Despite extensive research on fault rocks, and on their commercial importance, there is no non-genetic classification of fault breccias that can easily be applied in the field. The present criterion for recognising fault breccia as having no 'primary cohesion' is often difficult to assess. Instead we propose that fault breccia should be defined, as with sedimentary breccia, primarily by grain size: with at least 30% of its volume comprising clasts at least 2mm in diameter. To subdivide fault breccias, we advocate the use of textural terms borrowed from the cave-collapse literature – crackle, mosaic and chaotic. Image analysis is used to explore geometric discrimination between these visually assigned classes using samples from the well-understood Dent Fault, northwest England. Clast sphericity and surface roughness show some correlation with the breccia classes, but particle size distributions and their fractal dimension show none. A more useful parameter is dilation, as measured by the percentage of sample area occupied by clasts. Crackle breccia has >75% clasts, mosaic breccia 60-75% clasts, and chaotic breccia <60% clasts. The eye is also good at judging the tessellation (goodness-of-fit) of clasts, and a semi-quantitative approach to assessing this parameter is suggested. The average degree of rotational misfit of the clasts is strongly related to breccia class: crackle breccia involves less than 10° rotations, mosaic breccia 10-22° and chaotic breccia more than 22° rotations. Comparison charts are provided for semi-quantitative classification of fault breccias.



WOODCOCK, N. H., OMMA, J. E. & DICKSON, J. A. D., 2006. Chaotic breccia along the Dent Fault, NW England: implosion or collapse of a fault void? *Journal of the Geological Society, London* 163, 431-446.

2. The influence of ultrasonic mobilisation in laser-aided analytical procedures on particle size distributions in fault core rocks

Fabrizio Balsamo¹, Fabrizio Storti¹ & Yago Nestola¹

1. Università degli Studi Roma Tre, Dipartimento di Scienze Geologiche, Italy
Presenting author: balsamo@uniroma3.it

Keyword(s): fault core rocks, ultrasonic mobilisation, particle size distribution

Cataclastic rocks exert a primary control on the frictional strength, stability, seismic velocity, and permeability properties of fault zones. They form by progressive fragmentation, crushing, chipping, sliding, rotation and grinding of rock particles during faulting. Particle size distributions provide fundamental information for studying cataclasis because they can be related to specific fragmentation processes. The use of laser-aided analytical techniques provides the possibility to easily broaden the size range and to dramatically increase the sampling detail because of the small quantity of analysed material. This has been encouraging the increasing use of laser-aided particle size analysers in the study of poorly coherent cataclastic rocks. Ultrasonic mobilisation of disaggregated particles is commonly included in the analytical method of laser-aided particle size analysis, to facilitate and optimise laser activity. Ultrasonication, however, may influence the resulting particle size distribution because of collision-induced particle fragmentation, or agglomeration. To investigate the sensitivity of particle size data to the use and timing of ultrasonic particle mobilisation, we performed specific test analyses by systematic varying the duration of ultrasonic particle mobilisation preceding laser activation. These test analyses were carried out on fault core rocks developed in both carbonate platform rocks and quartz-rich clastic rocks faulted in soft-sediment conditions. Results of these tests indicate a significant sensitivity of particle size distribution data to ultrasonic mobilisation, thus questioning the meaning of many published datasets obtained by laser-aided analyses.

3. Microstructural comparison of major faults and minor damage zone faults, eastern Gulf of Suez rift

Christian Tueckmantel¹, Quentin Fisher¹ & Rob Knipe¹

*1. University of Leeds, School of Earth and Environment, Rock Deformation Research, U.K.
Presenting author: christian@rdr.leeds.ac.uk*

Keyword(s): *fault rock evolution, up-scaling of fault properties, normal faults, Gulf of Suez rift*

Knowledge of petrophysical properties of fault rocks is important to accurately predict fluid flow within structurally complex petroleum reservoirs. At present, most information of fault rock flow properties comes from analysing small-scale faults in the damage zones of large displacement structures because the petroleum industry seldomly cores seismic-scale faults. Faults present in core tend to have centimetre-scale throws at most (Fisher, 2005). A problem with this approach is that uncertainty exists as to whether the properties of the small-scale features are representative of those of seismic-scale faults. According to Fisher & Knipe (2001) there are many reasons why fault rocks along seismic-scale faults could have different fluid flow properties from those developed along smaller-scale features. Seismic-scale faults are often associated with major stress discontinuities above basement faults. Consequently, as well as having accommodated more strain, they often show prolonged activity, which means that they may have deformed under different stress conditions than small-scale faults. However, grain-size and permeability reductions in a small number of seismic-scale faults in the field and in rare core samples analysed by Fisher & Knipe (unpublished data) were found to be similar to their respective small-scale features in the surrounding damage-zone. Fisher & Knipe (2001) identify two reasons why the microstructure of seismic-scale faults is often similar to that of smaller-scale faults. First, the effective stress at the time of faulting may be a more important factor affecting grain-size distribution than the total strain. Second, each movement of a seismic-scale fault results in deformation in its damage zone. To further increase the amount of data relevant to this issue fieldwork was undertaken in the central eastern margin of the Gulf of Suez rift. We studied the ~100 m throw normal fault Humur B in the southern part of Wadi El Humur. The fault is located in the footwall of the ~1500 m throw Gamal fault which is part of the Rift Border fault system (Whitehouse, 2005). In the analysed outcrop the Lower Cretaceous Malha Formation is juxtaposed against itself. The host lithology of interest is medium grained, clean sandstone with 22% porosity. The footwall of Humur fault B is well exposed and comprises an up to 75 cm wide, highly deformed fault core and a ~10 m wide damage zone, defined by low displacement deformation bands. Humur fault B and its damage zone were mapped in detail. Several fault and host rock samples were analysed with scanning electron microscopy. Microstructure analysis reveals that cataclasis was the dominant deformation process. The sandstone host porosity was reduced to values between 8 and 20%. Adjacent to the main slip plane and along the fault core border of Humur fault B the sandstone is pervasively deformed. A small discontinuous domain along the fault core border comprises ultracataclasite. The damage zone deformation bands consist of ~1 mm wide cataclastic zones. The grain size distribution within a 5 mm and a >9 mm offset deformation band is approximately similar to the pervasively deformed samples within the core of the large-scale fault (see figure). Within the deformation bands the quartz grains are somewhat more angular and the ratio of grains with >50 µm diameter to smaller ones is slightly higher. However, it seems that the fault rock microstructure did not undergo significant changes after less than 1 cm offset was accumulated. Further slip was either accommodated without significant further grain size reduction or along newly formed bands,

ultimately resulting in pervasive deformation. Therefore this faulting regime provides an example of damage zone deformation that presents a reasonable analogue to the fault rock of the seismic-scale feature. This behaviour will be highly dependant on the lithology and the stress conditions at the time of faulting.

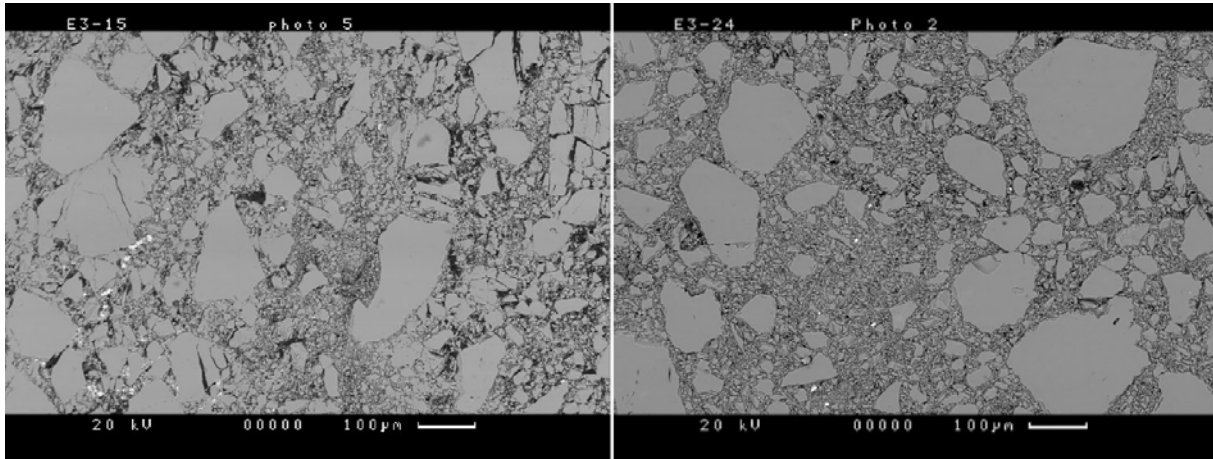


Figure 1. Backscattered scanning electron pictures, scale bars 100 μm . Left: Cataclastic deformation band with 5 mm offset in the damage zone of Humur fault B. Right: Fault rock directly adjacent to the main slip plane.

FISHER, Q. J., 2005. Recent advances in fault seal analysis as an aid to reservoir characterization and production simulation modelling. (pp. 1–8). Society of Petroleum Engineers.

FISHER, Q. J. & KNIPE, R. J., 2001. The permeability of faults within siliciclastic petroleum reservoirs of the North Sea and Norwegian Continental Shelf. *Marine and Petroleum Geology*, 18, 1063–1081.

WHITEHOUSE, P. S., 2005. Fault and fracture development in extensionally reactivated fault systems. PhD thesis, Royal Holloway, University of London.

4. Faults, fault rocks and fractures in basalts: the Faroe Islands, NE Atlantic Margin

Richard J. Walker¹, Jonathan Imber¹, Robert E. Holdsworth¹ & David J. Moy¹

*1. University of Durham, Department of Earth Sciences, Reactivation Research Group, U.K.
Presenting author: r.j.walker@dur.ac.uk*

Keyword(s): *Faroe-Shetland basin, transfer-zone*

To date, few field studies have focused on the characterisation of faults, fractures and associated fault rocks within continental flood basalt provinces (CFBs). The Faroe Islands are situated upon the Faroe platform on the NE Atlantic margin, and form part of the extensive Palaeogene flood basalts of the North Atlantic Igneous Province (NAIP), that cover much of the Faroe-Shetland basin (FSB). Existing seismic data and potential field modelling have proposed that many of the faults and fractures in the Faroes are related to NW-SE trending lineaments, interpreted as broad transfer-zones. The exceptional exposure of the Faroe Islands provides an opportunity to study sub-seismic scale faulting and fracturing that may be representative of the Faroe Islands Basalt Group (FIBG) and potentially analogous to the FSB beneath. The FIBG displays significant vertical and lateral variation, and is interspersed with sedimentary marker horizons (up to 25 m thick) laid down during periods of volcanic quiescence, providing an excellent opportunity to study the growth of faults, fractures and joints within these volcanic and sedimentary units. Previous structural studies have focused predominantly on lineament geometry by means of remote sensing, with no kinematic analysis, or discrimination of the nature of individual lineaments. Our detailed study of the individual faults and fault zones – the first attempted in this area - has revealed new constraints on the generation and relative timings of faults within the FIBG. Field observations reveal four distinct fault types: 1) individual fault surfaces with shear hydraulic fractures/veins; 2) broader fault zones comprising multiple fault clusters that display brecciation and tensile hydrofracture veins with abundant euhedral zeolite and calcite growth; and 3) open faults with shear hydraulic fractures/veins, bounding clastic fills, some of which may have experienced fluidization and injection events; 4) minor (<0.5 m) displacement faults, with 3-6 m wide fracture zones that focus fluid flow along the fault plane and in the hanging-wall. These different types are interpreted as forming at different depths and times, likely under varying differential stresses and pore-fluid pressure conditions. Future studies will use microstructural geochemical analysis, and fluid inclusion studies to verify preliminary interpretations of fault formation within the FIBG.

5. The nature and significance of transfer zones on the NE Atlantic margin: three case studies from the Faroe-Shetland Basin

David J. Moy¹, Jonathan Imber¹, Robert E. Holdsworth¹ & Richard J. Walker¹

*1. University of Durham, Department of Earth Sciences, Reactivation Research Group, U.K.
Presenting author: d.j.moy@durham.ac.uk*

Transfer zones are thought to occur along the length of the NE Atlantic Margin, varying in their tectonic and crustal signatures. Previous authors have suggested that some transfer zones originated due to reactivation of structures as old as 2.5 Ga, and they are often associated with oceanic fracture zones. Geological data suggest that transfer zones may have played an important role in the evolution of the NE Atlantic passive margin, through structural segmentation and offsetting of basinal depocentres on a variety of scales. The Faroe-Shetland Basin (FSB) is extensively covered by Cenozoic lavas which significantly affects imaging of the deeper structure in seismic data. The NW-SE transfer zones of the FSB have previously been defined from regional gravity and magnetic data and are commonly displayed on regional structural element maps of the basin. A recent study of palynological and heavy mineral data from the FSB suggests that NW-SE transfer zones may have acted as both conduits and barriers to sedimentation during the Paleocene. Nevertheless, the geometry and kinematics of transfer zones have not yet been clearly defined in offshore seismic datasets, despite the increased availability of high-quality 3D seismic data and steadily improving 2D seismic data quality across the margin. To date, there is only one published seismic example of a transfer zone in the FSB: the Victory Transfer Zone. This was initially interpreted as a Paleocene transpressional push-up structure. Analysis of this structure using the PGS MegaSurvey dataset strongly suggests that it is related to igneous intrusives at depth which have produced a non-circular hydrothermal vent complex. Another potential feature has been recognised associated with the Clair Transfer Zone, where there is a rapid change in basin structure along strike, which could be consistent with the presence of a transfer zone. This anomaly is seen to be highly localised and is more likely to be caused by faulting highly oblique to section views, gas effects or igneous sill and dyke activity. Thus, the seismic evidence for the Clair and Victory transfer zones remains enigmatic: the locations and geometries of the gas chimneys and/or igneous intrusions may have been influenced by transfer zones but, if they are present, the seismic data are unable to resolve individual transfer-related faults. In contrast, the Judd Fault Zone is a well-defined structural element that defines the southwest boundary to the FSB. It juxtaposes Precambrian basement that crops out on the Judd High to the southwest from the Cretaceous depocentre to the northeast. The faulting of the Rona Ridge rotates into the NW-SE Judd Fault, which was an active normal fault during the late Cretaceous. Small scale normal reactivation of the faults can also be seen to have occurred in the Eocene along a section of the fault. Fracture patterns within the Precambrian basement of the Judd High have been analysed using Schlumberger's Ant Tracking algorithm. We compare structural trends observed in the basement with those seen in the Mesozoic-Cenozoic cover to constrain the deep structure and verify the presence of fault / fracture patterns that could indicate strike-slip movement along this possible transfer zone. Seismic attribute analysis may also help to further constrain the nature of the proposed Clair and Victory transfer zones.

6. Seismicity of weak faults?

Jonathan Imber¹, Robert E. Holdsworth¹, Steven Smith¹ & Cristiano Collettini²

1. University of Durham, Department of Earth Sciences, Reactivation Research Group, U.K.

2. Università degli Studi di Perugia, Dipartimento di Scienze della Terra, Geologia Strutturale e Geofisica, Italy
Presenting author: jonathan.imber@durham.ac.uk

Studies of ancient faults (e.g. Median Tectonic Line, Outer Hebrides and Great Glen fault zones) exhumed from depths of c. 3 km or more suggest that many large-displacement intra-plate and plate-boundary faults have cores that contain foliated phyllosilicate-rich fault rocks (e.g. phyllonites and foliated cataclasites). The metamorphic conditions required to produce foliated phyllosilicate-rich fault rocks at these depths are likely to be met in many (perhaps most) large-displacement (offset >5 km) faults that cut continental basement rocks. This is certainly consistent with the recent recovery of such foliated rocks from the core of the San Andreas Fault at 4 km depth in the SAFOD borehole. High-strain experiments using analogue materials indicate that such faults should be both weak and aseismic, deforming by frictional-viscous flow. Some, such as the low-angle normal faults of the Apennines, Italy, seem to be consistent with this prediction and exhibit only abundant microseismicity ($M < 3$) during active slip, possibly related to hydrofracture and brittle slip events following periodic build-ups in fluid pressure during regional CO₂ degassing of the mantle. Elsewhere, however, seismological data suggest that other active large-displacement faults are able to generate large earthquakes and that some, though not all, faults may slip seismically (i.e. much of the displacement is accommodated by seismic slip). Thus, some exhumed large-displacement faults with phyllosilicate-rich cores are likely to have slipped seismically and/or generated large earthquakes during at least part of their displacement histories. There is some field evidence to support this contention: The Siberia Fault Zone, New Zealand contains foliated cataclasites that formed contemporaneously with pseudotachylyte, providing incontrovertible geological evidence that phyllosilicate-rich faults are capable of generating earthquakes. However, the magnitudes of the earthquakes that produced the pseudotachylytes are not known, nor is it clear how slip was partitioned between seismic and aseismic slip. The Wasatch Fault, Utah is an active normal fault that contains phyllonitic fault rocks exhumed from c. 11 km depth. Palaeoseismic studies show that it generated a series of $M \sim 7$ earthquakes throughout the Holocene. Extrapolation of the present day crustal loading rate back through the Holocene strongly suggests that the Wasatch Fault may have slipped seismically for the past c. 5000 years. We speculate that seismicity along faults with phyllosilicate-rich cores arises due to the long movement histories and complex internal geometries of large-displacement faults, which are difficult to resolve using geophysical data and recreate in laboratory experiments.

7. Fault growth in porous carbonate grainstones: examples from western Sicily, Italy

Emanuele Tondi¹ & Fabrizio Agosta¹

1. University of Camerino, Italy

Presenting author: emanuele.tondi@unicam.it

Keyword(s): deformation bands, strike-slip faults, carbonate grainstones, scaling properties

After field mapping, microstructural, and textural analyses of faults in Lower Pleistocene carbonate grainstones (Favignana Island, western Sicily), we document the interactive failure processes responsible for fault nucleation and growth. These involve strain localization into narrow bands, pressure solution, the subsequent shearing of the pressure solution products, and cataclasis as previously reported by Tondi *et al.* (2006) and Tondi (2007) in other carbonate grainstones. We also document how the transition from one deformation process to another, which is likely to be controlled by the changes in the material properties, is recorded by different ratios and distributions of the fault dimensional attributes. In particular, the results of our study allow us to: (i) identify two conjugate sets of right-lateral and left-lateral strike-slip faults trending NW and NNE, respectively; (ii) document a progression of fault nucleation from single compactive shear bands to zones of compactive shear bands, and then to zone of compactive shear bands that include cataclastic rocks and slip surfaces; (iii) recognize the linkage processes of lower-rank shear structures as responsible for fault growth; and (iv) define both architecture and scaling relationship among fault length, fault thickness, and fault displacement of strike-slip faults characterized by a different degree of growth. The products of the processes described above have a different impact on the subsurface fluid flow in porous carbonates. It is known that compactive shear bands have lower values of both porosity and permeability relative to the surrounding host rocks (Tondi, 2007). However, in this study we find that compactive shear bands containing well developed slip surfaces may form localized fluid pathways. This is nicely shown by the fluid escape structures present along the largest strike-slip faults of the area.

TONDI, E., 2006. Nucleation, development and petrophysical properties of faults in carbonate grainstones: evidence from the San Vito Lo Capo peninsula (Sicily, Italy). *Journal of Structural Geology*, 29 (4), 614-628.

TONDI, E., ANTONELLINI, M., AYDIN, A., MARCHEGIANI, L. & CELLO, G., 2006. Interaction between deformation bands and stylolites in fault development in carbonate grainstones of Majella Mountain, Italy. *Journal of Structural Geology*, 28, 376-391.

8. Evolution and stability of relay zones on a normal fault in the Taranaki Basin, New Zealand

Marc Giba¹, John J. Walsh¹, Andrew Nicol² & Conrad Childs¹

1. University College Dublin, School of Geological Sciences, Fault Analysis Group, Ireland

2. GNS Science, New Zealand

Presenting author: marc@fag.ucd.ie

Faults are rarely single surface features and usually consist of kinematically related fault segments, on one or more scales. Segmentation of faults is always accommodated by the formation of relay zones across which displacement is transferred between overlapping fault segments. Although previous studies have shown that increasing displacement often causes relay breaching and segment linkage, kinematic, as opposed to geometric, constraints on the stability and evolution of relay zones are sparse. In this talk we consider whether relay zones are geometrically stable or whether they change their map view shape as they accrue displacement. Specifically we investigate whether relay zones establish their shape early in their development and maintain the same overlapping segment geometry until intervening relay ramps become too steep and breaching occurs or whether the tips of overlapping fault segments continue to propagate changing the shape of the relay zone until breaching? The evolution of relays is addressed by examining the Pliocene-recent evolution of relays along a normal fault in the northern Taranaki Basin from high quality 3D seismic data. This area is characterised by sedimentation rates which exceed fault displacement rates, a condition which permits displacement backstripping of this syn-sedimentary growth fault and detailed reconstruction of the growth of relay zones. The Taranaki Basin is situated offshore south-west of the Northern Island of New Zealand. The Basin has a multiphase deformation history, with extension during the Late Cretaceous to Paleocene, followed by contraction in the Miocene and then, in the northern basin, by Pliocene to Recent backarc extension driven by subduction of the Pacific plate along the Hikurangi margin. We have analysed a fault along the western margin of the northern part of the Taranaki Basin, which has a maximum, Pliocene to Pleistocene, throw of about 2km. Underlying Late Cretaceous horizons have larger displacements (ca 2.5km) reflecting the fault's existence during the first extensional deformation phase. Reactivation of this approximately NNE-SSW striking fault was accompanied by upward propagation and the formation of new fault segments which are rotated up to 20° in a clockwise direction. This segmentation is attributed to a rotation in extension direction from the earlier to the later phase of extension, with the formation of individual segments and associated relay ramps within a ca 3km wide zone. Examination of displacement profiles highlights the transfer of displacement between segments, whilst sequence thickening and associated displacement changes indicate that the boundaries of relay zones were stable with no tip migration during ramp rotation. Upward decreases of displacement through the growth sequence, reflecting the displacement accumulation through time, are accompanied by a progressive increase in the structural integrity of relay ramps and a decrease in segment linkage. Kinematic analysis favours a model in which relays are formed rapidly and retain a geometrically stable shape in map view during progressive ramp rotation, which ultimately leads to eventual relay breaching.

9. Using geological rules and terrestrial laser scanning datasets to constrain uncertainty in three-dimensional structural models of sub-seismic scale fault networks

Jonathan Long¹, Jonathan Imber¹, Ruth Wightman¹, Richard Jones², Kenneth McCaffrey¹, Robert E. Holdsworth¹, Nick Holliman³ & Nicola De Paola¹

1. University of Durham, Department of Earth Sciences, Reactivation Research Group, U.K.

2. University of Durham, Department of Earth Sciences, Geospatial Research Limited, U.K.

3. University of Durham, e-Science Research Institute, U.K.

Presenting author: jonathan.long@durham.ac.uk

Keyword(s): *fault model, outcrop analog*

Three-dimensional (3D) seismic data have insufficient resolution to image faults with throws less than ca. 20 m. Despite their potential impact on reservoir performance, the true 3D structure of sub-seismic scale fault networks has only been determined in exceptional circumstances, for example by cutting serial sections through faults in unconsolidated sediments, or within active opencast mines. A further limitation to the 3D understanding of outcrop scale faults has been that most structural datasets from onshore analogues have been collected using traditional mapping techniques, which require the 3D geology and surface topography to be projected onto a 2-D plane (or along a 1-D scan line). Terrestrial laser scanning (TLS) now enables structural geologists to produce 3D representations of geological outcrops (“digital outcrop models”), but faults are generally recorded as intersections on the outcrop surface, rather than planes. We use a digital outcrop model of sub-seismic scale, post-depositional normal faults from SE Scotland to illustrate a methodology for extrapolating fault surface traces to create a fully 3D fault model. The faults are exposed on the foreshore and in cliffs behind the beach. We created a pseudo-3D seismic grid across the digital outcrop model and extrapolated fault sticks from the surface intersections using geologically-driven rules. The cliff section provides constraints on the range of permissible fault dips, fault heights, and the impact of host rock stratigraphy on fault bifurcation. The geometries of larger-scale post-depositional normal faults observed in 3D seismic datasets have been used to guide our interpretations of fault tip- and branch-lines geometries. These geological rules provide a conceptual framework to generate multiple 3D realisations from a single digital outcrop model, which could be used to further test the implications of small faults on production flow.

10. 3D modelling of the Pusteria and Sprechenstein-Mules fault system. Part 2: implications for the mechanical evolution of crustal-scale strike-slip faults

Andrea Bistacchi¹, Matteo Massironi², Luca Menegon² & Claudio Pellegrini¹

1. Università di Milano Bicocca, Dipartimento di Scienze Geologiche e Geotecnologie, Italy

2. Università di Padova, Dipartimento di Geoscienze, Italy

Presenting author: andrea.bistacchi@unimib.it

Keyword(s): 3D-modelling, mechanical models, Eastern Alps, fault zone architecture

New results on the mechanical evolution of the Pusteria and Sprechenstein-Mules fault system, obtained from a 3D fault zone architecture model, are presented. In a companion contribution (Part 1: geomodelling as applied to fault-zone architecture studies) we present theoretical considerations and the practical implementation, which allowed a 3D realistic model of the architecture of this strike-slip fault system to be reconstructed. The E-W Pusteria (Pustertal) line is the eastern segment of the Periadriatic lineament, the >600 km tectonic boundary between the Europe and Adria-vergent portions of the Alpine collisional orogen (Dal Piaz *et al.*, 2003). The crustal-scale Periadriatic lineament is characterized by a transcurrent polyphase activity of Tertiary age. The western edge of the Pusteria line is marked by the Mules tonalitic “lamella” and represents the tectonic divide between the Austroalpine basement to the N and the Bressanone Granite to the S. The Pusteria line, in turn, is cut by the later Sprechenstein-Mules fault, actually the kinematic linkage between the Pusteria system and the extensional Brenner detachment (Bistacchi *et al.*, 2003). At the map scale, this line is characterized by a complex network of dextral brittle fault zones, interconnected by contractional step-overs. A 3D geological model of the fault network, where each major fault segment is represented as a discrete surface, has been reconstructed from borehole data and a detailed 1:5000 geological map by means of the geomodeling package gOcad. In this model, fault cores are represented with triangulated surfaces, which carry properties such as core thickness and fault rock type. Damage zones are represented as fully-3D volumetric objects. Different properties, which concur in representing the “degree of damage”, are modelled as continuous or categorical functions: number and attitude of joint sets, fracture spacing, etc. A multi-criteria classification, which attempts to summarise the “degree of damage”, is proposed. The 3D model permits to visualize and quantitatively compare many features of this fault zone with predictions from mechanical models. A first-order influence on the evolution of fault rocks and fracturing in damage zones is exerted by composition and fabric of protoliths. This results in a marked asymmetry of damage zones when different tectonic units are juxtaposed across a fault segment. The model also highlights lobe-shaped stronger-damage volumes centred on step-overs, and lower levels of damage along rectilinear fault segments. These results can be compared with mechanical models, which predict stress intensity and orientation variations in step-overs and bends. Similar stress-concentrations have been detected where rocks of different composition are present on the hangingwall of the Sprechenstein-Mules fault, resulting in inhomogeneities of fault rocks and core zones along strike. The eastern tip of the Sprechenstein-Mules fault propagates for some km into the homogeneous Bressanone Granite. In this area, static models of stress concentrations at an advancing strike-slip fault tip have been compared with the distribution of fracturing in damage zones. Concluding, this 3D model provides new insights in the

architecture of a crustal-scale fault zone and provides quantitative data in 3D, which can be directly compared with results from mechanical models. In addition, the 3D structural model provides the basis for further studies. For instance, a relative permeability model can be derived from the structural model, based on qualitative inferences about the hydrogeological behaviour of damage and core zones. It highlights the architecture of relatively more permeable conduits and sealing boundaries. Enhanced damage in and around compressional step-overs might be the locus for more focused and important fluid flow. This point will be further investigated by means of geochemical data.

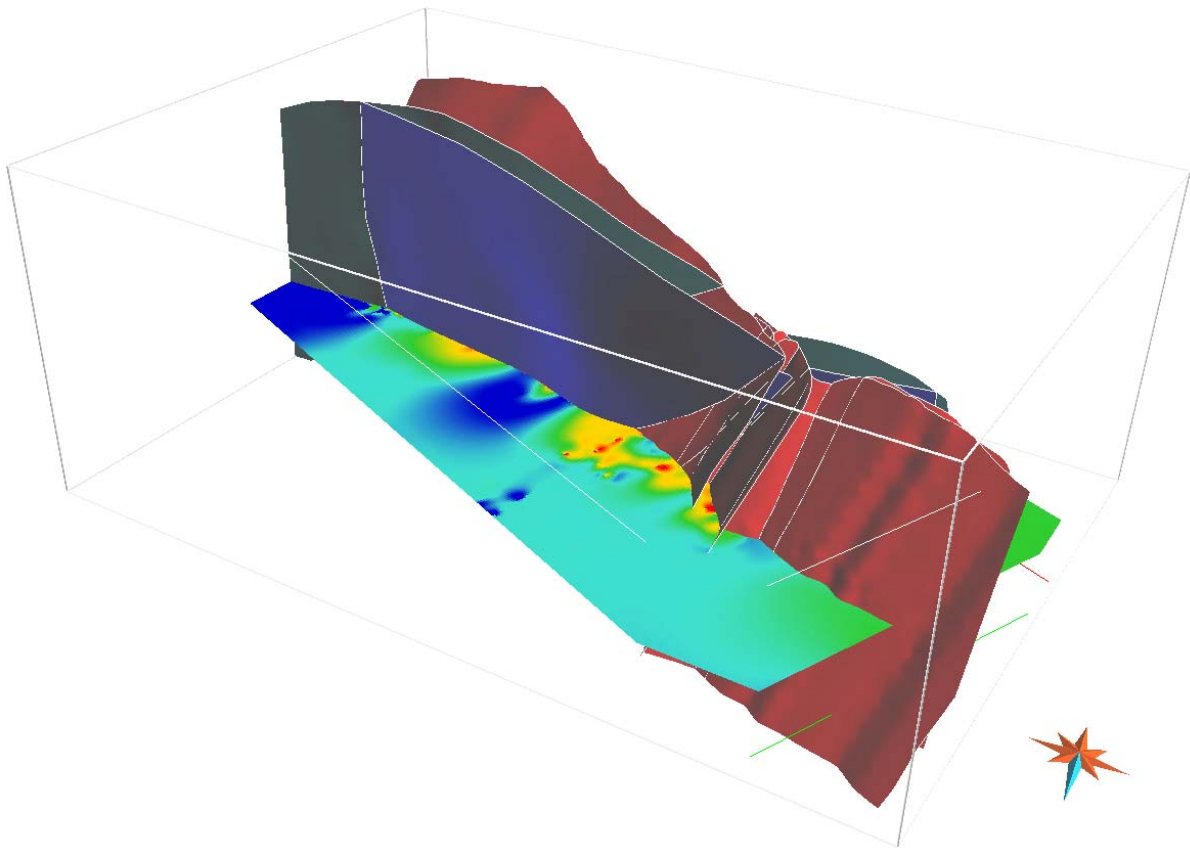


Figure 1. Fault network model, viewed from the NW, and horizontal cross section of the “degree of damage” volumetric property defined on damage zones. Lobe-shaped strong-damage volumes (red and orange) appear to be centred on step-overs. Bounding box is 8 x 5 x 1.5 km.

BISTACCHI, A., DAL PIAZ, G.V., DAL PIAZ, G., MARTINOTTI, G., MASSIRONI, M., MONOPOLI, B. & SCHIAVO, A., 2003. Carta geologica e note illustrative del transetto Val di Vizzate-Fortezza (Alpi Orientali). *Memorie di Scienze Geologiche-Padova* 55, 169–188.

DAL PIAZ G.V., BISTACCHI A. & MASSIRONI M., 2003. Geological outline of the Alps, *Episodes* 26 (3), pp. 174–179.

11. Reactivated steep basement shear zones as a locus for generation of brittle and ductile lateral thrust ramps and culmination walls in the Caledonian Moine Thrust Zone, NW Scotland

Graham Leslie¹ & Maarten Krabbendam¹

1. British Geological Survey, Edinburgh, U.K.

Presenting author: agle@bgs.ac.uk

Keyword(s): reactivation, Moine Thrust Zone

New detailed mapping and structural analysis in the Moine Thrust Zone (MTZ) by the British Geological Survey highlights previously unappreciated abrupt north-south lateral variations in both thrust architecture, and in the internal configuration of individual thrust sheets and culminations. We can now link these lateral variations to pre-, syn- and post-thrust displacements on reactivated sub-vertical faults and shear zones rooted in the Precambrian crystalline basement to the stratigraphical successions deformed in the MTZ. These discrete discontinuities in basement are a consequence of repeated Precambrian (2500 & c.1800 – 1600 Ma) deformation phases and typically trend WNW-ESE. They are thus aligned (sub)-parallel to the regional transport direction of the superimposed Caledonian thrusting. Analysis of piercing point displacements reveals that some basement shear zones experienced brittle reactivation prior to thrusting but after deposition of the Cambro-Ordovician sedimentary cover sequence and then again, both during and after thrusting. Thus, a layer-cake architecture had clearly been faulted prior to thrusting, creating a series of WNW-ESE trending steps of the order of 100 m high or more. In the Assynt Culmination of the MTZ, these steps strongly controlled the emergent thin-skinned thrust architecture in the sedimentary units, as well as the occurrence and limits of thicker (0.5 – 1 km) thrust sheets which also carry basement gneiss. Both thin- and thicker-skinned architecture is compartmentalized along steep WNW-ESE trending brittle-ductile lateral culmination walls at intervals of 5 – 8 km. At structurally higher levels in the hanging wall of the Moine Thrust, a km-scale WNW-ESE trending ductile steep culmination wall in Moine Supergroup metasediments is identified as the lateral termination of the Oykel Culmination. This culmination wall marks the termination of a c. 5 km thick thrust sheet and coincides with a steep gradient at the south-western limit of a deep regional gravity low. That gradient is believed to indicate the existence of a (long-lived) km-scale step in basement, one perhaps of several which acted to constrain lateral complexity at the regional scale throughout the evolution of the thrust belt.

12. Reactivated versus newly initiated faults: modelling of a normal fault system from the Suez rift using digital outcrop data

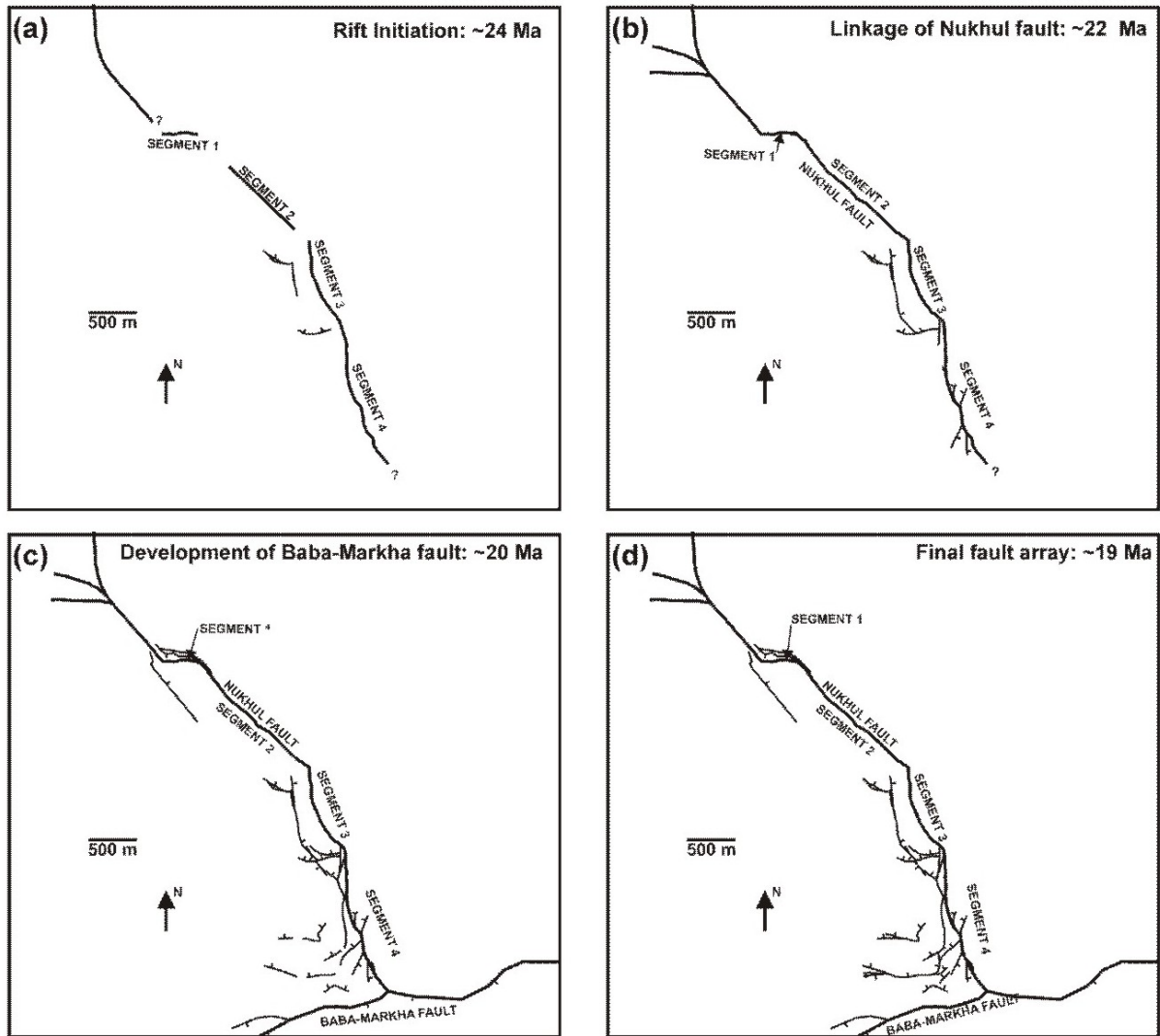
Paul Wilson¹, David Hodgetts¹, Robert L. Gawthorpe¹ & Franklin Rarity¹

1. University of Manchester, SEAES, U.K.

Presenting author: paul.wilson@manchester.ac.uk

Keyword(s): normal faults, fault growth, fault linkage, rifts

Models of normal fault growth and linkage fall into two types. In the first type, fault length increases as faults propagate laterally, and initially isolated faults link with other faults along strike to create longer faults (e.g. Cartwright *et al.* 1995; Cowie *et al.* 2000; Gawthorpe *et al.* 2003). In the second type, particularly applicable to reactivated faults, the fault length is established early in the history of the rift, leading to displacement accruing on a fault of approximately constant length (Nicol *et al.* 2005; Bull *et al.* 2006; Manzocchi *et al.* 2006). In real-world normal fault systems, it is likely that interaction between reactivated and newly initiated structures will influence the development of the fault array. We test this proposition in the Suez rift, which involves three sets of inherited basement structures, striking 140° (parallel to the rift-bounding faults), 000-020°, and 100-120° (e.g. Montenat *et al.* 1988). We use a LiDAR-based digital outcrop dataset, integrated with 'conventional' geological data, to create a tectono-stratigraphic model of the Nukhul half-graben of the Suez rift. We use the model to describe the distribution of displacement on faults within the half-graben, and to constrain the spatial and temporal evolution of the fault array. Syn-rift deposition in the Nukhul half-graben was controlled by the graben-bounding Nukhul fault. The fault can be divided into at least four segments based on strike of the segments and morphology of hangingwall strata. The segments of the fault became geometrically linked within the first 2.5 m.y. of rifting, as evidenced by the presence of early syn-rift Abu Zenima Formation strata at the segment linkage points. Fault-perpendicular anticlines in the hangingwall opposite the segment linkage points persist during a further 1.8 m.y. of syn-rift deposition, suggesting that the fault remains kinematically segmented following geometric linkage. We suggest this occurs because of sudden changes in fault strike at the segment linkage points that inhibit earthquake rupture propagation. Length/throw plots and throw contours on fault surfaces (generated using Badley Geoscience Ltd's Trap Tester software) show that minor faults in the array have different patterns of throw distribution. Antithetic faults in the hangingwall of the Nukhul fault show increasing throw with depth, while antithetic faults to the east-striking Baba-Markha fault have throw maxima within the upper syn-rift succession. This suggests that some faults in the array developed as upward-propagating structures initiated in pre-rift lithologies, while others initiated within the syn-rift succession and were related to the development of late transfer faults that link the major fault-block bounding faults. Numerical modelling and outcrop studies have shown that fault growth and linkage leads to a progressive decrease in the number of active faults, with displacement increasingly localised onto a few block-bounding structures as intra-block faults die out (e.g. Cowie *et al.* 2000; Gawthorpe *et al.* 2003). Our results show that at the half-graben scale, in complex rifts with several fault orientation sets, this progression may occur at different times for each fault set (see figure). In this case, the number of active faults will not simply decrease through time. Rather there may be transient highs in the number of active faults as faults initiate and develop in new orientations during the evolution of the half-graben.



- BULL, J.M., BARNES, P.M., LAMARCHE, G., SANDERSON, D.J., COWIE, P.A., TAYLOR, S.K. & DIX, J.K., 2006. High-resolution record of displacement accumulation on an active normal fault: implications for models of slip accumulation during repeated earthquakes. *Journal of Structural Geology* 28, 1146-1166.
- CARTWRIGHT, J.A., TRUDGILL, B.D. & MANSFIELD, C.S., 1995. Fault growth by segment linkage: an explanation for scatter in maximum displacement and trace length data from the Canyonlands Grabens of SE Utah. *Journal of Structural Geology* 17, 1319-1326.
- COWIE, P.A., GUPTA, S. & DAWERS, N.H., 2000. Implications of fault array evolution for synrift depocentre development: insights from a numerical fault growth model. *Basin Research* 12, 241-261.
- GAWTHORPE, R.L., JACKSON, C.A.-L., YOUNG, M.J., SHARP, I.R., MOUSTAFA, A.R. & LEPPARD, C.W., 2003. Normal fault growth, displacement localisation and the evolution of normal fault populations: the Hammam Faraun fault block, Suez rift, Egypt. *Journal of Structural Geology* 25, 883-895.
- MANZOCCHI, T., WALSH, J.J. & NICOL, A., 2006. Displacement accumulation from earthquakes on isolated normal faults. *Journal of Structural Geology* 28, 1685-1693.
- MONTENAT, C., D'ESTEVOU, P.O., PURSER, B., BUROLLET, P.-F., JARRIGE, J.-J., ORSZAG-SPERBER, F., PHILOBOS, E., PLAZIAT, J.-C., PRAT, P., RICHERT, J.-P., ROUSSEL, N. & THIRIET, J.-P., 1988. Tectonic and sedimentary evolution of the Gulf of Suez and the northwestern Red Sea. *Tectonophysics* 153, 161-177.
- NICOL, A., WALSH, J., BERRYMAN, K. & NODDER, S., 2005. Growth of a normal fault by the accumulation of slip over millions of years. *Journal of Structural Geology* 27, 327-342.

13. Hydrocarbon flow and accumulation in carbonate-hosted normal faults of the Majella Mountain, central Italy

Fabrizio Agosta¹ & Emanuele Tondi¹

1. University of Camerino, Italy

Presenting author: fabrizio.agosta@unicam.it

Keyword(s): *fault growth, fault permeability*

We document the structural control exerted by fractures and normal faults on the migration and accumulation of hydrocarbons in carbonate rocks. This study, conducted in the Roman Valley Quarry of the Majella anticline (central Italy), takes advantage on the presence of hydrocarbons in the form of tar within outcropping Miocene carbonate grainstones. By combining large-scale geological mapping with detailed analysis of the fractured, fragmented, and brecciated carbonates we assess: (i) the background deformation of the Miocene carbonate rocks, (ii) the processes of nucleation and growth of normal faults, (iii) the timing of fracturing and normal faulting with respect to the folding of the Majella anticline, and (iv) the overall fracture and fault permeability. Outside of the normal fault zones, in the carbonate host rock, by deciphering the failure modes and abutting relationships of the different fracture sets, we recognize the following structural elements: one set of discontinuous, bed-parallel Pressure Solution seams (PS), two orthogonal sets of bed-perpendicular PS, which abut against the bed-parallel PS, and two sets of low-angle to bedding PS that abut against the bed-parallel and bed-perpendicular PS sets. Within the normal fault zones, we also identify two sets of low-angle to bedding tail PS and one set of high-angle to bedding tail PS. These tail PS sets show the occurrence of both normal and left-lateral slip along the pre-existing, background elements, and formed during ongoing flexural slip and folding of the carbonate beds. Small, sub-vertical tail joints are present in the more intensively deformed domains of the fault zones, suggesting a switch of the deformation mechanisms from pressure-solution to opening-mode during the fault growth. The core of the normal faults may include breccia, grain-supported or matrix-supported cataclasites, and major slip surfaces depending on the degree of fault evolution. The tar distribution along the normal faults outcropping in the quarry is used as a marker to characterize the fracture and fault permeability. The larger normal fault zones behave as a combined barrier-conduit structure to fluid flow. The tar-free cataclasites are seals for cross-fault fluid flow, and surrounded by fluid conduits that localize in the fault breccias and major slip surfaces of the fault cores, and in the fractured and fragmented carbonates of the damage zones. On the contrary, the smaller normal faults channel the fluids primarily along the through going slip surfaces, which accumulate within the fragmented and brecciated carbonates. Considering the individual structural elements, one set of bed-perpendicular PS and the tail cracks structural elements, which are both NW-oriented and parallel to the current regional σ_{max} , result the most impregnated by tar. The larger normal faults thus form the principle pathways for fluids, which eventually migrate laterally through the smaller, connected faults, and accumulate within the fragmented and brecciated carbonates nearby, as well as in the more porous carbonate beds.

14. The structure and fluid flow properties of fault zones: inferences from combined field and laboratory studies

Daniel Faulkner¹ & Thomas Mitchell¹

*1. University of Liverpool, Earth and Ocean Sciences
Presenting author: faulkner@liv.ac.uk*

Quantifying the fluid flow properties of fault zones is important for understanding fault zone mechanics, predicting the distribution of fault-hosted economic deposits, and recovering hydrocarbons from structurally complex reservoirs. The fluid flow properties depend on the distribution of deformation within fault zones and the permeability of the individual fault components. The fault core can be a single, narrow zone of fault gouge, or consist of multiple strands with variably fractured lenses of country rock contained within them. Either structure will inhibit fluid flow across the fault zone, as typical laboratory values for the permeability of fault gouges in this direction is in the range 10^{-18} to 10^{-22} m². The multiple strand fault core provides the greatest opportunities for fluid entrapment. Although fault gouge exhibits significant permeability anisotropy (up to 3 orders of magnitude), fluid flow rates parallel to the fault within the fault core will still be low. Field, seismological and geophysical observations suggest that faults act as significant fluid conduits, and hence the zone of fractured rock surrounding the fault core (the damage zone) must act as a high permeability pathway. The damage zone consists of microscopic and macroscopic fracturing that decreases in intensity with distance from the fault core. In order to quantify the contribution of microscopic damage to the fluid flow properties, we measured the porosity and permeability evolution of initially low porosity crystalline rocks under simulated crustal conditions during progressive deformation to failure. The data show permeability enhancement from initial values of $\sim 10^{-21}$ to $\sim 10^{-17}$ m² immediately prior to failure. However, these values and the size of damage zones typically seen in the field are not sufficient to explain inferred fluid flow rates and imply that the macroscopic fracture network must play a significant role in fluid transport.

15. Signatures of the seismic cycle along ancient faults: CO₂-induced fluidization of brittle cataclasites in the footwall of a sealing low-angle normal fault

Steven Smith¹, Cristiano Collettini² & Robert E. Holdsworth¹

1. University of Durham, Department of Earth Sciences, U.K.

2. University of Perugia, Dipartimento Di Scienze Della Terra, Italy

Presenting author: steven.smith@durham.ac.uk

Keyword(s): *fault rocks, fluidization, fault-valve, interseismic, low-angle normal faults*

The Zuccale low-angle normal fault exposed on the island of Elba, Italy, is a crustal-scale structure with a displacement of 7-8km. It contains a pervasively foliated and low-permeability fault core composed of a sequence of fault rocks which have been exhumed from 3-6km depth. In the immediate footwall of the Zuccale Fault, cataclasites which were initially deformed by frictional mechanisms have experienced fluidization over areas of at least 10^{-2} to 10^{-3} km². Three internal variants of fluidized cataclasite are recognized with each related to a separate fluidization episode. All three variants of fluidized cataclasite preserve intrusive relationships with foliated fault rocks within the core of the Zuccale Fault. The boundary between the fluidized cataclasites and the fault core has a highly irregular nature and is warped into a series of meter-scale open folds. Fragments of foliated fault rock are found floating within the underlying fluidized cataclasites. On a grain-scale, fluidized cataclasites are characterized by a matrix-supported framework and there is no evidence for the operation of typical frictional deformation mechanisms. Clasts are sub-rounded to sub-angular and are frequently overgrown by carbonate cements. Immediately overlying the fluidized cataclasites, the core of the Zuccale Fault is highly altered and dominated by fresh carbonate growth, indicating that circulating fluids were rich in CO₂. Additionally, the fluidized cataclasites contain a clast-preferred orientation which indicates that the fluids were moving vertically within the footwall and spreading laterally as they encountered the low-permeability fault core. Our observations suggest that the fluidized cataclasites are a type of fault rock representative of the interseismic period along the Zuccale Fault. We propose a model whereby fluidized cataclasites develop in the immediate footwall of the Zuccale Fault across small fault patches during build-ups in fluid overpressure. The development of a critical fluid overpressure triggers brittle slip and hydrofracturing within the overlying fault core, which may account for the presence and the dimensions (10^{-1} to 10^{-3} km²) of slip patches which are known to produce microseismicity along currently active low-angle normal faults at depth in central Italy.

16. Dehydration and deformation of intact serpentinite under controlled pore pressure with pore volumetry

Ernest Rutter¹, Sergio Llana-Funez² & Katharine Brodie¹

1. University of Manchester, U.K.

2. University of Liverpool, U.K.

Presenting author: e.rutter@manchester.ac.uk

Keyword(s): serpentinite deformation, dehydration

The strength and ductility (deformability) of rocks in nature is believed to be strongly influenced by metamorphic reactions, especially when fluids are evolved and volume changes occur. Mechanical interactions between deformation and metamorphic reactions include (a) changes in the effective stress state through the evolution of fluid under pressure (e.g. H₂O or CO₂) in the case of devolatilization reactions, (b) changes to point defect chemistry of minerals (e.g. quartz) arising from changes in the activity of components of the fluid phase, (c) formation of reaction products sufficiently fine-grained to provoke a change in deformation mechanism to grain-size sensitive flow, (d) enhancement of intracrystalline plastic deformation through stresses arising from solid phase volume changes, and (e) weakening and enhancement of ductility through formation of new porosity. Serpentinites are well-suited to the study of deformation/metamorphism relations because the rock is initially strong yet can undergo substantial changes in mechanical properties in association with its dehydration reaction. It is also an important reaction in its own right because it is believed to play a key role in seismogenesis in subduction zones and in oceanic transform faults. The dehydration of lizardite occurs in the laboratory over the temperature range 500 to 580 °C, over a period from a few days to a few hours. We deformed intact cylinders of lizardite serpentinite under drained conditions, preventing the buildup of high pore fluid pressures, so that we could specifically study the influence on deformability of microstructural changes such as of grain size and porosity. In all experiments, pore volumetry was used, that enabled tracking of volume changes during the dehydration phase and during deformation, except when the duration of the deformation was comparable to the duration of the dehydration reaction. Samples were deformed at different temperatures, (a) before reaction onset, (b) during the course of the reaction, and (c) after the reaction has gone to completion, over a range of strain rates, in order to study its effect on strength and ductility. Complete reaction generates about 20% of new porosity if carried out at effective pressures low enough that pore collapse does not occur. Thus the deformation of the resulting porous rock is expected to behave in accordance with the concept of critical state soil mechanics, even at high temperatures. Here, the yield surface on a plot of deviatoric stress versus effective mean pressure shows a positive slope at low pressures, when dilatancy and faulting control failure. At higher pressures the yield surface displays a negative slope, characteristic of shear-enhanced compaction, until the condition is reached where failure by pore collapse can occur under hydrostatic pressure alone. The boundary line between dilatant and compactive failure is the critical state, at which deformation occurs at constant volume. The yield surface shows an elliptical form, which shrinks in size with decreasing strain rate and/or with increasing porosity. We found critical state-type behaviour in the serpentinite used in this study but, unexpectedly, the size of the yield surface also depended on the effective pressure at which the dehydration reaction was carried out. Thus at high pressures a linked framework microstructure of olivine grains was produced, leading to a higher yield strength. At low dehydration pressures, new olivine grains were more isolated, leading to relative weakness.

Stress/strain behaviour was characterized by strain hardening ductile flow, as pore collapse progressively occurred, until steady state flow at the critical state condition was attained. With decreasing strain rate the strength of the serpentinite decreased rapidly with a linear viscous characteristic. Microstructurally, the new olivine grains were composed of aggregates of ultrafine grained (100 nm) olivine, which we infer flowed by diffusion-accommodated grain boundary sliding, in the same way as we found in an earlier study of sliding along fault surfaces in dehydrating serpentinite. The observed rapidity with which serpentinite can relax deviatoric stress suggests that in subduction zones dehydrating serpentinite cannot support the stresses necessary to permit seismogenic failure, but instead, overpressured water released from dehydrating serpentinite permeates adjacent, non-dehydrating rocks such as gabbro. Coupled with stress transfer from the serpentinite, this is likely to favour seismicity in the gabbro. Serpentinite may act as a useful proxy for the mechanical behaviour of other (crustal) rock types taking part in dehydration reactions, but it must be remembered that the microstructural evolution we see in rapid, laboratory experiments (rapid nucleation and growth to produce fine grained reaction products) may not correspond to coarser grained aggregates produced during slower reaction with smaller thermal oversteps in nature. Unfortunately, during prograde reactions in nature, thermal equilibration and grain growth tend to outstrip deformation events, wiping out microstructural evidence of deformation/metamorphism relationships.

17. An analysis of micro-structural development in experimentally deformed polycrystalline pyrite using electron backscatter diffraction (EBSD)

Craig Barrie¹, Alan Boyle¹, Stephen Cox² & David Prior¹

1. University of Liverpool, Department of Earth and Ocean Sciences, U.K.

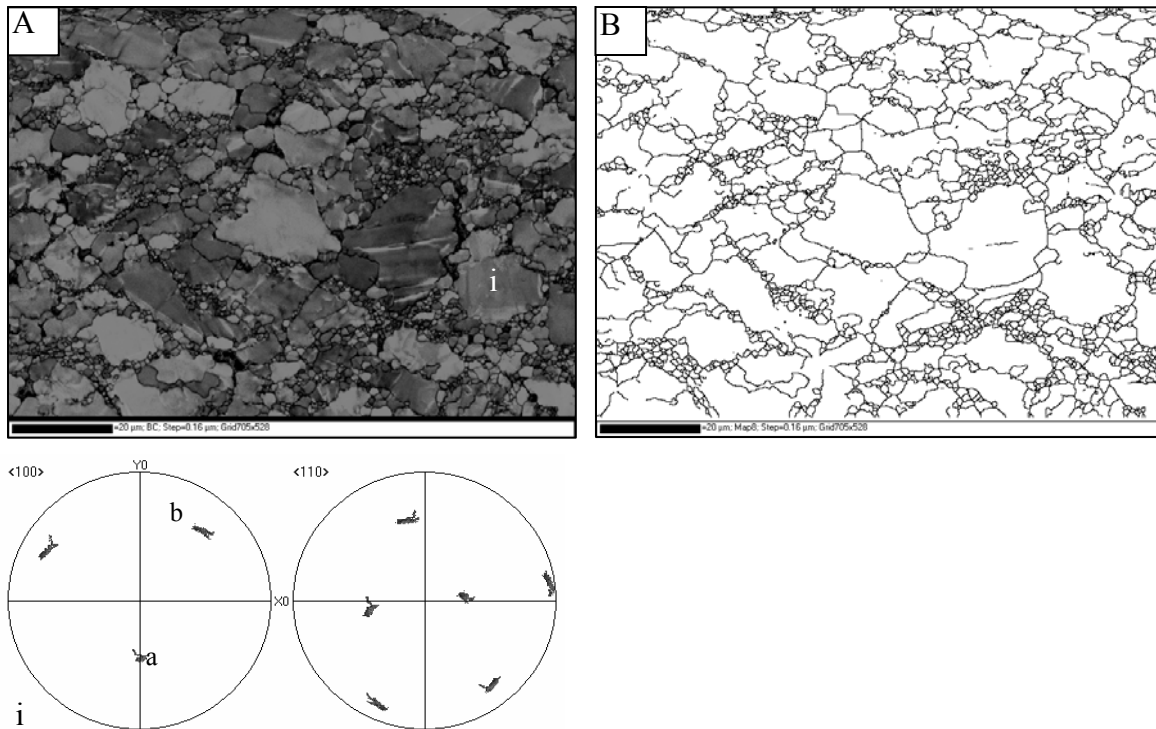
2. The Australian National University, Department of Earth and Marine Sciences, Australian National University, ACT 0200, Australia, stephen.cox@anu.edu.au

Presenting author: cbarrie@liverpool.ac.uk

Keyword(s): *pyrite, dislocation creep, recrystallisation, EBSD*

The identification of deformation mechanisms within pyrite (FeS₂) is essential in understanding of how ore bodies evolve through time. Many ore deposits have at some stage in their history undergone deformation and/or metamorphism at varying pressures and temperatures and so understanding how sulphides behave at these conditions is vital. Pyrite is not of economic importance but it is refractory in nature, preserving evidence of the ore bodies history not normally preserved in the more economic sulphides (i.e. chalcopyrite, sphalerite, etc). Recent work (Boyle *et al.*, 1998; Freitag *et al.*, 2004), utilising foreshatter orientation contrast (OC) imaging coupled with electron backscatter diffraction (EBSD) has allowed plastic deformation within pyrite grains to be readily identified and subsequently quantified allowing detailed systematic analysis of changing pyrite microstructures (Barrie *et al.*, 2007). In order to understand how the deformation mechanisms and microstructures within pyrite vary a range of experimentally deformed samples have been analysed using EBSD. The initial suite of samples, all from the Mt Lyell Mining and Railway Company, near Queenstown, Tasmania were deformed at a constant strain rate and confining pressure ($2 \times 10^{-4} \text{ s}^{-1}$; 300Mpa) but varying temperature (Cox *et al.*, 1981). The lowest temperature samples (550 and 600°C) show evidence for significant lattice misorientation with rotation often occurring about a $\langle 100 \rangle$ axis and the development of low-angle $\sim 2^\circ$ sub-grain boundaries. This suggests plastic deformation has occurred within the pyrite grains, specifically via dislocation creep. At 650°C and more so 700°C this misorientation is far less obvious and few if any sub-grain boundaries are present within pyrite grains. This suggests that with increasing temperature either the dominant deformation mechanism operating has changed (at about 650°C) or recovery and recrystallisation mechanisms are far more rigorous, removing misorientations from grains much more readily than at lower temperatures. Detailed analysis along grain boundaries suggests a systematic change in recrystallisation and recovery mechanisms with temperature. Between 550°C and 700°C recrystallisation changed from bulging at 550°C through sub-grain rotation (SGR) at 650°C and finally grain boundary migration (GBM) at 700°C. This systematic change suggests that in all of the samples analysed dislocation creep is likely to be the dominant deformation mechanism within pyrite grains. Much of the evidence for this dislocation creep however is removed at higher temperatures by recrystallisation and recovery mechanisms which appear to be much more important than at 550°C. These results do not correspond with those predicted by the proposed deformation mechanism map for pyrite (McClay and Ellis, 1981). This study suggests that the field for dislocation creep in pyrite occurs at a much wider range of conditions than previously predicted and in order for the deformation mechanism map to be of any future use it needs to be revised. The results presented in this study are part of a larger project, analysing both naturally and experimentally deformed pyrite samples with the aim of improved understanding of what deformation mechanisms operate under a wide range of

conditions.



BARRIE, C.D., BOYLE, A.P. & PRIOR, D.J., 2007. An analysis of the microstructures developed in experimentally deformed polycrystalline pyrite and minor sulphide phases using electron backscatter diffraction: *Journal of Structural Geology* 29, 1494-1511

BOYLE, A.P., PRIOR, D.J., BANHAM, M.H. & TIMMS, N.E., 1998. Plastic deformation of metamorphic pyrite: new evidence from electron backscatter diffraction and foreshorter orientation contrast imaging, *Mineralium Deposita* 34, pp. 71–81.

COX, S.F., ETHERIDGE, M.A. & HOBBS, B.E., 1981. The experimental ductile deformation of polycrystalline and single crystal pyrite, *Economic Geology* 76, pp. 2105–2117.

FREITAG, K., BOYLE, A.P., NELSON, E., HITZMAN, M., CHURCHILL, J. & LOPEZ-PEDROSA, M., 2004. The use of electron backscatter diffraction and orientation contrast imaging as tools for sulphide textural studies: example from the greens creek deposit (Alaska), *Mineralium Deposita* 39, pp. 103–113.

MCCLAY, K.R. & ELLIS, P.G., 1983. Deformation and recrystallization of pyrite, *Mineralogical Magazine* 47, pp. 527–538.

18. Behaviour of two-phase shear zones in high strain deformation experiments

Saskia ten Grotenhuis¹, Hans de Bresser¹ & Chris Spiers¹

*1. University of Utrecht, Faculty of Geosciences, HPT-Lab, The Netherlands
Presenting author: saskiatg@geo.uu.nl*

Flow laws used to model lithosphere dynamics are primarily based on data from low strain axial compression experiments on samples containing a single mineral phase, whereas deformation in the lithosphere is often localised in high strain shear zones and involve rocks that are in general polyphase. Deformation processes in these high strain shear zones lead to changes in the microstructure of the rock, resulting in foliated mylonitic microstructures. At present, quantitative understanding of the effect on rheology of developing microstructures in multiphase shear zones is still sparse. It is the aim of this study to help filling this gap, by performing high strain, direct shear, deformation experiments on salt-mica mixtures. The used experimental set-up is designed to generate a maximum shear strain of $\gamma = 5$. Salt (initial grain size 60 μm) and mica (muscovite, grain size 13 μm) powders have been mixed and cold-pressed into tablets to prepare the samples. The samples were heated at 500°C in Argon to dry before deformation. A series of mixtures, with mica content systematically varying from 0 to 50 %, has been tested at 200°C, 20-100 MPa confining pressure, and a strain rate $5 \cdot 10^{-4} \text{ s}^{-1}$. Under these conditions deformation in pure salt is dominated by climb-controlled dislocation creep, and in mica by frictional behaviour. The experiments show near constant flow stress at high strain, so no weakening or hardening. The dependence of the flow strength on mica content and confining pressure has been determined and the microstructures of the samples have been analysed. At relatively high confining pressure the flow stress increases with increasing mica content, indicating that the behaviour of the mica is stronger than that of the salt. Deformation is mainly concentrated in the salt grains. After deformation the samples were cut parallel to the shear direction, and analysed with SEM, BSE and EBSD. The BSE images were used to analyse the salt-mica distribution in the samples. The mica grains were found clustered in elongated patches of 10 to >100 μm long and max. 20 μm thickness, oriented at a small angle to the shear direction. The EBSD maps are used to analyse the grain size and shape, and CPO of the salt crystals. The salt grains are elongated, contain many subgrains and are reduced in grain size compared to the starting material to 7-9 μm . Both the size and the aspect ratio of the salt grains show a decreasing trend with increasing mica content. The decrease in grain size can most likely be explained by the higher stress, and therefore smaller recrystallised grain size, in samples with more mica. The lower aspect ratio could suggest that grain boundary sliding along the mica-salt contact plays an important role in the deformation of these samples. The decrease in intensity of the CPO with increasing mica content of the sample supports this conclusion. This suggests that the resulting strength of the samples is determined by a combination of the friction behaviour of the salt-mica interface and the dislocation creep in the salt crystals. At lower confining pressure the flow stress is less dependent on the mica content of the sample. Under these conditions grain boundary sliding along salt-mica contacts is probably the most important mechanism.

19. Boudins vs. mullions in the Ardenne Allochthonous: a century of academic debates in the “Terra Ardennensis Incognita”

Yves Vanbrabant¹ & Léon Dejonghe¹

1. Belgian Geological Survey, Brussels, Belgium

Presenting author: yves.vanbrabant@naturalsciences.be

Keyword(s): reworked boudins, academic debates

The famous boudin structures observed throughout the Ardenne Allochthonous in Belgium and Germany were coined for the first time in 1908 by Lohest *et al.* The boudins affect lower Devonian (meta-)sedimentary sequences (sandstone and silt-shale horizons). The structures are since their recognition a matter of academic debates regarding their origin. The main issue is related to the coexistence of stress and strain markers of two different tectonic events. The inter-boudin quartz veins indicate a layer-parallel tensile stress, while the obliquity of the cleavage in the fine-grained matrix with respect to the boudinage plane is related to a layer-parallel shortening event. The barrel-shaped boudin geometry is also a matter of discussions, since the aspect ratio (width/height ~ 0.5) is lower than the frequently referred value (>2) for typical boudins, in addition the layer interfaces between quartz veins show an atypical convexity (Figure 1). In our presentation, we first summarize the debate milestones from the initial purely descriptive definition of Lohest *et al.* (1908) to the more recent “geodynamic” models. In particular, we have to point out the papers by Rondeel & Voermans (1975) and Jongmans & Cosgrove (1993). They introduce a two-stage deformation model, namely boudinage by layer-parallel extension followed by a layer-parallel shortening. In this model, the shortening of pre-existing boudins explains the low aspect ratio and the strong convexity. The term “boudin” was remained. More recently, a set of papers by Kenis *et al.* (2002), Urai *et al.* (2001), refutes the term “boudin” and re-introduces the term “mullions” or “double-sided mullions”. The main argument is the aspect ratio, which seems incompatible with respect to typical boudins. In this model, the veining event is integrated with the Variscan orogeny with a progressive modification of the stress conditions and the interplay of the fluid pressure. In an advert for her contribution, Kenis & Sintubin (2007) wrote: “The current study irrefutable proves that the term ‘boudin’ should be abandoned to describe the particular ‘double-sided’ mullions in the Ardenne-Eifel area”. In our contribution, we will show that: 1) in contrast with the opinion of Kenis & Sintubin, the debate is not yet closed; 2) the model proposed by Kenis *et al.* (2002) is incompatible with the Mohr-Coulomb failure envelope model; 3) their model results from a mix-up of stress and strain concepts; 3) the narrow boudins exist and can readily be explained by the jointing of rocks. Our model is compatible with the one of Rondeel & Voermans (1975) and Jongmans & Cosgrove (1993). However, we consider that the boudins before the shortening event were already narrow with aspect ratio (width/height) close to 1. The latter value was reduced during the layer-parallel event to the current value (~ 0.5). Consequently, we suggest the use of “narrow reworked boudins” or simply “reworked boudins” terms to name the segmented layers observed through the Ardenne-Eifel area. Besides this academic debate we present a set of structures contrasting with reworked boudins. They are strongly influenced by the sedimentary sequences and provide new information on the structural evolution of the Ardenne-Eifel region, which is poorly known, but the reworked boudins.

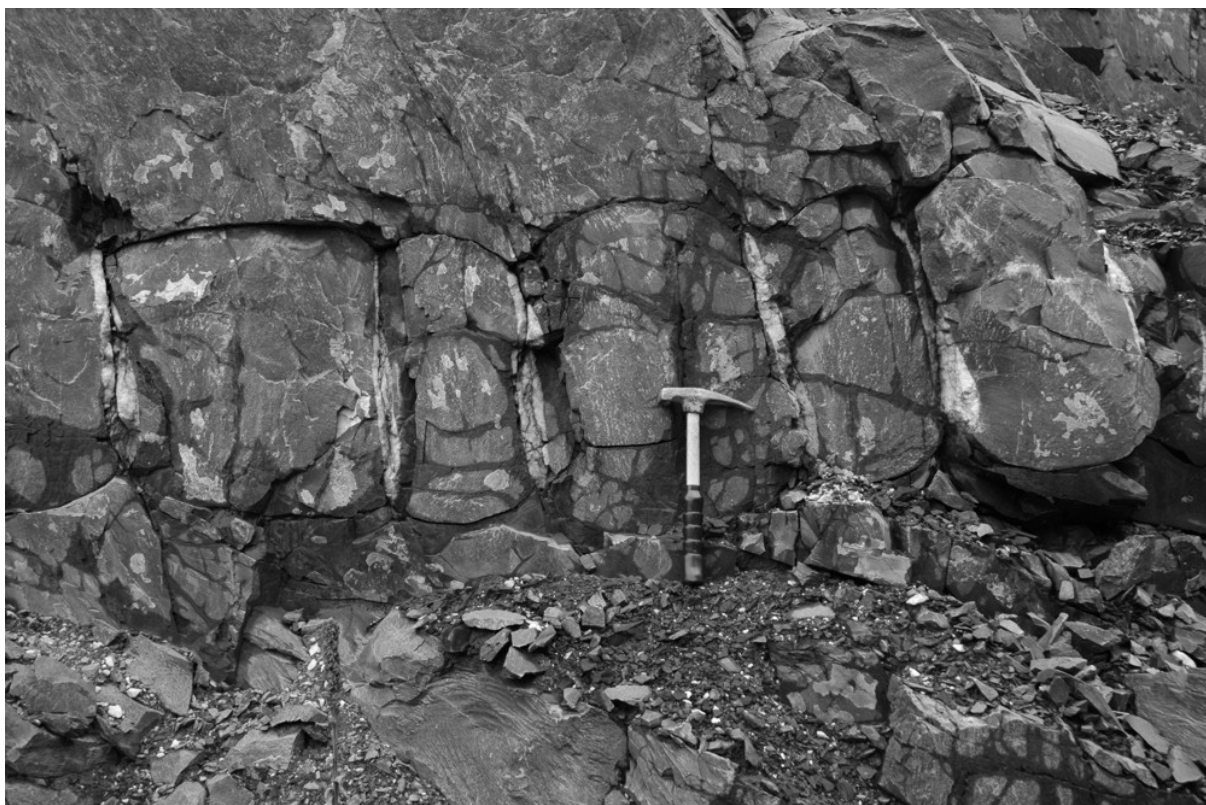


Figure 1. Example of reworked boudins from the “Sur les Roches” quarry (Bastogne, Belgium). The boudins show a barrel-shaped geometry with a low aspect ratio (width/height ~ 0.5) and a strong convexity of layer interfaces. A lens-shaped quartz vein separates two boudins.

JONGMANS, D. & COSGROVE, J.W., 1993. Observations structurales dans la région de Bastogne. *Annales de la Société géologique de Belgique* 116: 129-136.

KENIS, I., SINTUBIN, M., MUCHEZ, PH. & BURKE, E.A.J., 2002. The “boudinage” question in the High-Ardenne Slate Belt (Belgium): a combined structural and fluid-inclusion approach. *Tectonophysics* 348: 93-110.

KENIS, I. & SINTUBIN, M. 2007. About boudins and mullions in the Ardenne-Eifel area (Belgium, Germany). *Geologica Belgica* 10(1-2), 79-91.

LOHEST, M., STAINIER, X. & FOURMARIER, P., 1908. Compte rendu de la session extraordinaire de la Société géologique de Belgique, tenue à Eupen et à Bastogne les 29, 30 et 31 août et 1er, 2 et 3 septembre 1908. *Annales de la Société géologique de Belgique* 35: B351-B434.

RONDEEL, H.E. & VOERMANS, F.M., 1975. Data Pertinent to the Phenomenon of Boudinage at Bastogne in the Ardennes. *Geologische Rundschau* 64: 807-818.

URAI, J.L., SPAETH, G., VAN DER ZEE, W. & HILGERS, C., 2001. Evolution of mullion (formerly boudin) structures in the Variscan of the Ardennes and Eifel. *Journal of Virtual Explorer*, 3, 1-15. [url:http://virtualexplorer.com.au/2001/Volume3review/Urai2/index.html](http://virtualexplorer.com.au/2001/Volume3review/Urai2/index.html)

20. Crustal rheology of fine-grained siliciclastic rocks deforming by solution-precipitation processes

Janos L. Urai¹ & Manuel Sintubin²

1. RWTH Aachen University, Structural Geology, Tectonics and Geomechanics, Germany

2. K.U.Leuven, Geodynamics & Geofluids Research Group, Belgium

Presenting author: j.urai@ged.rwth-aachen.de

Keyword(s): *rheology, mullions*

Geomechanical models form an essential part with respect to our quantitative understanding of tectonic processes. In these models, a long-standing problem involves the quantification of the constitutive equations that describe the rheology of the middle crust (7-12 km). A combination of indirect methods has yielded first-order descriptions of the rheology of these rocks, but much is still unknown and controversial. Constraints on rock rheology are needed from careful field studies and mechanical modelling. We present a new method to quantify the rheology of fine-grained siliciclastic rocks, which are common in the middle crust (at around 400°C) and deform by solution-precipitation processes. We use a combined structural and numerical analysis of mullion structures pinned by pre-existing layer-perpendicular quartz veins to quantify the rheological parameters of the psammitic layers within the siliciclastic multilayer sequence during flow at geologic strain rates. The method is based on a parameter estimation scheme developed in structural mechanics. Results consistently converge towards a set of rheological properties, which are in agreement with observed microstructures and indicate that fine-grained psammitic rocks in the middle crust have a Newtonian, viscous, rheology, approximately ten times weaker than wet quartz (cf. quartz veins). Using information from folded multilayers in the same fine-grained siliciclastic multilayer sequence, we estimate the rheology of the pelitic layers, which are several times weaker than the psammites. These results are combined into a rheological model of the stratified siliciclastic multilayer sequence. This indicates a very weak middle crust, with important consequences for the tectonic style. Because siliciclastic rocks control the rheology of the middle crust in many sedimentary basins, our results provide new parameters for geodynamic modelling.

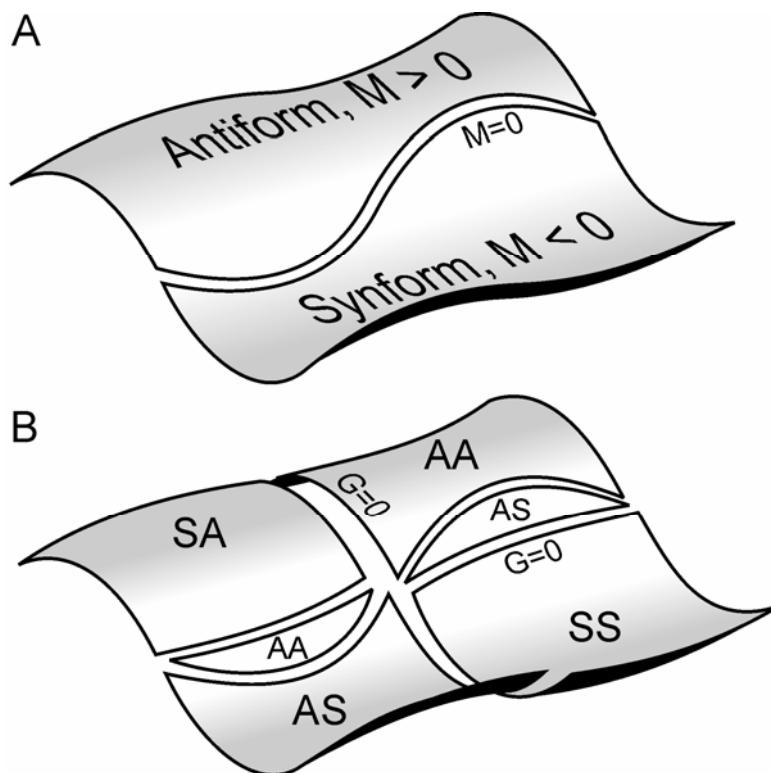
21. A 3D view of folds

Richard Lisle¹ & Yehua Shan¹

1. Cardiff University, U.K.

Presenting author: lisle@cardiff.ac.uk

The terms we currently use to describe folds (e.g. hinge line, inflection, fold limb, etc) are strongly biased towards the simple cylindrical model of fold geometry. This model is frequently adopted in situations where information on fold shapes is incomplete, and often little more than two dimensional. However with modern techniques of seismic mapping and GPS surveying of geological surfaces, it is possible to obtain truly 3D information from folded surfaces. These data reveal that the majority of open folds present in hydrocarbon provinces are highly non-cylindrical and therefore impossible to analyse using existing terms. This talk summarises a new approach for analysing complex non-cylindrical folds. The boundaries between antiforms and synforms are defined by lines of zero mean curvature, $M=0$ (Fig 1A). Antiforms ($M > 0$) and synforms ($M < 0$) are then subdivided on the basis of the values of Gaussian curvature, G (Fig 1B). Synclastic types ($G > 0$) are thus distinguished from anticlastic folds ($G < 0$). The figure below illustrates the four basic fold types. This approach leads to a division of a folded horizon into separate patches, each equating to an individual fold. For the first time, the number of folds on a given surface can be counted and studied as function of structural level, degree of smoothing of the data, scale of observations, etc. The new approach can be used to characterize the fold pattern arising from different strain environments (e.g., en echelon fold arrangements in strike slip zones).



22. Surface effects of active folding, illustrated with examples from the Tian Shan intracontinental mountain belt (China)

Aurelia Hubert-Ferrari & John Suppe

*Royal Observatory of Belgium, av. circulaire 3, 1180 Brussels, Belgium,
Department of Geosciences, Princeton University, Princeton, NJ 08544, USA, suppe@princeton.edu
Presenting author: aurelia.ferrari@oma.be*

Keyword(s): fold-and-thrust belt, active deformation

The combination of good surface exposure and subsurface imaging allow us to directly relate the anticlinal morphology to its deep active structure. The two studied Yakeng and Quilitak folds are located at the front of the Kuche-fold –and-thrust belt of the Southern Tianshan. The folds have fundamentally different folding mechanisms, which is reflected in their contrasting geomorphology. Seismic reflection profiles show that the Yakeng anticline is gentle detachment fold with limb dip generally less than 5-6 degrees. By measuring area of structural relief as a function of elevation we constrain its magnitude and the history of growth. The analysis yields a total shortening of 1200 m with the beginning of growth at horizon 14 time and an approximately linear upward decrease in shortening through the 2.4 km thick growth sequence. Furthermore during most of its growth Yakeng was completely buried with a constant ratio between shortening and cumulated sediment height of 0.2. A recent growth acceleration probably triggered by diapiric flow, leading to its topographic emergence. At the surface the low ridge formed by Yakeng anticline is similar to the deep structure. Its two-stage growth is also visible in the morphology. Yakeng emergence has been completely disrupted the river network and changed the sedimentation pattern. Before that time, wide alluvial fans were covering the northern part of the present Yakeng structural high. Finally a quantitative comparison between the warped surface of Yakeng and its deep shape shows that Yakeng topography is a direct image at reduced amplitude of its deep structure. Yakeng is thus a self-similar fold where the instantaneous uplift rate varies smoothly across the structure and is collocated to the finite uplift. In contrast, the Quilitak anticline does not directly reflect its deep structure. Quilitak is a complex fault-bend-fold having a deep width of 10 to 20 km and forming at the surface a 5 to 7 km wide mountainous ridge with a cumulated relief of ~1000 m. The edges of the Quilitak relief forms continuous linear front characterized by steep triangular facets. We demonstrate that this striking morphology corresponds to an active axial surface- or hinge- along which an abrupt change in bedding dip occurs. The Quilitak front is this a cumulative fold scarp resulting for the folding of an erosional surface south of Quilitak high across an active axial surface pinned to the underlying fault bend and thus fixed relative to the rocks. Fold scarp formation occurs because active axial surface are fixed locus of instantaneous uplift. Quilitak morphology thus directly reflects the deep kink-band folding mechanism which implies that active axial surface is a fixed locus of instantaneous uplift. Recent alluvial sediments deposited on top of the eroded southern front of Quilitak have recorded a bed-by-bed image of the formation of fold scarps. Quantitative sections logged in the field shows the whole complexity of processes occurring in hinges. The hinge appears to have a finite width within which progressive folding occurs. Furthermore the existence of marked unconformities or disconformities within the hinge points out the importance erosion/sedimentation processes relative to tectonic processes. Finally the folding kinematics can be modeled using a curved-hinge kink-band migration model where the sharp

axial-surface line used in fault-bend folding expands to be of finite ~110m width, and the wide axial surface zone behaves like curved similar fold. Our logged section can be fitted using this forward model of growth folding. The best fitting model then provides a measure of horizontal displacement for each bed-horizons.

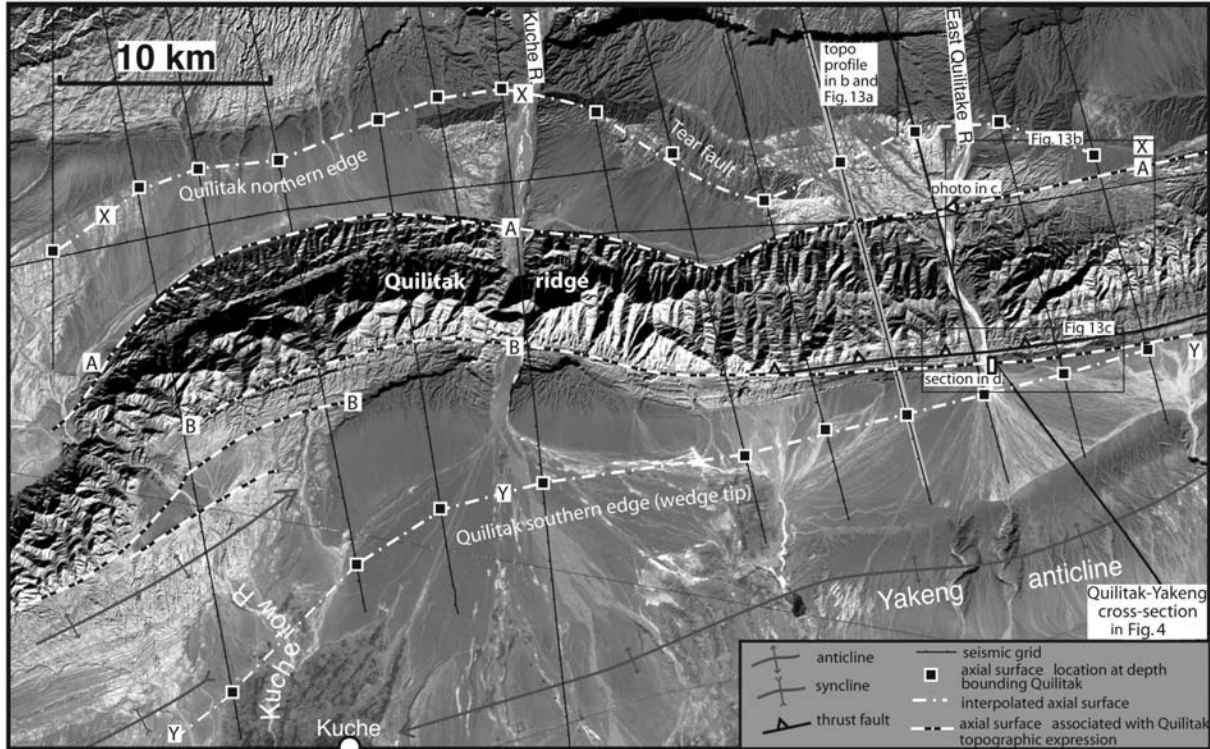


Figure 1. The Quilitak anticline: relationship between morphology and structure. Axial surface map was reported on top of Landsat image. Positions of seismic lines are indicated. The Quilitak topographic ridge as defined by its sharp edges A and B bears little apparent relation with the deep anticline width defined by the distance between axial surfaces X and Y.

23. Analogue modelling of material supply to a diapiric structure rising above an active basement fault

Stanislaw Burliga¹ & Hemin A. Koyi²

1. University of Wrocław, Institute of Geological Sciences, Poland

2. Uppsala University, Sweden

Presenting author: burliga@ing.uni.wroc.pl

Keyword(s): analogue modelling, diapir, salt tectonics, basin inversion

It is widely acknowledged that basement faults can trigger salt diapirs. However, little is known about the role of a basement fault in the overall growth of a diapir and how the hanging- and footwall portions of a basin contribute to salt supply. Using the Kłodawa Salt Structure (KSS) in central Poland as a prototype, a series of analogue models were carried out to investigate how the salt supply to a diapir is influenced by the presence of an active basement fault. KSS is a salt ridge built of Zechstein evaporite series located in the axial part of the former Mid-Polish Trough. This extensional basin was filled with Zechstein to Cretaceous sediments and was inverted in the Late Cretaceous to Paleogene time. The diapir was triggered in the Triassic above a basement fault. In the late Triassic, after intruding cover sediments, the diapir extruded, forming an overhang. In the models simulating this evolution, a ductile layer (PDMS) was spread over a rigid basement with an inbuilt normal fault. Different colours of the PDMS were used for the hanging- and footwall parts of the ductile layer in order to differentiate salt supply between the hanging- and footwall sides. During extension, a diapir was upbuilt by the sand cover above the basement fault. The ductile layer was allowed to extrude a wide overhang at the model “late Triassic” time. The diapir was later downbuilt with progressive extension. At the end of the extension, a part of the model was sectioned for photographing, whereas the remaining part was inverted, resulting in uplift of the hanging wall portion of the model. The model was eventually buried and sectioned for photographing. The experiments showed that at an early extensional stage, the diapir was primarily fed from the footwall side. Footwall material constitutes the uppermost portion of the structure and the dominant component of the overhang. Considering the upper, portion of the diapir – discordant with the overburden – footwall material made up between >70% of the diapir at the initial stage of its growth to about 55% in the mature diapir (Fig. a). Reverse movement on the basement fault resulted in an increase in the diapir height, overall thinning of its stem and larger supply of the ductile layer from the hanging-wall side into the basal footwall portion of the diapir. After the inversion, the footwall material constituted 65-75% of the structure above the reference line (Fig. b). Positioning the reference line at the base of depocentres that developed in the cover due to ductile layer withdrawal, still much larger amount of material was supplied from the footwall side. However, the difference was less contrasting and footwall material constituted 52-58% of the diapiric structure both at extensional and shortening stages of its development. The analogue models show that a diapir rising above an active normal fault is fed both by the footwall and hanging-wall sides. However, contribution from the hanging-wall to the upper segment of the diapir is remarkably smaller. The footwall material constitutes not only the footwall portion of the diapir, but also its topmost part on the hanging-wall side.

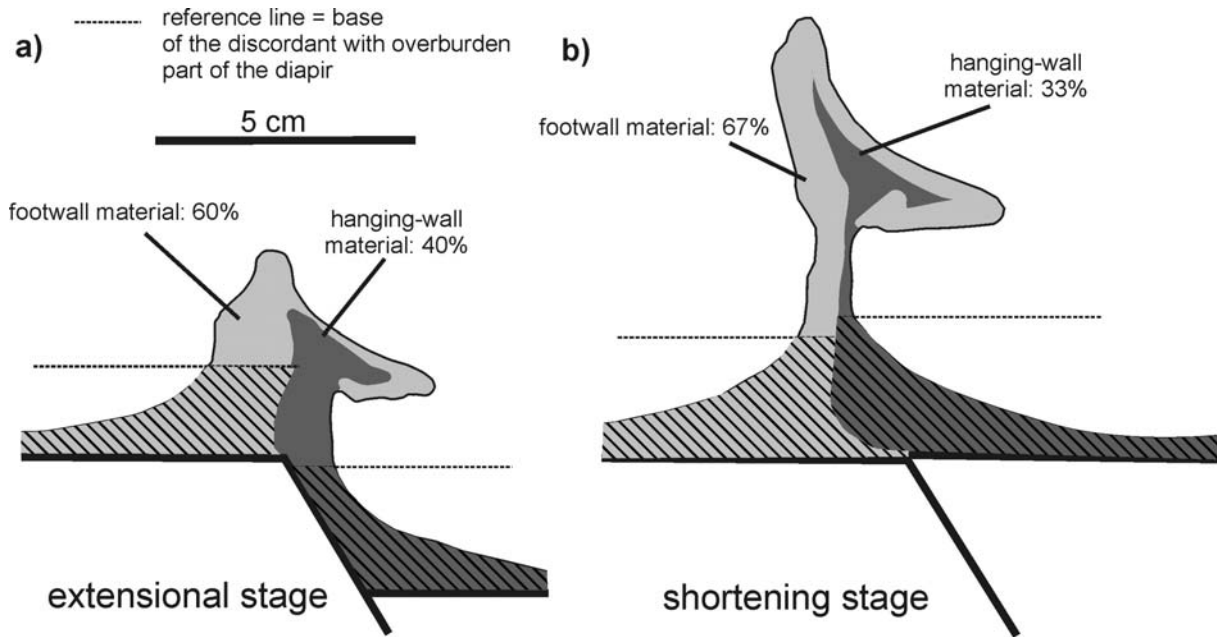


Figure 1. Distribution of hanging- and footwall material in a diapir rising above a basement fault: a) – after model extension, b) – after inversion

24. Syn-depositional formation of shear fabrics and folded laminations in turbidite sandstones: an example of deformation of granular media

Joris Eggenhuisen¹, Rob Butler¹, Bill McCaffrey¹ & Peter Haughton²

1. University of Leeds, School of Earth and Environment, U.K.

2. University College Dublin, Department of Geology, Ireland

Presenting author: j.eggenhuisen@earth.leeds.ac.uk

Keyword(s): shear localisation, growth folding, soft sediment deformation

Deformation of the substrate during submarine gravity flows has the potential to greatly influence deposit character and is an example of fluid assisted deformation of a granular medium. This presentation presents some of the structures that result, focussing on the occurrence of shear fabrics in a sedimentological facies usually referred to as 'mixed slurry', and folded ('convolute') laminations. 'Mixed slurry' facies, is a common facies in cores of the Britannia Sandstone Formation (Lower Cretaceous, UK North Sea sector). It occurs in sandstones with a significant percentage of clay. Relatively clay-poor dewatering structures define the texture of the facies. They are commonly folded and sheared. Assuming they initially formed sub-vertically, the sub-horizontal orientations of some of the dewatering structures indicate high shear strain values. Different sets of dewatering structures in different states of strain are often observed, the more continuous, vertical ones postdating more discontinuous and sheared ones. Discrete sub-horizontal shear planes dissect the dewatering structures in places, displacing all, even the least deformed, dewatering structures. These relations are interpreted as a transition from a uniform to a discrete distribution of shear strain indicating work hardening during ongoing dewatering. Occurrence of this facies in a 5cm-dm's scale banded pattern with clay poor, undeformed sandstone laminations, indicates that the observed deformation of the clay rich bands is syn-aggradational. In cases where this banding pattern is absent, the distinction between syn- and post-aggradational deformation is less easily made. The upper parts of turbidites often show convolute lamination. Here, we present outcrop examples from the Late Oligocene Macigno Formation (Tuscany, Northern Italy). Folded laminations thicken into the core of synforms and thin into anticlinal hinge zones, which is interpreted as evidence for growth. Erosional cut-off at the top of heavily convoluted sets of laminae by less or un-deformed laminae likewise points to the deformation taking place during aggradation of the bed. Where these structures are caused by shear coupling between the overriding flow and its substrate, their kinematics can help to reconstruct paleoflow direction and thus may be used as tools in cases where conventional paleoflow indicators are sparse. A recurring question in this type of study, though, is whether the stress driving the deformation is supplied by friction between the overriding flow and its substrate, or by gravity working on the sediments, which are deposited on a slope. Independent evidence of flow direction can be found in conventional paleoflow indicators, but independent evidence for the dip direction of the paleoslope is much less easy to obtain and must generally be deduced from the regional setting. Traditionally, sedimentologists regard depositional events as flow of water or air over a rigid substrate that might have a thin veneer of sediment grains in bedload transport. However, this implicitly assumed two-phase rheologic model of low viscosity water flowing over solid, unyielding substrate is much too simplistic.

25. Sediment loading drives folding in the South Caspian

Kenneth McCaffrey¹ & Richard Jolly²

1. University of Durham, Earth Sciences, U.K.

2. BP Exploration, Sunbury Upon Thames, U.K.

Presenting author: k.j.w.mccaffrey@durham.ac.uk

Keyword(s): folding, Caspian Sea

The South Caspian Basin provides an outstanding example of a rifted marginal basin now undergoing 3D contractional deformation. It is a young, deep basin which contains a prolific hydrocarbon system and thus is an extremely valuable natural laboratory with extensive industry data coverage. Folds and mud volcanoes are notable features of the basin and both are actively growing in the Cenozoic sedimentary sequence. Here, we discuss ongoing work to understand the dominant controls on the origin and evolution of the South Caspian structures. Within the basin, a thick fluvio-deltaic sequence is being actively folded into trains of 10-20km wavelength, 5-10km amplitude upright folds. The main spatial domains have been mapped in regional 2D seismic datasets. Linear, closely spaced fold arrays occur near the western and northern basin margins. Towards the basin centre folds display short, bifurcating hinge traces that form polygonal patterns in places. Mud volcanoes are found on or near fold crests and where hinge traces meet or are segmented. Our work suggests that the interaction between plate movements, basement influence and mechanical stratigraphy produce effects that vary spatially across the basin and with scale of observation. These interactions have produced fold geometries that are not typical of those developed by buckling alone as suggested previously, and that the mud and fold systems are linked by positive feedback mechanisms.

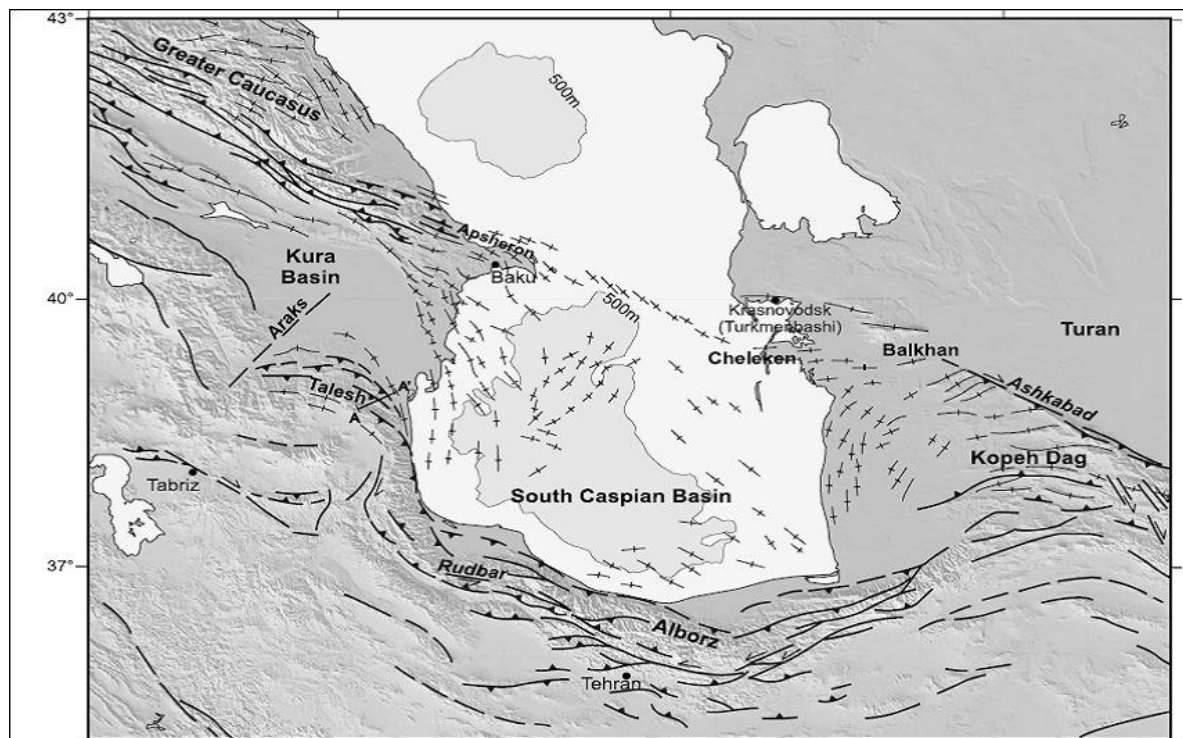


Figure 1. From: Jackson et al. GJI 2002

26. Tectonic evolution of the Caribbean-South America plate boundary at Colombia: implications for ocean-continent interactions

Rob Butler¹ & Douglas Paton¹

1. University of Leeds, SEE, Institute of Geophysics and Tectonics, U.K.

Presenting author: butler@see.leeds.ac.uk

The Caribbean Sea consists largely of thickened oceanic crust, part of an ancestral oceanic plateau of Cretaceous age, that has been in convergence with South America for at least the past 30 Myr. GPS-derived present plate motions for the western Caribbean relative to a fixed South America imply c. 1.5 cm/yr ESE convergence along the Colombian continental margin. Existing tectonic compilations show an active subduction thrust at the toe of the continental slope. Seismic data from a series of regional 2D surveys from offshore Colombia show a different story. There is active thrusting at the toe of slope, offshore Guajira, and in the Sinu accretionary prism (NE and SW on the margin respectively). However, the Plio-Quaternary Magdalena fan is largely undeformed. In the Sinu prism the late Pliocene reflector shows rather little deformation, implying only a few mm convergence over the past 2 Myr. There is even less young contraction evident off the Guajira. With the continental margin undergoing rather little active convergence, plate motion must be strongly partitioned into the continental interior, driving thrust systems on the margins of the Llanos foredeep and the Middle Magdalena basins. These inferences for the Myr-scale deformation are consistent with earthquake and available GPS data, although these are commonly interpreted as reflecting Nazca plate (Pacific side) indentation into South America. The proposal here is that the tectonics of the Colombia-Venezuelan margin reflects the buoyancy of the thick Caribbean oceanic crust. Convergence at the plate boundary is therefore partitioned onto the continental crust. Similar behaviour happened on the Pacific margin of Colombia with accretion of the Western Cordillera in early Tertiary times. The setting is an analogue for the model of subduction zone choking proposed by Davis (1995, EPSL) to explain the apparent cyclic nature of plate tectonics through Earth history. BHP Billiton and GX Technology are thanked for funding, permission to present these ideas and seismic data.

27. A structural transect through an accretionary complex, North-West Colombia

Steve Richardson¹

*1. University of Durham, Department of Earth Sciences, Science Labs, U.K.
Presenting author: s.e.j.richardson@durham.ac.uk*

Keyword(s): Colombia, accretionary complex, Sinu, restoration, balancing forward modelling

This project examines the subsurface geometry of compressional structures contained within the Sinú-San Jacinto Fold belt, located on the active, north western margin of Colombia. A 91 km long 2D seismic section through the fold belt was interpreted and subjected to geometric interrogation: Independent restoration and balancing of the structures was carried out. Additionally, forward modelling was performed in an attempt to recreate the observed deformation. The interpretation provides a rational geometry of the deforming subsurface of the Sinú folded belt. The geometry is that of an imbricate stack. Shortening is estimated at 22% (26 km) since the Late Pliocene. The stack contains multiple detachments. Uplift and re-activation of the detachment is interpreted to have occurred. Fault activity progresses down the stack in an alternating fashion with fault bend folding as the dominant folding mechanism. Piggyback basins have formed above fold limbs with folds and faults developing contemporaneously. The project was carried out for the completion of an MSc in structural geology and geophysics at Leeds University



Figure 1. A colombian beach (owner: tripowski taken from Flickr.com)

28. The role of strike-slip faulting in Peninsular Thailand

Ian Watkinson¹, Chris Elders¹ & Robert Hall¹

1. Royal Holloway University of London, Geology Department, Surrey, U.K.

Presenting author: i.watkinson@gl.rhul.ac.uk

The Khlong Marui Fault (KMF) and Ranong Fault (RF) are major NNE trending strike-slip structures which dissect Peninsular Thailand. They crop out for 220 km and 420 km respectively, appear to pass into the Andaman Sea to the west and the Gulf of Thailand to the east, and are assumed to be conjugate to the NW trending Three Pagodas Fault (TPF) and Mae Ping Fault (MPF) in northern Thailand. According to the lateral extrusion model, a diachronous reversal in shear sense on the NW trending faults correlates to northward movement of the Indian indenter during the India – Eurasia collision. It follows that the KMF and RF are expected to show the opposite shear sense and an inversion at the same time as the TPF. Field mapping reveals that both faults are defined by elongate cores of metamorphic rocks with dextral shear fabrics, bound by brittle sinistral strands. The cores are composed of amphibolite facies mylonites, migmatites, syn-kinematic granitoids, and lower grade sheared sediments. Two phases of ductile dextral shear – D1 and D2 - are separated by Campanian inter-kinematic magmatism. Palaeocene to Eocene post-kinematic granites constrain the end of D2, while D3, the brittle sinistral phase, deforms these granites, and has exhumed the metamorphic rocks. Minor dextral deformation, D4, occurred at shallow levels, and obliquely truncates the older fabrics. A metamorphic core complex at the northern end of the RF lies near the southernmost strand of the TPF. Its geometry is consistent with E-W extension, associated with D3. Basins at the ends of the fault are also orientated so that they should open during D3. However, both faults splay at their southern ends as they enter the Andaman Sea, and may die out entirely before they enter the Gulf of Thailand. In addition, syn-rift sediments in the basins pre-date the postulated D1/D2 to D3 inversion. It therefore seems likely that the faults did not control or drive extension in the basins during the D3 phase, but acted as accommodation structures. Syn-extension sedimentation on both sides of the peninsula continued from Mid Eocene to the end of the Oligocene. Miocene basin inversion correlates to the onset of D4 on the strike-slip faults. The D1/D2 to D3 inversion is consistent with the faults' hypothesised role as antithetic branches of the TPF. However, the sinistral phase on the TPF has previously been interpreted to occur 25 Ma after the equivalent D1/D2 interpreted here. This Upper Cretaceous – Palaeocene faulting is well before Himalayan continental collision, and may instead accommodate deformation in the over-riding plate during subduction of the Ceno-Tethys. The Eocene – Oligocene D3 phase is likely to represent reactivation of the D1/D2 fabrics at a shallower depth in response to locally driven basin extension, and resulted in exhumation of deep crustal rocks in the shear zone and in the metamorphic core complex.

29. Evolution of growth faults in a salt dominated slope, offshore Angola, West African margin

Emmanuel Adiotomre¹ & Robert L. Gawthorpe¹

1. University of Manchester, School of Earth, Atmospheric & Environmental Sciences, Basin Studies & Petroleum Geoscience, U.K.

Presenting author: adiotomre@postgrad.manchester.ac.uk

Keyword(s): growth faults, Angolan margin, geometric segments

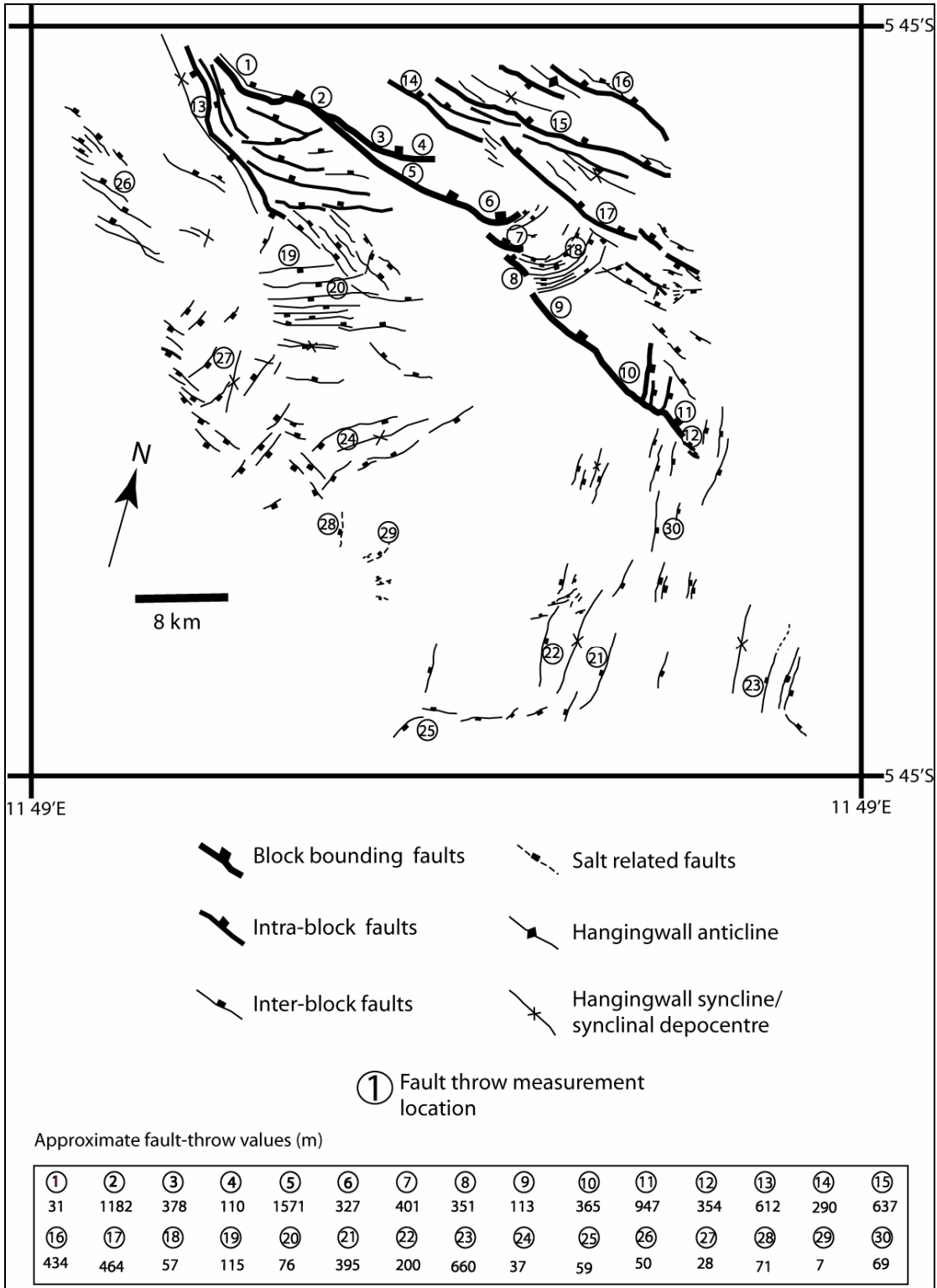
The morphology and geometric traces of fault structures observed in Block 17, offshore Angolan margin provide insights into the evolution of normal growth faults in shelf margin deltas prograding over mobile substratum. A summary structural map produced for the Angola Block 17 shows a population of normal faults that exhibits along-strike changes in structural style and trend. Slope topography is dominated by NW-SE trending growth faults and salt-cored folds at a high angle to the regional dip of the slope. Growth faults evolve by lateral propagation and linkage of segments to form major fault zones c. 50 km long, that give the shallow section tilted fault-block topography. The trace geometry of principal fault zone shows right-stepping, overlapping 14 geometric segments c. 100m to 4 km in lateral extent, that are characterised along-strike with intact and breached relay zones. The overlap of geometric segments varies from a few cm to km scale. The displacement-distance plot for geometric fault segments dominantly bears some resemblance to the 'C'-type plots which suggest that fault segments propagates from a localised nucleation point. Higher displacement values are associated with geometric segments of greater overlap. Geometric segments shows undulations along their trace that indicate rapid changes in fault strike and secondary linkage areas with splay or relay faults. Seismic section across two centrally located relays shows that in each case the relay bounding fault segments rejoin at shallower horizons to form a single fault. Lateral termination of the principal fault trace is characterised by en échelon configuration of geometric segments that soft-linked towards the climax of fault system evolution. Large fault displacements (~1.6 km) on main block-bounding faults are marked by the development of significant changes in synfault stratal architecture in hangingwall depocentres. In these depocentres, there are wedge-shaped stratal packages that thicken towards faults, stratal horizons that onlap intrabasinal highs, and unconformities. Time-travel thickness maps generated for chosen horizons shows the development of more open continuous hangingwall depocentres in shallow section compared with more isolated depocentres at deeper horizon levels.

CHILDS, C. *ET AL.*, 1994. Fault overlap zones within developing normal fault systems. *Journal of the Geological Society, London*, 152, 535-548.

CHILDS, C., NICOL, A., WALSH, J. J. & WATTERSON, J., 2003. The growth and propagation of synsedimentary faults. *Journal of Structural Geology*, 25, 633-638.

MARCHAL, D. *ET AL.*, 2003. Geometric and morphologic evolution of normal fault planes and traces from 2D-4D data. *Journal of Structural Geology*, 25/1, 135-158.

SOLIVA, R. & BENEDICTO, A., 2004. A linkage criterion for segmented normal faults. *Journal of Structural Geology*, 26/12, 2251-2267.



30. Interaction of tectonic, sedimentary and diapiric processes in the origin of mélanges: examples from the Messinian of NW Italy (Tertiary Piedmont Basin)

Andrea Festa¹ & Francesco Dela Pierre¹

1. Università di Torino, Dipartimento di Scienze della Terra, Italy
Presenting author: andrea.festa@unito.it

Keyword(s): *mélanges, tectonic, sedimentary processes, diapiric processes*

Chaotic deposits or mélanges are a significant component of ancient orogenic belts and of present-day accretionary complexes. Their origin is commonly attributed to tectonic disruption and mixing of originally coherent sequences, gravitational submarine downslope movements and shale diapirism, caused by the rising towards the sea floor of overpressured, fluid-permeated fine grained sediments. Despite valuable criteria having been proposed to discriminate among these mechanisms (e.g. Orange, 1990; Orange and Underwood, 1996; Pini, 1999), the recognition of the role played by each of these processes in the geologic record is problematic, due to the strong facies convergence of their products and to the fact that later deformation and metamorphism often obscure the prevailing forming processes. Moreover, these mechanisms are not mutually exclusive, and can coexist and interact in a complex way. In northwestern Italy, the Messinian succession is made up of chaotic sediments, consisting of a fine-grained unconsolidated matrix enveloping blocks of different size and composition, including gypsum and a wide range of carbonate facies. The study of these sediments, including geologic mapping and integrated stratigraphic, and structural observations, allow to evaluate the relative contribution, the time relationships, and the causative links between tectonic, sedimentary, and diapiric processes in the genesis of chaotic sediments of Messinian age. It appears that these mechanisms, triggered by regional tectonic deformation, impacted on each other and operated sequentially in a short time span (Dela Pierre *et al.*, 2007). Faulting was responsible for the disruption of an originally coherent stratigraphic succession, favored the failure of mechanically weakened sediments and encouraged shale diapirism through the creation of mechanical discontinuities working as conduits for the rising of overpressured sediments. Loading provided by deposition of gravitative chaotic sediments could have contributed (together with the circulation of methane-rich fluids in the sedimentary column) to diapir intrusion, which in turn caused a partial reorganisation of the dismembered sediments produced by the other two processes. Large volumes of Messinian chaotic sediments characterize many sectors of the Mediterranean area. In these sedimentary bodies, the imprint left by gravitational movements can usually be seen. However, it must be taken into account that in the highly mobile geodynamic setting where these deposits formed, slope failure was likely to be the prevailing process, able to completely conceal the traces of both tectonic faulting and shale diapirism: the role played by these latter mechanisms in the genesis of the chaotic sediments (or mélanges) could thus underestimated (Dela Pierre *et al.*, 2007).

DELA PIERRE, F., FESTA, A. & IRACE, A., 2007. Interaction of tectonic, sedimentary, and diapiric processes in the origin of chaotic sediments: An example from the Messinian of Torino Hill (Tertiary Piedmont Basin, northwestern Italy): Geological Society of America Bulletin, v. 119, no 9/10, p. 1107-1119.

ORANGE, D.L., GEDDES, D.S. & MOORE, J.C., 1993. Structural and fluid evolution of a young accretion complex: the Hoh rock assemblage of the western Olympic Peninsula, Washington: Geological Society of America Bulletin, v. 105, p. 1053-1075.

ORANGE, D.L. & UNDERWOOD, M.B., 1995. Patterns of thermal maturity as diagnostic criteria for interpretation

of melanges: *Geology*, v. 23, p.1144-1148.

PINI, G. A., 1999. Tectonosomes and Olistostromes in the Argille Scagliose of the Northern Apennines, Italy: *Geological Society of America, Special Paper 335*, 73 p.

31. Effect of bedrock structures upon formation of glacial megagrooves by Pleistocene ice streams in NW Scotland: implications for structural interpretation of remote sensing images in formerly glaciated terrains

Maarten Krabbendam¹, Tom Bradwell¹ & Stuart Clarke¹

1. British Geological Survey, Edinburgh, U.K.

Presenting author: mkrab@bgs.ac.uk

Keyword(s): glacial, remote sensing, structure

Megagrooves are large-scale erosional bedforms cut straight into bedrock, formed underneath ice sheet. These features occur in large 'fields' over areas several 10 km² developed parallel to former ice flow. They are generally interpreted as the 'footprint' of a palaeo ice stream in which the ice flow velocity was 10 – 100 times greater than that of the surrounding ice. A large field of east-west trending megagrooves has been discovered east of Ullapool in the NW Highlands of Scotland, formed during Pleistocene ice sheet glaciation. Individual grooves are typically 5-15 m deep, 10-30 m wide and 500 – 3000 m long. Spacing of megagrooves is typically 100 – 200 m. Broadly three types occur: parabolic, asymmetric 'bench' shaped and V-shaped; the latter presumably modified by (subglacial) melt water erosion. The megagrooves continue right over the present-day watershed. The bedrock geology of the megagroove field comprises psammites of the Moine Supergroup, in the hangingwall of the Moine Thrust. The Moine psammites in this area have a well-developed, gently southward dipping bedding and strong bedding-parallel foliation, giving a 'flaggy' appearance. In addition there are NNE and ESE trending sets of joints. There is a clear link between the megagroove presence and type of megagroove and the orientation of the intersection between bedding/foliation and the ground surface. On east and west-facing slopes, megagrooves are poorly developed. On gently south-dipping dip-slopes megagrooves are poorly developed, but once initiated are deep (>10 m) parabolic features. On north-facing slopes, asymmetric megagrooves are developed, with gentle dip-slopes and steep steps (typically 2-5 m high). These bedforms are akin to cuestas but only developed where the intersection between bedding/foliation and the ground surface trends east-west, parallel to palaeo ice flow. The joint systems appear to have facilitated 'side-ways' plucking, thus so that glacial erosion enhanced the stepped faces, rather than destroying them. Analysis of satellite and DEM images in Northern Scotland and Northern England has shown that linear erosional features are well developed where the strike of bedrock structure is parallel to rapid palaeo ice flow (eg. Ben Hope – Loch Naver area in Northern Scotland and Tyne Gap in Northern England). In contrast, important bedrock structures such as the Moine Thrust that are oriented at high angles to palaeo ice flow have little expression on remote sensing images. In the depositional régime of an ice sheet, drumlins and other depositional features may develop a strong linear landscape largely independent of bedrock structure, as for instance in eastern Northumberland. Thus, the interpretation of bedrock structure from remote sensing in formerly glaciated terrains must take the character and dynamics of the former ice sheet into account.

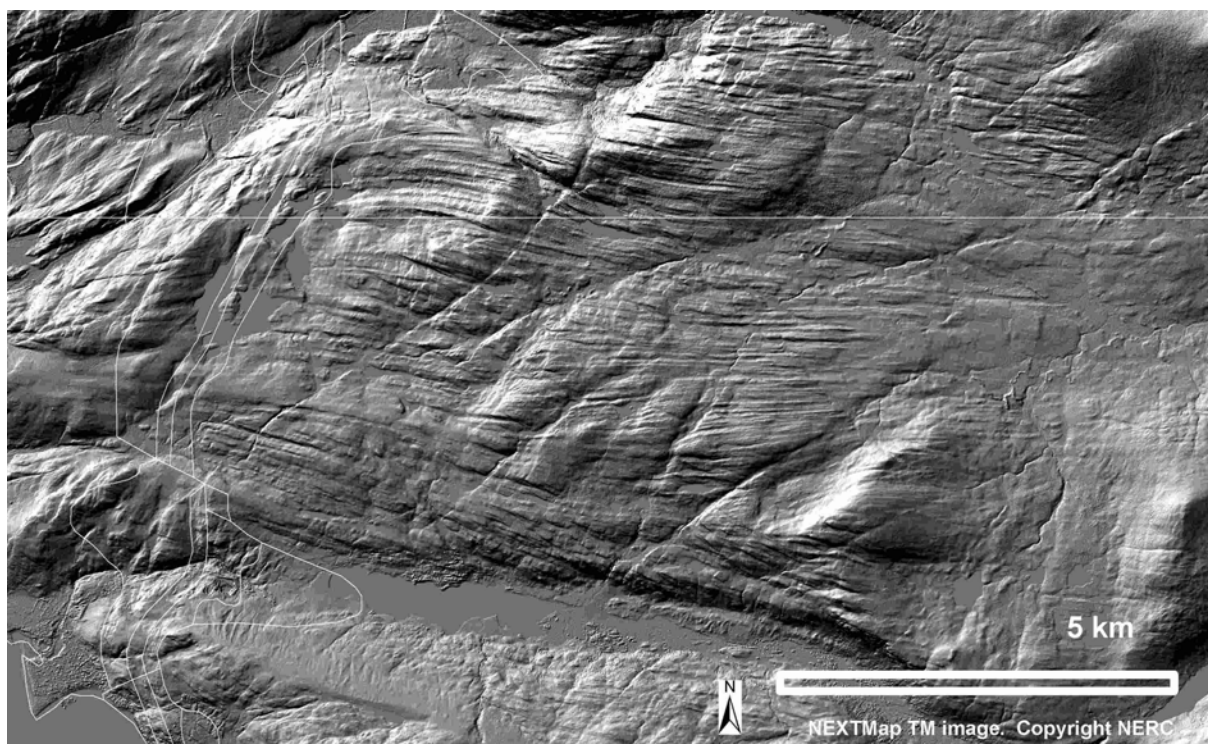


Figure 1. NEXTMap (Intermap Technologies) DEM image of the megagrooves east of Ullapool. Copyright NERC.

32. The analysis and mapping of geological structures using high-resolution Digital Elevation Models

Stuart Clarke¹, Linda Austin², Stuart Egan² & Graham Leslie¹

1. British Geological Survey, Edinburgh, U.K.

2. Keele University, U.K.

Presenting author: smcl@bgs.ac.uk

Keyword(s): structure, remote sensing

Traditionally, geologists have made extensive use of aerial photography, supported by regional-scale Digital Elevations Models (DEMs), for geological analysis and interpretation. This approach has proved extremely useful but has two principle drawbacks. The interpretation of aerial photography is somewhat subjective and is strongly influenced by temporal factors such as vegetation cover and lighting directions at the time of acquisition. Regional DEMs, whilst providing largely objective pictures, are generally of insufficient resolution to allow analysis at large mapping scales, such as the standard 1:10 000-scale used by the British Geological Survey. It is only recently that high-resolution and high-accuracy DEMs have become generally available. One such example is the NEXTMap Britain DEM dataset (Intermap Technologies, 2003), providing a five-metre post spacing with one-metre (%95 RMSE) vertical accuracy for the whole of Great Britain. Numerical processing of these data has provided datasets that are extremely useful in the geological analysis of well-featured landscapes underlain by comparatively simple, gently dipping strata and the analysis of glacially sculptured landscapes, both at scales as large as 1:10 000 (e.g. Clarke *et al.*, 2007) In this work, we extend the application of NEXTMap Britain DEM data to the geological analysis of more structurally complex terranes. We apply recognised processing techniques of hill-shading and slope analysis (1st and 2nd derivative mapping) to extract structural data such as regional dip-azimuths and fault relationships at a range of scales, and develop new processing approaches based on aspect analysis that allow the extraction of structurally related features, and thus the identification of both brittle (faults and fractures) and ductile (folding, fold hinges and axes) deformation structures at 1:10 000-scale. We apply these techniques to the geological analysis and interpretation of varied structural settings from North Wales and northern England to compare this approach with traditional aerial photograph interpretation. In so doing, we are able to demonstrate the extreme usefulness of high-resolution DEMs for the geological survey of these more structurally complex terranes.

CLARKE, S.M., MILLWARD, D. & EVEREST, J., 2007. The use of NEXTMap digital elevation models for geological mapping in well-featured terrains: a case study from Northern England, U.K. *Geomorphology* (under review).

INTERMAP TECHNOLOGIES, 2003. Intermap. Product handbook and quick start guide. Intermap Technologies Inc. Denver Co. U.S.A.

33. Syn-depositional tectonics in a deep-water “mini-basin” setting, Tabernas, SE Spain

Lucie Baudouy¹, Peter Haughton¹ & John J. Walsh²

1. University College Dublin, UCD School of Geological Sciences, Ireland

2. University College Dublin, UCD School of Geological Sciences, Fault Analysis Group, Ireland

Presenting author: lucie.baudouy@ucd.ie

The interplay between tectonics and sedimentation is reasonably well understood in continental and shallow marine basins. However, there are fewer cases where structural controls on deep-marine turbidite deposition and the propagation of faults through wet near sea-bed deposits can be demonstrated. Gravity currents are very sensitive to small gradient changes and hence should be affected by even subtle sea floor deformation. Flows may be re-routed, modified to become more or less erosive, or undergo partial or whole-scale containment in local fault-controlled depressions (‘mini-basins’). On-going deformation may also destabilize and cause previously deposited turbidites to be locally remobilized. Gradient changes may reflect structural tilting, the development of seabed fault scarps, or substrate shale or salt mobility. In this talk, we describe the geology of intrabasinal fault zones and the evolution of a transient fault-controlled mini-basin on the floor of the Tabernas Basin in SE Spain based on new mapping and structural analysis. The well exposed Neogene Tabernas Basin was a relatively small and narrow (~20 km long and ~10 km wide) strike-slip basin which was elongated in an E-W direction, sub-parallel to a bounding strike-slip fault. The fill is dominated by turbidites which are affected by both syn- and post-depositional faults. A number of oblique-slip intrabasinal faults that propagated to the palaeo-sea bed can be identified. These provided local ponded accommodation for gravity currents and influencing current pathways and slope stability. The early basin fill was characterised by extensive east-facing, axial slopes into which slope channels were incised and bypassed sediment. As the intra-basinal faults appeared at the sea bed, they bounded local areas of rapid subsidence that became deeps analogous to mini-basins into which turbidity currents and mass transport complexes were preferentially trapped and ponded. Occasional mass transport complexes and numerous slides attest to the tectonic activity and associated slope instability on the flanks of the mini-basin. They are attributed to collapse of either intrabasinal fault scarps or, in most cases, the oversteepened margins of the sub-basin. Excellent outcrop exposures permit 3D definition of slumped units and reconstruction of part of their internal structure and their geometry. Detailed analysis helps define the impact of tectonics on sedimentation and slope failure, and shows how strike-slip mini-basins are characterised by particularly unstable slopes with episodic whole scale slumping, sliding and failure of the onlap wedges. Analogies can be drawn with structurally-controlled depressions in the Marmara Sea, and the fill style of salt-controlled mini-basins in the Gulf of Mexico.

34. Sediment distribution and architecture around early Alpine intra-basinal structures, Champsaur Basins, SE Ecrins, France

Jamie Vinnels¹, Rob Butler¹, Bill McCaffrey¹, Henry Lickorish², Gillian Apps³ & Frank Peel³

1. University of Leeds, School of Earth and Environment, U.K.

2. Calgary, Alberta, Canada

3. BHP Billiton, Houston, Texas, U.S.A.

Presenting author: jamie@earth.leeds.ac.uk

Keyword(s): Alpine, turbidites

Within the Eocene to Oligocene deposits of the Alpine Foreland Basin are preserved a series of perched, interconnected flysch troughs, whose development was influenced by early uplift of the Alpine foreland. Within these remnants, well-constrained interpretations of sediment architectures have been developed by many workers and used to resolve both intra- and inter-basinal filling histories. These interpretations can be used to constrain aspects of the structural development of the foreland basin into which they were deposited. Presented here is an outcrop case study from the Eastern and Western Champsaur Basins, found today in the Ecrins region of SE France, and separated by the modern Selle Fault. These basins record the deposition of deep-water sediments onto the fringes of the ancestral Pelvoux Massif, itself deformed by local early Alpine related fold and thrust structures. Although earlier work suggests that the Pelvoux Massif had a pronounced positive paleo-topographic expression, this study suggests that the ancestral Pelvoux Massif did not form a significant bathymetric barrier, and that sediment routing pathways passed over and around this area and continued much further around the Alpine foreland. Presented here is a reconstruction of the bathymetric template of the Eastern Champsaur Basin prior to turbidite deposition. Within the subsequent fill, both facies and associated net to gross variations are observed to vary systematically around an intra-basinal high, (the bathymetric expression of an early Alpine structure), which is thought to have partially contained the turbidity current, allowing a relatively finer fraction of the flow to be striped downstream, to the NW. Although the distal preserved remnants of the Eastern Champsaur Basin are truncated by the Selle Fault Zone; the sedimentology of the truncated basin fill suggests that turbidity currents were dispersing over and beyond this structure. Within the easternmost part of the Western Champsaur Basin is a NE-dispersing submarine channel, structurally truncated in its distal persevered section by the Selle Fault. Its form and internal architecture suggest it probably connected to deeper bathymetric levels towards the NE when active, and was therefore likely to have been of greater axial extent than its preserved dimensions. The Selle Fault is interpreted to be the modern expression of a structure that separated the volcanoclastic Western Champsaur Basin and the siliciclastic Eastern Champsaur Basin. Thus both Western and Eastern Champsaur Basins are inferred to have originally connected to deeper bathymetric levels towards the N or NW, suggesting that the ancestral Pelvoux Massif did not form a significant bathymetric barrier. Whether the separate turbidite systems that they represent coalesced downstream at some point remains an open question. This presentation shows that stratigraphic analysis on deformed basin fills at basin scale may help constrain the broader evolution of the Alpine foreland basin.

35. Structural and tectonic basis for some far-reaching new insights on the dynamics of the Earth's mantle

Miles Osmaston¹

1. The White Cottage, Woking, Surrey, U.K.

Presenting author: miles@osmaston.demon.co.uk

Keyword(s): two-layer mantle, cratonic tectospheres, mantle flow tectonics, Black Sea opening, Balkan tectonics, Western Alps, Greenland motions, Caribbean plate motions, atmospheric oxygen, Palaeoproterozoic glaciation

Two of the most controversial questions concerning mantle behaviour are the great depth of cratonic tectospheric keels (e.g. Gu *et al.*, 1998; Agee, 1998) and whether the base of the upper mantle is a substantial barrier to flow (Osmaston, 2003). Individually the arguments for each are indecisive and have hitherto been regarded as the province of seismologists and mantle modellers. But if both are true we can by-pass these arguments because there should be major dynamical consequences for plate motions, susceptible to direct observation (Osmaston, 2006). My recent contention that both are true (Osmaston, 2007) to two successive audiences at IUGG 2007 (seismologists and then - by invitation - to lithosphere specialists) seems to warrant a degree of repetition to a TSG audience much closer to the structural observations. The point is that if the 660 is indeed a barrier to mantle flow and keels extend nearly that far we need to ask: (a) Where does the mantle come from to put beneath a widening ocean? and (b) Where does it go as two cratons approach one another? In an Atlantic-Arctic context we find two examples of (a). First, the widely-evident eastward motions of the Caribbean and Scotia Sea plates appears to record the eastward flow, at depth, of mantle to put beneath the widening S Atlantic. Second, the intra-Eocene Eureka folding from Ellesmere Island to Svalbard, across northern Greenland, is seen (Osmaston, 2006) as due to drag upon Greenland's keel by mantle being drawn to put under the widening Eurasia Basin. Significantly the compression began at the moment Greenland became detached on both sides and ended when the NE Atlantic offered a sufficient gap for the flow. In an Alpine belt setting we have a complex example of (b). My recent studies show that the Western Alps were primarily the result of up to 250km westward motion of northern Adria/Italy in the early Oligocene, using a formerly-straight Insubric-Pusteria-Gailtal fault-Line, before the Giudicaria NE-ward offset differentially compressed the Eastern Alps. This dextral motion is recorded in a shear zone extending all the way to the Black Sea in the Danube delta area, north of the probably Neo-Archaeon Moesian block, long known for its mysterious westward 'indenter' behaviour. Westward flow of mantle from between the converging Arabian and Russian tectospheres in the Caucasus has evidently driven this motion by impinging upon the cratonic keel of Moesia, opening the western Black Sea, and it may explain the present deep seismicity below the SE Carpathians (Vrancea). This westward motion of Moesia and ultimately of the entire Balkan Peninsula appears first (mid-K) to have built the N-S volcanic and granitic arc on the W side of Moesia, progressing westward to the Dinarides and finally to the Western Alps and Apennines. Thus the dominantly N-S closure of Africa and Eurasia now yields a mechanism for the broadly concurrent E-W components of compression in the Alpine belt. If the Earth now has a 2-layer mantle, when and how did it change from the whole-mantle convective pattern surely driven by the high heat generation in the early Earth? The answer is highly significant for us all. The interval 2.49-2.2Ga marks the convective hiatus during the changeover. MOR collapse and sea-level fall led to lower atmospheric CO₂, glaciations during 2.45-2.3Ga and the Great Oxygenation Event at ~2.3Ga when oxygenic life

had finally won its battle against the reducing chemical action of MORs. In this sense, therefore, we all are the living proof of that changeover.

AGEE, C. B., 1998. Phase transformations and seismic structure in the upper mantle and transition zone. In *Ultrahigh pressure mineralogy: physics and chemistry of the Earth's deep interior*, (ed. R. J. Hemley), *Reviews in Mineralogy*. 37, 165-203.

GU, Y., DZIEWONSKI, A. M. & AGEE, C. B., 1998. Global de-correlation of the topography of transition zone discontinuities. *Earth Planet. Sci. Lett.* 157, 57-67.

OSMASTON, M. F., 2003. What drives plate tectonics? Slab pull, ridge push or geomagnetic torque from the CMB? A new look at the old players vis-a-vis an exciting new one. XXIII IUGG 2003, Sapporo, Japan. Abstracts CD, p. B129, Abstr #016795-2.

OSMASTON, M. F., 2006. Global tectonic actions emanating from Arctic opening in the circumstances of a two-layer mantle and a thick-plate paradigm involving deep cratonic tectospheres: the Eureka (Eocene) compressive motion of Greenland and other examples. In *ICAM IV, Proc. Fourth International Conference on Arctic Margins, 2003* (ed. R. Scott & D. Thurston). Dartmouth, NS, Canada: OCS Study MMS 2006-003, pp.105-124: Also published on: <<http://www.mms.gov/alaska/icam>>

OSMASTON, M. F., 2007. Cratonic keels and a two-layer mantle tested: mantle expulsion during Arabia-Russia closure linked to westward enlargement of the Black Sea, formation of the Western Alps and subduction of the Tyrrhenian (not the Ionian) Sea (abstr). In XXIV IUGG 2007, Perugia, Italy, July 2007. Session JSS 011 Earth Structure and Geodynamics. (See also <http://osmaston.nmpc.co.uk>).

36. Displacement-length scaling relations of normal faults and paleoearthquakes in the active Taupo Rift, New Zealand

John J. Walsh¹

1. University College Dublin, School of Geological Sciences, Fault Analysis Group, Ireland
Presenting author: john@fag.ucd.ie

Keyword(s): fault growth, earthquake

The relation between maximum displacement and length provides important information about the scaling properties of faults and earthquakes. Displacement-length plots typically reveal slopes of 1-1.5 for ancient fault systems and 1 for historical earthquakes. Active normal faults in the Taupo rift, however, provide slopes of 0.5-0.7 for paleoearthquakes and faulted volcanic surfaces ranging up to ca. 60 ka in age, with slopes of 1 or greater on older surfaces. The low slopes are attributed to two principal factors: increased variability of displacement rates on short-time scales and sampling bias. Fault interaction and displacement transfer in the rift locally enhances or diminishes the growth of individual faults, a complexity in behaviour which introduces an increase in the scatter of displacement-length relationships derived from progressively younger horizons, representing shorter time scales (horizons range from 2,000 to 300,000 years in age). The bulk of our data are from a digital elevation model of displaced geomorphic surfaces with a vertical resolution of ~2 m, which leads to an under-sampling of small faults and a reduction in lengths of at least 100-200 m on younger mapped surfaces. Both of these sampling artefacts introduce a systematic under-sampling of low displacement-length faults particularly for those faults with lengths of <1 km, and therefore lead to a decrease in the slope of the displacement-length relation. In this talk we investigate the extent to which earthquake faulting is capable of reproducing the increased scatter on displacement-length plots for data representing progressively shorter time scales. Using a stochastic model in which earthquake populations ranging from power-law (i.e. Gutenberg-Richter) to nearly characteristic (i.e. same-sized) are placed over a fault surface, we show that, contrary to general opinion, it is not possible to define earthquake scaling from conventional trench data (i.e. kinematic constraints from trenches across active faults). Our model contrasts with classic slip-dependent or time-dependent earthquake models, which are underpinned by assumptions of how slip accumulates at each point on a fault surface, and instead examines the accumulation of slip over the entire fault surface. Despite its simplicity, we show that it is capable of reproducing the variability in displacement-length relationships on different scales, and therefore of providing a rationale for the unpredictable nature of earthquake accumulation. This model combined with sampling biases is capable of explaining the derived relationships between displacement and length.

37. Active tectonics in northern France

Koen Verbeeck¹, Jean-Pierre Colbeaux², Sara Vandycke³, Françoise Bergerat⁴, Kris Vanneste¹, Christophe Tesnière², Michel Sébrier⁴, Toon Petermans¹ & Thierry Camelbeeck¹

1. Royal Observatory of Belgium, Brussels, Belgium

2. Parc Naturel Régional Scarpe-Escaut, Saint-Amand-Les-Eaux, France

3. Faculté Polytechnique de Mons, Belgium

4. Laboratoire de Tectonique - UMR 7072 CNRS-UPMC, Paris, France

Presenting author: koen.verbeeck@oma.be

Keyword(s): active fault, historical earthquake, northern France

One of the most severe earthquakes that affected northwestern Europe during historical times occurred in the Strait of Dover on April 6, 1580 (Melville *et al.*, 1996). This event, with an estimated magnitude around 6.0, shook a large area of northwest Europe including parts of France, England, Belgium, the Netherlands, and Germany. The most affected regions were Flanders, Kent, Artois and in particular the city of Calais. Another destructive earthquake occurred in the North of France on September 2, 1896 (M=5.0). It was felt over a smaller area (Lancaster, 1896). The farthest city where it was felt, near Jodoigne in Belgium, is around 170 km from the epicentral region. The earthquake caused damages interpreted as intensity VII (MSK-scale) in its epicentral area, between the cities of Lens and Arras. The region where these two events occurred separates the Flemish plain to the north and the chalky Boulonnais-Artois plateau to the south. This corresponds to a NW-SE-striking North-facing escarpment that is underlined by hill alignments from Boulogne to Cambrai. As in the Weald, Wessex, and southern North Sea basins, the Artois alignments correspond to small, fault-related anticlines resulting from the early Tertiary tectonic inversion, during which faults slipped in a reverse sense to that during the Mesozoic. Gravity data suggest that the faults have lengths ranging from 15 to 40 km and are arranged en-echelon in longer fault zones (Everaerts et Mansy, 2001). They have slightly different orientations in the Boulonnais (WNW-ESE) and in the Artois (NW-SE). The faults have influenced the river development, independently of lithological contacts, suggesting possible Quaternary tectonic activity. Quaternary activity of the Marqueffles fault has been invoked at the archeological site of Biache-Saint-Vaast (Colbeaux *et al.*, 1981). There, fluvial deposits and the overlying loess are affected by a small dextral horizontal displacement that occurred along WNW-ESE and NNE-SSW faults. We undertook specific geomorphological, geological and geophysical investigations to identify evidence of active tectonics in this bordering region between the Flemish plain and the Artois hills.

COLBEAUX, J.-P., SOMME, J. & TUFFREAU, A., 1981. Tectonique quaternaire dans le Nord de la France: L'apport du gisement paléolithique de Biache-Saint-Vaast: Bulletin de l'Association française pour l'étude du Quaternaire, v. 3, p. 183-192.

EVERAERTS, M. & MANSY, J.-L., 2001. Le filtrage des anomalies gravimétriques; une clé pour la compréhension des structures tectoniques du Boulonnais et de l'Artois (France): Bulletin de la Société Géologique de France, v. 172, p. 267-274.

LANCASTER, M.A., 1896. Le tremblement de terre du 2 septembre 1896: Ciel et Terre, v. 14.

MELVILLE, C., LEVRET, A., ALEXANDRE, P., LAMBERT, J. & VOGT, J., 1996. Historical seismicity of the Strait of Dover-Pas de Calais: Terra Nova, v. 8, p. 626-647.

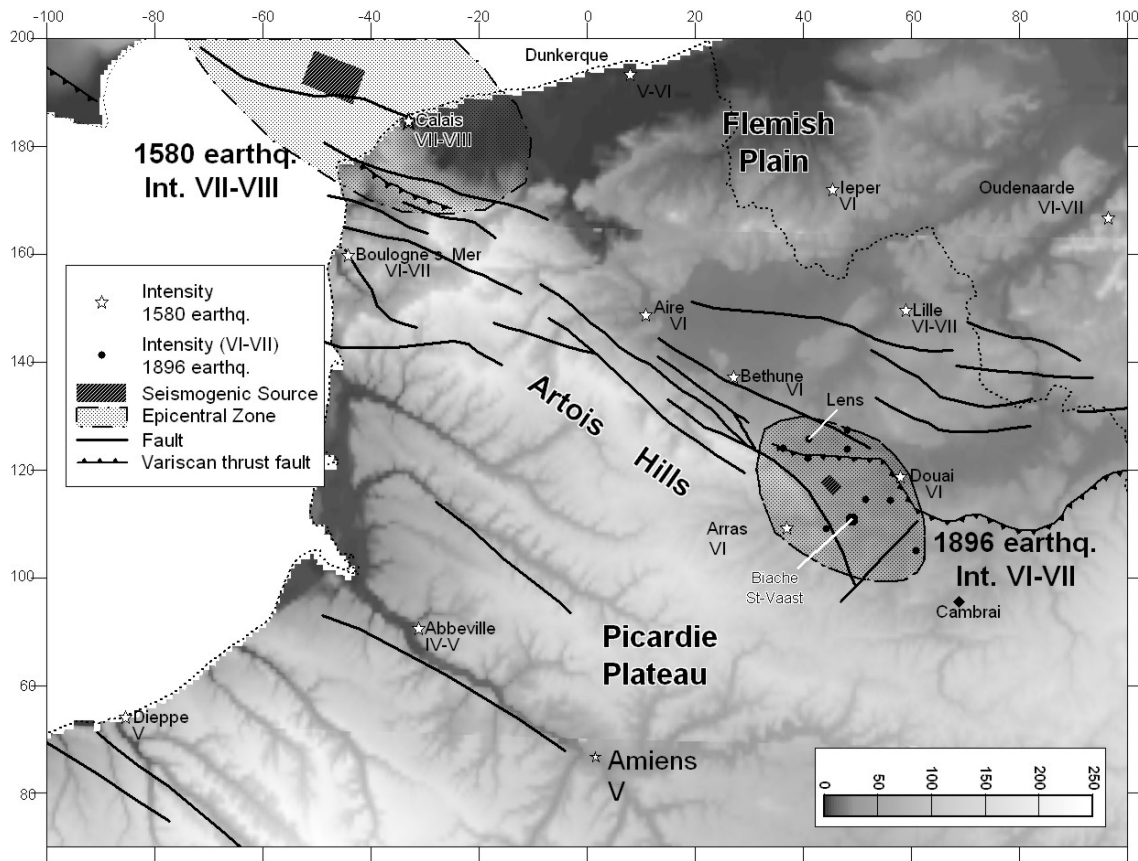


Figure 1. DEM map of the investigated region with the major faults and the source zones and some maroseismic information of the 1580 and 1896 earthquakes (projection: Belgian Lambert 72 and coordinates in km).

38. New paleoseismic evidence for prehistoric surface rupturing in the intraplate Lower Rhine graben area

Kris Vanneste¹, Koen Verbeeck¹, Florias Mees² & Dimitri Vandenberghe³

1. Royal Observatory of Belgium, Brussels, Belgium

2. Royal Museum for Central Africa, Department of Geology and Mineralogy, Tervuren, Belgium

3. Ghent University, Geological Institute, Laboratory of Mineralogy and Petrology, Belgium

Presenting author: kris.vanneste@oma.be

Keyword(s): paleoseismology, Geleen fault, prehistoric earthquake

We studied two paleoseismic trenches on the central section of the Geleen fault, a branch of the southwestern border fault zone of the Roer Valley graben. As the fault is characterized by low slip rates (ca 0.03 mm/yr), the geomorphic expression of its central part, traversing Late Glacial and Holocene sediments in the Belgian Maas River valley, is subdued compared to the northwestern and southeastern sections, which intersect older Quaternary deposits. Only in a few places a subtle fault scarp, less than 1 m high, can be recognized. The surface trace of the fault was mapped using electric tomography and GPR, and shows a distinct bend associated with a stepover, but it is not clear if this represents a segment boundary. The trenches provide convincing arguments for two surface-rupturing earthquakes. In the first trench, the most recent paleoearthquake has resulted in 1 m vertical displacement of a Late Glacial fluvial terrace and overlying eolian deposits. We identified a discontinuity truncating fault splays, which, on one wall, coincides with a prehistoric, man-made stone pavement. In the second trench, we attribute a displaced soil profile, buried below structureless sediment in the downthrown block, to the same event. Macroscopic identification of the event horizon is not straightforward because most stratification is obliterated down to 1 m depth, but thin-section analysis confirmed the presence of an in situ soil below, and of colluvial sediment above. In both trenches this event is associated with liquefaction, including a series of sand blows and a gravel dike. These features are unambiguous evidence for strong co-seismic shaking. OSL and radiocarbon dating in the second trench constrain the event between 2.5 ± 0.3 and 3.1 ± 0.3 kyr, and between 2790 ± 20 and 3770 ± 50 calibrated years before AD 2005, respectively. We also found evidence that it occurred at a time when the area was being cultivated. In the second trench, we observed additional 0.4 m offset for fluvio-eolian sands below an erosional gravel pavement correlating with a regional deflation horizon. This gravel pavement also truncates several soft-sediment deformations, and is interpreted as the event horizon. The associated colluvial wedge was most likely eroded, however. OSL dating constrains the age of this event between 15.9 ± 1.1 and 18.2 ± 1.3 kyr. This penultimate event is not recorded in the first trench, where the oldest deposits have been IRSL-dated at 12.9 ± 3.8 kyr. The ages obtained for the two paleoearthquakes are in good agreement with those obtained in earlier trenches further north, suggesting that the Geleen fault defines a single, 30-km-long segment.

39. A multidisciplinary approach to paleoseismic behaviour of the Conclud fault (Iberian Chain, Spain)

Paloma Lafuente¹, José Luis Simón¹, Luis Eduardo Arlegui¹, Carlos Luis Liesa¹ & Miguel Ángel Rodríguez-Pascua²

1. Universidad de Zaragoza, Dep. Geodinámica, Spain

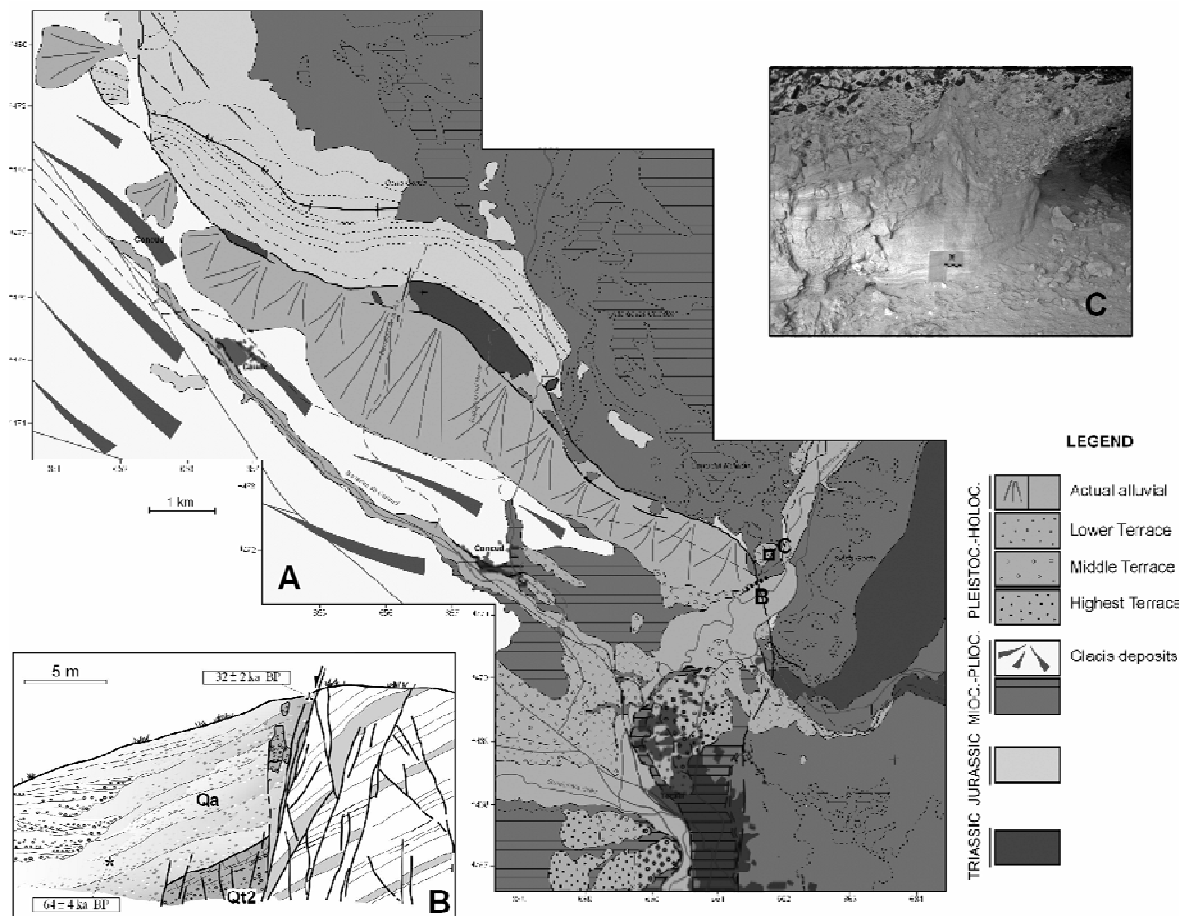
2. Universidad San Pablo, Dep. Ciencias Ambientales y Recursos Naturales, Madrid, Spain

Presenting author: palomalt@unizar.es

Keyword(s): normal fault, Conclud fault, paleoseismology, active tectonics

The Conclud fault constitutes the northeastern boundary of the southern sector of the Jiloca graben (Iberian Chain, Teruel, Spain), and has been active during most of the Late Pliocene and Quaternary, under a still acting multidirectional extension field (sigma1 vertical, sigma2 \approx sigma3; Simón, 1989; Cortés, 1997; Arlegui *et al.*, 2004), with sigma3 trending ENE. It is a practically pure normal fault, with an overall NW-SE strike, veering to N-S in its southeastern end (where it articulates with the Teruel fault). We present here the characterization of the fault's activity, using structural, paleoseismological and morphotectonic methods. From the displacements measured in some dated stratigraphic levels, slip rates corresponding to different periods have been calculated: 0.07 mm/year since Late Ruscinian (3.6 Ma, displacement of 255 m); 0.23-0.33 mm/year since Middle Pleistocene ($116 \pm 10 - 169 \pm 4$ ka, displacement of 39 m); 0.23 mm/year during a lapse within Late Pleistocene (32 ± 6 ka, displacement of 7.5 m). An outcrop close to Teruel city shows deposits of a very recent fluvial terrace displaced 2 m by a normal fault, probably a secondary branch of the Conclud fault, that could represent its latest movement, around 15 ka ago (Simón *et al.*, 2005). Considering the fault length (at least 13.5 km), its non-segmented character, and using empirical correlations proposed by different authors (Wells & Coppersmith, 1994; Stirling *et al.*, 2002; Pavlides & Caputo, 2004), its potential moment magnitude (6.37 to 6.78) and associated coseismic displacement (between 0.35 and 2.02) have been calculated. Using coseismic displacements and slip rates, recurrence periods between 1.1 and 28.9 ka are inferred. The results obtained from the correlation proposed by Stirling *et al.* (2002) differ from those of Wells & Coppersmith (1994) and Pavlides & Caputo (2004) equations, both of them being more conservative. However, if the displacement measured in the lower terrace (2 m) does actually represent the latest movement of the fault 15 ka ago, the results obtained from Stirling *et al.* (2002) correlation (2.02 m of coseismic displacement and recurrence periods of 6.3 to 28.9 ka) are more consistent. This could be confirmed or rejected after a more exhaustive paleoseismic study of the fault. Some liquefaction structures interpreted as seismites have been found in sand levels of the middle fluvial terrace adjacent to the fault. That confirms the occurrence of earthquakes with $M \geq 5-5.5$ during Pleistocene times, one of those around 90 ka BP. Earthquakes with moment magnitudes as calculated by means of empirical methods (between 6.37 and 6.78) are capable to generate this structures. Also geomorphic analysis of the fault indicates that it is active. Two geomorphic indexes have been calculated: mountain-front sinuosity and stream-gradient index. These, together with other geomorphological evidences such as conserved facets, allow us to classify fault's activity: between classes 2 (rapid) and 3 (slow) according to McCalpin (1996), and active to moderate according to Silva *et al.* (2003). Both classifications establish slip rates for each activity class. In this case, slip rates ranging from 0.05 to 0.5 mm/year (McCalpin, 1996) or higher than 0.03 mm/year (Silva *et al.*, 2003) would correspond to our fault. This result fits well with data obtained from structural methods. In summary, all the results obtained through different

approaches indicate that the Conclud fault should be considered as an active fault.



- ARLEGUI, L.E., SIMÓN, J.L., LISLE, R.J. & ORIFE, T., 2004. El campo de esfuerzos extensional plioceno-cuaternario en el entorno de la falla de Conclud (fosa del Jiloca, Teruel). *Geotemas*, 6(3), 131-134.
- CORTES, A.L., 1999. Evolución tectónica reciente de la Cordillera Ibérica, Cuenca del Ebro y Pirineo centro-occidental. Tesis doctoral, Universidad de Zaragoza, 409p.
- MCCALPIN, J.P., 1996. *Paleoseismology*. Academic Press, 588 p.
- PAVLIDES, S. & CAPUTO, R., 2004. Magnitude versus faults' surface parameters: quantitative relationships from the Aegean Region. *Tectonophysics*, 380, 159-188.
- SILVA, P.G., GOY, J.L., ZAZO, C. & BARDAJÍ, T., 2003. Fault-generated mountain fronts in southeast Spain: geomorphologic assessment of tectonic and seismic activity. *Geomorphology*, 50, 203-225.
- SIMÓN, J.L., 1989. Late Cenozoic stress field and fracturing in the Iberian Chain and Ebro Basin (Spain). *Journal of Structural Geology*, 11 (3), 285-294.
- SIMÓN, J.L., LAFUENTE, P., ARLEGUI, L.E., LIESA, C.L. & SORIANO, M.A., 2005. Caracterización paleosísmica preliminar de la falla de Conclud (fosa del Jiloca, Teruel). *Geogaceta*, 38, 63-66.
- STIRLING, M., RHOADES, D. & BERRYMAN, K., 2002. Comparison of Earthquake Scaling Relations Derived from Data of the Instrumental and Preinstrumental Era. *Bulletin of the Seismological Society of America*, 92 (2), 812-830.
- WELLS, D.L. & COPPERSMITH, K.J., 1994. New Empirical Relationships among Magnitude, Rupture Length, Rupture Width, Rupture Area, and Surface Displacement. *Bulletin of the Seismological Society of America*, 84, 4, 974-1002.

40. Geological and archaeoseismological evidence of neotectonic activity in the Fethiye-Burdur Fault Zone (Eşen Basin, SW Turkey)

Baris Yerli¹, Johan H. ten Veen¹ & Manuel Sintubin²

1. Ruhr University, Institute for Geology, Mineralogy and Geophysics, Bochum, Germany

2. K.U.Leuven, Geodynamics & Geofluids Research Group, Belgium

Presenting author: baris.yerli@rub.de

Keyword(s): *neotectonic, archaeoseismology, Fethiye-Burdur fault zone, southwest Turkey, earthquake*

The Fethiye-Burdur Fault Zone (FBFZ) in southwestern Turkey forms an important, but only moderately well studied lineament connecting three tectonic provinces. Each of these are characterised by different processes associated with the incipient and imminent collision of tectonic plates in the Eastern Mediterranean. The FBFZ is regarded as a single tectonic element, based on the linear arrangement of individual faults, some of which showed recent seismic activity. Despite this almost unquestioned notion, there are a number of uncertainties that regard the origin and orientation of fault segments, the fault kinematics and the age of activity of individual segments. Within the FBFZ, the Eşen Basin formed as a ca. 15 km wide and 30 km long, N-S trending graben. Our study of this basin builds on information from the geological, historical and recent time scales and as such aims at reconstructing the full basin evolution. A structural analysis in combination with tectonosedimentary information infers that during the Late Miocene - Pliocene, E-W extension caused the development of N-S normal faults along which basin-margin alluvial fans were deposited in a lake environment. In the Pleistocene the faulted basin margin became segmented by a system of NE-SW trending normal faults. Subsequently, the Mio-Pliocene fault-block tilted basin fill was unconformably overlain by Pleistocene alluvial fan deposits that were sourced from broad NE-SW fault-related valleys transecting the original basin margin. The nowadays terraced Pleistocene conglomerates are segmented and back-tilted through continuous activity of these NE-SW faults in younger Quaternary times. Historic activity of these faults is inferred from earthquake-induced damage to the Lycian (Hellenistic- Roman) city of Pinara. We used LIDAR (Light Detection and Ranging) to produce a 3D model of the Roman theatre. This quantitative datasets allows us to demonstrate a significant tilt of the theatre's seating rows toward the basin margin fault, attesting to historic fault activity. We further present the first results of a Georadar (GPR) profiling campaign that aimed at the recognition of active faults in present-day lowland areas. The preliminary data show that many of the NW-SE trending faults cut the uppermost Holocene deposits and transect the overall N-S trending basin. The integration and combination of various geological and geophysical techniques allowed us to obtain important information on the timing and magnitude of faulting in the Eşen Basin. Furthermore, our data importantly helps to acknowledge the, until now underestimated, seismic risk in the area.

41. Is present-day coastal recession of the eastern English Channel guided by the tectonic state of stress of NW Europe?

Anne Duperret¹, Sara Vandycke², Albert Genter³ & Rory N. Mortimore⁴

1. Université du Havre, Laboratoire de Mécanique, Physique et Géosciences, France

2. Faculté Polytechnique de Mons, Géologie fondamentale et appliquée, Belgium

3. BRGM (French Geological Survey), Orléans, France

4. University of Brighton, Applied Geology Research Unit, U.K.

Presenting author: anne.duperret@univ-lehavre.fr

Keyword(s): chalk cliffs, collapses, paleostress, English Channel

Recession of chalk cliffs along the eastern English Channel varies between 0.2 m/year in NW France and 0.35 m/year in South England for the last 30-125 years respectively (Costa *et al.*, 2004; Dornbusch *et al.*, 2006). As Cretaceous chalk rocks provide excellent records of brittle tectonics and consequently to reconstructing the stress history during the mesozoic period, a paleo-stress analysis of Normandie-Picardie meso-scale faults has been performed and completed with paleostress studies realised in East Sussex (Vandycke, 2002) in order to establish the various phases and chronology of tectonic stresses in eastern English Channel since upper Cretaceous. A comparison between the cliff collapse occurrences, pre-existing fractures and the corresponding state of stress allows deciphering the type of faults and thus the corresponding state of stress currently submitted to reactivation in collapse triggering. The paleostress analysis realised on late Cretaceous chinks of Normandie-Picardie and East Sussex has evidenced various successive states of stress. In France, three extensional events are outlined: WNW-ESE extension, N-S extension and NE-SW extension. The WNW-ESE extension phase is only revealed on Turonian-Coniacian chinks and thus assumed to be the older one. The N-S and NE-SW extension phases are younger as revealed on Turonian to Campanian chinks. Normal faults, joints and master-joints associated to the NE-SW extension phase represent the most common brittle tectonics of Normandie-Picardie coastal chinks. In UK, the paleostress field evolution recorded in the late Cretaceous chinks of East Sussex (UK) has evidenced extensional and strike-slip events, with the following sequence of paleo-stress: (1) NE-SW extension, (2) N-S compression, (3) E-W extension and (4) NE-SW extension (Vandycke, 2002). Some correlations have been established between scar collapses and fault occurrence at 13 locations in France and 3 locations in UK. Scar collapses may present fractures or not. On a basis of 20 observed scar collapses in Normandie, 16 of them are laterally limited and/or contain fractures and 4 of them are not linked to fracture. Most of the faults reported within the scar collapses belong to the NE-SW extension phase. In UK, the analysis has been conducted on 6 scars observed at 3 locations: a wedge failure and two vertical collapses have occurred on strike-slip faults linked to the N-S compression phase and E-W extension in Campanian chinks (at Newhaven and Peacehaven), whereas joints linked to the last NE-SW extension phase have guided three vertical collapses in Santonian chinks (at Birling Gap). This coastal section presents also the highest erosion rate of the East Sussex coast with a mean retreat of 60 to 80 cm/year (Dornbusch *et al.*, 2006), which reinforces the idea that jointing may be a preponderant fracture type when involved in collapse processes. The N-S compressional event observed in East-Sussex, that appears also in the Isle of Wight (UK), is associated to folding and due to the Oligocene structural inversion along E-W trending structures of the Wessex basin located in southern England (Vandycke, 2002). Brittle structures associated to this state of stress guide some recent cliff collapses in East Sussex. In

Normandie-Picardie coastline, no brittle structures linked to a N-S compressional event have been reported at meso-scale, except the Bray fault inversion during late Cretaceous (Wyns, 1980), and consequently there is no collapses guided by this state of stress. Most of the collapses linked to brittle tectonics are apparently geometrically guided by the younger state of stress recorded in the chalk of NW France: the NE-SW extension phase. Coastal cliff collapses and the subsequent coastal recession of the eastern English Channel are mainly guided by the brittle tectonics originated from the present-day state of stress of NW Europe (NE-SW phase) in NW France. In East Sussex, this actual state of stress is concealed by the preponderant influence of the older N-S compression event linked to the Tertiary inversion system.

COSTA, S., DELAHAYE, D., FREIRÉ-DIAZ, S., DI NOCERA, L., DAVIDSON, R. & PLESSIS E., 2004. Quantification of Normandy and Picardy chalk cliff retreat by photogrammetric analysis, in: Mortimore R.N. and Duperret A. (eds), Coastal chalk Cliff Instability. Geological Society, London, Engineering Geology Special Publications, 20, 139-148.

DORNBUSCH, U., ROBINSON, D.A., MOSES, C., RENDEL, W. & COSTA, S., 2006. Retreat of chalk cliffs in the eastern English Channel during the last century, *Journal of Maps*, 71-78.

VANDYCKE, S., 2002. Paleostress records in Cretaceous formations in NW Europe: extensional and strike-slip events in relationships with Cretaceous-Tertiary inversion tectonics, *Tectonophysics*, 119-136.

WYNS, R., 1980. Apports de la microtectonique à l'étude de l'anticlinal du pays de Bray: proposition d'un mécanisme de pli en compression avec décrochements associés, *Bulletin de la Société Géologique de France*, 7, t. XXII, n04, 681-684.

42. Paleostress based on seismic data – examples from the NW Groningen and Dutch offshore gas fields

Heijn van Gent¹, Stefan Back², Janos L. Urai¹, Peter A. Kukla² & Klaus Reicherter³

1. RWTH Aachen University, Structural Geology, Tectonics and Geomechanics, Germany

2. RWTH Aachen University, Geological Institute, Germany

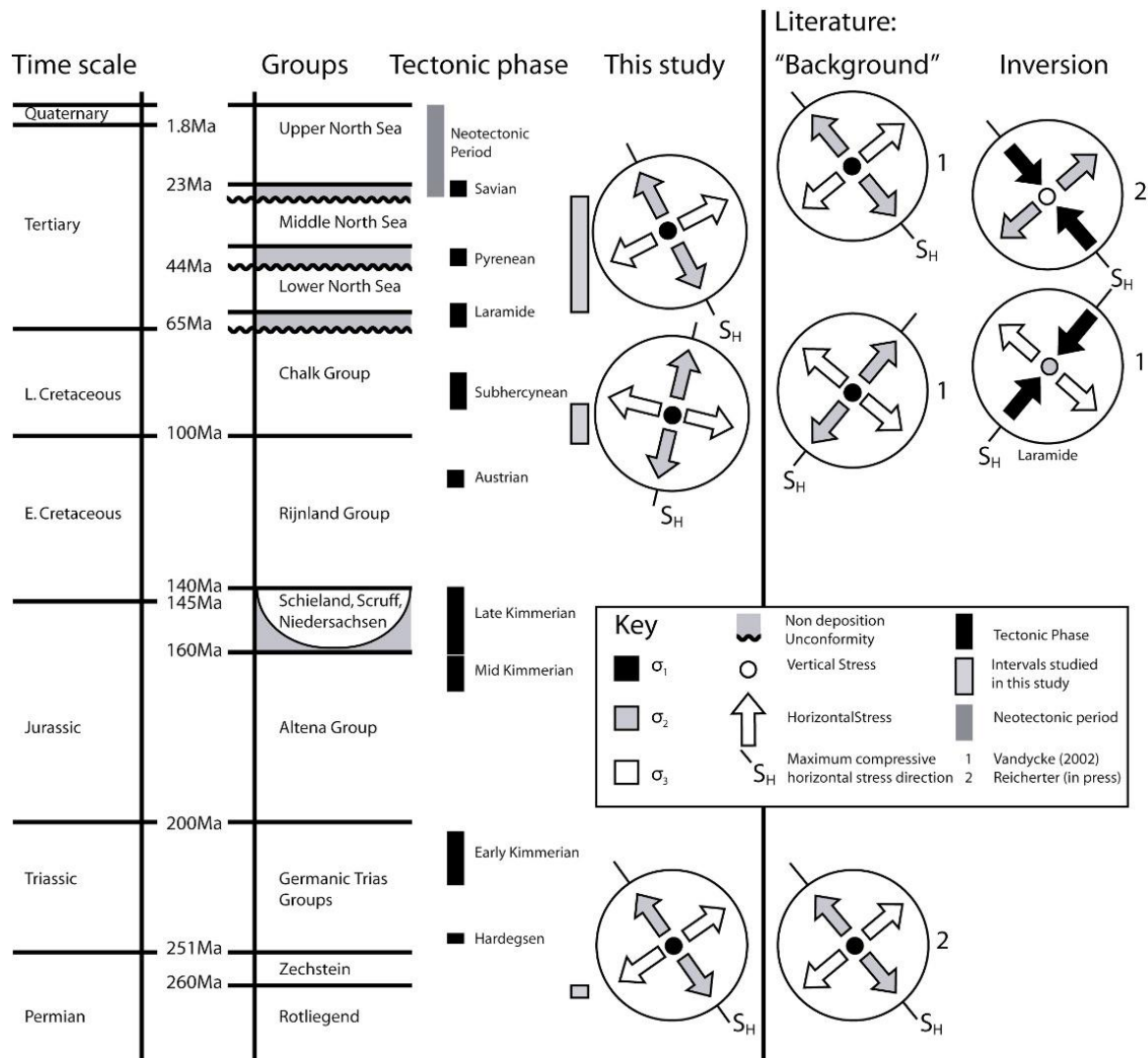
3. RWTH Aachen University, Neotectonics and Natural Hazards, Germany

Presenting author: h.vangent@ged.rwth-aachen.de

Keyword(s): paleostress, 3D reflection seismic data

Knowledge of the paleostress state is essential to understand the tectonic evolution of the crust (e.g. Gruenthal and Stromeyer, 1994), and for the oil industry knowledge of paleostress field could explain patterns of fault leakage, reservoir diagenesis and hydrocarbon migration (DuRouchet, 1981; Gartrell and Lisk, 2005). The “traditional”, field based paleostress methods (e.g. Bergerat, 1987; Vandycke, 2002; Caiazza *et al.*, 2006) cannot be performed in many active sedimentary basins, because direct fault observations are not possible. We present a workflow based on the reconstruction of interpreted 3D seismic datasets. The workflow entails three steps, (1) a high resolution seismic interpretation of the 800 km² study area is done, concentrating on horizons and major faults, (2) using 3D reconstruction software the direction of slip on the main faults is determined for different time periods, which is then used (3) to estimate the paleostress tensor, using the kinematic NDA method (Sperner *et al.*, 1993). A similar workflow is discussed by Gartrell and Lisk (2005) for the Miocene deformation in the Timor Sea (N Australia) but here a structurally more complex setting is studied and a paleostress stratigraphy is estimated spanning roughly 250 Myr. Results are presented for the NW corner of the Groningen field, the Netherlands, as well as first results from an offshore shallow field in the North Sea, and statistical analyses of the results. For the Groningen field, paleostress data is secured for three tectono-stratigraphic groups: the Tertiary North Sea Group, the Upper Cretaceous Chalk Group, and the Upper Permian Rotliegend Horizon. The tectonic phases are separated by horizons that were flat after reconstruction, indicating a period of tectonic quiescence. The calculated paleostress tensors for these intervals fit well with published data (see figure and e.g. Vandycke, 2002 and Bergerat, 1987 and refs. therein). As the North Sea Group deformation falls within the Neotectonic period, we compare our results with the present stress field from the World Stress Map (Reinecker *et al.*, 2005). The maximum compressive horizontal stress of our study fits well with the general trend in NW Europe. Data from the offshore gas field is integrated with the Groningen results. The results of Gartrell and Lisk (2005) and the present study show that there is clear potential for the use of seismic data for paleostress analyses, but major issues that require further attention include the scale of the analyses, the assumption of stress field homogeneity, the extraction of reliable movement directions from seismics, and the basic assumptions of stress analysis techniques. Field based studies can be considered field scale, while seismic methods cover larger areas. The scale and homogeneity issues are addressed with a bootstrapping analysis of the data, which shows that the stress might be calculated for sub-areas of 200km² of the same data set, but the splitting of the area results in a reduction of the used number of faults. The slip direction estimation is not entirely unambiguous, so an additional study is performed where near sub-seismic faults are studied in the Chalk of the Groningen field. Based on the geometry, size and distribution, we assume these to be pure dip-slip faults. The paleostress result from this dataset gives the same stress orientation and stress ratio as the

major faults, but are of better quality, with a better misfit histogram. Furthermore, we used a statistical Monte Carlo analysis to estimate the effects of artificial measurement errors introduction in the slip direction on the paleostress calculations. We introduced random errors using three different normal distributions in three different datasets, repeating the process 50 times. We find that different methods react differently on the introduction of errors. The spread of the results increases with increasing standard deviation and in some cases different results are produced, but generally the results can be considered as robust.



BECKER, A., 1993. An attempt to define a "neotectonic period" for central and northern Europe. *Geol. Rund.* 82, 67-83.

BERGERAT, F., 1987. Stress Fields in the European platform at the time of Africa-Eurasia collision. *Tectonics* 6, 99-132.

CAIAZZO, C., ASCIONE, A. & CINQUE, A., 2006. Late Tertiary-Quaternary tectonics of the Southern Apennines (Italy): New evidences from the Tyrrhenian slope. *Tectonophysics* 421, 23-51.

DU ROUCHET, J., 1981. Stress Fields, A key to Oil Migration. *AAPG Bull.* 65, 74-85.

GARTRELL, A.P. & LISK, M., 2005. Potential New Method for Paleostress estimation by Combining Three-dimensional Fault Restoration and Fault Slip Inversion Techniques: First Test on the Skua Field, Timor Sea. In: Boulton, P. & Kaldi, J. (Eds.), *Evaluating fault and cap rock seals. AAPG Hedberg Series 2*, 23-26.

GRUENTHAL, G. & STROMEYER, D., 1994. The recent crustal stress field in Central Europe sensu lato and its quantitative modelling. *Geologie en Mijnbouw* 73, 173-180.

REICHERTER, K., FROITZHEIM, N., REINECKER, J., JAROSINSKI, M., POPRAWA, P., ZUCHIEWICZ, W., BADURA, J., STACKEBRANDT, W., HANSEN, M. B. & HÜBSCHER, C. (in press). Alpine tectonics II - Central Europe north of the Alps. In: McCann, T. (Ed.), *Geology of Central Europe. Special Publication Geological Society of London*,

London.

REINECKER, J., HEIDBACH, O., TINGAY, M., SPERNER, B. & MÜLLER, B., 2005. The release 2005 of the World Stress Map (www.world-stress-map.org).

SPERNER, B., RATSCHBACHER, L. & OTT, R., 1993. Fault-striae analysis: a Turbo pascal program for graphical presentation and reduced stress tensor calculation. *Computers & Geosciences* 19, 1361-1388.

VAN ADRICHEM-BOOGAERT, H.A. & KOUWE, W. F. P., 1993-1997. Stratigraphic Nomenclature of the Netherlands; revision and update by RGD and NOGEPa. TNO-NITG, Med. Rijks Geol. Dienst, Haarlem, 50, pp. 50.

VANDYCKE, S., 2002. Paleostress records in Cretaceous formations in NW Europe: extensional and strike-slip events in relationships with Cretaceous-Tertiary inversion tectonics. *Tectonophysics* 357, 119-136.

43. Natural fractures in shales and their importance for gas production

Julia Gale¹ & Jon Holder¹

1. The University of Texas at Austin, U.S.A.

Presenting author: julia.gale@beg.utexas.edu

Keyword(s): shale, opening mode fractures

Shales make up a substantial proportion of the sedimentary record and in petroleum exploration have mostly been regarded as source or seal rocks. Recent developments in the continental US, however, have seen shale increasingly exploited for both gas and oil, where shale is the source, reservoir and seal. This presentation highlights recent work on one of the most important geological parameters in shale-gas reservoirs; the natural fracture system. Gas in these reservoirs is commonly extracted using hydraulic fracture treatments. Evidence from microseismic monitoring of hydraulically induced fracture growth shows that hydraulic fractures sometimes propagate away from the present-day maximum horizontal stress direction. One likely cause is that natural opening-mode fractures, which are present in most shales, act as weak planes that reactivate during hydraulic fracturing. Knowledge of the geometry and intensity of the natural fracture system is therefore necessary for effective hydraulic fracture treatment design. Using core and outcrop studies from several shales we review common fracture types, their characteristics, and the mechanical properties of the host rocks. Examples include Devonian Woodford Shale from the Permian basin in west Texas and Mississippian Barnett Shale of the Fort Worth basin in north central Texas. Fractures are commonly steep ($>75^\circ$) narrow (<0.05 mm), sealed with calcite, and are present in en echelon arrays. Most are undeformed, but there are examples that have been deformed by compaction. There are also examples of bedding-parallel sealed fractures. Yet other fractures are closely associated with concretions and diagenetic alteration of discrete layers. We consider fracture origin in the context of burial history and diagenetic evolution of the host rock. We tested the effect of calcite-sealed fractures on tensile strength of shale with a bending test. Samples containing natural fractures have half the tensile strength of those without and always break along the natural fracture plane. In Barnett shale examples the junction between the fracture-wall rock and cement is weak because the dominant calcite cement grows mostly over non-carbonate grains and there is no chemical bond between cement and wall rock. Thus, even completely sealed fractures are prone to reactivation. We consider the range of common fracture cements and host rock compositions in an effort to predict under which circumstances the fractures are likely to be weakest. We consider the natural fractures to have grown subcritically. We measured the subcritical crack index of different shale facies. The subcritical index is generally high, in excess of 100, but does show variability with facies. Geomechanical modeling, using the index as an input parameter, predicts fractures are clustered. Although the narrow steep fractures of the most common type are sealed and probably do not enhance reservoir permeability their population may follow a power-law size distribution. By analogy with fractured chalks we infer that the largest fractures in this distribution would be open and present in widely spaced clusters, spaced several hundred metres apart. This prediction has been confirmed in some horizontal image logs. In a few shales hydraulic fracture stimulation has not been necessary for gas production. In these cases horizontal wells are drilled to intersect open natural fractures and therefore knowledge of the open fracture distribution is crucial.

44. The record of a tectonic inversion in the Lower Devonian Ardenne-Eifel basin (Belgium, Germany): a switch from bedding-normal to bedding-parallel quartz veins

Koen Van Noten¹, Christoph Hilgers², Janos L. Urai² & Manuel Sintubin¹

1. Katholieke Universiteit Leuven, Geodynamics & Geofluids Research Group, Belgium

2. RWTH Aachen, Geologie-Endogene Dynamik, Germany

Presenting author: koen.vannoten@geo.kuleuven.be

Keyword(s): quartz veins, Lower Devonian, Variscan orogeny, tectonic inversion, High-Ardenne slate belt

Interesting scenarios for fluid redistribution arise during transitions between two stress regimes. A compressional inversion, i.e. the transition from an extensional to a compressional stress regime, in a sedimentary basin at the onset of orogeny is accompanied by an increase in maximum sustainable overpressure (cf. Sibson 2004). In the northern frontal part of the Rhenohercynian foreland fold-and-thrust belt, more specific in the periphery of the High-Ardenne slate belt (HASB; Germany), two successive types of quartz veins, i.e. bedding-normal and bedding-parallel veins, are interpreted to reflect the late Carboniferous compressional inversion affecting the Ardenne-Eifel sedimentary basin. Fracturing and sealing occurred in upper-crustal levels in a Lower Devonian, low-grade metamorphic siliciclastic multilayer sequence. A detailed structural study allowed recognising different cross-cutting early bedding-(sub)perpendicular vein-generations suggesting that fracturing/veining occurred in a less anisotropic stress field than in the central HASB, where a regular and regionally consistent array of veins is present (cf. Kenis & Sintubin 2007 and references therein). Veins in the periphery consist of quartz showing stretched elongate-blocky crystals. Curvature of crystals is a primary growth feature, not the result of later deformation. Discontinuous elongate crystals and repeated solid-inclusion bands and trails indicate a crack-seal mechanism and reflect that these extension veins were repeatedly opened and sealed during vein formation. Macroscopic observations such as bedding-parallel dissolution seams, veins remaining perpendicular to bedding across fold hinges and cleavage cross-cutting the veins, indicate that bedding-normal veining occurred early in deformation history, presumably still during burial. Subsequent deformation led to incipient formation of new subgrains in the original crystals. The presence of bedding-parallel quartz veins at the interface between two lithologies is the first evidence of the compressional stress regime. Bedding-parallel veins in the periphery of the HASB show a pronounced composite bedding-parallel fabric, consisting of bedding-parallel host-rock inclusion bands and bedding-perpendicular inclusion trails. Quartz crystals show a strong variability in grain size and suffered a weak recrystallisation during progressive veining and subsequent deformation. The formation of bedding-parallel veins has caused considerable debate in literature and several models have been postulated concerning their origin. Micro- and macroscopic observations indicate that some veins in the periphery of the HASB are formed due to bedding-parallel thrusting predating the formation of folds and the regional development of cleavage. This thrusting reflects a brittle deformation in upper-crustal levels that may be equivalent to the ductile mullion development in mid-crustal levels in the central part of the HASB.

SIBSON, R. H., 2004. Controls on maximum fluid overpressure definitions conditions for mesozonal mineralisations. *Journal of Structural Geology* 26, 1127-1136.

KENIS, I. & SINTUBIN, M., 2007. About boudins and mullions in the Ardenne-Eifel area (Belgium, Germany). *Geologica Belgica* 10(1-2), 79-91.

45. Vein-cleavage fabrics associated to a late-orogenic destabilisation of the Variscan cleavage in the High-Ardenne slate belt (Belgium)

Hervé Van Baelen¹, Philippe Muchez¹ & Manuel Sintubin¹

*1. Katholieke Universiteit Leuven, Geodynamics & Geofluids Research Group, Belgium
Presenting author: herve.vanbaelen@geo.kuleuven.be*

Keyword(s): tectonic inversion, quartz veins, cleavage, kink bands, crenulation, Variscan orogeny, Ardennes

The High-Ardenne slate belt, forming part of the northern frontal parts of the Rhenohercynian foreland fold-and-thrust belt, consists of intensely shortened siliciclastic Lower Devonian metasediments. Contraction of this thick Lower-Devonian sequence took place at lower greenschist facies conditions during the Visean – early Namurian Sudetic stage of the Variscan orogeny (~320 Ma), giving rise to a pervasive cleavage, forming the main structural fabric in the slate belt. Our current research allows recognising an important tectonic inversion during a late stage of the Variscan orogeny, expressed by (1) decametre-scale, south-verging folds (F2), affecting the pre-existing south-dipping main Variscan cleavage; (2) kink bands and crenulation cleavages, often related to southward dipping, low-angle normal shear zones and (3) veins that cross-cut the main Variscan cleavage. These veins can be further subdivided into three vein types. A first vein set consists of rather long, but thin veins. The cross-cut cleavage planes can easily be traced from one side of the vein to the other. These veinlets may form the precursor of a second type of veins, the lens-shaped veins. These lensoid veins display a more complex vein-cleavage geometry, e.g. radial disposition of the cross-cut cleavage at the vein tip. The vein-cleavage cross-cutting relationship strongly suggests that the veins, or fluid-filled gaps (?), were highly mobile structures during their evolution. The internal deformation is accommodated by foliation-parallel slip in the surrounding slates (instead of crack-tip propagation), allowing the transfer of the cross-cut cleavage from one vein-wall to the other. A third vein type is represented by large-scale, fault-related, south-dipping veins, locally crosscutting the hinges of the south-verging F2 folds, again juxtaposing different cleavage-vein geometries at both sides of the veins. The sense of shear deduced from these different vein types confirms the top-to-the-south shear deformation determined from the folded, kinked and crenulated cleavage planes surrounding the veins. The quartz veins will be further studied from a microthermometric point of view, to investigate the role of fluid pressures during deformation. High fluid pressures, possibly inherited from the main stage of the Variscan orogeny, may have triggered or facilitated the deformation related to this late Variscan tectonic inversion.

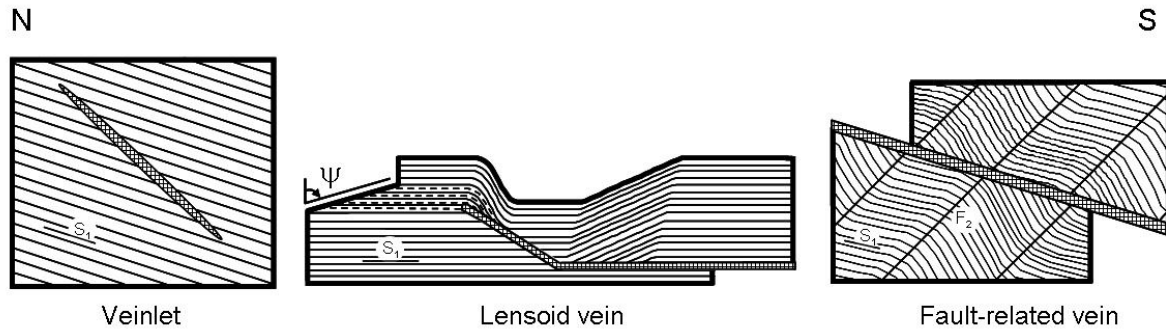


Figure 1. For explanation see text.

46. Natural alteration of chalk in contact with air versus transformation due to shearing: examples in the Mons Basin (Belgium)

Suzanne Raynaud¹, Olivier Richard¹, Françoise Bergerat² & Sara Vandycke³

1. Géosciences Montpellier, France

2. Laboratoire de Tectonique, Paris VI, France

3. Faculté Polytechnique de Mons, Belgium

Presenting author: suzanne.raynaud@gm.univ-montp2.fr

Keyword(s): *chalk, hardpan, normal faulting, shear, porosity, Mons Basin (Belgium)*

Some studies about matrix transformations of chalk along fault planes (Gaviglio *et al.*, 1997, 1999, Schroeder *et al.*, 2006) demonstrated an important decreasing of the porosity, resulting from both dissolution and crystallization linked to the shear process. Behind the fault plane, a heterogeneous zone of about 15 cm width is formed showing a decrease of the porosity and of the permeability. The most noteworthy changes occur within the very first millimetres. Some other studies (Raynaud 2004, Ventalon, 2005; Ventalon *et al.*, 2005) concerning the natural alteration of carbonated rocks in contact with air also establish the occurrence of petrophysical variations in few millimetres width zone, called hardpan. In this zone the calcite dissolved in the rock by the rain water crystallises after the water evaporation. The result is a decreasing of the porosity. The question is: which part of the petrophysical transformations observed along the fault planes are resulting from tectonic process or from hardpan formation? A first study has been carried out in the Mons basin, on faulted and non faulted samples of chalk, knowing the age of their exhumation. We present herein the results for two samples: the first one in a non faulted chalk, the second one along a fault plane, both being exhumed since three years. In the CBR quarry of Harmignies, in the Obourg chalk, two natural surfaces which are three years old are sampled. The surface H3 is a fault surface, the surface H4 is a ordinary quarry surface. A reference chalk piece H5 is sampled at 20 cm depth. The H3 and H4 surfaces were exposed to weathering for three years. For the three samples we made thin sections perpendicular to the sample surface. The calcitic patina is developed only in the first mm under the surface (Raynaud *et al.* 2004, Ventalon *et al.* 2005). By SEM, we took a succession of pictures of the surface to the depth. We present here the study of the evolution of the surfacic porosity measured on SEM views of H3 and H4 compared to the surfacic porosity reference value H5. This method allows to detect the porosity variation at micrometric scale but we chose a 0,05 mm scale with the aim to smooth the micrometric rock heterogeneities. In figure 1, the hardpan thick corresponds to the rock thickness (about 5 mm) in which the surfacic porosity is less than the reference value. Then, we observe a zone in which the surfacic porosity is higher than the reference value. This zone is qualified as a dissolving zone. This evolution is similar to the porosity evolution observed in the Burdigalian limestones in the South of France. In figure 2, after a high porosity under the fault surface, the porosity decreases. It is minimum at 2.5 mm, increases to 35% at 17 mm and after futher increases to 45%. Previous analyses on fault planes in the same chalk (Schroeder *et al.*, 2007) have been made using a low pressure mercury porosimeter. These studies indicated a porosity of the intact chalk ranging between 40 and 44%. Close to the fault planes, the porosity is about 30 to 35%. In previous studies, variation of petrophysical properties along normal fault plane have been associated to dissolution process induce by

shearing. The hardpan formation is a natural phenomena which modifies the chalk surfaces. So, we conclude that the porosity profile under the faulted surface results from the superposition of tectonic and hardpan formation events.

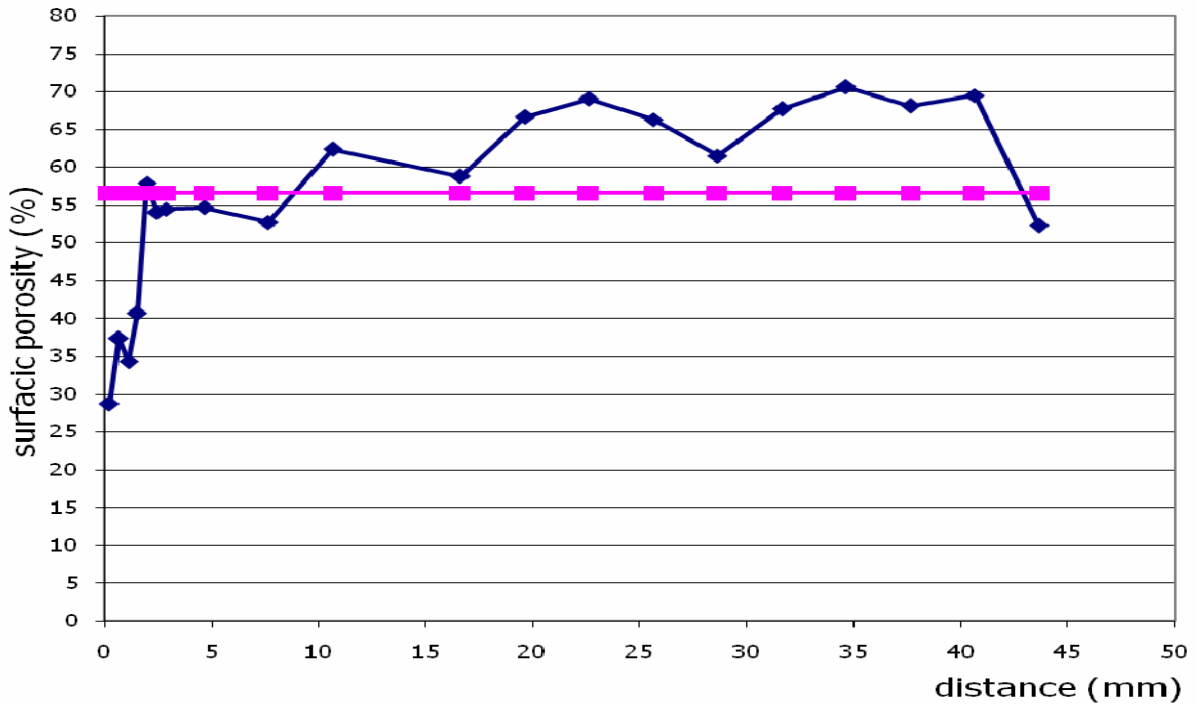


Figure 1. Sample H4. Hardpan (calcitic patina) alone. Surfacic porosity (%) along a transect from surface to depth.

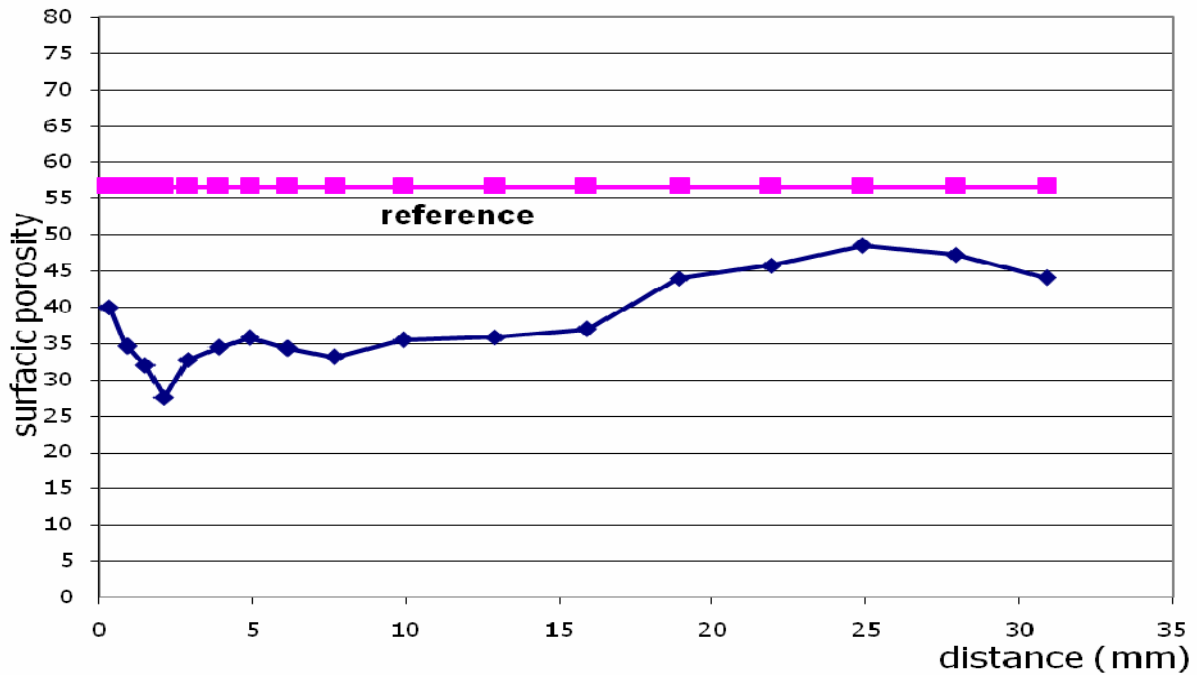


Figure 2. Sample H3. Fault Surface. Surfacic porosity (%) along a transect from surface to depth.

- GAVIGLIO, P., ADLER, P., THOVERT, J.F., VANDYCKE, S., BERGERAT, F., BEKRI, S. & LESTIDEAU R., 1997. Grain-scale microstructures and physical properties of faulted chalk. *Bull. Soc. géol. Fr.*, 168, 6, p. 727-739
- GAVIGLIO, P., VANDYCKE, S., SCHROEDER, CH., COULON, M., BERGERAT, F., DUBOIS, C. & POINTEAU, I., 1999. Matrix strains along normal fault planes in the Campanian White Chalk of Belgium: structural consequences. *Tectonophysics*, 309, p.41-56
- RAYNAUD, S., SEIDEL, J.L., EMBLANCH, C., VIGNARD, G. & GALL, J.Y., 2004. An altered stone zone under the polychromatic layer. The stone retable of the Narbonne cathedral (SW France), 199-210. In *Architectural and sculptural stone in man-cultivated landscape*, Petr.Siegl and Richard Prikryl. Carolinum Press Prague.
- SCHROEDER, CH., GAVIGLIO, P., BERGERAT, F., VANDYCKE, S. & COULON, M., 2006. Faults and matrix deformations in chalk: contribution of porosity and sonic wave velocity measurements. *Bull. Soc. Géol. France*, 4, 203-213.
- VENTALON, S., RAYNAUD, S. & DE LA BOISSE, H., 2005. L'évolution dans le temps de la surface des pierres calcaires. Exemple du calcaire de Beaulieu. Colloque « pierres et patrimoine européen: économie de la pierre de l'Antiquité à la fin du 18ème siècle en Europe ». Château-Thierry, 18-21 octobre 2005.

47. In-situ observation of fluid-filled-pores in Boom Clay (Belgium) using cryo-FIB-SEM technology: first results

Guillaume Desbois¹ & Janos L. Urai¹

*1. RWTH, Aachen University, Geologie - Endogene Dynamik, Germany
Presenting author: g.desbois@ged.rwth-aachen.de*

Keyword(s): Boom clay, in-situ porosity, cryo-SEM, FIB, EDX

Mudrocks form seals for hydrocarbon accumulations, aquitards and chemical barriers. The sealing capacity is controlled either by the rock microstructure or by chemical interactions between minerals and the permeating fluid. A detailed knowledge about the sealing characteristics is of particular interest in Petroleum Science. Other fields of interest are the storage of anthropogenic carbon dioxide and radioactive waste in geologic formations. A key factor to the understanding of sealing by mudstones is the study of their porosity. Early studies of clay porosity have used dried fractured samples but clay is a wet, nominally hydrous mineral and the drying of the samples damages the natural structure of pores and leads to the development of artefact structures due to clay mineral dehydration and desiccation. Hildenbrand and Urai (2003) have investigated clay porosity by mercury and Wood's metal injection to calculate the porosity and the average pore size. However, this approach gives an indirect description of pores in clays. For instance, much is still unknown and fundamental information is missing because the impossibility to observe in-situ the elusive wet components in clay. What are the distribution and the geometry of individual pores? How are pores connected? Are the pores fluid-filled? If so, which is the nature of these fluids? An alternative is to study wet samples using a high-resolution cryogenic SEM which allows stabilization of wet media at cryo-temperature, in-situ sample preparation by ion gun excavation and observations of the frozen fluids at high resolution, combined with a micro-chemical analysis using EDX. At the present time, the cryo-SEM technology has been used widely in Life Sciences for about thirty years but it has only very recently been used in Geosciences. We have applied the cryo-FIB-SEM method to investigate in-situ porosity of natural wet clay. The clay samples are fine grained Boom clays (Belgium) which are of special interest because in Belgium the Boom Clay is considered as a potential host formation for the geological disposal of high-level and long-lived radioactive waste. We present here the first pictures of in-situ pores in clay. The most spectacular result is certainly the first observation of fluid filled clay pores within FIB cross-sections. Water phase sublimation experiments suggest that these pores are not all filled with the same fluid. More over, our observations done on Boom clay samples show that the pores are distributed in two size populations organized parallel to the layering of the clay sheets. Thus, we are convinced that the cryo-FIB-SEM method is very promising for further detailed and systematic in-situ investigation of clay pores.

HILDENBRAND, A. & URAI, J.L., 2003. Investigation of the morphology of pore space in mudstones—first results. *Marine and Petroleum Geology*, 20(10):1185-1200.

48. Evolution of brittle deformation and fault growth in a high porosity sandstone analogue from the Cretaceous of the Bassin du Sud-Est, Provence, France

Elodie Saillet¹ & Christopher Wibberley²

1. UMR Géosciences Azur, Valbonne, France

2. TOTAL, TOTAL - Exploration et Production, Pau, France

Presenting author: saillet@geoazur.unice.fr

Keyword(s): reservoirs, porous sandstones, cataclastic deformation bands (CDBs), “Bassin du Sud-Est”

Faulting in porous sandstone produces zones of deformation bands rather than planar fracture surfaces (Aydin, 1978; Aydin and Johnson, 1978, 1983; Antonellini *et al.*, 1994; Du Bernard, 2002; Torabi *et al.*, 2007). Cataclastic deformation bands (CDBs) are brittle shear zones that form through the combined effects of compaction and cataclasis. Porosity and grain size reduction associated with CDBs formation cause strain hardening, and the result is the initiation of a new band, adjacent to the first (Aydin, 1978; Aydin and Johnson, 1978, 1983). Continued deformation may possibly result in the development of localised slip surfaces at the edge of deformation band zones (Aydin and Johnson, 1983; Antonellini and Aydin, 1995; Shipton and Cowie, 2001). However, the mechanical causes and consequences of this localisation are not clear. Understanding the evolution of fault geometrical and hydromechanical properties during fault growth and network development is of major importance in fluid flow prediction in the crust. This contribution is based on field and laboratory data of CDBs, obtained in the Upper Cretaceous high-porosity sands and sandstones of the Southeast France in the “Bassin du Sud-Est”. This complete field and multi-scale study is based on three main research axes: (i) A complete and systematic field study based on scan lines totalling 717 meters long; (ii) A microstructural and a statistic porosity and granulometry analysis based on samples extracted from the outcrops previously mapped in detail. (iii) A permeability study based on the same samples. Based on our different methods of analysis, the main results can be summarized as follows: (1) For each outcrop, the position of all visible CSBs was recorded along one meter wide scan-lines perpendicular to the main structures and through their damage zones. This systematic field study of CDBs shows: (i) The overall CDB density is low to moderate, with the predominance of thin CDBs; (ii) A few zones present an anomalous CDB density increase, where CDBs are organized in clusters patterns, with sometimes a localized main slip plane. (2) The CDBs characterisation based on field data show us the predominance of thin CDBs, with small thickness and displacement, suggested to correspond to strain hardening processes by addition of individual deformed strands. Larger faults are also present with different spatial distribution characteristics. (3) Microstructural studies show a drastic reduction of pores and grains size with fault displacement and thickness increase. (4) The grain and pores size reduction is quantified with the computer programme NIH Image, and shows a two order scale reduction between the host rock and a mature fault. (5) There is an important permeability reduction between the host sands, the thin CDBs and the larger faults. This study based on multi-scale field data suggests two main ideas: (i) Clusters of thin CDBs can evolve into larger faults; (ii) Thin CDBs and CDBs cluster increase by a strain hardening process whereas larger faults grow by strain softening processes. Those different analysis methods exhibit the evidence of a transition in growth mechanism from thin CDBs to larger ultracataclastic fault zones. These larger fault zones form preferentially in contexts where a previous generation of CDBs

already exists, suggesting the influence of previous structural heritage on further fault network growth.

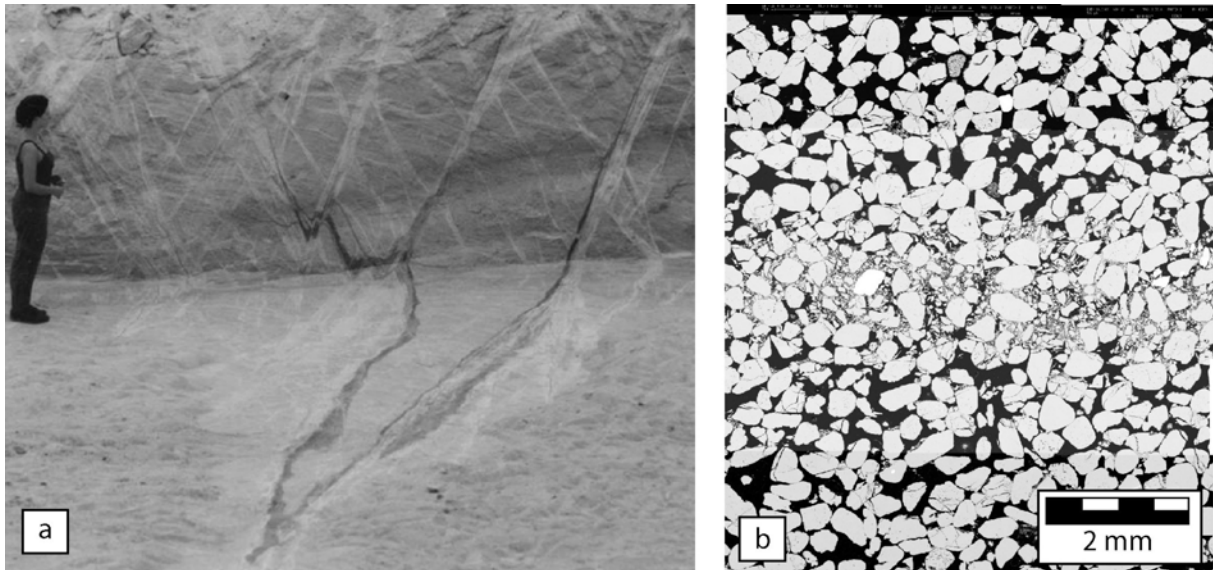


Figure 1. (a) Field view of red iron-deposits in the sands adjacent to the CDBs in the Massif d'Uchaux areas, corresponding to recent fluid flow. (b) Scanning electron micrograph showing the details of the grain fracturation and reduction for a single strand CDB in the sands of Bédoin area.

- ANTONELLINI, M.A., AYDIN, A. & POLLARD, D.D., 1994. Microstructure of deformation bands in porous sandstones at Arches National Park, Utha: *Journal of Structural Geology*, v.16, p.941-959.
- ANTONELLINI, M.A. & AYDIN, A., 1995. Effect of faulting on fluid flow in porous sandstones: geometry and spatial distribution: *AAPG Bulletin*, v.79, p.642-671.
- AYDIN, A., 1978. Small faults formed as deformation bands in sandstones: *Pure and Applied Geophysics*, v.116, p. 913-930.
- AYDIN, A. & JOHNSON, A.M., 1978. Development of faults as zones of deformation bands and as slip surfaces in sandstone: *Pure and Applied Geophysics*, v.116, p. 931-942.
- AYDIN, A. & JOHNSON, A.M., 1983. Analysis of faulting in porous sandstones: *Journal of Structural Geology*, v.5, p.19-31.
- DEBRAND-PASSARD, S. & COURBOULEIX, S., 1984. Synthèse géologique du Su-Est de la France: *Mém. BRGM*, no.126.
- DU BERNARD, X., LABAUME, P., DARCEL, C., DAVY, P. & BOUR, O., 2002. Cataclastic slip band distribution in normal fault damage zones, Nubian sandstones, Suez rift: *Journal of Geophysical Research*, v.107, p.103-114.
- SHIPTON, Z.K. & COWIE, P.A., 2001. Damage zone and slip-surface evolution over μm to km scales in high-porosity Navajo sandstone, Utah. *Journal of Structural Geology*, v.23, 1825-1844.
- TORABI, A., BRAATHEN, A., CUISAT, F. & FOSSEN, H., 2007. Shear zones in porous sand: Insight from ring-shear experiments and naturally deformed sandstones. *Tectonophysics* v.437, 37-50.
- WIBBERLEY, C.A.J., PETIT, J.P & RIVES, T., 2007. The mechanics of fault distribution and localization in high-porosity sands, Provence, France: In: Lewis, H. & Couples, G.D. (eds.) *The Relationship between Damage and Localisation*. Geological Society, London, Special Publication 289, 19-46.

49. DEM simulation of shear induced mixing in layered sand-clay sequences – initial results

Steffen Abe¹, Joyce Schmatz¹ & Janos L. Urai¹

*1. RWTH Aachen University, Geologie-Endogene Dynamik, Germany
Presenting author: s.abe@ged.rwth-aachen.de*

Keyword(s): Discrete Element Modelling, sand-clay mixing

An important sealing mechanism in fault zones of sand-clay sequences is mechanical mixing of sand and clay. For the case of perfect mixing, a 1 mm thick clay gouge is transformed into a 3 mm thick sand-clay gouge with the same low permeability and a better sealing capacity. The process of mixing has been discussed in the literature and was identified in laboratory experiments, but its rate as a function of sand and clay properties is poorly understood. In this project, a Discrete Element (DEM) simulation is used to investigate the micro-mechanics of the mixing between sand and clay during shear of a layered sequence. Initial work has been performed using a 2D model but the approach can easily be extended to full 3D simulations. The simulation model consist of 2D box sequence of alternating layers of sand and clay which are represented by DEM particles with different size and frictional properties. On the boundaries orthogonal to the layering a constant normal stress is applied whereas on the boundaries parallel to the layers periodic boundary conditions have been implemented. The model is then sheared perpendicular to the orientation of the layers by moving the edges of the model with a constant velocity. Due to the periodic boundary conditions the model enables arbitrarily large displacements, only limited by the computational cost. The displacements applied to the models in the simulations presented here did result in total shear strains of more than 30. The results from these initial simulations show that a number of important features of real shear deformations of sand-clay multilayer sequences are also present in the model, such as shear localization and mixing between sand and clay. Results obtained from the DEM simulations are compared with data obtained from laboratory experiments where a simple shear deformation is applied to a sand-clay multilayer sequence.

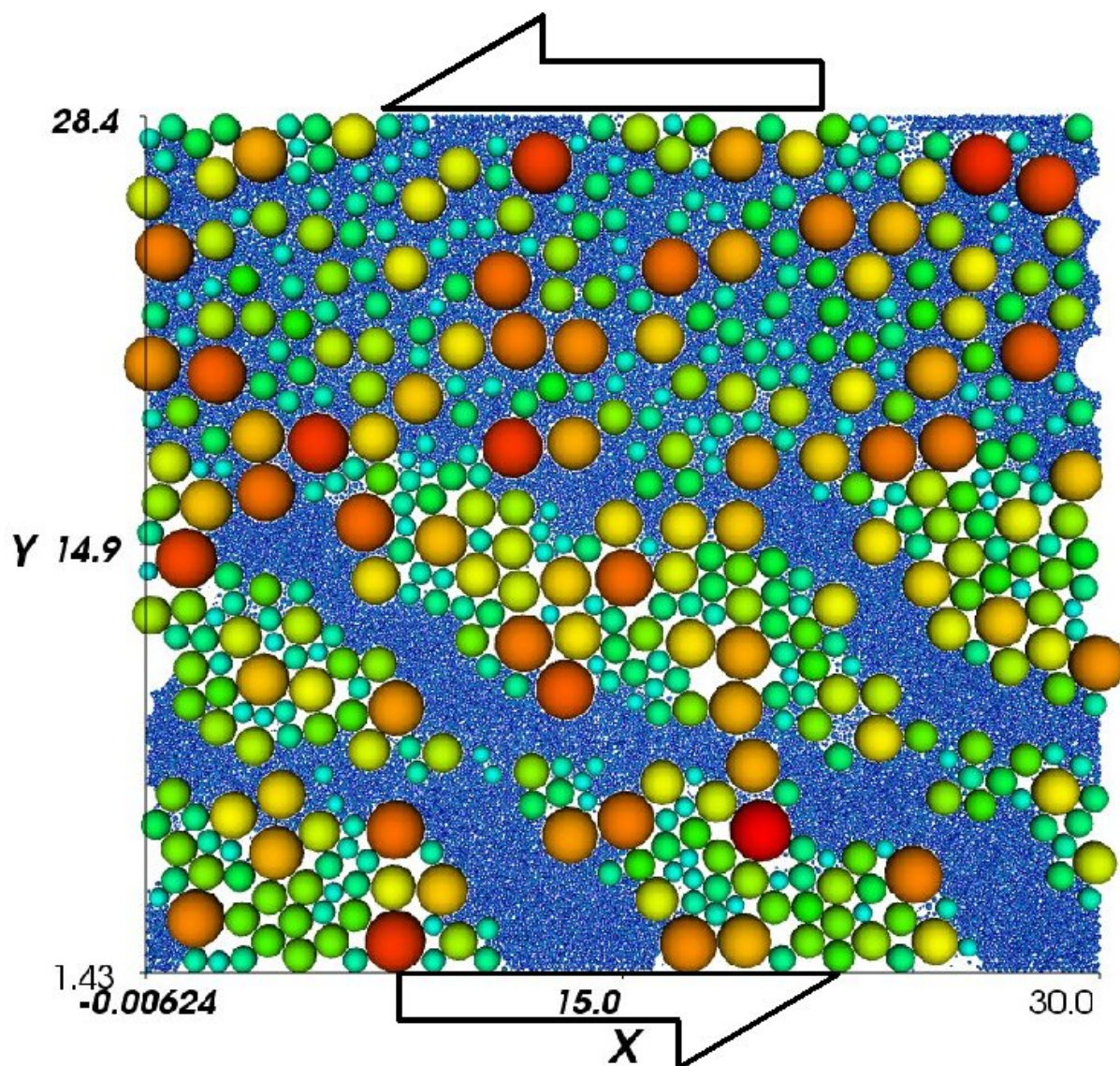


Figure 1. Mixing of clay (blue) and sand (green-red) grains in a DEM simulation after 775% shear strain

50. Elasticity, strength, friction and porosity relations in Discrete Element Method (DEM) models of cohesive granular materials

Martin Schöpfer¹, Steffen Abe², Conrad Childs¹ & John J. Walsh¹

1. University College Dublin, School of Geological Sciences, Fault Analysis Group, Ireland

2. RWTH Aachen University, Geologie-Endogene Dynamik, Germany

Presenting author: martin@fag.ucd.ie

Keyword(s): porosity, friction angle

Laboratory tests of sedimentary rocks (e.g. sandstones, limestones) indicate that rock strength, angle of internal friction and Young's modulus decrease with increasing porosity. If core samples for rock mechanics testing are not available, rock physical properties are estimated using empirical relations, i.e. Young's modulus is estimated from a sonic log and other properties (unconfined compressive strength, friction angle) using other empirical relations. Since some of these empirical relations are poorly constrained, our study attempts to provide an improved mechanical basis for their determination. The Discrete Element Method (DEM), in which rock is represented by bonded spherical particles, is used to investigate the shape of failure envelopes and relations between friction angle and porosity. A series of confined triaxial extension and compression tests were performed on samples generated with different particle packing methods in order to test whether the mechanical properties of the model material are predominantly controlled by particle size distribution or porosity. The impact of pre-existing cracks, which were modelled as non-bonded contacts, on mechanical properties was also investigated. Our 3D DEM models for both uniform (Fig. 1a) and power-law (Fig. 1b) particle size distributions and varying cement content demonstrate that the friction angle decreases (almost) linearly with increasing porosity and is independent of particle size distribution. Young's modulus and strength decrease with increasing porosity, whereas Poisson's ratio is (almost) porosity independent. The unconfined compressive strength to tensile strength (UCS/T) ratio is controlled by model porosity, but also by the proportion of bonded contacts, i.e. UCS/T increases with increasing crack density. Young's modulus and strength decrease and Poisson's ratio increases with increasing crack density. All our 3D DEM model property relations (strength, friction angle, stiffness) are consistent with continuum mechanics predictions and empirical rock property relations. The modelling results not only provide a rationale for empirical relationships between the mechanical properties of rock and other parameters, but also underpin improved methods for the calibration of DEM model materials.

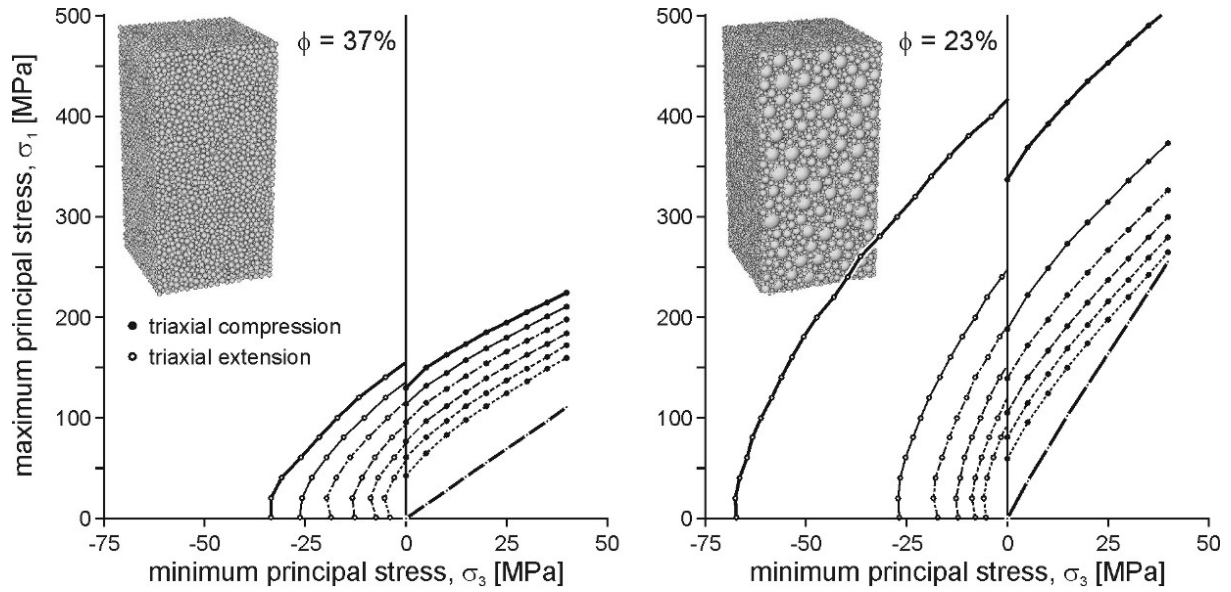


Figure 1. Failure envelopes in principal stress graphs obtained for two models with different porosities but identical particle and bond properties. The strongest materials are fully bonded, whereas the weakest materials are non-bonded. The envelopes in-between were obtained from partially bonded models.



Poster presentations

(in order of presentation)

Poster presentations: table of contents

1. Towards an understanding of the seismic properties of major fault zones	90
Rochelle Taylor	90
2. 3D modelling of the Pusteria and Sprechenstein-Mules fault system. Part 1: geomodelling as applied to fault-zone architecture studies	92
Andrea Bistacchi, Matteo Massironi & Luca Menegon	92
3. The Asquempont Detachment System, Anglo-Brabant Deformation Belt, Belgium: state-of-the-art	94
Timothy N. Debacker, Kris Piessens, Alain Herbosch, Walter De Vos & Manuel Sintubin	94
4. Geometry and evolution of the Nansha trough foreland thrust and fold belt of South China Sea, China	97
Shimin Wu, Huaifu Lu & Shengli Wang	97
5. Grain boundary migration in quartz: not a simple story.....	98
Helena Bergman & Sandra Piazzolo	98
6. The effect of grain size sensitive flow on synthetic calcite ‘conglomerates’.....	99
Alexander Edwards, Stephen Covey-Crump & Ernest Rutter	99
7. The fabrics and kinematics of anhydrite rocks from central Italy	100
Rebecca Hildyard, Daniel Faulkner, David Prior, Nicola De Paola & Cristiano Colletini	100
8. Experimental dehydration and deformation of Volterra Gypsum: preliminary experiments and overview.....	102
Sergio Llana-Funez, Daniel Faulkner & John Wheeler.....	102
9. The role of fluid-filled grain boundaries in substructure development: new insights from see-through deformation experiments.....	104
Joyce Schmatz & Janos L. Urai	104
10. The centennial of the terms ‘boudin’ and ‘boudinage’ - a historical retrospect	106
Manuel Sintubin	106
11. The compaction dependent cohesion and tensile strength of gypsum powder – the effect on scaled analogue models	109
Heijn van Gent, Marc Holland & Janos L. Urai	109
12. The Hazar pull-apart along the East Anatolian Fault: structure and active deformation.....	111
Aurelia Hubert-Ferrari, David Garcia, Jasper Moernaut, Maarten Van Daele, Emre Damci, Xavier Boes, Jeff Fraser, Namik Cagatay & Marc De Batist.....	111
13. 3D joint density mapping	112
Michael Drews & Hagen Deckert	112
14. Deformation-controlled fluid migration in a middle to upper-crustal level: a research strategy for the western part of Armorica (Brittany, France)	114
Isaac Berwouts, Philippe Muechez & Manuel Sintubin.....	114
15. Structural control on the Dikulushi Cu-Ag deposit, Katanga, Democratic Republic of Congo	116
Maarten Haest, Philippe Muechez & Sara Vandycke	116
16. Global search for intrusive mud systems: analogues for the subsurface.....	118
Katie Roberts, Richard Davies, Simon Stewart & Kenneth McCaffrey	118
17. The geological and geodynamic evolution of the Northumberland Trough region, northern England: insights from the numerical modelling of lithosphere deformation and basin formation	119
Linda Austin, Stuart Egan & Stuart Clarke.....	119
18. The Quenast plug: a mega-porphyroclast during the Brabantian Orogeny (Senne valley, Brabant Massif, Belgium)	121
Timothy N. Debacker & Manuel Sintubin	121
19. The post-Triassic uplift and erosion history of the southwest UK	123
John E. Kelly & Jonathan P. Turner	123
20. Characterising fractured basement using the Lewisian Complex: implications for petroleum potential in the Clair Field.....	124
Jennifer Martin, Robert E. Holdsworth, Kenneth McCaffrey, Andy Conway, Stuart Clarke.....	124
21. Structural styles and timing of deformation on the Stublick – Ninety-Fathom Fault, Northern England, U.K.	126
Stuart Clarke, David Millward & Katie Whitbread.....	126

1. Towards an understanding of the seismic properties of major fault zones

Rochelle Taylor¹

1. University of Manchester, U.K.

Presenting author: rochelle.taylor@student.manchester.ac.uk

Keyword(s): *fault zone, seismic properties*

Understanding and characterizing fault zone structure at depth is a key part of predicting the slip behaviour of faults in the brittle crust. Field studies of the surface outcrop of faults can provide valuable insights into fault zone structure, but are often hampered by poor and/or incomplete exposure, and may only show fault rocks formed at one depth if movements are purely strike-slip. Some faults now exposed at the surface have suffered significant modification during exhumation, such as overprinting of seismogenic structures by continued slip. To image active faults at depth requires remote sensing techniques. Thus seismology can potentially give information on the spatial distribution of seismicity, the size and extent of the fault zone, the fluid pressure within fault zones and the level of fracture damage within the fault zone, but presently seismic studies of fault zones are not 'calibrated' against a forward model of expected properties based on field studies of real fault rocks. If an improved understanding of the controls on the seismic properties of well characterized fault rocks (P/S wave velocity, attenuation, shear wave splitting, dispersion) were available, this would result in a better understanding of the physical properties of fault zones at depth. This study forms part of a collaborative investigation involving the universities of Manchester and Liverpool that uses the Carboneras fault zone in S.E. Spain as an analog for certain types of major fault zone, and involves specifically: Characterization of the surface structure of the Carboneras fault zone (CFZ) by detailed geological mapping. Laboratory measurement over a range of physical conditions (pressure/temperature/pore fluid pressure) of the seismic properties of representative samples collected from the CFZ. Construction of a synthetic seismic fault zone model based on surface mapping and laboratory measurements, for comparison with results from active experiments, which it is hoped eventually will be carried out in this region. This work follows the same approach that was adopted for producing a synthetic deep seismic reflection profile of lower crustal rocks of the Ivrea-Verbano zone, NW Italy, based on geological mapping, section construction, laboratory seismic measurements and seismic modelling that was recently carried out by researchers from this department and Royal Holloway, University of London. Several recent field studies have used 'seismic fault zone waves' to help interpret fault zone contiguity and dimensions (such as width) and the contrasting physical properties with the country rock. These waves consist of head waves and waves trapped in the slower rocks of the fault core. Head waves occur where seismic energy is transported along material interfaces with the velocity and motion polarity of body waves within the faster medium. These waves arrive in the slower velocity medium before the direct arrivals and can be misinterpreted as direct arrivals. Trapped waves are internally-reflected, slow seismic energy transported within low velocity layers (i.e. waveguides). To be able to model fault zone wave propagation from forward modelling should represent a substantial aid to their interpretation when detected from field seismic studies. Work currently focuses on the extension of earlier geological mapping in the CFZ so that the whole of the exposed tract, some 30 km long, is characterized in a way suited to the seismic modelling. Rock sampling effectively involves dealing with rocks in three different states of friability. The country rocks are sufficiently cohesive not to present problems. Clay-bearing fault gouge is being sampled

in the same way as was used for taking samples for permeability measurements (by hammering oriented copper tubes into the rock). Highly fractured and friable non-clay-bearing fault rocks pose special problems that have to be addressed on an individual basis. Ultrasonic acoustic velocity measurements are made using standard equipment over confining and pore pressure ranges appropriate to the upper 10km of the continental crust and we attempt to account for frequency-dependent effects using static elastic property determinations. Pore volumetry is used because fault rocks can be quite porous and pore collapse under effective pressure can have a significant modifying effect on seismic properties.

2. 3D modelling of the Pusteria and Sprechenstein-Mules fault system. Part 1: geomodelling as applied to fault-zone architecture studies

Andrea Bistacchi¹, Matteo Massironi² & Luca Menegon²

1. Università di Milano Bicocca, Dipartimento di Scienze Geologiche e Geotecnologie, Italy

2. Università di Padova, Dipartimento di Geoscienze, Italy

Presenting author: andrea.bistacchi@unimib.it

Keyword(s): 3D modelling, fault zone architecture, Eastern Alps

In this contribution we present theoretical considerations and the practical implementation which allowed a 3D realistic model of the architecture of the Pusteria and Sprechenstein-Mules fault system (Eastern Italian Alps) to be reconstructed. In a companion contribution (Part 2: implications for the mechanical evolution of crustal-scale strike-slip faults) we present some results of this model, regarding the mechanical evolution of the fault system. A 3D geological model of the fault network, where each major fault segment is represented as a discrete surface, has been reconstructed from borehole data and a detailed 1:5000 geological map by means of the geomodeling package gOcad. In this model, continuous fault surfaces are discretised as triangulated surfaces interpolated with the DSI algorithm (Mallet, 2002). This algorithm is particularly well suited to model natural objects, such as fault networks, because, while retaining the imposed topology, it allows for different concurrent constraints to be set: hard and soft constraints on position, constraints on attitude, constraints on intersection with other fault surfaces, etc. The 3D fault network model has been interactively validated by means of retrodeformation of the Sprechenstein-Mules fault. The accuracy of the model has been evaluated with techniques described in Bistacchi *et al.* (2007). Having reconstructed the geometry and topology of the fault network, the next step is to populate the model with fault rocks and structural/geomechanical properties. Continuous or categorical properties (the latter being the result of some sort of classification) can be represented in a 3D geomodel as discrete functions defined either on volumetric or surface objects, and both these data structures has been used in our model for damage and core zones respectively. In any case, available classification and representation schemas have been modified and adapted in order to account for the scale and spatial resolution of the 3D model. Core zones are assumed to have their mean surfaces coincident with surfaces of the fault network. The finite thickness of cores is not represented explicitly, with volumetric objects, because of the very low thickness of these objects with respect to areal extension. Therefore, we prefer to represent fault core thickness as a continuous property of fault surfaces. Also fault-rock classification and other continuous or categorical properties have been represented as discrete functions of surfaces of the fault network. Hence, each fault core in the model is represented with a triangulated surface, which carries properties such as core thickness and fault rock type (these properties can be visualized with isopachs or with a categorical colour-coded legend). Several problems and limitations have arisen in the interpolation and/or simulation of these properties, but in general the very flexible DSI algorithm can be applied successfully. The relationships between thickness of the fault core, type of fault rock, lithology of the host rock, and topological position in the fault network can be very effectively highlighted by means of this representation. On the other hand, damage zones can be represented as fully-3D volumetric objects. Different properties, which concur in representing the “degree of damage”, are modelled as continuous or categorical functions defined on different 3D portions of the

damage zones: number and attitude of joint sets, fracture spacing, etc. A multi-criteria classification, which attempts to summarise the “degree of damage”, is proposed. As is shown in the companion contribution (Part 2: implications for the mechanical evolution of crustal-scale strike-slip faults), this 3D model provides new insights in the architecture of a crustal-scale fault zone and provides quantitative data in 3D, which can be directly compared with results from mechanical models. In the future, this kind of model might also be used as an input dataset for more detailed and realistic mechanical or hydraulic models.

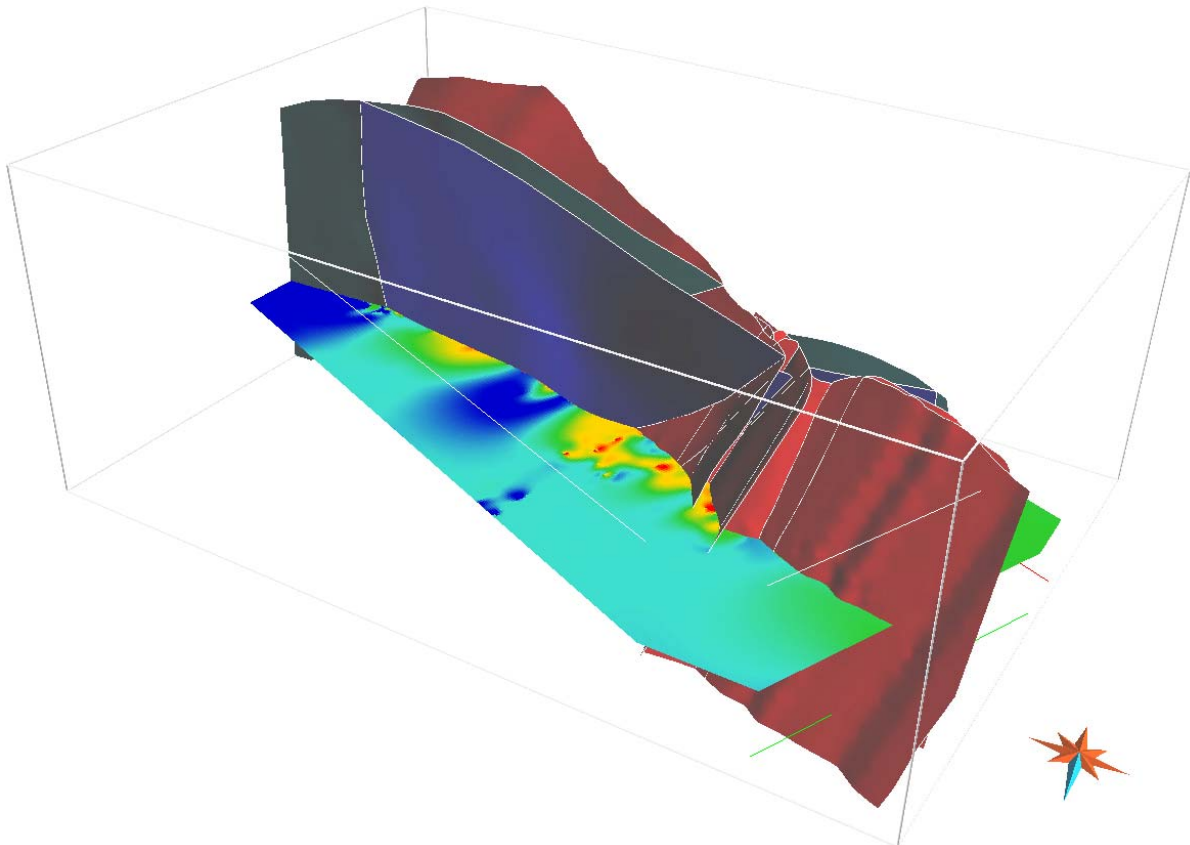


Figure 1. Fault network model, viewed from the NW, and horizontal cross section of the “degree of damage” volumetric property defined on damage zones. Lobe-shaped strong-damage volumes (red and orange) appear to be centred on step-overs. Bounding box is 8 x 5 x 1.5 km.

BISTACCHI, A, MASSIRONI, M., DAL PIAZ, G.V., DAL PIAZ, G., MONOPOLI, B., SCHIAVO, A.& TOFFOLON, G., 2007. 3D fold and fault reconstruction with an uncertainty model: An example from an Alpine tunnel case study. *Computers and Geosciences*, doi:10.1016/j.cageo.2007.04.002
MALLET, J.L., 2002. *Geomodeling*. Oxford University Press, New York, NY, 624pp.

3. The Asquempont Detachment System, Anglo-Brabant Deformation Belt, Belgium: state-of-the-art

Timothy N. Debacker¹, Kris Piessens², Alain Herbosch³, Walter De Vos²
& Manuel Sintubin⁴

1. Universiteit Gent, Geology & Pedology, Belgium

2. Geological Survey of Belgium, Brussels, Belgium

3. Université Libre de Bruxelles, Département des Sciences de la Terre et de l'Environnement, Belgium

4. Katholieke Universiteit Leuven, Geodynamics & Geofluids Research Group, Belgium

Presenting author: timothy.debacker@ugent.be

Keyword(s): extensional detachment, low-angle normal fault

In order to explain the juxtaposition of the lowermost Ordovician Chevlipont Formation and the Lower to lower Middle Cambrian Oisquercq Formation at Virginal (Sennette valley), Mortelmans (1955) suggested the presence of an important reverse fault, the Virginal fault. At Asquempont, in the vicinity of Virginal, Legrand (1967) described a fault zone between the Chevlipont Formation and the Oisquercq Formation, and named this fault the Asquempont fault. Also he considered this fault as an important reverse fault, adding, however, that the fault is steeply NE-dipping and that it contains a quartz vein-bearing damage zone. A re-examination of the latter outcrop by Debacker (Debacker 2001; Debacker *et al.*, 2003, 2004) demonstrated that the actual limit between the Chevlipont Formation and the Oisquercq Formation consists of a pre-cleavage fault zone oriented at low angles to the steeply inclined bedding that is cross-cut by a steeply NE-dipping, quartz vein-bearing post-cleavage normal fault zone. The same pre-cleavage fault zone is also encountered at Virginal (Sennette valley; cf. Mortelmans, 1955) and at Quenast (Senne valley). As there is only evidence for one single progressive deformation event within the Brabant Massif, and cleavage development and folding are cogenetic (e.g. Sintubin, 1999; Debacker *et al.*, 2005a), the pre-cleavage nature of this fault zone suggests a pre-folding origin. In several boreholes to the WNW of the Senne-Sennette outcrop area, quite similar contacts occur between subhorizontal to gently dipping beds of the Oisquercq Formation and the overlying Ordovician. This confirms the expected pre-folding fault origin and, more importantly, suggests a normal sense of movement instead of a reverse sense. This led Debacker (Debacker 2001; Debacker *et al.*, 2003, 2004) to redefine the fault zone separating the Oisquercq Formation and the Chevlipont Formation in the Senne-Sennette outcrop area as the Asquempont Detachment, being a pre-cleavage and pre-folding extensional fault zone oriented at low angles to bedding, with an activity between the Caradoc and the time of cleavage development. In the Dyle-Thyle outcrop area, to the east of the Senne-Sennette area, the Asquempont Detachment, renamed as the Asquempont Detachment System, is suggested to form the limit between the Lower Cambrian Blanmont and Tubize formations on the one hand and the Upper Cambrian Mousty Formation on the other hand (Debacker *et al.*, 2005b). During the construction of a new geological map of the Brabant Massif, Piessens *et al.* (2005) demonstrated the presence of the Asquempont Detachment System in several boreholes in the unexposed parts to the WNW of the Senne-Sennette outcrop area. On the basis of the hanging wall and footwall stratigraphy, these authors deduced an initial NNE-dip for this detachment system, this being fully compatible with the outcrop data. Moreover, also Piessens *et al.* (2005) inferred that this detachment system should occur also along the north-side of the Brabant Massif (cf. Debacker *et al.*, 2003). Upon re-examining the Jodoigne Formation in the Gette outcrop area, to the NE of the Dyle-Thyle outcrop area, Herbosch *et al.* (accepted) proposed a new stratigraphic position for

this formation, and were able to explain the proximity between the lowermost Cambrian Blanmont Formation and the Middle to Upper Cambrian Jodoigne Formation by means of the Asquempont Detachment System. This is fully compatible with the NNE-dip inferred by Piessens *et al.* (2005) and also forms the first strong outcrop indication for the presence of the Asquempont Detachment System along the N-side of the Brabant Massif. The Asquempont Detachment System can now be traced for at least 110 km in a WNW-ESE-direction, and extends for at least 75 km in a NNE-SSW-direction. It is responsible for the removal of a sedimentary pile estimated at between 3.5 and 6 km thick and its activity can be constrained between the Caradoc and the time of cleavage development. Several questions remain to be answered, however: a) Is there a relationship with the large-scale slumping in the Caradoc?; b) What is the relationship with the Late Ordovician – lower Silurian magmatic activity?; c) Is the detachment system reflected by the degree of burial metamorphism?; d) How does the detachment system fit into the basin development and inversion history?; e) What are the cause and formation mechanism of this detachment system?

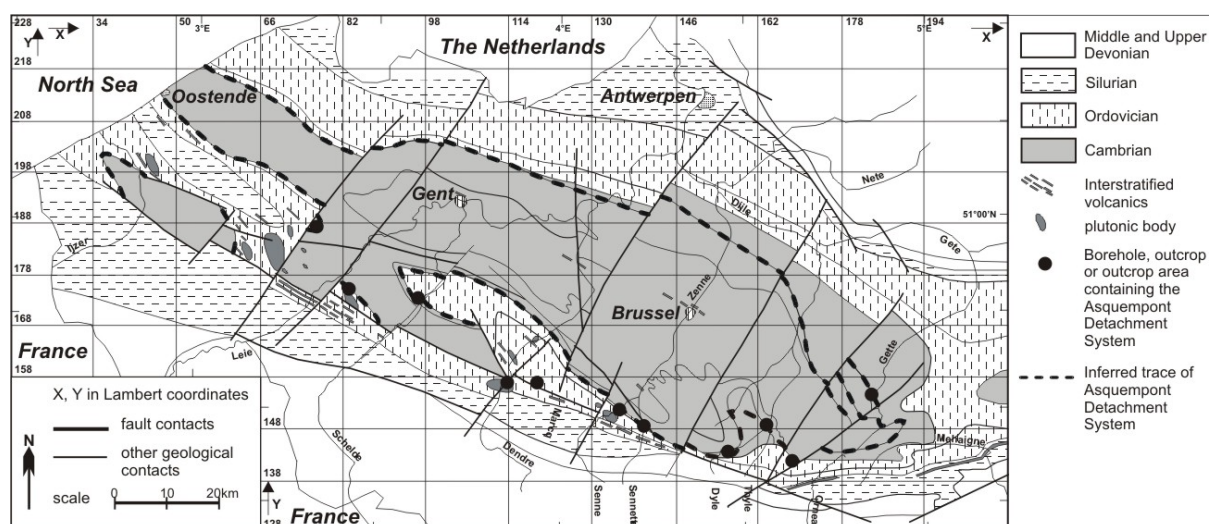


Figure 1. Geological map of the Brabant Massif, showing the occurrences and inferred trace of the Asquempont Detachment System

- DEBACKER, T.N., 2001. Palaeozoic deformation of the Brabant Massif within eastern Avalonia: how, when and why? Unpublished Ph.D. thesis, Laboratorium voor Paleontologie, Universiteit Gent.
- DEBACKER, T.N., DEWAELE, S., SINTUBIN, M., VERNIERS, J., MUCHEZ, PH. & BOVEN, A., 2005a. Timing and duration of the progressive deformation of the Brabant Massif, Belgium. *Geologica Belgica* 8, 20-34.
- DEBACKER, T.N., HERBOSCH, A. & SINTUBIN, M., 2005b. The supposed thrust fault in the Dyle-Thyle outcrop area (southern Brabant Massif, Belgium) re-interpreted as a folded low-angle extensional detachment. *Geologica Belgica* 8, 53-69.
- DEBACKER, T.N., HERBOSCH, A., SINTUBIN, M. & VERNIERS, J., 2003. Palaeozoic deformation history of the Asquempont-Virginal area (Brabant Massif, Belgium). *Memoirs of the Geological Survey of Belgium* 49, 30 p.
- DEBACKER, T.N., HERBOSCH, A., VERNIERS, J. & SINTUBIN, M., 2004. Faults in the Asquempont area, southern Brabant Massif, Belgium. *Netherlands Journal of Geosciences* 83, 49-65.
- HERBOSCH, A., DEBACKER, T.N. & PIESSENS, K. (accepted). The stratigraphic position of the Cambrian Jodoigne Formation redefined (Brabant Massif, Belgium). *Geologica Belgica*.
- LEGRAND, R., 1967. Ronquières. Documents géologiques. Mémoires pour servir à l'Explication des Cartes Géologiques et Minières de la Belgique 6, 1-60.
- MORTELMANS, G., 1955. Considérations sur la structure tectonique et la stratigraphie du Massif du Brabant. *Bulletin de la Société belge de Géologie, de Paléontologie et d'Hydrologie* 64, 179-218.
- PIESSENS, K., DE VOS, W., BECKERS, R., VANCAMPENHOUT, P., DE CEUKELAIRE, M., DEBACKER, T., SINTUBIN, M. & VERNIERS, J., 2005. Opmaak van de pre-Krijt subcropkaart van het Massief van Brabant voor invoering in de Databank Ondergrond Vlaanderen. Eindverslag voor het Ministerie van de Vlaamse Gemeenschap Afdeling Natuurlijke Rijkdommen en Energie. 90p.

SINTUBIN, M., 1999. Arcuate fold and cleavage patterns in the southeastern part of the Anglo-Brabant fold belt (Belgium): tectonic implications. *Tectonophysics* 309, 81-97.

4. Geometry and evolution of the Nansha trough foreland thrust and fold belt of South China Sea, China

Shimin Wu¹, Huafu Lu² & Shengli Wang²

1. South China Sea Institute Of Oceanology, Guangzhou, China

2. Nanjing University, China

Presenting author: smwu@scsio.ac.cn

Keyword(s): deformation, foreland basin, South China Sea, Nansha Trough

The Nansha trough foreland thrust and fold belt is a thin-skinned foreland thrust and fold belt of Late Miocene to Quaternary age that deforms early Tertiary through Quaternary reef limestone, shale, silty sandstone strata. Four fault-related fold zones in NE trends distribute from NW to SE of the belt. The folds include the fault-bend fold, fault-propagation folds, detachment folds, structure wedges etc. Growth strata analyses indicate that the fold zone and related faults emplace from SE to NW. The balance geological cross sections show approximate 22.87% (~18.75km) shortening for the thrust and fold belt. Combined with adjacent area tectonic study, a “scissors type” subduct and collide model was suggested. The evolutionary history of Nansha trough foreland basin has a close link to the Paleo-South China Sea and current South China Sea.

5. Grain boundary migration in quartz: not a simple story

Helena Bergman¹ & Sandra Piazzolo¹

1. Stockholm University, Sweden

Presenting author: bergman@geo.su.se

Keyword(s): microstructures, annealing, quartz

We present observations of microstructures in naturally annealed quartzite from the contact aureole of Ballachulish (Scotland), using cathodoluminescence (CL) and electron backscatter diffraction (EBSD). The study and interpretation of microstructures developed in naturally thermally altered rocks, plays an important role in unravelling the history and dynamics of processes recorded in the Earth's crust. CL images reveal a series of fine-scale alternating bands of bright and dark luminescent material that are interpreted to represent different positions of migrating grain boundaries during growth. These bands can be viewed as time series during the migration of grain boundaries providing the unique opportunity to directly track the grain boundaries movement and its relation to crystallographic orientation and grain boundary shape. The analysis of the only weakly deformed samples, collected at an increasing distance from the intrusion gives a temperature and duration of growth profile. Four such profiles were analysed, each including samples ~20m, ~400m and ~900m from the intrusion. An overall increase in grain size and straighter grain boundaries with decreasing distance to the contact is recorded. In addition, we observe a marked anisotropy of grain boundary properties. A number of grain boundaries grow at a late stage bulges which are approaching a triangular shape, hence increasing not decreasing the grain boundary surface area. We believe these represent low-energy surfaces related to crystal facets. Preliminary results suggest that grain boundary energy and/or mobility is connected to the c-axis orientation of the two grains involved during grain growth. Neighbouring grains separated by a high mobility boundary, as recorded in broad CL-bands, have a high angle between their c-axes. The opposite holds for low angle boundaries. Features such as single grain boundaries movement while surrounding grain boundaries stay stable underline the fact that indeed even in quartz grain boundary anisotropies do play a role during grain growth. In samples which exhibit up to 10 vol% feldspar, we observe interesting interferences of quartz grain boundary movement with feldspar. Grain boundaries that have moved more or less perpendicular to a feldspar grain show a fan-like pattern with wider dark bands between the bright bands, than further away from the feldspar grain. This may be due to pinning at the quartz-feldspar boundary, resulting in stepwise movement along that boundary. Here, EBSD data show no crystallographic change over the CL-bands. Furthermore, there is a marked increase of Dauphiné twinning with decreasing distance to the contact which is attributed to the phase transition from beta to alpha quartz. Our study shows that the combination of detailed cathodoluminescence and EBSD analysis is a powerful tool to link directly swept areas, growth direction and lattice orientation in crystalline materials. With this technique it is possible to analyse the mechanism of grain growth and grain boundary migration after a growth event.

6. The effect of grain size sensitive flow on synthetic calcite 'conglomerates'.

Alexander Edwards¹, Stephen Covey-Crump¹ & Ernest Rutter¹

1. University of Manchester, School of Earth, Atmospheric and Environmental Sciences, Rock Deformation Laboratory, U.K.

Presenting author: alexander.edwards@postgrad.manchester.ac.uk

Keyword(s): calcite, grain size sensitive, stress, strain

Naturally deformed clastic rocks such as breccias and conglomerates provide a useful way to study strain but grain size sensitive deformation processes potentially compromise many of commonly used methods of determining strain in such rocks at high temperatures. In order to explore this matter quantitatively, we have performed a number of deformation experiments on synthetic calcite 'conglomerates' at temperatures where we can vary the rate-dependence of grain size-sensitive deformation processes in clasts and matrix. In order to control the microstructures of the experimental samples, specimens were fabricated by mixing granulated Solnhofen Limestone with powders of Chelometric grade calcite. The mixtures were tumbled for 3 hours duration to ensure uniform intermixing of the powders, and were then hot isostatically pressed at 144 MPa and 700°C for three days. The resulting samples are fully dense and comprise sub-spherical Solnhofen clasts <90µm in diameter, in a foam-textured matrix of Chelometric calcite with a grain size of, 18µm ±3µm. An initial set of deformation experiments were performed on pure Chelometric grade samples to establish the flow behaviour of the matrix. Subsequent experiments are being performed on samples in which the volume fraction of clasts:matrix is being varied in the range 10:90 to 30:70. In order to assess the accuracy of strain measurements made on deformed conglomerates and in particular, the potential complicating influence of grain size-sensitive flow on those measurements, Fry and Rf/phi methods are being used to determine the matrix and clast strains respectively in the experimental samples, and after which clast strains are compared with the imposed bulk strains on the samples. Comparisons with strains obtained in like manner from a naturally deformed polygenetic clastic rock such as those in the Dalradian rocks at Onich, Scotland will also be presented.

7. The fabrics and kinematics of anhydrite rocks from central Italy

Rebecca Hildyard¹, Daniel Faulkner¹, David Prior¹, Nicola De Paola² & Cristiano Collettini³

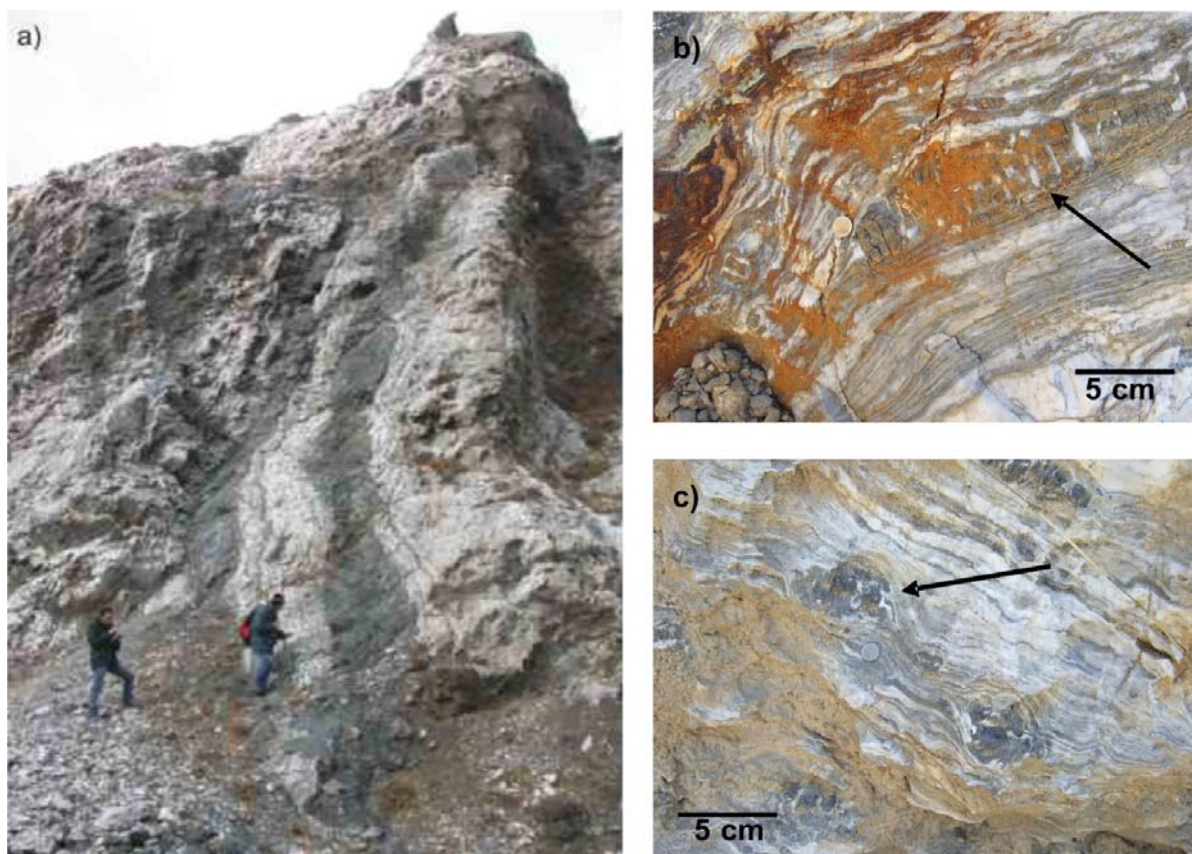
1. University of Liverpool, Department of Earth and Ocean Science, U.K.

2. University of Durham, Earth Science Department, Reactivation Research Group, U.K.

3. Università di Perugia, Dipartimento di Scienze della Terra, Gruppo di Geologia Strutturale e Geofisica, Italy
Presenting author: rebecca.hildyard@liverpool.ac.uk

Keyword(s): anhydrite deformation fabrics

In the Northern Apennines of central Italy a sequence of evaporitic rocks have been recognized as a detachment horizon (ductile behaviour) active during a Cretaceous to Quaternary stage of shortening and thrusting (Bally *et al.* 1986; Barchi *et al.* 1998a). It has been suggested that the later, Miocene – Recent, post-collisional extension was accommodated along these horizons and recently, it was observed that the nuclei of the 1997-1998 Colfiorito earthquake sequence (in the Umbria-Marche Apennines) were located along extensional normal faults within these evaporitic rocks (brittle behaviour) (e.g. Miller *et al.* 2004). In general, an understanding of the mechanisms and processes that lead to the change from distributed, ductile behaviour of detachment zones to localised, brittle faulting within evaporite horizons is important as this has implications for fluid flow through fault zones within evaporitic rocks and also for the seismogenic properties of these areas (De Paola *et al.*, In Press). The Triassic Evaporites are a 1.5 to 2 km thick package of alternating layers of evaporite and dolostones (Figure 1a). Below 1 km depth 95% of the evaporite is anhydrite and at shallower depths re-hydration has occurred and gypsum is dominant. During the early shortening phase of deformation, the Triassic Evaporites developed a compositional layer (cm – m scale Ca-sulphates interbedded with cataclastic dolostones) and mesoscale flow structures, e.g. isoclinal folds (Figure 1b). These structures are overprinted by a tectonite fabric which results in an over all “gneissic” fabric within the evaporites now seen close to the surface (Figure 1c) (Paola *et al.* 2007). Although highly detailed macroscopic observational studies have been carried out on the Triassic Evaporites at the surface, the associated microstructures (both from depth and at the surface) are poorly constrained. This work aims to characterize the early compressional, and therefore ductile, microstructures and crystallographic fabrics seen in anhydrite samples from boreholes drilled to ~3km depth. Optical and SEM techniques will be used, including Electron Backscatter Diffraction (EBSD) to map out the crystallographic preferred orientation (CPO) of the anhydrite rocks from depth. These analyses will constrain both the kinematics and the deformation mechanisms (i.e. diffusion creep and/or dislocation creep etc.) which were operative at the time. This type of analysis has not previously been attempted for anhydrite rocks. Once a significant data set has been established for the borehole anhydrites it is hoped that new techniques can be developed to measure the CPOs of gypsum rocks collected from the surface, which have undergone exhumation and rehydration, to establish whether the original, ductile anhydrite fabrics have any control on the inherited fabrics within the gypsum.



- BALLY, A., BURBI, L., COOPER, C. & GHELARDONI, R., 1986. Balanced sections and seismic reflection profiles across the Central Apennines. *Memorie della Societa Geologica Italiana* 35: 257-310.
- BARCHI, M. R., DE FEYTER, A., MAGNANI, M., MINELLI, G., PIALLI, G. & SOTERA, B., 1998a. The structural cycle of the Umbria-Marche fold and thrust belt. *Memorie della Societa Geologica Italiana* 52: 557-578.
- MILLER, S. A., COLLETTINI, C., CHIARALUCE, L., COCCO, M., BARCHI, M. & KAUS, B. J. P., 2004. Aftershocks driven by a high-pressure CO₂ source at depth. *Nature* 427(6976): 724-727.
- PAOLA, N. D., COLLETTINI, C., TRIPPETTA, F., BARCHI, M. R. & MINELLI, G., 2007. A mechanical model for complex fault patterns induced by evaporite dehydration and cyclic changes in fluid pressure. *Journal of Structural Geology* 29(10): 1573-1584.

8. Experimental dehydration and deformation of Volterra Gypsum: preliminary experiments and overview

Sergio Llana-Funez¹, Daniel Faulkner¹ & John Wheeler¹

*1. University of Liverpool, Department of Earth Sciences, U.K.
Presenting author: slf@liverpool.ac.uk*

Keyword(s): experimental deformation, gypsum

Experimental dehydration of gypsum, simultaneous to the application of differential stresses may provide valuable insight of controlling processes during the evolution of faults and its relation to seismicity (fault-valve behaviour or seismic pumping). Gypsum is directly involved in the development of some faults in the upper crust and from the mechanical point of view its syn-tectonic dehydration may be an analogue to similar metamorphic transitions in other hydrated minerals in subduction zones. Experimentally, gypsum is very accessible to deformation and petrological experiments since its yield strength is about 90 MPa at 100 MPa and it dehydrates at measurable rates (days) at temperatures slightly over 80 °C. The complete dehydration to anhydrite involves a reduction in volume of the solids of 38 % and bulk volume increase of 12%, which allows to monitor the progress of the reaction. In laboratory experiments (at strain rates of $\sim 10^{-5} \text{ s}^{-1}$), dry gypsum deforms by a combination of twinning and cataclasis. Stress-strain curves show the development of stress drops in relation to the formation of short-lived cataclastic bands. The formation of these bands is reduced but still present when samples are wet. We present preliminary results on the isothermal dehydration of Volterra gypsum at atmospheric pressure and various temperatures and on the deformation of dry specimens at room temperature at various confining pressures. Two series of simple heating experiments of Volterra gypsum samples at room pressure, using intact and powdered specimens, provide reference data for future experiments under confining and differential stress. Heating experiments were run at constant temperature between 80 °C and 140 °C in intact specimens and at 86 °C and 97 °C using powders with five different grain size fractions: <0.063, 0.063-0.125, 0.125-0.25, 0.25-0.5 and >0.5 mm. The complete dehydration of gypsum to anhydrite implies a weight loss of 21 % upon removal of water. The weight reduction of solids was used to estimate the progress of the reaction. The reaction is characterized by an initial stage under 10 % reaction where rates accelerate, which is followed by a linear stage for about 50 to 70% of the reaction and a final third stage with decelerating reaction rates. All tests run above 85 °C reached about 90 % reaction. Those below 85 °C seem to converge to a lower final fraction (~ 75 %) suggesting partial dehydration, very likely to bassanite. The temperature dependence of the linear rates indicates in an Arrhenius plot that the full dehydration of gypsum has an activation enthalpy of $96.0 \pm 0.4 \text{ kJ/mol}$. The two temperatures tested with powdered specimens are consistent with this activation enthalpy, although the higher values of y-axis intercepts ($\ln k$) indicate that reaction rates are about one order of magnitude faster. This is interpreted in relation to the very large initial porosity of the un-compacted powdered specimens (>45 % porosity). There is an additional marginal increase in rates in powdered specimens as the grain size decreases eight-times. A first series of deformation tests on dry gypsum have also been run at room temperature, at strain rates of $2 \cdot 10^{-5} \text{ s}^{-1}$ and confining pressures of 13, 50, 100, 146, 190 MPa. Tests were run in a triaxial rig using 20 mm diameter by 45 mm length specimens. Stress-strain curves show well-defined yield points and an almost straight plastic behaviour with a slight strain hardening component, similar to previous work in literature. The grain fracturing associated with the generation of cataclastic bands during experimental deformation of gypsum has the potential of affecting

the dehydration kinetics by the associated increase in surface area of smaller gypsum fragments.

9. The role of fluid-filled grain boundaries in substructure development: new insights from see-through deformation experiments

Joyce Schmatz¹ & Janos L. Urai¹

1. RWTH Aachen, Geologie-Endogene Dynamik, Germany

Presenting author: j.schmatz@ged.rwth-aachen.de

Keyword(s): grain boundary mobility, fluid inclusions, chemical weakening

Subgrain boundaries (SGB) and grain boundaries (GB) play a major role in microstructural development, and therefore the physical and chemical properties of a crystalline material. In this study particular attention is given to the presence of fluids on GB as this is of crucial importance to the behaviour of the Earth's crust and mantle. The role GB properties and behaviour in the mechanical properties of materials remains poorly understood and is therefore often oversimplified. For example, the role of recrystallization on the rheology of rocks is described with grain size sensitive flow laws whereas effect of GB fluid is approximated in separate equations, based on the principle of enhanced diffusion processes. It is well known that physical properties such as pore fluid pressure as well as chemical processes such as mineral reactions and mass transfer play a major role during deformation and recovery, but there are not many quantitative statements on how fluid-filled GB and fluid inclusions affect GB and SGB structure and mobility. In this study we address, amongst others, questions like: What is the magnitude of velocity of a fluid-filled GB? How is a fluid phase distributed and reorganized during recrystallization and recovery? Which role does pore fluid chemistry play in weakening processes and substructure development? What is the impact of viscosity and the interplay with variable boundary conditions such as stress, strain rate and temperature? For this purposes we use a newly developed see-through deformation apparatus, which provides a fluid pressure system that controls confining pressure (up to 30 MPa) and can be used for temperatures up to 200°C, first established by Schenk and Urai (2005). We deform natural and synthetic samples of rock salt in the presence of saturated brine. As halite has a cubic crystal structure observations in transmitted light only acquaint us with information on high angle GB and phase boundaries. To improve our knowledge on substructure development we also employ a simplified setup of the deformation rig, which goes without the controlled fluid pressure system, and therefore allows fast and efficient deformation experiments on the rock analogue camphor. The camphor experiments are conducted in the presence of fluid with different viscosities, namely water (H₂O), ethylene glycol, and glycerin, which are poor solvents of camphor. Reference experiments with camphor-saturated ethanol (see also Walte *et al.*, 2003) have also been conducted. Fluid-filled GB in halite experiments show high mobility during dynamic and metadynamic stages as well as the ability to incorporate isolated fluid inclusion and to distribute them along GB or leave them behind as secondary fluid inclusions. Fluid-filled GB in camphor experiments show the ability to pin high angle GB and therefore decrease mobility. During static phases this equalizes: surface energy seems to override pinning effects of the fluid phase and GB, fluid-filled or not (microscopic resolution), equilibrate with a comparable magnitude of velocity. A strong tendency for the formation of low angle GB at existing isolated fluid inclusions is observed. An evaluation of the first results shows that chemical reactions play a crucial role, rather than physical effects such as pore fluid pressure. This agrees with studies by Kronenberg (1994). Experiments done with ethanol show comparable results to halite

experiments and a minor tendency to the formation of SGB compared to setups with a non-solving fluid phase. The interaction of GB with the fluid phase shows strong reliance on particle coherency (Humphreys, 1996). In future setups we will investigate the differences in substructure development of analogous experiments done with and without a fluid phase.

HUMPHREYS, F. J. & HATHERLY, M., 1996. Recrystallization and related annealing phenomena, Pergamon, 497pp.

KRONENBERG, A. K., 1994. Hydrogen speciation and chemical weakening of quartz. Silica: Physical behavior, geochemistry, and materials applications. P. J. HEANEY, C. T. PREWITT & GIBBS, G. V. Washington, Mineralogical Society of America 29: 123-176.

SCHENK, O. & URAI, J.L., 2005. The migration of fluid-filled grain boundaries in recrystallising synthetic bischofite: first results of in-situ high-pressure, high-temperature deformation experiments in transmitted light. *Journal of Metamorphic Geology* 23, 695-709.

WALTE, N.P., BONNS, P.D., PASSIER, C.W. & KOEHN, D., 2003. Disequilibrium melt distribution during static recrystallization. *Geology* 31, 1002-1012.

10. The centennial of the terms 'boudin' and 'boudinage' - a historical retrospect

Manuel Sintubin¹

1. Katholieke Universiteit Leuven, Geodynamics & Geofluids Research Group, Belgium
Presenting author: manuel.sintubin@geo.kuleuven.be

Keyword(s): boudinage, history

The first geometrical description of the particular quartz-vein occurrence in the Bastogne area (Belgium) goes back to 1888 when Gosselet mentions in his chapter on metamorphism in the Ardenne that "*tous ces filons de quartz ... sont limités au grès et s'arrêtent à la cornéite*". In his work on the origin of the metamorphic rocks in the Bastogne area, Stainier (1907) presents an extensive inventory of the occurrence and geometry of these veins, demonstrating the regional occurrence and significance of the veins and associated structures. To explain these particular structures, he invokes a polyphase brittle-ductile deformation sequence: "*... c'est grâce à la préexistence des filons quartzeux et des crevasses que l'on peut expliquer l'allure en chapelet et l'allure en petites voussettes, unique en Ardenne, que présentes les bancs de grès de la région. Si ces bancs de grès n'avaient pas présenté des fissures, la poussée tangentielle du grand ridement les aurait plissées en voûtes ou bassins ordinaires; ou bien, si la poussée avait été trop forte, elle aurait déterminé la production de failles inverses de refoulement. Au lieu de cela, chaque compartiment d'un banc de grès, devenu indépendant des ses voisins dont il était séparé par un joint quartzeux, s'est arqué, pour son compte, en une petite voussette ou bien s'est renflé en saucisson ou grain de chapelet*". To Stainier the sequence of events was evident: first fracturing and veining, then layer-parallel shortening, all prior to the main Variscan folding and cleavage development. To demonstrate the work of Stainier, a field trip was organised by the Société Géologique de Belgique. On August 31st, 1908, at the *Carrière Collignon* near Bastogne, Lohest introduced the terms 'boudin' and 'boudinage' in order to facilitate discussions: "*Lorsque l'on voit ces segments renflés sur une surface de stratification étendue, mise à nu par l'exploitation, on croirait voir une série d'énormes cylindres ou boudins alignés côté à côté ... sur l'initiative de M. Lohest on a fréquemment utilisé, pour la facilité du langage, les néologismes de boudiner et de boudinage.*" (Lohest *et al.* 1908). At this early stage, these terms were used purely descriptive to indicate the series of sausage-like structures, lying side by side. Already during the field trip, a discussion unfolds on the relative timing of the different deformation features, setting the stage for a century long discussion on the development of these particular structures observed at Bastogne. In the first half of the 20th century numerous models were proposed with variable chronologies with respect to the development of the different deformation features (Corin 1932, Holmquist 1931, Quirke 1923, Wegmann 1932), clearly demonstrating the uncommon nature of the structures (cf. Quirke 1923). Although these authors often mentioned that the 'boudins' at Bastogne were seemingly related to 'pinch-and-swell' structures as described by e.g. Ramsay (1866) and Harker (1889), it was generally agreed that they did not fully resemble, primarily because of the strongly different aspect ratio of the segments (Holmquist 1931, Walls 1937). Cloos (1947), however, did not make this clear distinction, and the term 'boudinage', applied to both types of structures, obtained its current kinematic definition referring to a process of disruption of layers, bodies or foliation planes within a rock mass in response to bulk extension along the enveloping surface (cf. Goscombe *et al.* 2004). Eversince confusion only got worse, in particular when very similar structures in the North Eifel region were described as 'mullions' (Pilgers & Schmidt 1957). In an attempt

to relate the ‘mullions’ of the North Eifel – considered as layer-parallel shortening structures (i.e. cusped-lobate folding) – and ‘boudins’ of Bastogne – at that time considered as extension structures – terms such as L-boudins or ‘*auslängungs-boudins*’ and K-boudins or ‘*verkürzungs-boudins*’ were introduced (Brühl 1969). The ‘mullions’ of Pilgers and Schmidt (1957) became ‘half-boudins’ (Brühl 1969). Quickly, it was acknowledged that this new terminology was definitively not the solution to the confusing, taking into account that the association of the term ‘boudinage’ with bulk extension was already too entrenched in English literature (Mukhopadhyay 1972). Mukhopadhyay (1972) and Spaeth (1986), more recently corroborated by Urai *et al.* (2001), considered the structures in the Ardenne-Eifel region as mullions. Apart from them the idea of ‘shortened boudins’ gained, however, ground, primarily based on the atypical aspect ratio of the segments (Jongmans & Cosgrove 1993, Lambert & Bellière 1976, Rondeel & Voermans 1975), an idea still persistent to date (Vanbrabant & Dejonghe 2006). A century of debate primarily focused on the cusped-lobate – sausage-like – geometry of the sandstone-pelite bedding interface, largely ignoring the quartz veins. Renewed interest in the quartz veins allowed constraining the formation conditions and kinematic significance of the veins with respect to the overall structure development (Kenis *et al.* 2005a, Kenis *et al.* 2002). A numerical modelling approach (Kenis *et al.* 2004) ultimately corroborated the mullion model and even allowed to use the particular cusped-lobate morphology to constrain the rheology of the deforming middle crust (Kenis *et al.* 2005b). Ultimately, the hypothesis initially postulated by Stainier in 1907 becomes remarkably up to date!

- BRÜHL, H., 1969. Boudinage in den Ardennen und in der Nordeifel als Ergebnis der inneren Deformation. *Geologische Mitteilungen* 8, 263-308.
- CLOOS, E., 1947. Boudinage. *Transactions of the American Geophysical Union* 28(4), 626-632.
- CORIN, F., 1932. A propos du boudinage en Ardenne. *Bulletin de la Société belge de Géologie* 42, 101-117.
- GOSCOMBE, B. D., PASSCHIER, C. W. & HAND, M., 2004. Boudinage classification: end-member boudin types and modified boudin structures. *Journal of Structural Geology* 26(4), 739-763.
- GOSSELET, J., 1888. L’Ardenne. *Mém. Expl. Carte géol. France*, 1-889.
- HARKER, A., 1889. On local thickening of dykes and beds by folding. *Geological Magazine* 6(69-70).
- HOLMQUIST, P. J., 1931. On the relations of the “boudinage-structure”. *Geol. Fären. Färhandl.* 53, 193-208.
- JONGMANS, D. & COSGROVE, J. W., 1993. Observations structurales dans la région de Bastogne. *Annales de la Société géologique de Belgique* 116, 129-136.
- KENIS, I., MUCHEZ, P., VERHAERT, G., BOYCE, A. J. & SINTUBIN, M., 2005a. Fluid evolution during burial and Variscan deformation in the Lower Devonian rocks of the High-Ardenne slate belt (Belgium): sources and causes of high-salinity and C-O-H-N fluids. *Contribution to Mineralogy and Petrology* 150, 102-118.
- KENIS, I., SINTUBIN, M., MUCHEZ, P. & BURKE, E. A. J., 2002. The “boudinage” question in the High-Ardenne slate belt (Belgium): a combined structural and fluid inclusions approach. In: *Tectonophysics* (edited by Labaume, P., Craw, D., Lespinasse, M. & Muchez, P.). *Tectonophysics* 348, 93-110.
- KENIS, I., URAI, J. L., VAN DER ZEE, W., HILGERS, C. & SINTUBIN, M., 2005b. Rheology of fine-grained siliciclastic rocks in the middle crust - evidence from structural and numerical analysis. *Earth and Planetary Science Letters* 233, 351-360.
- KENIS, I., URAI, J. L., VAN DER ZEE, W. & SINTUBIN, M., 2004. Mullions in the High-Ardenne Slate Belt (Belgium). Numerical model and Parameter Sensitivity Analysis. *Journal of Structural Geology* 26(9), 1677-1692.
- LAMBERT, A. & BELLIERE, J., 1976. Caractères structuraux de l’éodévonien aux environs de Bastogne. *Annales de la Société géologique de Belgique* 99, 283-297.
- LOHEST, M., STAINIER, X. & FOURMARIER, P., 1908. Compte rendu de la session extraordinaire de la Société Géologique de Belgique, tenue à Eupen et à Bastogne les 29, 30 et 31 août et le 1, 2 et 3 septembre 1908. *Annales de la Société géologique de Belgique* 35, B351-B434.
- MUKHOPADHYAY, D., 1972. A note on the mullion structures from the Ardennes and North Eifel. *Geologische Rundschau* 61, 1037-1049.
- PILGERS, A. & SCHMIDT, W., 1957. Die Mullion-Strukturen in der Nord-Eifel. *Abh. Hess. Landesamtes Bodenforsch.* 20, 1-53.
- QUIRKE, T. T., 1923. Boudinage, an unusual structural phenomenon. *Geological Society of America Bulletin* 34,

649-660.

RAMSAY, A. C., 1866. The Geology of North Wales. *Memoirs of the Geological Survey of Great Britain* 3, 1-75.

RONDEEL, H. E. & VOERMANS, F. M., 1975. Data pertinent to the phenomenon of boudinage at Bastogne in the Ardennes. *Geologische Rundschau* 64, 807-818.

SPAETH, G., 1986. Boudins and Mullions in devonischen Schichtfolgen der Nordeifel und Ardennen - Erscheinungsbild, Entstehung und Umformung. *Nachrichten Deutsche Geologische Gesellschaft* 35, 74-75.

STAINIER, X., 1907. Sur le mode de gisement et l'origine des roches métamorphiques de la région de Bastogne. *Mémoire de l'Académie royal de Belgique, classe des Sciences. Collection 4^e, 2ième série.*

URAI, J. L., SPAETH, G., VAN DER ZEE, W. & HILGERS, C., 2001. Evolution of mullion (formerly boudin) structures in the Variscan of the Ardennes and Eifel. *Journal of the Virtual Explorer* 3, 1-15.

VANBRABANT, Y. & DEJONGHE, L., 2006. Structural analysis of narrow reworked boudins and influence of sedimentary successions during a two-stage deformation sequence (Ardenne-Eifel region, Belgium-Germany). *Memoirs of the Geological Survey of Belgium* 53, 1-43.

WALLS, R., 1937. A new record of boudinage-structure from Scotland. *Geological Magazine* 74, 325-332.

WEGMANN, C. E., 1932. Note sur le boudinage. *Bulletin de la Société géologique de France* 52, 477-491.

11. The compaction dependent cohesion and tensile strength of gypsum powder – the effect on scaled analogue models

Heijn van Gent¹, Marc Holland¹ & Janos L. Urai¹

1. RWTH Aachen University, Geologie - Endogene Dynamik, Germany

Presenting author: h.vangent@ged.rwth-aachen.de

Keyword(s): material properties, scaled analogue modelling, gypsum powder, Cam Clay model

Sandbox modelling has been used extensively over the last decades to model shallow geological processes. The materials used to date are however not well scaled for studying rocks with a high brittleness index, i.e. materials that are strong in comparison to the mean effective stress. Typically, materials like sand and clay do not develop brittle, dilatant structures observed in rocks like basalt and carbonate at shallow crustal depth, and recently it was realised that sand has only an “apparent” cohesion, with shear stress/ normal stress plots curving towards zero at very low normal stress tests (Schellart, 2000). The use of truly cohesive powders is becoming increasingly common in (scaled) structural analogue modelling (Sims *et al.*, 2003; Galland *et al.*, 2006; Holland *et al.*, 2006). In scaled models of extension, compression and transpression, we have been using commercial gypsum powder. This powder has a measurable, non-compacted, true cohesion of 50Pa and tensile strength of 5Pa. Measurements are done using a modified Jenike Shear Cell (van der Zee, 2001) at low normal stress, supported by odometer compaction data and tensile strength data, measured using a pharmaceutical machine described by (Schweiger and Zimmermann, 1999). Using an overcompaction and relaxation approach in respect to the shear cell measurements, and increasing the initial load in the tensile strength measurements, we observe that both cohesion and tensile strength are linearly dependent of the amount of precompaction and the related pore space reduction. The coefficient of internal friction does not dependent on compaction, and remains constant around 0.6. Combining data from all methods, allowed us to define the material properties of the powder, using a modified, 3D Cam Clay model, which is used in Soil Mechanics (Lambe and Whitman, 1969), showing tensile and shear failure and compaction relations in a single plot. In extension experiments we observe failure type transitions of tensile fractures to dilatational fractures with fault plane asperities and from dilatational fractures to shear fractures, at consistent depths in the model throughout the model series. We couple these transitions to the increase of powder strength with compaction due to depth in the experiment, similar to compaction in sedimentary basins. Using the empirical relations for the material, we reconstructed stress states at different depths of the model, which are consistent with the failure type transition observations. Due to the cohesive nature of the powder, further interesting observations include very discrete fractures, the creation of fault plane asperities and their subsequent filling by gravitational transport, the evolution of fault arrays and overstepping of normal faults, and rigid block rotation and disintegration which were quantified using a Particle Image Velocimetry analysis (PIV, e.g. (Adam *et al.*, 2005; Holland *et al.*, 2006) in respect to kinematics, strain and rotation.

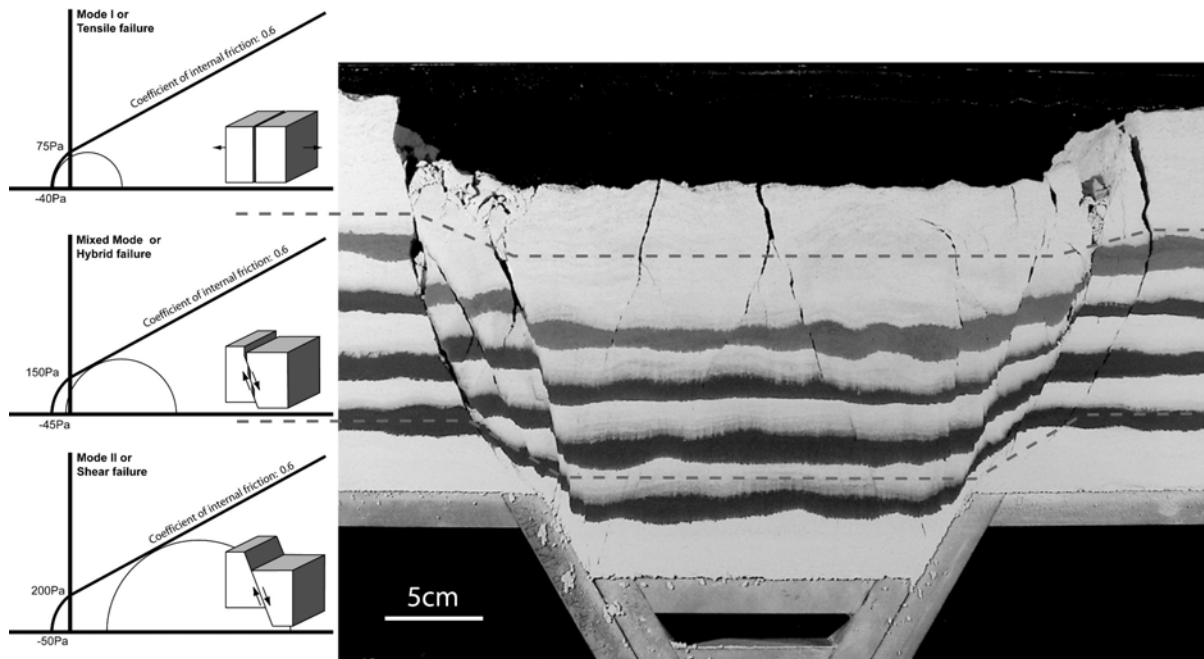


Figure 1. The effects of increases in cohesion and tensile strength are expressed by changes in the failure type with depth. Mohr diagrams are scaled using data from the material properties.

ADAM, J., URAI, J. L., WIENEKE, B., ONCKEN, O., PFEIFFER, K., KUKOWSKI, N., LOHRMANN, J., HOTH, S., VAN DER ZEE, W. & SCHMATZ, J., 2005. Shear localisation and strain distribution during tectonic faulting--new insights from granular-flow experiments and high-resolution optical image correlation techniques. *Journal of Structural Geology* 27(2), 283.

GALLAND, O., COBBOLD, P. R., HALLOT, E., DE BREMOND D'ARS, J. & DELEVAUD, G., 2006. Use of Vegetable oil and silica powder for scale modelling of magmatic intrusion on a deforming brittle crust. *Earth and Planetary Science Letters* 243, 786-804.

HOLLAND, M., URAI, J. L. & MARTEL, S., 2006. The internal structure of fault zones in basaltic sequences. *Earth and Planetary Science Letters* 248(1-2), 286-300.

LAMBE, T. W. & WHITMAN, R. V., 1969. *Soil Mechanics*. John Wiley & Sons, Inc, New York.

SHELLART, W. P., 2000. Shear test results for cohesion and friction coefficients for different granular materials: scaling implications for their usage in analogue modelling. *Tectonophysics* 324(1-2), 1-16.

SCHWEIGER, A. & ZIMMERMANN, I., 1999. A new approach for the measurement of the tensile strength of powders. *Powder Technology* 101(1), 7-15.

SIMS, D. W., MORRIS, A. P., FERRILL, D. A., WYRICK, D. Y. & COLTON, S. L., 2003. Physical models of pit chain formation over dilatational faults in Mars. *Lunar and Planetary Science XXXIV*.

VAN DER ZEE, W., 2001. Dynamics of fault gouge development in Layers sand-clay sequences. Shaker Verlag, Aachen, PhD thesis

12. The Hazar pull-apart along the East Anatolian Fault: structure and active deformation

Aurelia Hubert-Ferrari¹, David Garcia¹, Jasper Moernaut², Maarten Van Daele², Emre Damci³, Xavier Boes¹, Jeff Fraser¹, Namik Cagatay³ & Marc De Batist²

1. Royal Observatory of Belgium, Brussels, Belgium

2. Ghent University, Renard Centre of Marine Geology, Belgium

3. Istanbul Technical University, Eastern Mediterranean Centre for Oceanography and Limnology, Turkey

Presenting author: aurelia.ferrari@oma.be

Keyword(s): *strike-slip faulting, seismic survey*

The Hazar Lake occupies 20 km long, 5 km wide, 200 m deep pull-apart basin along the East Anatolian strike-slip Fault, which accommodates -together with the North Anatolian Fault- the westward extrusion of the Anatolian block. The lake is a major structure along the East Anatolian Fault, and is located within 100 km of at least three major dams on the Euphrates-Tigris river system. It was the locus of two earthquakes of magnitude 7.1 and 6.7 in respectively 1874 and 1875. This poorly studied lake (only approximate bathymetric map, no geophysical survey, or sedimentological information) was the focus in summer 2007 of a multidisciplinary study in order to constrain its structure and sedimentation, and to propose a coherent scenario of the 1874-1875 earthquake sequence. We present here a fault map of the pull-apart basin constrained by seismic profiles obtained with sparker (400-1500 Hz) and with a mean spacing of 500 m between the profiles. The structural pull-apart, a 210 m deep basin with a fault step of less than 3 km, represents only 1/3 of the present lake extent and is located at the lake northeastern extremity. Further southwest, the lake is a half-graben with the main fault system bounding the southeast edge of the lake with a fault trace showing varying level of complexities with alternating small-scale pull-apart and push-up structures. Finally a first sketch of the structural development of the basin can be proposed.

13. 3D joint density mapping

Michael Drews¹ & Hagen Deckert¹

*1. University of Mainz, Institut für Geowissenschaften, Germany
Presenting author: michaeldrews@gmx.com*

Keyword(s): photogrammetry, 3D joint analysis

The characterization of joint density is commonly based on measuring the frequency of joint intersections along a line of predefined orientation. Conventional techniques are largely based on extrapolating one-dimensional measurements of discontinuity sets into three dimensions (e.g. S.D. Priest, 1993). Instead, we use digital photogrammetry for acquiring both orientation and position of fracture planes in an outcrop. This technique provides significant improvements for mapping and analysis of rock faces. The key advantage of this method over individual measurements is particularly the generation of a spatial point cloud and/or surface model referenced in 3D space. To analyse joint distributions in three dimensions the idea of counting planes intersected by one scanline has to be extended. We present a newly developed algorithm for analysing 3D joint networks based on photogrammetric images. The main idea is, that a population of joints distributed in three dimensions has to be analysed by sets of scanlines in all directions and of equal length. To provide reasonable data acquisition for a 3D investigation of joint distributions the mapping area has to be a sphere. Scanlines in such a spherical mapping space (SMS) should meet the following conditions (Fig.1): 1. All scanlines have to be radially distributed and have to cut the centre of the SMS, respectively. 2. The orientations of the scanlines should be generated to result in an equal distance distribution on the surface of the SMS. This idea coincides with the theoretical calculation of 3D frequency loci after Hudson and Priest (1983). In our study, these uniformly distributed origins of scanlines are derived from the Recursive Zonal Equal Area Sphere Partitioning (EQ-) Toolbox (Leopardi, 2006). With the resulting coordinates for 800 points on the upper hemisphere of a sphere from the EQ-Toolbox and by fulfilling the above mentioned conditions it is possible to create a fully automated algorithm, which is able to acquire spatially referenced data of total and directional joint density from three dimensional joint frequency loci. Thus, SMSs can be used to divide an outcrop into sub-domains and allows to address and map possible inhomogeneities in the frequency or density of joints in the investigated area. The application of our algorithm can be used to analyse 2.5D data derived from laser scanning or photogrammetry techniques (Fig. 1) as well as 3D data derived from generic fracture networks or CT scans. Our algorithm has been successfully applied for studying fracture density variations in sedimentary rocks of the Taunus Quartzite in Germany. To test our method a comparison between visualizations of theoretical frequency loci and the frequency loci produced by our method has been carried out for homogeneous generic fracture sets and inhomogeneous fracture sets of the Taunus Quartzite. We were able to determine and visualize total joint density maps from the generated surface models and additional joint density maps created for certain scanline directions (e.g. along the normal of the preferred orientation of a joint set) (Fig.2). This is useful for further interpretations in terms of rock quality designation as well as hydraulic conductivity estimations in hydrocarbon reservoirs, geothermal systems, and veining and alteration in hydrothermal ore deposits.

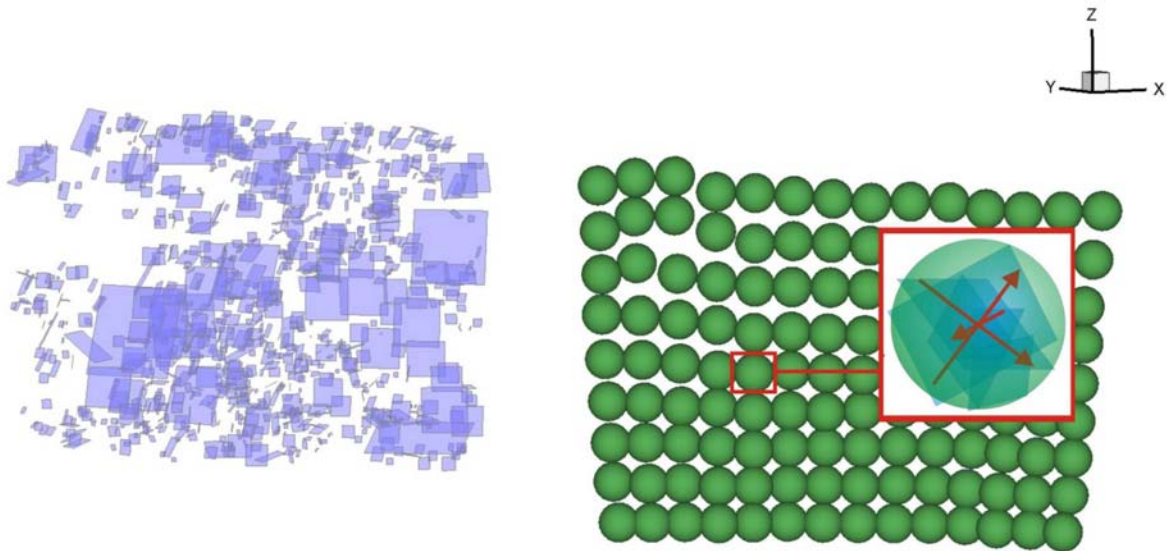


Figure 1. Left: Digitised joint planes derived from photogrammetry techniques. Right: SMS, each including a unit number of scanlines, distributed on the surface of a 3D image of an outcrop.

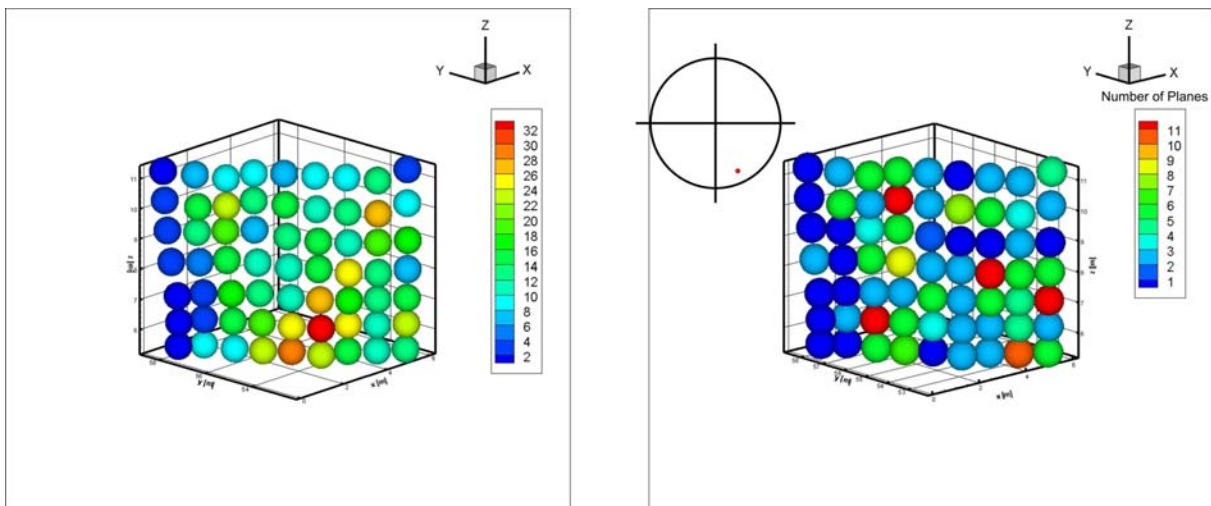


Figure 2. Left: Map of total joint density of a surface model of the Taunus Quartzite, Germany. Right: Map of joint density created for scanline directions along the normal of the preferred orientation of a joint set of the Taunus Quartzite. The red dot in the equal area plot shows the orientation of the surface normal of the mean set orientation.

HUDSON, J.A. & PRIEST, S.D., 1983. Discontinuity frequency in rock masses. *Int. J. Rock Mech. Min. Sci. & Geomech. Abstr.*, 20, 2, 73-89.

LEOPARDI, P., 2006. Distributing points on the sphere - Partitions, separation, quadrature and energy. Doctoral thesis, University of new South Wales, School of Mathematics and Statistics, Department of Applied Mathematics, pp. 232.

PRIEST, S.D., 1993. *Discontinuity analysis for rock engineering*. Chapman & Hall Inc., London, pp. 473.

14. Deformation-controlled fluid migration in a middle to upper-crustal level: a research strategy for the western part of Armorica (Brittany, France)

Isaac Berwouts¹, Philippe Muchez¹ & Manuel Sintubin¹

1. Katholieke Universiteit Leuven, Geodynamics & Geofluids Research Group, Belgium

Presenting author: isaac.berwouts@geo.kuleuven.be

Keyword(s): Armorican Massif, Léon Domain, fluid flow, metamorphism, research strategy

Quartz veins in siliciclastic metasediments and igneous rocks of the western part of Armorica (Brittany, France) have been described since long (Chauris & Hallégouët, 1973). Nevertheless, no detailed and/or regional research has been done on the exact significance of these veins with respect to deformation processes. This research project will determine P-T-X properties of vein-forming fluids, metamorphic conditions and the nature of the fluid system (open or closed). In a final stage, conclusions can be drawn on fluid properties and fluid migration in the western part of Armorica and vein formation during deformation. Objectives will be pursued by a research strategy containing two parts. Firstly, field observations will enable the mapping and description of the quartz veins and their geological context. Secondly, optical microscopy, microthermometry, chlorite geothermometry, Raman spectrometry, stable isotope and X-ray diffraction analyses are used to constrain the origin of the veins. The research strategy will focus on three particular target areas: the western part of the Central Armorican Terrane (CAT), the North Armorican Shear Zone (NASZ) and the Léon Domain (see figure 1). These regions underwent different grades of metamorphism (Rolet *et al.*, 1994), which will be important during analysis of chemical properties of the fluids. The study areas in the Central Armorican Terrane are the Monts d'Arrée, the Elorn valley and the Saint-Rivoal valley (see figure 1). During earlier research, seven different vein generations could be identified and framed within the deformation history (van Noorden *et al.*, 2007). On the basis of this vein paragenesis, geochemical analysis allowed to determine an increase in methane due to changing redox conditions during deformation. A future regional study of the veins can relate the fluid chemistry with the degree of metamorphism. The NASZ will be studied along outcrops spread out over 50 km from Landiviseau to Belle-isle-en-terre (see figure 1). This will lead to a better understanding of the properties of this regional-scale shear zone. Key outcrops will be sampled and analyzed to understand small-scale phenomena in the neighbourhood of the NASZ and the importance of the NASZ in regional-scale fluid migration. Sampled veins, covering the poorly exposed Léon Domain, will make it possible to get an overview of the geochemical properties of fluids during different stages of deformation in this allochthonous. The samples are being investigated by microthermometry and petrography. Further research, by XRD and chlorite geothermometry will give some information about changing P-T-X conditions during and after vein formation.

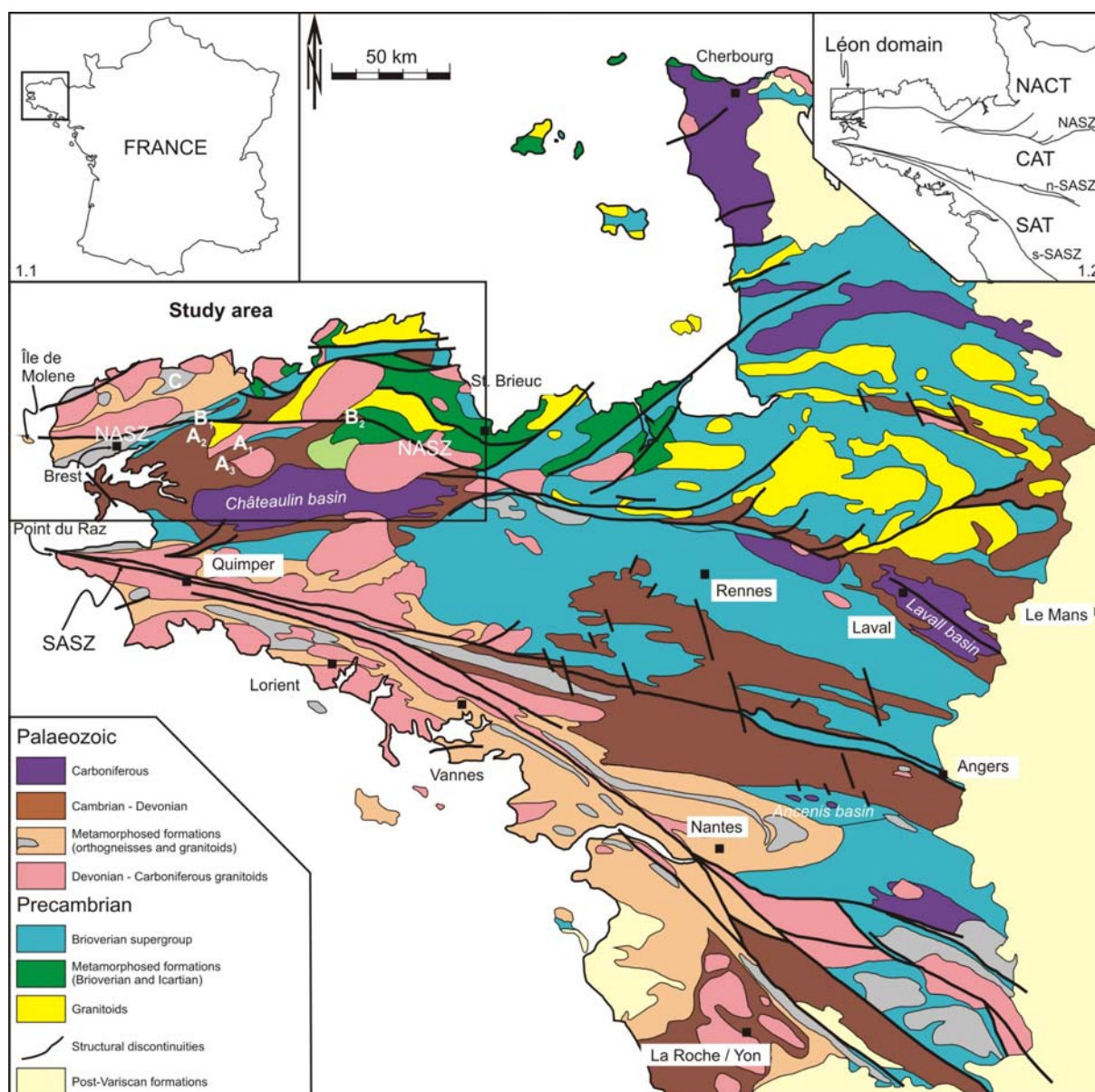


Figure 1. Schematic geological map of the Armorican Massif (after Le Corre et al. 1991), with inset (1.1) indicating its location in France, and inset (1.2) showing the subdivision of the Armorican Massif into the North Armorican composite terrane (NACT), Léon Domain, Central Armorican Terrane (CAT), and South Armorican terrane (SAT). Abbreviations: NASZ, North Armorican shear zone; n-SASZ, northern branch of the South Armorican shear zone; s-SASZ, southern branch of the South Armorican shear zone; A1: Monts d'Arrée; A2: Elorn valley; A3: Saint-Rivoal valley; B1: Landiviseau; B2: Belle-Isle-en-Terre; C: Léon Domain

CHAURIS, L. & HALLEGOUËT, B., 1973. Les relations du Paléozoïque inférieur avec le socle précambrien du pays de Léon, le long de la vallée de l'Elorn (Finistère). *Comptes Rendus de l'Académie des Sciences, Paris* 19, 277-280.

LE CORRE, C., AUVRAY, B., BALLEVRE, M. & ROBARDET, M., 1991. Le Massif Armoricaïn. In: Piqué, A. (Editor), *Massifs Anciens de France*. Louis Pasteur University, Strasbourg, 31-103.

ROLET, J., GRESSELIN, F., JEGOZO, P., LEDRU, P. & WYNS, R., 1994. Intracontinental Hercynian Events in the Armorican Massif. In: Keppie, J.D. (Editor), *Pre-Mesozoic Geology in France and related areas*, Springer-Verlag, 195-219.

VAN NOORDEN, M., SINTUBIN, M. & DARBOUX, J.-R., 2007. Incipient strain partitioning in a slate belt: evidence from the early Variscan Monts d'Arrée slate belt (Brittany, France). *Journal of Structural Geology* 29, 837-849.

15. Structural control on the Dikulushi Cu-Ag deposit, Katanga, Democratic Republic of Congo

Maarten Haest¹, Philippe Muchez¹ & Sara Vandycke²

1. Katholieke Universiteit Leuven, Geodynamics & Geofluids Research Group, Belgium

2. Faculté Polytechnique de Mons, Belgium

Presenting author: maarten.haest@geo.kuleuven.be

Keyword(s): structural control, Dikulushi Cu-Ag deposit

The deposit of Dikulushi is a high grade vein-type Cu-Ag mineralisation in the Kundelungu Plateau region in the southeast Katanga province of the Democratic Republic of Congo. The Kundelungu Plateau is a triangular shaped area to the north of the Lufilian Arc, which contains part of the Central African copperbelt, the largest known sediment-hosted copper province in the world. The Lufilian Arc and the Kundelungu Plateau comprise Neoproterozoic sedimentary rocks of the Katanga Supergroup that attain an overall thickness of more than 7000 m. The Lufilian orogeny imposed a northeast-directed shortening on the Kundelungu Plateau region (Coward and Daly 1984), forming several gentle, northwest-oriented anticlines above subparallel detachment surfaces at depth (Trefois and Fernandez 2000). The Dikulushi mine is located close to the hinge zone of one of these anticlines. Four different lithologies are recognised in the Dikulushi mine (Fig.1): 1) a dolomite breccia is exposed in the far western corner (Carbonate Unit), 2) brown coloured conglomerates, sandstones and shales build up the eastern part (Sandstone Unit) and both lithologies are separated by a north-northwest-oriented zone of ductile deformed shale (Shale Unit) and a breccia that contains dolomite, sandstone and basalt fragments in a shale matrix (Breccia Unit). The Shale Unit is bordered by two north-northwest-oriented faults that are covered with slickenlines, which record a dip-slip movement. The ductile deformed shale was emplaced upward in between both faults and this probably caused brecciation and the local development of kink folds in the overlying dolomite-sandstone sequence. The zone of ductile deformed shale is regarded as a thrust that could be the surface expression of a detachment at depth, responsible for the formation of the anticline to the west of the mine. The brecciated layers in the west and nonbrecciated sandstone layers in the central part of the mine are crosscut by several east-west- and northeast-oriented faults. The Main Fault Zone (MF in Fig.1) is an east-west-oriented reverse fault zone that borders the Breccia Unit to the north. The Northern Fault (NF in Fig.1) is a northeast-oriented normal fault that borders a zone of northeast-oriented faults to the north. Both the Main Fault Zone and the Northern Fault are covered with slickenlines that point to an oblique-slip fault movement, which is evidence for the reworking of these faults. The contact zone between both faults functioned as a damage zone that was a favourable site for the migration of mineralising fluids. At this location developed a Cu-Pb-Zn-Fe mineralization consisting of chalcopyrite, bornite and chalcocite, with minor pyrite, arsenopyrite, sphalerite and galena, with dolomite, calcite and quartz as gangue minerals. The northeast-oriented fault direction was reactivated several times, with at least one phase of dextral strike-slip that developed the Southern Fault. The fault surface of the Southern Fault is covered with slickenlines that record a pure strike-slip movement, which confirms its neofomed character. These northeast-oriented fault zones were sites of remobilization and enrichment of the previously deposited Cu-Pb-Zn-Fe mineralization. The remobilized sulfides consist of Ag-rich chalcocite, with barite, calcite and quartz as gangue minerals.



Figure 1. Geological map of the mine showing the stratigraphy, the main fault directions, the 0.5% Cu envelope and the alteration pattern, characterized by a decoloring of the red rocks (SstU=Sandstone Unit, CU=Carbonate Unit, ShU=Shale Unit, BU=Breccia Unit, NF=Northern Fault, SF=Southern Fault, MF=Main Fault Zone).

COWARD, M. P. & DALY, M. C., 1984. Crustal lineaments and shear zones in Africa - Their relationship to plate movements. *Precambrian Research*, 24, p. 27-45.

TREFOIS, P., & FERNANDEZ, M., 2000. Updating the geological map of Katanga (D.R. of Congo) with space imagery combined to archive data compilations [abs]. Fourteenth International Conference on Applied Geologic Remote Sensing, Las Vegas, Nevada, 2000, p. 369-376.

16. Global search for intrusive mud systems: analogues for the subsurface

Katie Roberts¹, Richard Davies¹, Simon Stewart² & Kenneth McCaffrey³

1. University of Durham, Department of Earth Sciences, CeREES (Centre for Research into Earth Energy Systems), U.K.

2. BP Azerbaijan, Sunbury on Thames, U.K.

3. University of Durham, Department of Earth Sciences, Reactivation Research Group, U.K.

Presenting author: k.s.roberts@durham.ac.uk

Keyword(s): mud volcano, intrusive feeder system

Mud volcanoes are an important global mechanism for the escape of fluid and gasses from sedimentary basins, however, little is known about the 3D geometry of their feeder systems. Two end-member theories on geometry currently exist; (a) mud transport takes place through linked mud-dyke complexes (determined by seismic interpretation) and (b) mud moves diapirically (identified in fossil and present day deltas). Detailed investigation is required to determine how such systems intrude the crust and how fluid-sediment mixes utilize the conduit system. The conduits penetrate some of the largest hydrocarbon reservoirs in the world located in the South Caspian Sea, resulting in this research being of huge commercial importance. Recent reconnaissance has yielded several types of intrusion where: (1) muds are intruded through sandstone beds utilizing thrust faults as pathways (Yasamal Anticline, Baku (Az)); (2) mud infills pre-existing joints in the centre of anticlines (Kichik Harami volcano, Ali-Bayramly (Az)); and (3) mud intrudes through small scale, sinuous hydrofractures (Kichik Harami volcano, Ali-Bayramly (Az)). We review these examples. Ongoing work will test the hypothesis that mud transport is through linked mud dykes collectively forming highly efficient conduit systems capable of transporting and re-cycling tens of cubic kilometres of mud and fluid from depths of 1-5 km. If this hypothesis is correct, it would counter the common conception of kilometre-wide mud-diapir systems, and thus downgrade the role of diapirism to an ancillary process. Here we intend to employ a scaled approach to the problem: Seismic interpretation of the several mud volcano systems within the AGC fields and Shah Deniz (South Caspian Sea), will be combined with field-based studies, initially focused in Trinidad, Azerbaijan and Brunei. In addition, records of drilling induced 'blow-outs' will be reviewed, as fracturing, fluid flow and entrainment of sediment are a documented feature of such events (e.g. Sidoarjo mud volcano – Java, May 2006). The structure of these conduits is still unknown and the global search for a subsurface analogue should have an important role in understanding the subsurface roots of volcanoes in more detail.

17. The geological and geodynamic evolution of the Northumberland Trough region, northern England: insights from the numerical modelling of lithosphere deformation and basin formation

Linda Austin¹, Stuart Egan¹ & Stuart Clarke²

1. Keele University, School of Physical and Geographical Sciences, Earth Sciences and Geography, U.K.

2. British Geological Survey, Edinburgh, U.K.

Presenting author: l.austin@epsam.keele.ac.uk

Keyword(s): geodynamics, numerical modelling, extensional tectonics

The numerical modelling of the interaction of geological and geodynamic processes has proved to be a valuable tool for explaining the causes and magnitude of regional subsidence and uplift in response to continental tectonics. In particular, geodynamic modelling can be used to investigate the effects of deep processes that are poorly constrained by subsurface and surface data. In this work, we apply 2D and 3D numerical modelling techniques, combined with the analysis of surface and subsurface data, to investigate the structural, stratigraphic and geodynamic evolution of the Carboniferous block and basin structure of northern England. This region includes the Alston Block, a Carboniferous high that is bounded to the north by the Stublick-Ninety Fathom fault system, the Northumberland Trough, and the Solway Basin to the East (Chadwick *et al.*, 1995). The region has experienced a complex subsidence and uplift history and the emphasis of this investigation is to apply and further develop 2D and 3D lithosphere-scale tectonic modelling techniques to determine the interplay of geological and geodynamic processes that have controlled basin structure and stratigraphy. The analysis of surface data from fieldwork and subsurface geophysical data has been used to produce regional cross-sections showing present day structure and stratigraphy across the region. These cross-sections have been constructed and analysed within a 3D co-ordinate frame to show regional variations in basin depth and burial history, as well as the position and magnitude of movement along major faults. In addition, the availability of deep geophysical data has provided constraint on Moho depth and, therefore, the variation of crustal thickness across the region. The analysis of structural data gathered from outcrop studies and published material has provided an overview of the tectonic and stratigraphic evolution of the region, including the extent and timing of extension, thrust and wrench deformational events. Numerical modelling that includes structural, thermal, isostatic and surface processes (e.g. Egan and Meredith, 2007) has been applied to the study area. Initially, a 2-D kinematic modelling approach has been used provide insights into the structural, thermal and isostatic evolution of the Northumberland Trough region and to test the compatibility of a variety of tectonic scenarios, including uniform lithosphere extension and depth-dependent stretching. Models that reconcile the observed amount of fault-controlled deformation with the magnitude of overall thinning of the crust generate comparable amounts of subsidence to that observed in the basin structures. These results also highlight some the limitations of a 2D modelling approach such that faults are considered as 2D objects and it is not possible to consider variations in isostatic loading outside the plane of the section being considered. Further development of modelling algorithms is now taking place in order to generate a realistic 3D model of the structural, geodynamic and stratigraphic evolution of Northumberland Trough region throughout Carboniferous times.

- CHADWICK, R.A., HOLLIDAY, D.W., HOLLOWAY, S. & HULBERT, A.G., 1995. The structure and evolution of the Northumberland-Solway Basin and adjacent areas. Subsurface Memoir. British Geological Survey/HMSO, London.
- EGAN, S.S. & MEREDITH, D.J., 2007. A kinematic modelling approach to lithosphere deformation and basin formation: application to the Black Sea. In: Karner, G.D., Manatschal, G. & Pinheiro, L.M. (eds) *Imaging, Mapping and Modelling Continental Lithosphere Extension and Breakup*. Geological Society, London, Special Publications, 282, 73-198.

18. The Quenast plug: a mega-porphyroclast during the Brabantian Orogeny (Senne valley, Brabant Massif, Belgium)

Timothy N. Debacker¹ & Manuel Sintubin²

1. Universiteit Gent, Geology & Pedology, Belgium

2. Katholieke Universiteit Leuven, Geodynamics & Geofluids Research Group, Belgium

Presenting author: timothy.debacker@ugent.be

Keyword(s): strain, X-ray pole figure goniometry, AMS

The Quenast plug is a quartz microdiorite situated in the southern part of the single-phase deformed Lower Palaeozoic Anglo-Brabant deformation belt (Brabant Massif, Belgium). This microdiorite is interpreted as a steeply NE-plunging feeder pipe or volcano neck (André & Deutsch, 1984; André, 1991, André, pers. comm. 2000). Although the intrusive nature of this magmatic body was already suggested 166 years ago (Galeotti, 1835), its age remained unknown for a long time (cf. Galeotti, 1835; Dumont, 1848; Corin, 1965). Finally, André & Deutsch (1984) obtained a U-Pb zircon cooling age of 433 ± 10 Ma for the plug. This age ranges from the middle Hirnantian to the basal Ludfordian (upper Ludlow), according to the time-scale of Gradstein *et al.* (2004), and clearly predates the Givetian angular unconformity at the southern rim of the Brabant Massif (Legrand, 1967; Van Grootel *et al.*, 1997), thus suggesting a pre-kinematic (pre-Brabantian) plug emplacement (André & Deutsch, 1984). However, this absolute age interval partly overlaps with the recently proposed late Llandovery – late Emsian(-Eifelian?) time interval for the long-lived Brabantian Orogeny (Debacker *et al.*, 2005). In addition, the stratigraphic age of the volcanic rocks of the late Caradoc – early Ashgill Madot Formation in the Fauquez area (Vanmeirhaeghe *et al.*, 2005), sometimes regarded as being derived from the Quenast plug (André, 1991), is considerably older than 433 ± 10 Ma. Judging from published structural field observations, there appears to be no agreement on whether or not the Quenast plug was emplaced prior to the Brabantian Orogeny. An analysis of the fracture orientations in the plug led Jedwab (1950) to conclude a late-syntectonic to post-tectonic, Early Devonian origin of the plug. In contrast, Corin (1965) mentions a curvature of the Lower Palaeozoic rocks around the Quenast plug, thus suggesting a pre-tectonic age. Taking into account the poor results of the previous structural studies inside the magmatic body, possibly caused by the competence of the rock and the difficulties in distinguishing cooling fractures and flow banding from tectonic features (cf. Jedwab, 1950), we focussed on the direct surroundings of the Quenast plug. In the fine-grained Ordovician siliciclastic deposits surrounding the Quenast plug, a variety of structural features demonstrate that the Quenast plug was emplaced prior to the Brabantian deformation event. These features include: a) a large-scale bending of the cleavage, mimicking the shape of the plug; b) a concomitant change in the orientation of the transverse fractures; c) a marked variation in cleavage intensity around the plug, with a high-strain zone along the NE-side of the plug and a low-strain zone along the NW-side of the plug; d) contractional and dilational kink bands. In combination with the elliptical cross-section of the plug, these features indicate that the Quenast plug can be regarded as having acted as a mega-porphyroclast during the Brabantian deformation event. The different structural features are discussed and related to the geometry and deformation of the Quenast plug. The emplacement age of the Quenast plug has implications for the timing of the Asquempont Detachment System (Debacker *et al.*, 2003, 2004). Using the observations in this work, a preliminary attempt can be made at

estimating the amount of shortening across the Quenast plug. Further work, concentrating on the magnetic fabric within the plug, will shed further light on the behaviour of the actual microdiorite during the Brabantian deformation event.

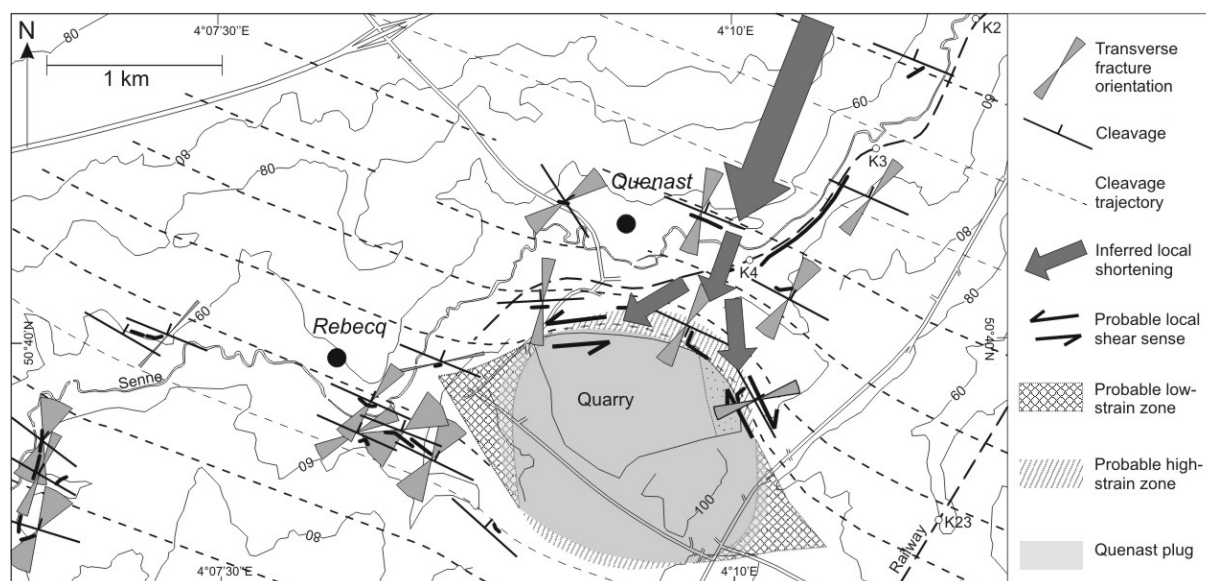


Figure 1. Simplified topographic map with inferred cleavage trajectories, inferred shortening direction, inferred and observed local shear sense, and inferred low- and high-strain zones around the Quenast plug. Note that the extent of the high- and low-strain zones is unknown.

- ANDRE, L., 1991. Caledonian magmatism. *Annales de la Société Géologique de Belgique* 114, 315-323.
- ANDRE, L. & DEUTSCH, S., 1984. Les porphyres de Quenast et de Lessines: géochronologie, géochimie isotopique et contribution au problème de l'âge du socle Précambrien du Massif du Brabant (Belgique). *Bulletin de la Société belge de Géologie* 93, 375-384.
- CORIN, F., 1965. Atlas des roches éruptives de Belgique. *Mémoires pour servir à l'Explication des Cartes géologiques et minières de la Belgique* 4, 1-190.
- DEBACKER, T.N., DEWAELE, S., SINTUBIN, M., VERNIERS, J., MUCHEZ, PH. & BOVEN, A., 2005. Timing and duration of the progressive deformation of the Brabant Massif, Belgium. *Geologica Belgica* 8, 20-34.
- DEBACKER, T.N., HERBOSCH, A., SINTUBIN, M. & VERNIERS, J., 2003. Palaeozoic deformation history of the Asquempont-Virginal area (Brabant Massif, Belgium). *Memoirs of the Geological Survey of Belgium* 49, 30 p.
- DEBACKER, T.N., HERBOSCH, A., VERNIERS, J. & SINTUBIN, M., 2004. Faults in the Asquempont area, southern Brabant Massif, Belgium. *Netherlands Journal of Geosciences/Geologie en Mijnbouw* 83, 49-65.
- DUMONT, A., 1848. Mémoire sur les terrains ardennais et rhénan de l'Ardenne, du Rhin, du Brabant et du Condros: seconde partie: terrain rhénan. *Mémoires de l'Académie royale de la Belgique, Classe des Sciences* 22, 1-451.
- GALEOTTI, 1835. Aperçu géologique du Brabant méridional. Séance du 18 mai 1835. Extrait du Mémoire sur la Constitution géognostique de la province du Brabant (ouvrage couronné par l'Académie royale des sciences et belles-lettres de Bruxelles, dans la séance du 7 mai 1835). *Bulletin de la Société géologique de France (1ère série)* 6, 264-272.
- GRADSTEIN, F.M., OGG, J.G & SMITH, A.G., 2004. A geological time scale 2004. Cambridge University Press, Cambridge.
- JEDWAB, J., 1950. Introduction à l'étude structurale de la microdiorite de Quenast. *Bulletin de la Société belge de Géologie, de Paléontologie et d'Hydrologie* 59, 225-230.
- LEGRAND, R., 1967. Ronquières. Documents géologiques. *Mémoires pour servir à l'Explication des Cartes Géologiques et Minières de la Belgique* 6, 1-60.
- VAN GROOTEL, G., VERNIERS, J., GEERKENS, B., LADURON, D., VERHAEREN, M., HERTOGEN, J. & DE VOS, W., 1997. Timing of subsidence-related magmatism, foreland basin development, metamorphism and inversion in the Anglo-Brabant fold belt. *Geological Magazine* 134, 607-616.
- VANMEIRHAEGHE, J., STORME, A., VAN NOTEN, K., VAN GROOTEL, G. & VERNIERS, J., 2005. Chitinozoan biozonation and new lithostratigraphical data in the Upper Ordovician of the Fauquez and Asquempont areas (Brabant Massif, Belgium). *Geologica Belgica* 8, 145-159.

19. The post-Triassic uplift and erosion history of the southwest UK

John E. Kelly¹ & Jonathan P. Turner¹

*1. University of Birmingham, GEES, Earth Sciences, U.K.
Presenting author: jek517@bham.ac.uk*

Keyword(s): AFTA, exhumation, sonic velocity analysis, sediment porosity

The Birmingham group has established that kilometres-scale exhumation (uplift and erosion) affected the sedimentary basins of southern Britain during the Cretaceous and Cenozoic driven by horizontal shortening of formerly extensional basins (inversion). In this study, we describe the distribution and chronology of exhumation, presenting results from the southwest UK, South Wales and offshore in the Bristol Channel and contiguous South Celtic Sea basins. Our data demonstrate that larger magnitude exhumation has occurred on the basin margin faults, particularly along the southern South Celtic Sea-Bristol Channel Basin margin, rather than in the centre of the offshore basins. This is consistent with footwall uplift which has been shown to occur further north along the Mohcras fault. Contrary to the short wavelength variations in exhumation that characterise the Cardigan Bay Basin and Saint Georges Channel Basin the distribution of exhumation across the present study area is more uniform, alluding to a broader uplift that affected the wider region. In addition the area lacks the large magnitude variations across faults that have been shown further north in the East Irish Sea Basin and Cardigan Bay Basin. Thermal history studies based on Apatite Fission Track Analysis (AFTA) and vitrinite reflectance data have revealed three main cooling events: an Early Jurassic (200-180Ma), Early Cretaceous (125-120Ma) and Miocene (20-15Ma) events. A number of samples also show a Variscan event (290-260Ma) and an earlier Miocene (Neogene) event (75-50Ma). Several different sediment porosity approaches have been taken involving both velocity-depth and porosity-depth relationships resulting in total exhumation estimates of between 0.75-3km. Flexural isostatic modelling software has been used to test the plausibility of the pre-exhumation stratigraphic architecture implied by the AFTA and sediment porosities. Forward models are based on basin-normal cross-sections that have been constructed using onshore geological maps, seismic data, including the deep-imaging BIRPS SWAT profiles, borehole logs and field observations.

20. Characterising fractured basement using the Lewisian Complex: implications for petroleum potential in the Clair Field

Jennifer Martin¹, Robert E. Holdsworth¹, Kenneth McCaffrey¹, Andy Conway², Stuart Clarke³

1. Durham University, Earth Sciences, Reactivation Research Group, U.K.

2. ConocoPhillips, Aberdeen, U.K.

3. British Geological Survey, Edinburgh, U.K.

Presenting author: j.c.martin@durham.ac.uk

Keyword(s): Clair Field, connected volume, Lewisian Gneiss complex, terrain, fractured basement

This project focuses on characterising two- and three-dimensional fault patterns in onshore Lewisian Gneiss as an analogue for offshore basement reservoir potential in the Clair Field. The Clair field lies 75km west of Shetland in the Faroes-Shetland basin. It covers an area of 220km² and lies under 150m of water. The field has reservoirs in Devonian and Carboniferous sediments and potentially in the fractured basement rocks. The basement of the Clair field is poorly understood so by creating fracture analogues for the field, from its onshore equivalent, will hopefully provide valuable constraints upon the likely 'connected volume' which will maximise production in this potentially significant hydrocarbon reservoir.

Thus the scientific aims of the project are three-fold.

Firstly, what is the Clair basement? The current consensus is that the Lewisian is made up of a series of terrains which stretch from the mainland of Scotland, to the Outer Hebrides and as far north as Shetland. Basement material recovered from the Clair field is considered to have affinities with the Lewisian so the emphasis here is which terrain does it belong to? The focus will be on the Assynt and Rhiconich terrains which form a large part of the mainland Lewisian. This will be established using careful optical thin section analysis, field work and core logging to place the Clair basement within this terrain system. The cores from the Clair basement will also be characterised in terms of their fracture arrays in order to compare and contrast these features with the fracture networks seen onshore.

Secondly, what are the fracture patterns in the onshore Lewisian complex? Can the patterns seen at outcrop be scaled up to what is seen regionally in 2D and 3D? Ultimately do these onshore patterns relate to what is seen on seismic and therefore are they a potential fracture network analogue for the Clair Field basement?

Finally, what are the dominant controls on the fracture patterns? Previous work has suggested many hypotheses for the possible controls on fracturing including lithology and intensity of pre-existing fractures. Part of the task here is to establish whether the fracture networks vary between the Assynt and Rhiconich terrains and the reasons behind that variation, if it exists.

Using natural fracture datasets from onshore outcrops in the Lewisian Gneiss Complex, NW Scotland, a series of 2D fracture models down to the millimetre scale, using line sampling and photomosaics will be constructed. This will be supplemented further by using ground-based laser scanning (LIDAR) to collect a digital dataset, again down to millimetre scale, that can

then be used to create 3D fracture network models for the outcrops. To assess the scalability of the fracture networks, a regional scale analysis of lineaments will be conducted using digital surface models created from the NEXTMap Britain (Intermap Technologies, 2003) digital elevation model (DEM). In order to compare with the fracture networks in the Clair Field, seismic reflection attribute fault maps will also be analysed.

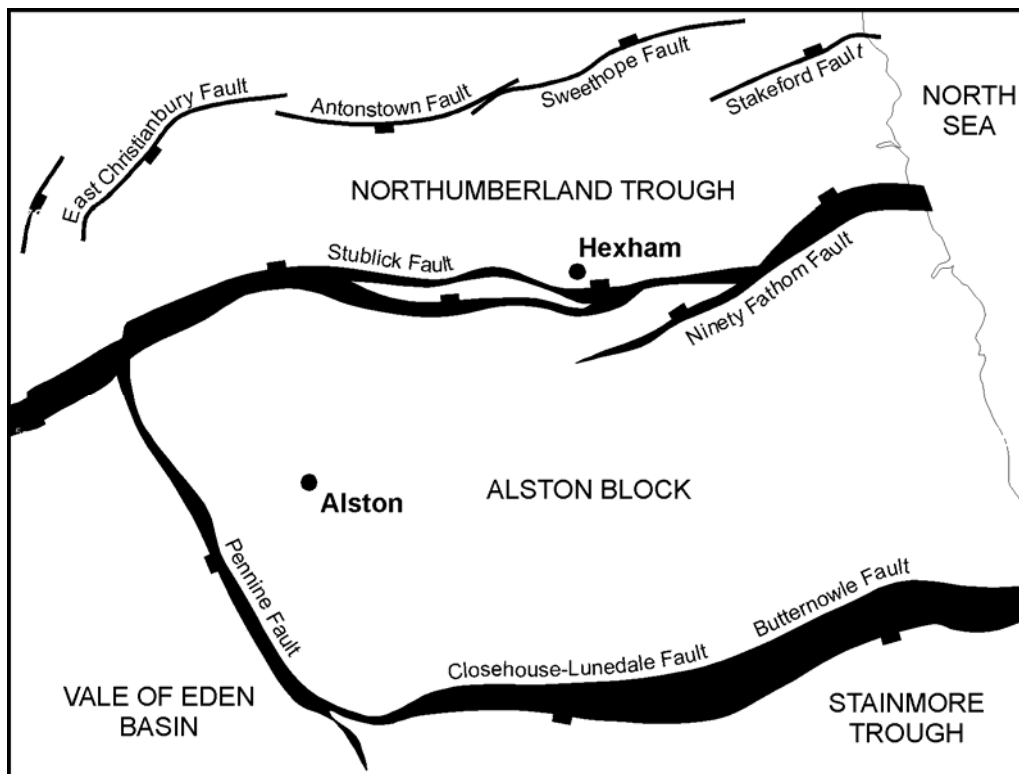
21. Structural styles and timing of deformation on the Stublick – Ninety-Fathom Fault, Northern England, U.K.

Stuart Clarke¹, David Millward¹ & Katie Whitbread¹

*1. British Geological Survey, Edinburgh, U.K.
Presenting author: smcl@bgs.ac.uk*

Keyword(s): Stublick Fault

Early Carboniferous extension across Northern England defined a ‘block and basin’ structure in which large asymmetric half-graben developed as a result of varied azimuths and magnitudes of extension on major block-bounding fault systems. The Northumberland trough, bounded to the south and controlled by the Stublick - Ninety-fathom Fault System (Fig.), is one such example. New, detailed 1:10 000-scale mapping across parts of the Stublick – Ninety Fathom Fault System highlights a number of structural styles and cross-fault relationships of Carboniferous strata. These variously result from syn-sedimentary deformation, the interaction of en-echelon major fault segments and complexly interrelated syn- and antithetic minor faults in both the footwall and hanging-wall, and late Carboniferous folding and reactivation of both major and minor structures. In this work we combine detailed mapping and modelling of structural styles observed at surface with subsurface mining data, geophysical data and stratigraphical interpretations to examine the structural evolution of the Stublick – Ninety-Fathom Fault System and constrain timing of deformation. Comparison of structural styles on the Stublick – Ninety-Fathom Fault System with those related to other major Carboniferous faults of northern England and inferred by other workers to result from transtensional and transpressional regimes, will set the structural evolution of the Stublick - Ninety-Fathom Fault System into the context of regional stress fields that have dominated the geological evolution of Northern England.





Author index

Author index

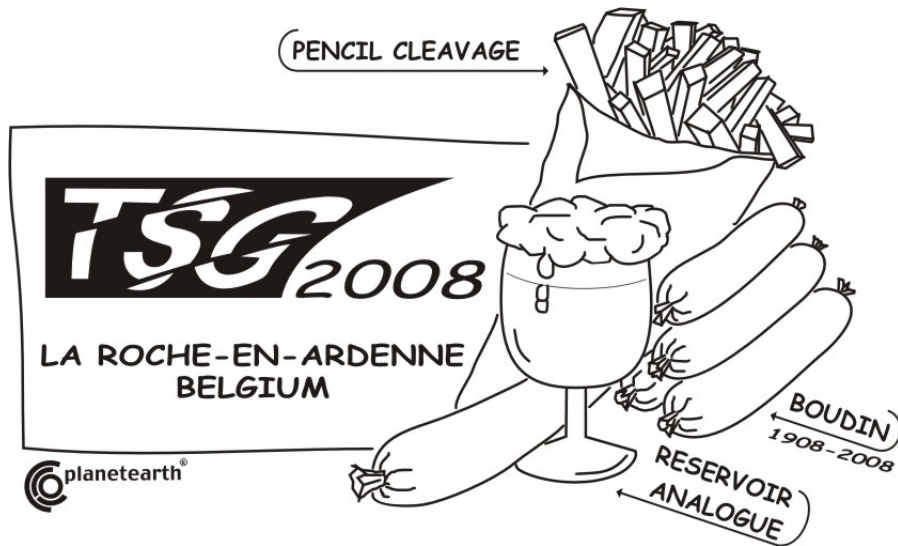
Author	Abstract number	Page number
Steffen Abe	talk 49,50	82,84
Emmanuel Adiotomre	talk 29	48
Fabrizio Agosta	talk 7,13	19,27
Gillian Apps	talk 34	56
Luis Eduardo Arlegui	talk 39	63
Linda Austin	talk32, poster17	54,119
Stefan Back	talk 42	68
Fabrizio Balsamo	talk 2	13
Craig Barrie	talk 17	32
Lucie Baudouy	talk 33	55
Françoise Bergerat	talk 37,46	60,76
Helena Bergman	poster 5	98
Isaac Berwouts	poster 14	114
Andrea Bistacchi	talk10, poster2	22,92
Xavier Boes	poster 12	111
Alan Boyle	talk 17	32
Tom Bradwell	talk 31	52
Katharine Brodie	talk 16	30
Stanislaw Burliga	talk 23	41
Rob Butler	talk 24,26,34	43,45,56
Namik Cagatay	poster 12	111
Thierry Camelbeeck	talk 37	60
Conrad Childs	talk 8,50	20,84
Stuart Clarke	talk31,32, poster17,20,21	52,54,119,124,126
Jean-Pierre Colbeaux	talk 37	60
Cristiano Colletini	talk6,15, poster7	18,29,100
Andy Conway	poster20	124
Stephen Covey-Crump	poster 6	99
Stephen Cox	talk 17	32
Emre Damci	poster 12	111
Richard Davies	poster 16	118
Marc De Batist	poster 12	111
Hans de Bresser	talk 18	34
Nicola De Paola	talk9, poster7	21,100
Walter De Vos	poster 3	94
Timothy N. Debacker	poster 3,18	94,121
Hagen Deckert	poster 13	112
Léon Dejonghe	talk 19	35
Francesco Dela Pierre	talk 30	50
Guillaume Desbois	talk 47	79
Michael Drews	poster 13	112
Anne Duperret	talk 41	66
Alexander Edwards	poster 6	99
Stuart Egan	talk32, poster17	54,119
Joris Eggenhuisen	talk 24	43
Chris Elders	talk 28	47
Daniel Faulkner	talk14, poster7,8	28,100,102
Andrea Festa	talk 30	50
Quentin Fisher	talk 3	14
Jeff Fraser	poster 12	111
Julia Gale	talk 43	71

*Author index TSG annual meeting 2008
La Roche-en-Ardenne, Belgium*

David Garcia	poster 12	111
Robert L. Gawthorpe	talk 12,29	25,48
Albert Genter	talk 41	66
Marc Giba	talk 8	20
Maarten Haest	poster 15	116
Robert Hall	talk 28	47
Peter Haughton	talk 24,33	43,55
Alain Herbosch	poster 3	94
Rebecca Hildyard	poster 7	100
Christoph Hilgers	talk 44	72
David Hodgetts	talk 12	25
Jon Holder	talk 43	71
Robert E. Holdsworth	talk 4,5,6,9,15, poster20	16,17,18,21,29,124
Marc Holland	poster 11	109
Nick Holliman	talk 9	21
Aurelia Hubert-Ferrari	talk22, poster12	39,111
Jonathan Imber	talk 4,5,6,9	16,17,18,21
Richard Jolly	talk 25	44
Richard Jones	talk 9	21
John E. Kelly	poster 19	123
Rob Knipe	talk 3	14
Hemin A. Koyi	talk 23	41
Maarten Krabbendam	talk 11,31	24,52
Peter A. Kukla	talk 42	68
Paloma Lafuente	talk 39	63
Graham Leslie	talk 11,32	24,54
Henry Lickorish	talk 34	56
Carlos Luis Liesa	talk 39	63
Richard Lisle	talk 21	38
Sergio Llana-Funez	talk16, poster8	30,102
Jonathan Long	talk 9	21
Huafu Lu	poster 4	97
Jennifer Martin	poster20	124
Matteo Massironi	talk10, poster2	22,92
Kenneth McCaffrey	talk9,25, poster16,20	21,44,118,124
Bill McCaffrey	talk 24,34	43,56
Florias Mees	talk 38	62
Luca Menegon	talk10, poster2	22,92
David Millward	poster 21	126
Thomas Mitchell	talk 14	28
Jasper Moernaut	poster 12	111
Kate Mort	talk 1	12
Rory N. Mortimore	talk 41	66
David J. Moy	talk 4,5	16,17
Philippe Muchez	talk45, poster14,15	74,114,116
Brendan J. Murphy	plenary lecture	5
Damian R. Nance	plenary lecture	5
Yago Nestola	talk 2	13
Andrew Nicol	talk 8	20
Miles Osmaston	talk 35	57
Douglas Paton	talk 26	45
Frank Peel	talk 34	56
Claudio Pellegrini	talk 10	22
Toon Petermans	talk 37	60

*Author index TSG annual meeting 2008
La Roche-en-Ardenne, Belgium*

Sandra Piazzolo	poster 5	98
Kris Piessens	poster 3	94
David Prior	talk17, poster7	32,100
Franklin Rarity	talk 12	25
Suzanne Raynaud	talk 46	76
Klaus Reicherter	talk 42	68
Olivier Richard	talk 46	76
Steve Richardson	talk 27	46
Katie Roberts	poster 16	118
Miguel Ángel Rodríguez-Pascua	talk 39	63
Ernest Rutter	talk16, poster6	30,99
Elodie SAILLET	talk 48	80
Joyce Schmatz	talk49, poster9	82,104
Martin Schöpfer	talk 50	84
Michel Sébrier	talk 37	60
Yehua Shan	talk 21	38
José Luis Simón	talk 39	63
Manuel Sintubin	talk20,40,44,45, poster3,10,14,18	37,65,72,74,94,106,114,121
Steven Smith	talk 6,15	18,29
Chris Spiers	talk 18	34
Simon Stewart	poster 16	118
Fabrizio Storti	talk 2	13
John Suppe	talk 22	39
Rochelle Taylor	poster 1	90
Saskia ten Grotenhuis	talk 18	34
Johan H. ten Veen	talk 40	65
Christophe Tesnière	talk 37	60
Emanuele Tondi	talk 7,13	19,27
Christian Tueckmantel	talk 3	14
Jonathan P. Turner	poster 19	123
Janos L. Urai	talk20,42,44,47,49, poster9,11	37,68,72,79,82,104,109
Hervé Van Baelen	talk 45	74
Maarten Van Daele	poster 12	111
Heijn van Gent	talk42, poster11	68,109
Koen van Noten	talk 44	72
Yves Vanbrabant	talk 19	35
Dimitri Vandenberghe	talk 38	62
Sara Vandycke	talk37,41,46, poster15	60,66,76,116
Kris Vanneste	talk 37,38	60,62
Koen Verbeeck	talk 37,38	60,62
Jamie Vinnels	talk 34	56
Richard J. Walker	talk 4,5	16,17
John J. Walsh	talk 8,33,36,50	20,55,59,84
Shengli Wang	poster 4	97
Ian Watkinson	talk 28	47
John Wheeler	poster 8	102
Katie Whitbread	poster 21	126
Christopher Wibberley	talk 48	80
Ruth Wightman	talk 9	21
Paul Wilson	talk 12	25
Nigel Woodcock	talk 1	12
Shimin Wu	poster 4	97
Baris Yerli	talk 40	65



PART III

List of participants

Tectonic Studies Group Annual Meeting 2008

January 8th - 10th, 2008

List of participants

Abe, Steffen	s.abe@ged.rwth-aachen.de	RWTH Aachen Geologie-Endogene Dynamik, Lochnerstrasse 4-20, 52056, Aachen, Germany
Adiotomre, Emmanuel	emmanuel.adiotomre@postgrad.manchester.ac.uk	University of Manchester, Basin Studies and Petroleum Geoscience, Williamson Building Oxford Road, M13 9PL, Manchester, UK
Agosta, Fabrizio	fabrizio.agosta@unicam.it	University of Camerino, via Gentile III da Varano, 62032, Camerino Macerata, Italy
Austin, Linda	l.austin@epsam.keele.ac.uk	Keele University, Earth Sciences and Geography School of Physical and Geographical Sciences, Keele University, ST5 5BG, Keele, UK
Balsamo, Fabrizio	balsamo@uniroma3.it	Dipartimento di Scienze Geologiche Roma Tre University L.go S. L. Murialdo1, 146 Roma Italy
Barrett, Tony	barrett.ap@btinternet.com	SEAES University of Manchester, Williamson Building, Oxford Road, M13 9PL, Manchester, UK
Barrie, Craig	cdbarrie@liverpool.ac.uk	University of Liverpool, Dept. of Earth and Ocean Sciences, L69 3GP, Liverpool, UK
Baudouy, Lucie	lucie.baudouy@ucd.ie	University College Dublin, School of Geological Sciences, Belfield, 4, Dublin, Ireland
Bergman, Helena	bergman@geo.su.se	Department of Geology and Geochemistry, Stockholm University, Svante Arrhenius VÅg 8C, 106 91, Stockholm, Sweden
Berwouts, Isaac	isaac.berwouts@geo.kuleuven.be	Katholieke Universiteit Leuven, Celestijnenlaan 200E, 3001, Leuven, Belgium
Bistacchi, Andrea	andrea.bistacchi@unimib.it	Dipartimento di Geologia, Univeristy of Milano Bicocca, Piazza della Scienza 4, 20126, Italy
Blake, Oshaine	oshaine@liverpool.ac.uk	University of Liverpool, Dept of Earth & Ocean Sciences, 4 Brownlow Street, L69 3GP, Liverpool, UK
Burliga, Stanislaw	burliga@ing.uni.wroc.pl	University of Wroclaw, Institute of Geological Sciences, pl. M. Borna 9, 50 – 204, Wroclaw, Poland
Butler, Rob	butler@earth.leeds.ac.uk	University of Aberdeen, Dept of Geology, Aberdeen, AB24 3UE, Aberdeen, UK
Clarke, Stuart	smcl@bgs.ac.uk	British Geological Survey, Murchison House, West Mains Road, EH93LA, Edinburgh, UK
Crider, Juliet	Juliet.Crider@wwu.edu	Western Washington University, Dept. of Geology, 98225, Bellingham, WA, USA
Debacker, Timothy	timothy.debacker@ugent.be	UGent, Krijgslaan 281 S8, 9000 Gent, Belgium
Deckert, Hagen	drewsilson@gmx.de	Institut fur Geowissenschaften, University of Mainz, Becherweg 21, 55099 Mainz, Germany
Desbois, Guillaume	g.desbois@ged.rwth-aachen.de	Geologie - Endogene Dynamik – RWTH Aachen University, Lochnerstr. 4-20, 52056 Aachen, Germany
Drews, Michael	MichaelDrews@gmx.com	Institut fur Geowissenschaften, University of Mainz, Becherweg 21, 55099 Mainz, Germany
Duperret, Anne	anne.duperret@univ-lehavre.fr	Université du Havre, 25 rue Philippe Lebon, BP540, 76056 Le Havre, FRANCE
Edwards, Alexander	xela_103@hotmail.com	University of Manchester, Williamson Building, Oxford Road, m13 9pl Manchester, UK

*Participants TSG annual meeting 2008
La Roche-en-Ardenne, Belgium*

Eggenhuisen, Joris	j.eggenhuisen@earth.leeds.ac.uk	University of Leeds, School of Earth and Environment, Earth Sciences, LS2 9JT Leeds, UK
Faulkner, Daniel	faulkner@liv.ac.uk	University of Liverpool, Earth and Ocean Sciences, L69 3GP Liverpool, UK
Festa, Andrea	andrea.festa@unito.it	Dipartimento Scienze della Terra - Universita di Torino, Via Valperga Caluso 35, 10125 Torino, Italy
Fitton, James	james_fitton@urscorp.com	University of Manchester, Oxford Road, M13 9PL Manchester, UK
Franceschi, Guy	tech@gfconsult.be	gf consult, Antwerpsesteenweg 644, B-9040 Gent, Belgium
Gale, Julia	julia.gale@beg.utexas.edu	Bureau of Economic Geology, Jackson School of Geosciences, The University of Texas at Austin, University Station Box X, 78713-8924 Austin, Texas, USA
Garcia, David	davidgm08@gmail.com	Royal Observatory of Belgium, Avenue Circulaire 3, 1180Brussels, Belgium
Giba, Marc	marc@fag.ucd.ie	Fault Analysis Group, School of Geological Sciences, University College Dublin, Belfield 4, Dublin, Ireland
Glover, Claire	claire.glover@postgrad.manchester.ac.uk	University of Manchester, SEAES, Williamson Building, Oxford Road, M13 9PL Manchester, UK
Haest, Maarten	Maarten.Haest@geo.kuleuven.be	Katholieke Universiteit Leuven, Celestijnenlaan 200E, 3001 Heverlee, Belgium
Hansford, Joanna	joanna@rdr.leeds.ac.uk	Rock Deformation Research, University of Leeds, LS2 9JT Leeds, UK
Harper, Nick	geonick@hotmail.co.uk	University of Leeds, 8 Beeches End, Boston Spa, Wetherby, West Yorkshire, LS23 6HL Leeds, UK
Havenith, Hans-Balder	havenith@sed.ethz.ch	University of Liege, Sart Tilman, B19, 4000 Liege, Belgium
Hildyard, Rebecca	rebecca.hildyard@liverpool.ac.uk	University of Liverpool, Department of Earth and Ocean Sciences, L69 3GP, Brownlow Hill, L69 3RZ Liverpool, UK
Hubert-Ferrari, Aurelia	aurelia.ferrari@oma.be	Royal Observatory of Belgium, Av. circulaire 3, 1180 Brussels, Belgium
Hus, Rob	rhus@frogtech.com.au	FrOG Tech, 6/50 Geils Court, PO-Box 250, ACT 2600 Deakin West, Australia
Imber, Jonathan	jonathan.imber@durham.ac.uk	University of Durham, Department of Earth Sciences, DH1 3LE Durham, UK
Irving, Alan	alan.irving@total.com	Total E&P UK, Geoscience Research Centre, Crawpeel Road, Altens Ind Est, AB12 3FG Aberdeen, UK
Kelly, John	jek517@bham.ac.uk	University of Birmingham, Earth Sciences, Aston Webb Building, Edgbaston, B15 2TT Birmingham, UK
Krabbendam, Maarten	mkrab@bgs.ac.uk	British Geological Survey, Murchison House, West Mains Road, EH9 3LA Edinburgh, UK
Laduron, Dominique	dominique.laduron@uclouvain.be	Universite catholique de Louvain, Geologie, Place L.Pasteur 3, 1348 Louvain-la-Neuve, Belgium
Lafuente, Paloma	palomalt@unizar.es	Universidad de Zaragoza, C/Pedro Cerbuna 12, 50009 Zaragoza, Spain
Leslie, Graham	agle@bgs.ac.uk	British Geological Survey, Murchison House, West Mains Road, EH9 3LA Edinburgh, UK
Lisle, Richard	lisle@cardiff.ac.uk	Cardiff University, Park place, CF10 3YE Cardiff, UK

*Participants TSG annual meeting 2008
La Roche-en-Ardenne, Belgium*

Llana-Funez, Sergio	slf@liverpool.ac.uk	University of Liverpool, 4 Brownlow Street, L69 3GP Liverpool, UK
Long, Jonathan	jonathan.long@durham.ac.uk	Durham University, Department of Earth Sciences, DH1 3LE Durham, UK
Martin, Jennifer	pcb7339@hotmail.com	University of Durham, 76 Annand Rd, DH11PP Durham, UK
McCabe, Nicola	nikki@rdr.leeds.ac.uk	Rock Deformation Research, Earth Sciences, University of Leeds, LS2 9JT Leeds, England
McCaffrey, Ken	k.j.w.mccaffrey@durham.ac.uk	Durham University, Earth Sciences, DH1 3LE Durham, UK
Moy, David	d.j.moy@durham.ac.uk	Durham University, Science Labs, DH1 3LE Durham, UK
Murphy, Brendan	bmurphy@stfx.ca	St. Francis Xavier University, Department of Earth Sciences, Antigonish, Nova Scotia Canada
Nollet, Sofie	sofie.nollet@exxonmobil.com	URC/ExxonMobil, 1035 Rutland Street, 77008 Houston, USA
O'Connor, Victoria	viki@rdr.leeds.ac.uk	Rock Deformation Research Ltd, Earth Sciences, School of Earth and Environment, University of Leeds, LS2 9JT Leeds, England
Osmaston, Miles	miles@osmaston.demon.co.uk	The White Cottage, Sendmarsh, Ripley, GU23 6JT Woking, UK
Ramsay, John	john.ramsay@ethz.ch ramsay-dietrich@wanadoo.fr	Cratoule, Issirac, F-30760 St. Julien de Peyrolas, France
Raynaud, Suzanne	suzanne.raynaud@gm.univ-montp2.fr	Géosciences, Montpellier, France
Richardson, Steve	s.e.j.richardson@dur.ac.uk	Durham University, St Marys College, Elvet Hill Road, DH1 3LR Durham, UK
Roberts, Katie	k.s.roberts@durham.ac.uk	University of Durham, Department of Earth Sciences, University Science Labs, South Road, DH1 3LE Durham, UK
Rutter, Ernest	e.rutter@manchester.ac.uk	University of Manchester, School of Earth Sciences, M13 9PL Manchester, Great Britain
Saillet, Elodie	saillet@geozaur.unice.fr	UMR Geosciences Azur, 250 Avenue Albert Einstein, 6560 Valbonne, France
Sathar, Shanvas	shanvas.sathar@liv.ac.uk	University of Liverpool, Dept of Earth & Ocean Sciences, 4 Brownlow Street, L69 3GP Liverpool, UK
Schmatz, Joyce	j.schmatz@ged.rwth-aachen.de	Geologie-Endogene Dynamik, RWTH Aachen, Lochnerstrasse 4-20, 52056 Aachen, Germany
Schöpfer, Martin	martin@fag.ucd.ie	Fault Analysis Group, School of Geological Sciences, University College Dublin, Belfield, Dublin 4, Ireland
Sintubin, Manuel	manuel.sintubin@geo.kuleuven.be	Katholieke Universiteit Leuven, Geodynamics & Geofluids Research Group, Celestijnenlaan 200E, 3301 Leuven, Belgium
Smith, Steven	steven.smith@durham.ac.uk	University of Durham, Department of Earth Sciences, DH1 3LE Durham, UK
Somovilla de Miguel, Ion Ander	nuevodentro8@hotmail.com	Universidad de Zaragoza, C/Pedro Cerbuna 12, 50009 Zaragoza, Spain
Stewart, Iain	istewart@plymouth.ac.uk	University of Plymouth, Drakes Circus, PL4 8AA Plymouth, UK
Taylor, Rochelle	rochelle.taylor@student.manchester.ac.uk	University of Manchester, Williamson Building, Oxford Road, M13 9PL Manchester, England

*Participants TSG annual meeting 2008
La Roche-en-Ardenne, Belgium*

ten Grotenhuis, Saskia	saskiatg@geo.uu.nl	Faculty of Geosciences, Budapestlaan 4, 3584 CD Utrecht, the Netherlands
Tondi, Emanuele	emanuele.tondi@unicam.it	University of Camerino, Via Gentile III da Varano, 62032 Camerino, Italy
Tueckmantel, Christian	christian@rdr.leeds.ac.uk	University of Leeds, Rock Deformation Research, School of Earth and Environment, LS2 9JT Leeds, UK
Urai, Janos L.	j.urai@ged.rwth-aachen.de	RWTH, Lochnerstrasse 4-20, D-52056 Aachen, Germany
Van Baelen, Hervé	herve.vanbaelen@geo.kuleuven.be	Katholieke Universiteit Leuven, Celestijnenlaan 200E, 3001 Leuven, Belgium
van Bever Donker, Jan	jvanbeverdonker@uwc.ac.za	University of the Western Cape, Private Bag X17, 7535 Bellville, South Africa
van Gent, Heijn	h.vangent@ged.rwth-aachen.de	Structural Geology, Tectonics and Geomechanics
van Noorden, Michiel	michiel@badleys.co.uk	Badley Geoscience Ltd., North Beck House, North Beck Lane, PE23 5NB Hundleby, UK
Van Noten, Koen	koen.vannoten@geo.kuleuven.be	Geodynamics & Geofluids Research Group, Katholieke Universiteit Leuven, Celestijnenlaan 200E, 3001 Leuven, Belgium
Vanbrabant, Yves	yves.vanbrabant@naturalsciences.be	Geological Survey of Belgium, Rue Jennerstraat 13, 1000, Brussels, Belgium
Vandycke, Sara	Sara.Vandycke@fpms.ac.be	Faculté Polytechnique de Mons/FNRS, 9 rue de Houdain, 7000 Mons, Belgium
Vanneste, Kris	kris.vanneste@oma.be	Royal Observatory of Belgium, Ringlaan 3, B-1180 Brussel, Belgium
Verbeeck, Koen	koen.verbeeck@oma.be	Royal Observatory of Belgium, Avenue Circulaire 3, 1180 Brussels, Belgium
Vinnels, Jamie	jamie@earth.leeds.ac.uk	School of Earth and Environment, University of Leeds, LS2 9JT Leeds, UK
Walker, Richard	r.j.walker@durham.ac.uk	Durham University, Dept. of Earth Sciences, University of Durham, DH1 3LE Durham, UK
Walsh, John	john@fag.ucd.ie	University College Dublin, School of Geological Sciences, Fault Analysis Group, Ireland
Watkinson, Ian	i.watkinson@gl.rhul.ac.uk	Royal Holloway University of London, 24 Elmbank Avenue, TW20 0TJ Englefield Green, Surrey, UK
Wilson, Paul	Paul.Wilson@manchester.ac.uk	University of Manchester, Williamson Building, Oxford Road, M13 9PL Manchester, England
Woodcock, Nigel	nhw1@esc.cam.ac.uk	University of Cambridge, Department of Earth Sciences, Downing Street, CB2 3EQ Cambridge, UK
Wouters, Laurent	l.wouters@nirond.be	ONDRAF/NIRAS, Kunstlaan 14, 1210 Linden, Belgium
Wu, shimin	smwu@scsio.ac.cn	south china sea institute of oceanology, West Xingang Road 164, 510301 guangzhou, P.R.China
Yerli, Baris	baris.yerli@rub.de	Institute for Geology, Mineralogy and Geophysics, Ruhr University, Univeritätsstrasse 150, 44801 Bochum, Germany



PART IV

Field trip guide

January 11th, 2008

“A TASTE OF THE ARDENNES”

Manuel Sintubin¹, Sara Vandycke² & Timothy N. Debacker³

¹Geodynamics & Geofluids Research Group, Department of Earth & Environmental Sciences, Katholieke Universiteit Leuven, Celestijnenlaan 200E, B-3001 Leuven

²Géologie Fondamentale et Appliquée, Faculté Polytechnique de Mons, rue de Houdain, 9, B-7000 Mons

³Vakgroep Geologie & Bodemkunde, Universiteit Gent, Krijgslaan 281 S8, B-9000 Gent

Safety information for field trip participants

- ✓ The attendees of the field trip must take responsibility for their own and other participants' safety. In order to ensure the safety of all participants the organisers reserve the right to limit or refuse attendance at the field trip.
- ✓ Should you be unsure either of the risks involved or your suitability for the field trip, you must seek advice from the organisers. You must declare any disabilities or medical conditions that may affect your ability to safely attend the field trip.
- ✓ The field trip leaders will give a safety briefing at the start of the field trip.
- ✓ Inform the field trip leaders if you leave the field trip early.
- ✓ The field trip leaders are not expected to provide First Aid. Ensure you have adequate supplies for your own needs.
- ✓ Wear appropriate clothing and footwear for the locality, time of year and as recommended. Anticipate potential changes in weather conditions. The field trip organisers will advise on any personal protective equipment that participants need (e.g. hard hat, high visibility vest, goggles). These **MUST** be worn if asked for. Failure to do so may lead to your exclusion from the field trip. The organisers do not automatically provide personal protective equipment.
- ✓ Children and animals will not be allowed on the field trip.
- ✓ The leader's decision is final on any matter relating to the field trip.
- ✓ No list can cover every safety issue. Always be alert for yourself and others around you.
- ✓ We visit two quarries in exploitation. Hard hats compulsory! Please approach exploitation front with caution! Be cautious for falling rocks!
- ✓ By attending the field trip, you have agreed to these terms without prejudice.

Introduction to the field trip “A taste of the Ardennes”

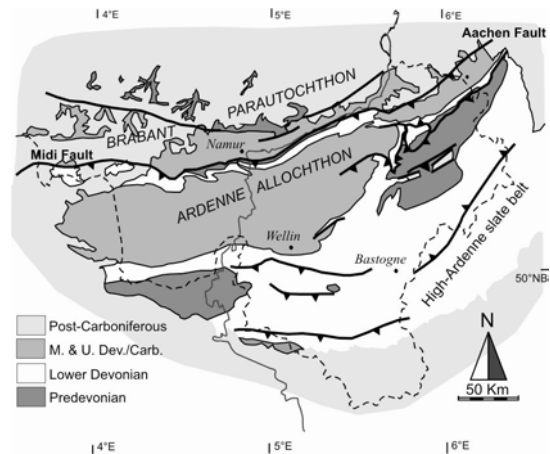
In one day – particularly in winter – it is nearly impossible to give you a good idea of what the Ardennes has to offer geologically. More than 500 million years European history has sculpted the scenic landscapes of the Ardennes in Belgium, Northern France and Western Germany.

We choose three outcrops to give you just a “*taste of the Ardennes*”. These outcrops are, moreover, places where our research group in Leuven, Mons and Gent were active in recent years.

The **Mardasson quarry at Bastogne** (STOP A) is the locality where exactly one century ago the term ‘boudin’ and ‘boudinage’ were used for the first time. We will examine the particular structures in the High-Ardenne slate belt that are the result of brittle-ductile deformation in the middle crust at the onset of the Variscan orogeny.

The **Fond des Vaulx quarry at Wellin** (STOP B) is situated in the limestone belt – the *calestienne* – along the southern side of the Dinant fold-and-thrust belt. It offers the opportunity to study Variscan and post-Variscan brittle tectonics and the relationship between active tectonics and karst dynamics.

The **Chemin de Ronde section at Namur** (STOP C) is situated at the northernmost front of the Variscan orogen in the Brabant parautochthon. This outcrop allows us to examine a number of synsedimentary and penecontemporaneous soft-sediment deformation features, reflecting a progressive accumulation of deformation at different stages of the Variscan orogeny affecting its foreland.



Manuel Sintubin
Sara Vandycke
Timothy Debacker

The geology of the Ardennes in a nutshell

by Manuel Sintubin

The Ardennes is one of the Palaeozoic massifs in Northwest Europe. It is part of the Rhenish massif. These massifs expose rocks belonging to the Rhenohercynian zone of the Variscan orogen (figure 1). The **Rhenohercynian zone** represents the northern external parts of the Central European Variscides. It forms of a thin-skinned foreland fold-and-thrust belt, telescoping the Devonian-Carboniferous rift and platform sediments of the southern passive continental margin of the 'Old Red Continent' (Oncken et al. 1999) (figure 4).

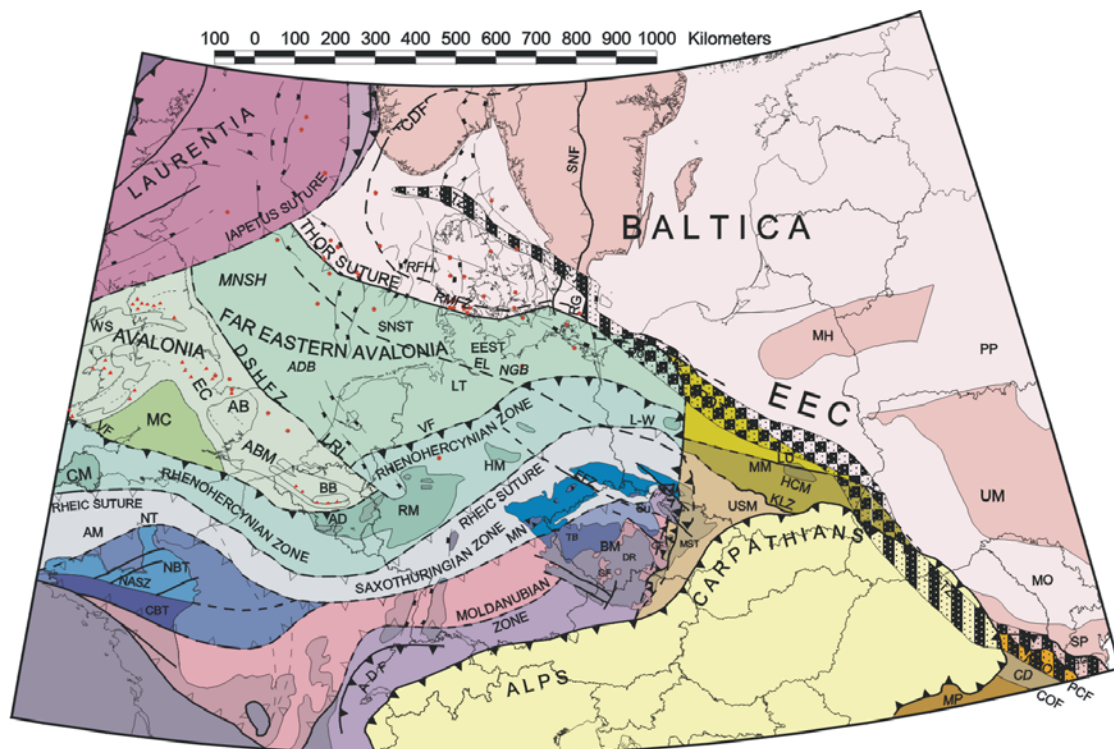


Figure 1 – Terrane map of Palaeozoic Europe (Winchester & Team 2002). The Ardennes (AD), part of the Rhenish massif (RM), is situated in the Rhenohercynian zone at the northern front of the Pan-European Variscan orogen. The Ardennes is situated north of the Rhenic suture, thus belonging to the Avalonia terrane.

The northern part of the Rhenohercynian foreland fold-and-thrust belt (figure 4), as exposed in the Ardennes (figure 2), comprises the **Ardenne allochthon**, which is thrust over the **Brabant parautochthonous foreland** during the latest Carboniferous 'Asturian' stage (~300 Ma) of the Variscan orogeny (e.g. Mansy & Lacquement 2003, Meilliez et al. 1991). The **Brabant parautochthon** (*Namur synclinorium*) represents the deformed Carboniferous foreland basin, covering Middle to Upper Devonian platform sediments and the Lower Palaeozoic **Brabant basement**. The latter is characterised by an early Palaeozoic orogenic event, the 'Brabantian' orogeny (see Verniers et al. 2002 and references therein). This tectonometamorphic event took place from the late Llandovery to the Eifelian (Debacker 2001, Debacker et al. 2005), coinciding with the onset of the development of the rift basin in the Ardenne-Eifel realm during the early Devonian (Oncken et al. 2000).

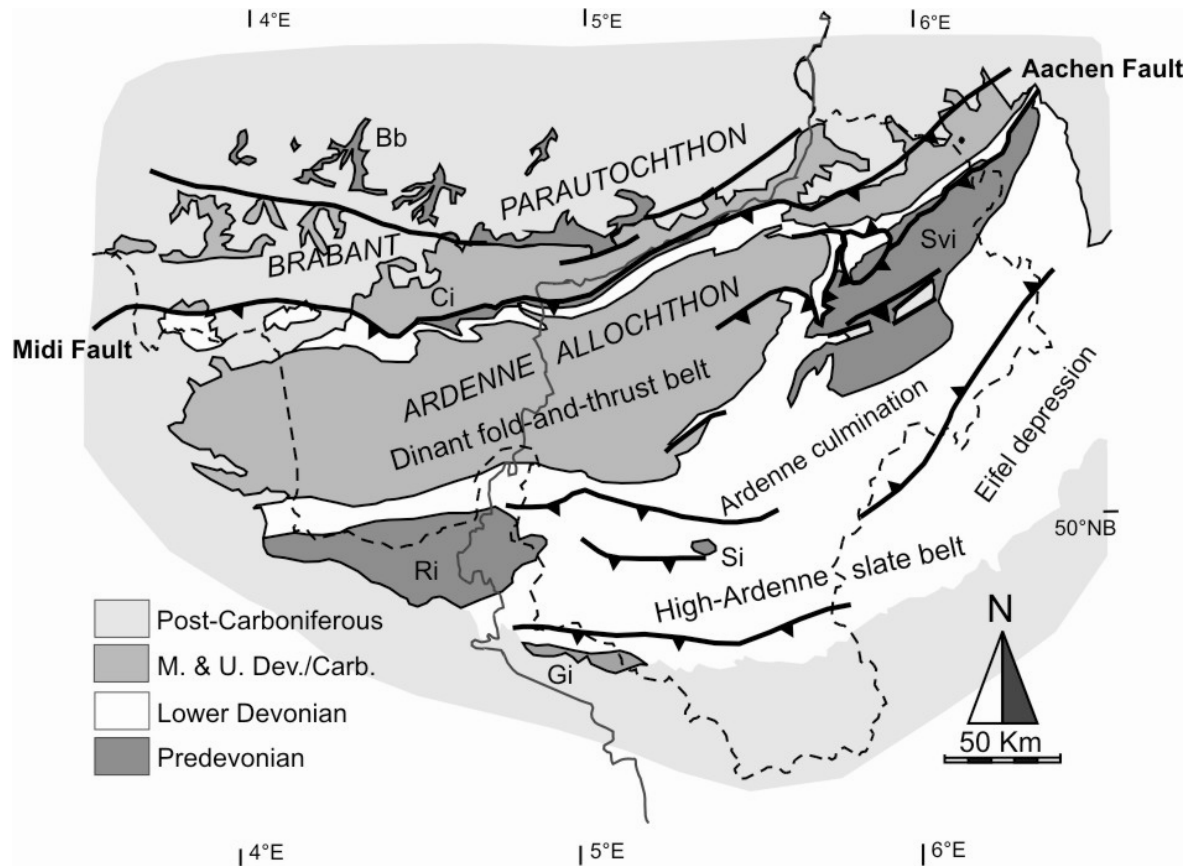


Figure 2 – Schematic geological map of the Ardenne-Eifel area (Belgium, Germany, France) with indication of the main tectonostratigraphical domains. Bb: Brabant basement; Ci: Condroz inlier; Svi: Stavelot-Venn inlier; Ri: Rocroi inlier; Si: Serpont inlier; Gi: Givonne inlier.

The main Variscan thrust, separating the Brabant parautochthon from the Ardenne allochthon, has different names along strike: the *Midi fault* in the west, the *Condroz thrust* in the central part, and the *Aachen fault* in the east. In the frontal area the total displacement is estimated at 20 to 40 km (see e.g. Adams & Vandenberghe 1999). The Ardenne allochthon consists of the **Dinant fold-and-thrust belt** (*Dinant synclinorium*) and the **High-Ardenne slate belt** (*Ardenne anticlinorium* & *Eifel synclinorium*). The Variscan deformation in the Dinant fold-and-thrust belt is controlled by the presence of relatively competent rock formations in the Devonian-Carboniferous sedimentary sequence (Lacquement 2001, Meilliez & Mansy 1990). Contrary, the deformation in the High-Ardenne slate belt, predominantly composed of pelitic rocks of early Devonian age, is controlled by this thick, relatively homogeneous pile of incompetent rocks, which eventually led under low-grade metamorphic conditions to the development of a slate belt.

The High-Ardenne slate belt is, furthermore, composed of the **Ardenne culmination** (*Ardenne anticlinorium*), which involves predominantly siliciclastic metasediments of Lochkovian age, and the **Eifel depression** (*Eifel synclinorium*), which consists of Lower Devonian siliciclastic metasediments. In the west, these sediments are of Pridolian to Pragian age, while towards the northeast the metasediments progressively young up to the Eifelian. The backbone of the Ardenne culmination is formed by a number of Lower Palaeozoic basement inliers, i.e. the Rocroi-Serpont and Givonne inliers in the west and the Stavelot-Venn inlier in the northeast (figure 2). The predominantly siliciclastic metasediments in these basement inliers are of Cambrian to middle Ordovician age, and possibly reflect an early Palaeozoic rift basin development (Verniers et al. 2002). These basement inliers are seen as

footwall short-cuts of crustal ramps (Oncken et al. 2000, Plesch & Oncken 1999) (figure 4). Whether or not the Lower Palaeozoic rocks, exposed in the basement inliers, were affected by a middle Ordovician orogenic event, the so-called 'Ardennian' orogeny (Michot 1980), remains to date a matter of debate (see e.g. Delvaux de Fenffe & Laduron 1991, Hugon 1983, Hugon & Le Corre 1979, Lacquement 2001, Le Gall 1992, Van Baelen & Sintubin 2008).

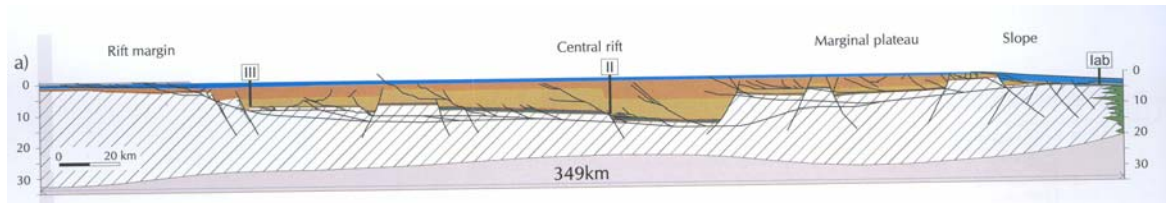


Figure 3 – Reconstruction of the southern passive margin of the Old Red Continent (Oncken et al. 2000) during the Middle Devonian. The Rhenohercynian ocean is situated at the eastern extremity of the section (green: oceanic crust). The early Devonian rift basin fill (brown) is covered by the Middle Devonian carbonate platform (blue). Note the total length of the section, 349 km.

The thick Lower Devonian sequence in the High-Ardenne slate belt reflects the rapid syn-rift basin fill, particularly active during the Pragian (Oncken et al. 2000, Oncken et al. 1999), in the northern part of the developing Rhenohercynian ocean (figure 3). In the central part of this ocean, a rift-drift transition occurred during the Emsian (~400 Ma), marking the onset of the post-rift sedimentation in the Ardenne-Eifel realm. This post-rift sedimentation, characterised by the development of a carbonate platform in a passive margin setting lasted until the end of the Viséan (~325 Ma). More specifically, there were two phases of carbonate platform development, the first in the Eifelian-Frasnian and the second in the Tournaisian-Viséan, interrupted by the return of terrigenous sedimentation during the Famennian.

During the early Viséan (~335 Ma) the Rhenohercynian ocean was closed (southern Rhenish massif). At the end of the Viséan, basin closure and the northerly prograding Variscan deformation front reached the southern parts of the Ardenne-Eifel realm. During the Carboniferous, foreland basins developed ahead of the Variscan orogen. Deformation in the High-Ardenne slate belt took place during the late Viséan – early Namurian 'Sudetic' stage (~325 Ma) of the Variscan orogeny (Fielitz & Mansy 1999, Piqué et al. 1984). Variscan deformation eventually ended in the Stephanian (Kasimovian) 'Asturian' stage (~300 Ma) when the Dinant fold-and-thrust belt and the Brabant parautochthon were incorporated in the Variscan orogen (figure 4).

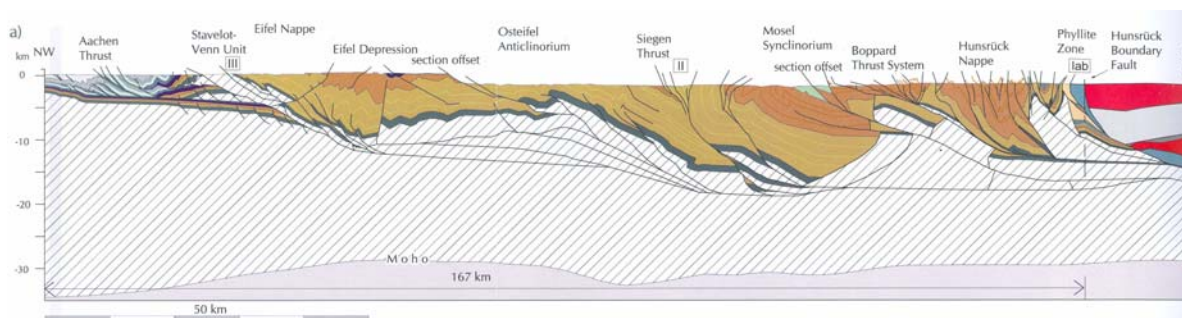


Figure 4 – Balanced cross-section of the Rhenohercynian foreland fold-and-thrust belt (Oncken et al. 2000), bounded to the southeast by the upper plate (Saxothuringian zone) and the Rhenohercynian suture (Phyllite zone). The High-Ardenne slate belt comprises the Stavelot-Venn unit, the Eifel nappe and the Eifel depression. Northwest of the Stavelot-Venn unit the northeastern extension of the Dinant fold-and-thrust belt is exposed. Note the total length of the section, 167 km.

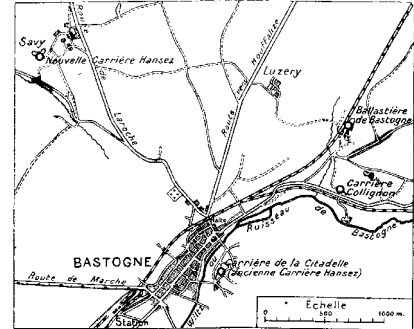
STOP A – Bastogne – Mardasson quarry: “About boudins, veins and mullions”

by Manuel Sintubin in collaboration with Ilse Kenis, Philippe Muechez & Janos L. Urai

INTRODUCTION

Together with the Collignon quarry, the Mardasson quarry, originally called the *Ballastière de Bastogne* (Gosselet 1888), is the locality where in August 1908 during a field trip organised by the *Société Géologique de Belgique* the term ‘boudin’ and ‘boudinage’ were used for the first time in order to facilitate the discussion with respect to particular structures in the Lower Devonian metasedimentary series, resembling sausages lying side by side (Lohest et al. 1908).

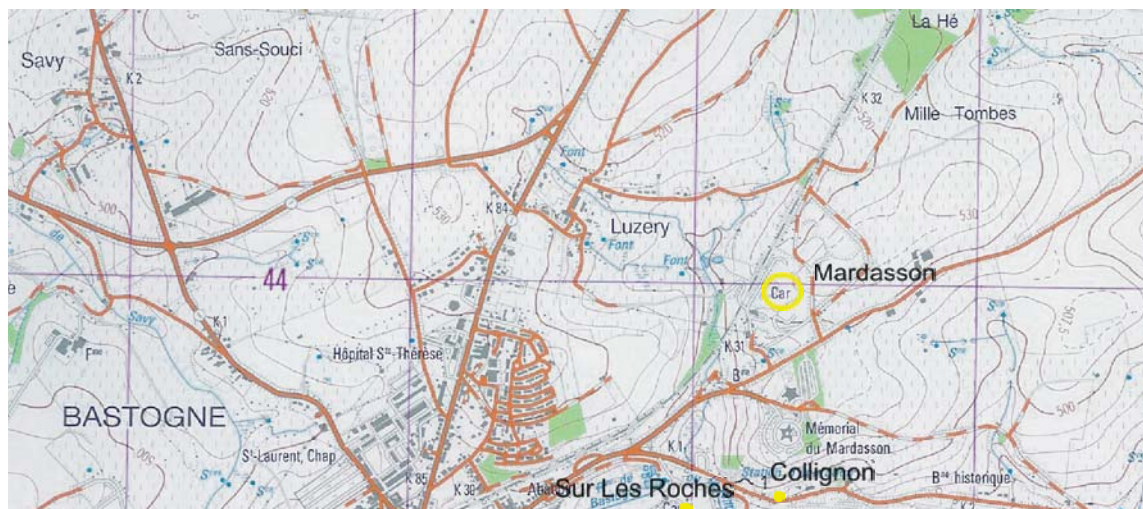
To celebrate the centennial, we revisit this locality. The brittle-ductile structures exposed have been in the centre of a century of debate. Today, these structures turn out to be very particular, expressing a brittle-ductile deformation at the onset of the Variscan orogeny.



Logistics – Terrain

The Mardasson quarry is located north of the war memorial of Mardasson, east of the city of Bastogne. The geographical coordinates of the quarry correspond to 50°00'50"N and 5°44'21"E.

This is a quarry in exploitation. Hard hats compulsory! Please approach exploitation front with caution!



Map: 1:25.000 sheet 60/7-8 Longchamps-Longvilly

Contact: Enrobage Stockem, route de Bouillon 222, B-6700 Arlon, tel.: +32 (0)63 24 52 00; fax: +32 (0)63 22 77 16; e-mail: enrobage.stockem@cobonet.be.

Aims

The purpose of this visit is:

1. to visit the site where the term 'boudin' and 'boudinage' has been coined in 1908;
2. to visit the type locality of the mineral 'bastonite';
3. to examine brittle-ductile deformation in the middle crust.

Points to debate:

1. did fracturing and veining occurred at the same time and in similar conditions?
2. is there evidence for boudinage, i.e. bulk layer-parallel extension?
3. are these brittle-ductile structures reworked boudins or mullions?
4. what is the regional significance of the occurrence of these brittle-ductile structures?

GEOLOGICAL SETTING OF THE BASTOGNE AREA

The Bastogne area is located in the **High-Ardenne slate belt**, the southern part of the **Ardenne allochthon** (figure A1). The latter forms part of the foreland fold-and-thrust belt at the northern front of the Central European Variscides, resulting from the telescoping of a Palaeozoic passive margin (Renohercynian zone). The High-Ardenne slate belt consists of a thick sequence of Lower Devonian siliciclastic, predominantly argillaceous, metasediments.

The Lower Devonian deposits, exposed in the High-Ardenne slate belt, reflect the rapid syn-rift sedimentation, particularly active during the Pragian (Oncken et al. 1999) in the **Ardenne-Eifel rift basin**. This basin, part of the Renohercynian ocean, develops within the continental passive margin of the 'Old Red Continent'. In the more central part of the Renohercynian ocean a rift-drift transition occurred during the early Emsian (~400 Ma)

(Franke 2000, McKerrow et al. 2000, Oncken et al. 2000, Oncken et al. 1999), marking the onset of post-rift sedimentation in the Ardenne-Eifel realm, characterised by the development of carbonate platforms. During the early Visian (~335-330 Ma)

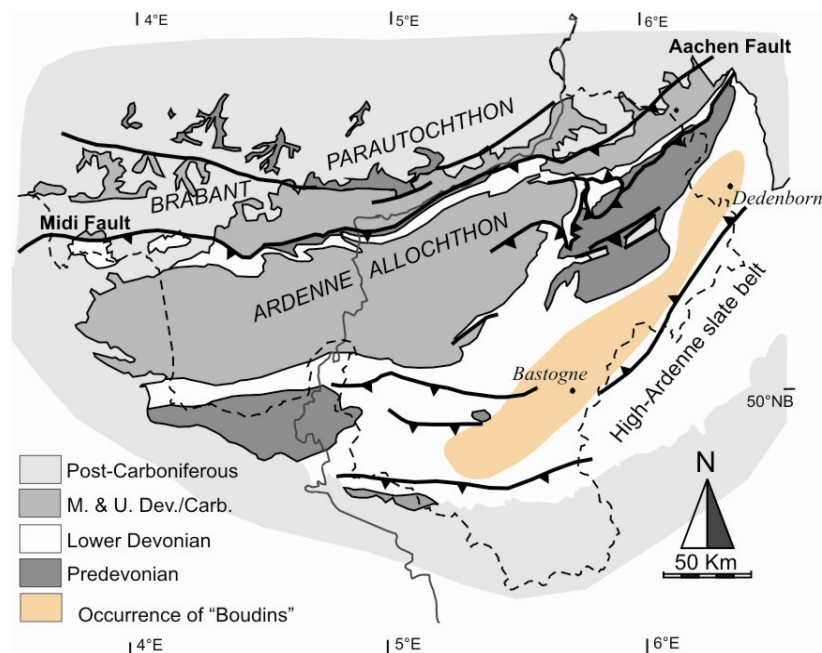


Figure A1 – Schematic geological map of the Ardenne-Eifel area (Belgium, Germany) with indication of the main tectonostratigraphical domains. The regional extend of the occurrence of the brittle-ductile structures is indicated. Bastogne and Dedenborn are indicated.

convergence of the Rheohercynian ocean heralded the Variscan orogeny. By the end of the Viséan (~325 Ma) basin closure and the prograding Variscan deformation front reached the southern parts of the Ardenne-Eifel realm. Peak deformation in the High-Ardenne slate belt occurred during Serpukhovian to Bashkirian times (~325-310 Ma) (Plesch & Oncken 1999) with a shortening rate of ~14mm/a (Oncken et al. 1999).

The metasediments of the High-Ardenne slate belt underwent a metamorphism that is believed to be pre- to early synkinematic with respect to the prograding Variscan deformation and is considered to have a burial origin (Fielitz & Mansy 1999). In the Bastogne area the maximum metamorphic temperature conditions are estimated to range between 365 and 400°C (Beugnies 1986, Darimont et al. 1988). At peak metamorphism pressure conditions are estimated to range between 170 and 180 MPa (Beugnies 1986, Darimont et al. 1988). An overall geothermal gradient of 40 to 50°C/km is considered to be present during the burial and deformation of the rocks in the High-Ardenne slate belt (Darimont 1986, Helsen 1995, Kenis et al. 2000, Schroyen 2000).

Bastonite



In quartz veins of the Bastogne area a dark mica can be observed. This hydrobiotite is described as extremely poor in potassium (Klement 1888) and is named bastonite after its type locality. It is one of the richest NH_4^+ -dark micas (Bos et al. 1987, Kenis et al. 2002).



The High-Ardenne slate belt consists of open to relatively closed folds with a dominant, steeply S-dipping axial planar cleavage. The overall grain in the Bastogne area is NE-SW. Fold hinge lines plunge weakly to the NE. Most folds are metric to hectometric and seem largely synchronous with the pervasive cleavage development.

Mardasson Quarry

*In the quarry grey-blue metasiltstones, intercalated with grey-blue quartzites are exposed. The quartzite layers are discontinuous, showing sedimentary wedges, dichotomy, etc. Stratigraphically the rocks belong to the **Mirwart formation** (Bultynck & Dejonghe 2001), which is considered to have a Lochkovian-Pragian age (formerly Siegenian 1).*

The quarry is situated in the wide hinge of a hectometric open antiform (hinge line orientation: 235/10). The axial planar cleavage has an average orientation of 150/61.

A HISTORICAL RETROSPECT

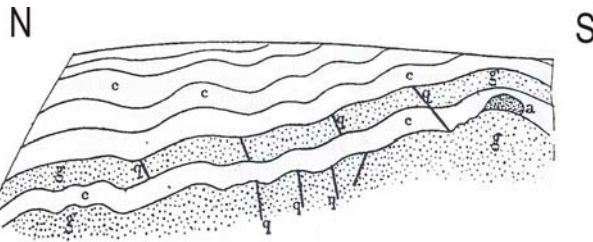


Figure A2 – First sketch of the brittle-ductile structures in the Mardasson quarry (*Ballastière de Bastogne*) by Gosselet in 1888. c: cornéite; g: grès; q: quartz vein.

The first geometrical description of the particular quartz-vein occurrence in the Bastogne area (Belgium) goes back to 1888 when Gosselet mentions in his chapter on metamorphism in the Ardenne that *“tous ces filons de quartz ... sont limités au grès et s’arrêtent à la cornéite”*. In his work on the origin of the metamorphic rocks in the

Bastogne area, Stainier (1907) presents an extensive inventory of the occurrence and geometry of these veins, demonstrating the regional occurrence and significance of the veins and associated structures. To explain these particular structures, he invokes a polyphase brittle-ductile deformation sequence: *“... c’est grâce à la préexistence des filons quartzeux et des crevasses que l’on peut expliquer l’allure en chapelet et l’allure en petites voussettes, unique en Ardenne, que présentes les bancs de grès de la région. Si ces bancs de grès n’avaient pas présenté des fissures, la poussée tangentielle du grand ridement les aurait plissées en voûtes ou bassins ordinaires; ou bien, si la poussée avait été trop forte, elle aurait déterminé la production de failles inverses de refoulement. Au lieu de cela, chaque compartiment d’un banc de grès, devenu indépendant des ses voisins dont il était séparé par un joint quartzeux, s’est arqué, pour son compte, en une petite voussette ou bien s’est renflé en saucisson ou grain de chapelet”*. To Stainier the sequence of events was evident: first fracturing and veining, then layer-parallel shortening, all prior to the main Variscan folding and cleavage development.

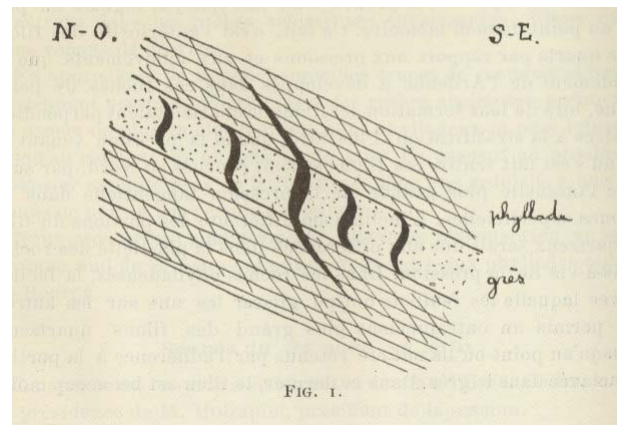


Figure A3 – An illustration of the original “boudins” in the report of the field meeting in Bastogne of the Société Géologique de Belgique (Lohest et al. 1908).

To demonstrate the work of Stainier, a field trip was organised by the Société Géologique de Belgique. On August 31st, 1908, at the Carrière Collignon near Bastogne, Lohest introduced the terms ‘**boudin**’ and ‘**boudinage**’ in order to facilitate discussions (Lohest et al. 1908):

*“Lorsque l’on voit ces segments renflés sur une surface de stratification étendue, mise à nu par l’exploitation, on croirait voir une série d’énormes cylindres ou **boudins** alignés côté à côté ... sur l’initiative de M. Lohest on a fréquemment utilisé, pour la facilité du langage, les néologismes de boudiner et de **boudinage**.”*

At this early stage, these terms were used purely descriptive to indicate the series of sausage-like structures, lying side by side. Already during the field trip, a discussion unfolds on the relative timing of the different deformation features, setting the stage

for a century long discussion on the development of these particular structures observed at Bastogne.

In the first half of the 20th century numerous models were proposed with variable chronologies with respect to the development of the different deformation features (Corin 1932, Holmquist 1931, Quirke 1923, Wegmann 1932), clearly demonstrating the uncommon nature of the structures (cf. Quirke 1923). Although these authors often mentioned that the 'boudins' at Bastogne were seemingly related to 'pinch-and-swell' structures as described by e.g. Ramsay (1866) and Harker (1889), it was generally agreed that they did not fully resemble, primarily because of the strongly different aspect ratio of the segments (Holmquist 1931, Walls 1937). Cloos (1947), however, did not make this clear distinction, and the term 'boudinage', applied to both types of structures, obtained its current kinematic definition referring to a process of layer-parallel extension.

Boudinage

Boudinage refers to the disruptions of layers, bodies or foliation planes within a rock mass in response to bulk extension along the enveloping surface (Goscombe et al. 2004).



Ever since confusion only got worse, in particular when very similar structures in the North Eifel region were described as '**mullions**' (Pilgers & Schmidt 1957). In an attempt to relate the 'mullions' of the North Eifel – considered as layer-parallel shortening structures (i.e. cusped-lobate folding) – and 'boudins' of Bastogne – at that time considered as extension structures – terms such as L-boudins or '*auslängungs-boudins*' and K-boudins or '*verkürzungs-boudins*' were introduced (Brühl 1969). The 'mullions' of Pilgers and Schmidt (1957) became 'half-boudins' (Brühl 1969). Quickly, it was acknowledged that this new terminology was definitively not the solution to the confusing, taking into account that the association of the term 'boudinage' with bulk extension was already too entrenched in English literature (Mukhopadhyay 1972). Mukhopadhyay (1972) and Spaeth (1986), more recently corroborated by Urai et al. (2001), considered the structures in the Ardenne-Eifel region as mullions. Apart from them the idea of 'shortened boudins' gained, however, ground, primarily based on the atypical aspect ratio of the segments (Jongmans & Cosgrove 1993, Lambert & Bellière 1976, Rondeel & Voermans 1975), an idea still persistent to date (Vanbrabant & Dejonghe 2006).

A century of debate primarily focused on the cusped-lobate – sausage-like – geometry of the sandstone-pelite bedding interface, largely ignoring the quartz veins. Renewed interest in the quartz veins allowed constraining the formation conditions and kinematic significance of the veins with respect to the overall structure development (Kenis et al. 2005a, Kenis et al. 2002). A numerical modelling approach (Kenis et al. 2004) ultimately corroborated the mullion model and even allowed to use the particular cusped-lobate morphology to constrain the rheology of the deforming middle crust (Kenis et al. 2005b). Eventually, the hypothesis initially postulated by Stainier in 1907 becomes remarkably up to date!

THE BRITTLE-DUCTILE STRUCTURES

Describing the particular structures in the Bastogne area, we make a clear distinction between two distinct structural features (figure A4): (1) the veins, and (2) the cusped-lobate morphology of the bedding interface. Although we consider both features separately, a regional survey shows that both features are spatially closely related and are kinematically linked. If veins are not present, the cusped-lobate morphology of the bedding interface is lacking.

Where to find the structures?

These brittle-ductile structures are limited both in stratigraphic and regional extent (Kenis 2004, Urai et al. 2001). They only occur in formations of Upper Lochkovian to Pragian age. Regionally, their occurrence is limited to the southern limb of the Ardenne culmination (figure A1), coinciding with the region of highest metamorphic grade (Fielitz & Mansy 1999) and representing the deepest parts of the Eifel-Ardenne rift basin (Oncken et al. 1999).

Veins – geometrical characteristics

The veins show the following geometrical characteristics:

- ✓ commonly *lens-shaped*;
- ✓ oriented *perpendicular to bedding*, independent of orientation of bedding;
- ✓ limited to the *most competent parts of the multilayer sequence*, i.e. the sandstone layers; mostly *limited to one single bed*;
- ✓ systematic array of *parallel veins*, very continuous in the longitudinal direction;
- ✓ *regular spacing*; spacing in relation to bed thickness;
- ✓ *aspect ratio* (height/width) of the segments in between two adjacent veins ranges from 1 to 7 (even up to 20).

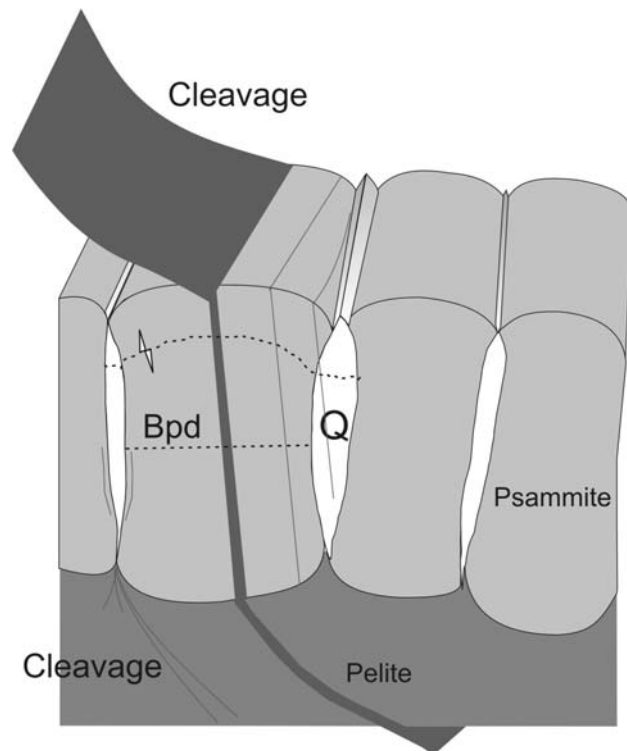


Figure A4 – Synthetic figure of the brittle-ductile structures in the Ardenne-Eifel area. Q: quartz vein; Bpd: bedding-parallel dissolution seam; gray lines represent the tectonic cleavage (Kenis & Sintubin 2007).

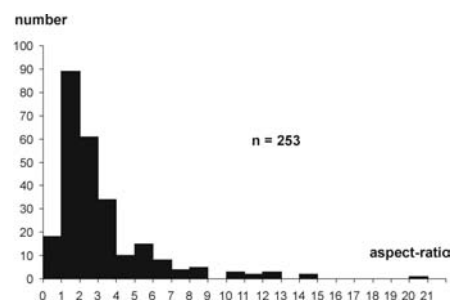


Figure A5 – Histogram representing the aspect ratio (height/width) of the segments between the veins (Kenis & Sintubin 2007).

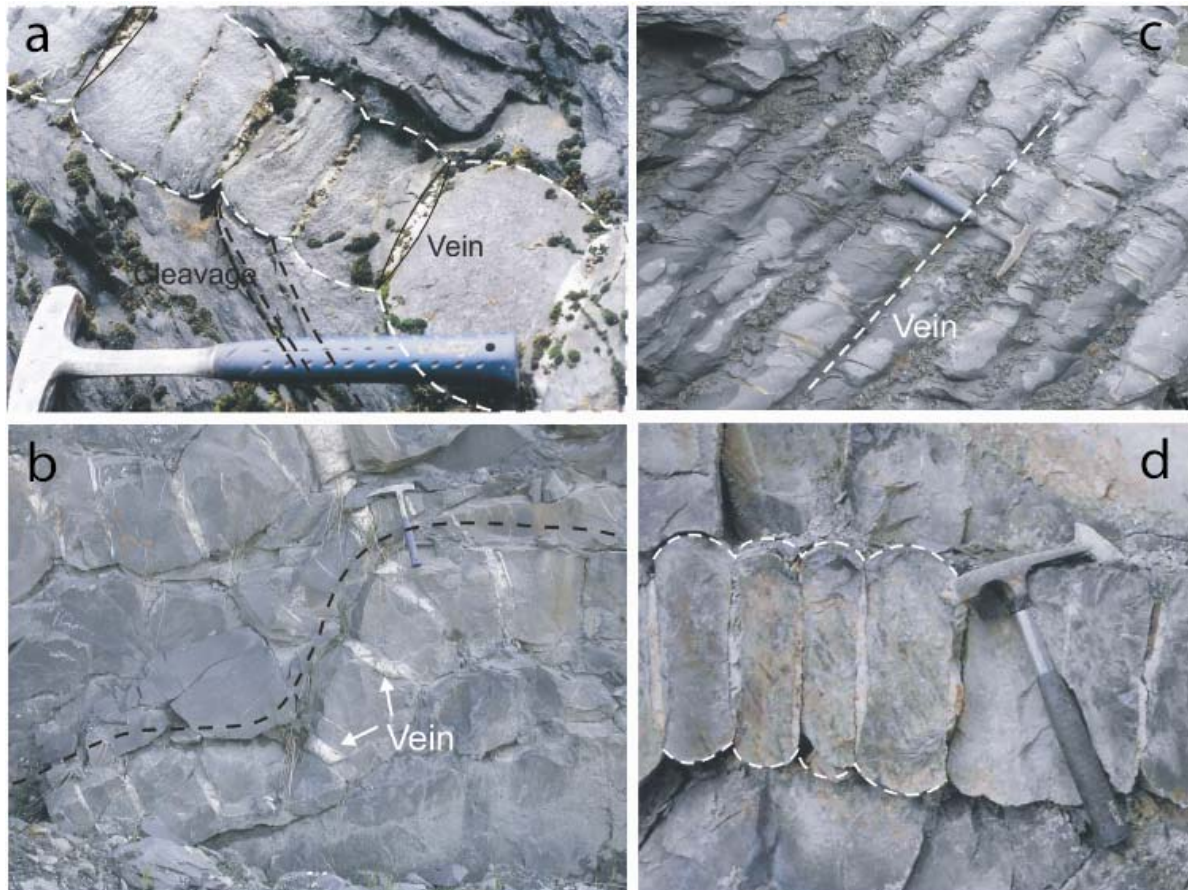


Figure A6 – Different geometrical aspects of the brittle-ductile structures (Kenis & Sintubin 2007). (a) lens-shaped veins in a single layer with a regular spacing, perpendicular to bedding; the bedding interface shows a cusped-lobate morphology. (b) small-scale fold of a segmented sandstone layer. (c) vein-bedding intersection indicative of the longitudinal continuity of the veins. (d) particular aspect ratio.

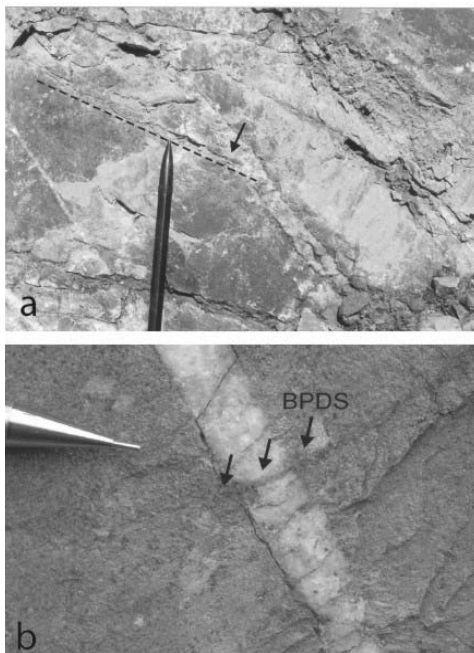


Figure A7 – (a) Variscan cleavage (black dashed line) cross-cutting the veins. (b) bedding-parallel dissolution seams (BPDS) cross-cutting the veins. (Kenis & Sintubin 2007).

A number of features allow constraining the relative timing of the veining:

- ✓ *prior to Variscan folding and cleavage development* (always perpendicular to bedding; cleavage cross-cuts veins);
- ✓ occurred in beds in a *horizontal, depositional, disposition* (perpendicular to bedding);
- ✓ *prior to maximum burial conditions* (bedding-parallel dissolution seams cross-cutting the veins).

It is therefore fair to assume that veining occurred during the last stages of the deep burial of the sediments within the Ardenne-Eifel rift basin, thus most probably during the early Viséan (~340 Ma).

Veins – mineralogy and fabric

The veins predominantly consist of quartz, but also contain chlorite, muscovite, biotite (bastonite), pyrite, chalcopyrite, ilmenite, and feldspar (figure A8). Native gold and silver have also been described in the veins at Bastogne (Hatert et al. 2000). In general, the vein minerals all are well-crystallized and no indications for a different timing of the formation of the different minerals could be observed, such as broken mineral fragments enclosed by other minerals, crosscutting relationships, etc.

The vein quartz shows a number of microstructures characteristic of crystal plasticity (Kenis et al. 2005a). Large cores of quartz grains abundantly occur. Grain sizes range between 500 μm and 1 cm. Quartz grains show undulose extinction and contain deformation lamellae, evolving to the subgrains (figure A9). Sometimes, the vein quartz shows a core-mantle structure. Grain size of smaller grains ranges between 40 and 120 μm .

The vein-quartz fabric is indicative for dislocation creep, evolving to recovery and dynamic recrystallization by subgrain rotation and grain-boundary migration. These microstructures comply with regime 2 of experimental dislocation-creep regimes that corresponds to natural temperature conditions of 350 to 500°C (Stipp et al. 2002). This temperature range is conform with the metamorphic temperatures of the host rock (Fielitz & Mansy 1999).

In contrast with the vein quartz, the host rock only contains evidence for quartz dissolution and overgrowth, suggesting that solution-precipitation creep was the dominant deformation mechanism responsible for the deformation of the sandstone (figure A9). The absence of notable dislocation creep deformation of

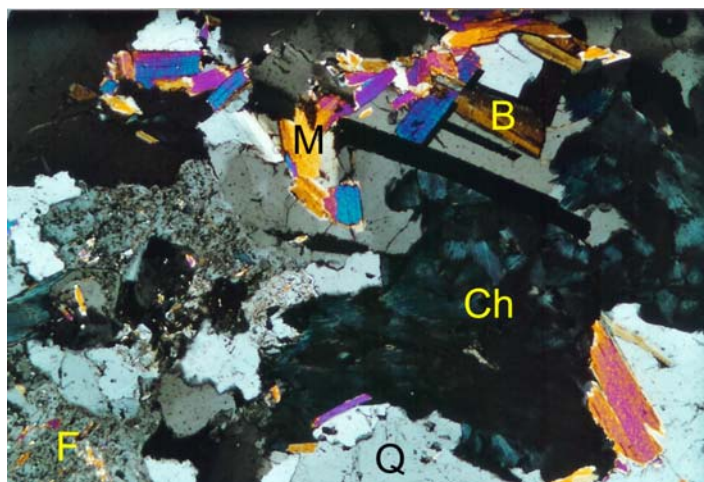


Figure A8 – Mineralogy of the veins. Q: quartz; Ch: chlorite; B: biotite (bastonite); M: muscovite; F: feldspar (width of picture is 2 mm) (Kenis et al. 2005a).

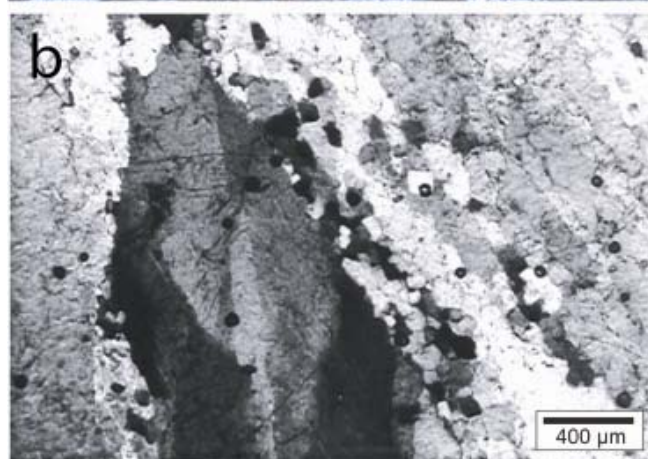
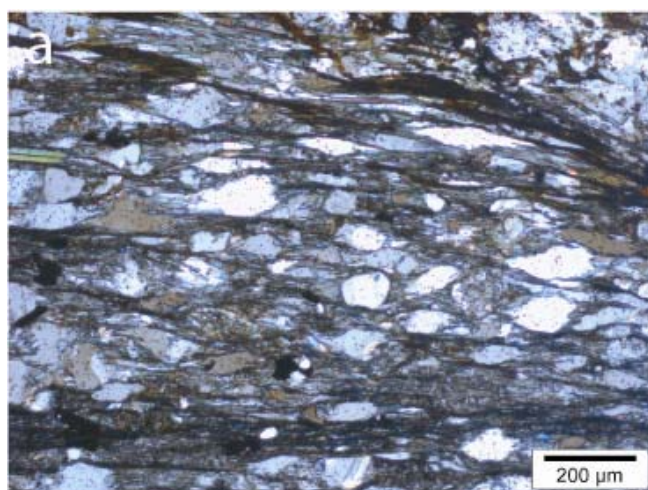


Figure A9 – (a) sandstone matrix with microstructures indicative of solution-precipitation creep. (b) microstructure in the vein quartz indicative of dislocation creep (Kenis et al. 2005a).

quartz in the sandstone suggests that the differential stress remained too low for dislocation creep to be competitive with solution-precipitation creep. The flow stress in the quartz veins was much higher, causing an inhomogeneous stress field in the different materials. The latter difference will cause buckling of the interface at the onset of the Variscan shortening (Kenis et al. 2005a).

Veins – fluid-inclusion characteristics

Fluid inclusions (~510 in 13 samples – size ranging from 2 to 20 μm) occurring in veins from ten different localities enabled to reconstruct a temporal and spatial evolution of the chemical composition of the fluids during veining and subsequent Variscan deformation. Using petrography, microthermometry (using a USGS-modified fluid-inclusion stage) and Laser Raman Spectroscopy, four types of fluid inclusions were identified in the vein quartz (figures A10, A11 & A12):

Type 1 inclusions (A1)

- ✓ found in samples of vein quartz in both the epizone and anchizone;
- ✓ occur in growth zones and are therefore assigned a primary origin; also occur as isolated inclusions;
- ✓ mixed aqueous-gaseous fluid inclusions (H_2O - NaCl - CO_2 -other gases);
- ✓ low to high salinity; between ~0 and 3.5 eq.wt% NaCl in anchizone; between 0.6 and 17 eq.wt% NaCl in epizone;

Type 2 inclusions (A2)

- ✓ only found in samples of vein quartz in the epizone;
- ✓ occur spatially associated with A1 primary inclusions and are morphological similar; also observed in growth zones;
- ✓ gaseous (CO_2 - N_2 -(CH_4)) fluid inclusions;

Type 3 inclusions (G1)

- ✓ only found in samples of vein quartz in the epizone;
- ✓ inter-grain, trail-bound inclusions occurring along the surface of former microcracks and are thus described as secondary fluid inclusions;
- ✓ the composition of this gaseous fluid type varies from a CO_2 - N_2 -(CH_4) composition to a pure N_2 -(CH_4) composition;

Type 4 inclusions (W1)

- ✓ found in samples of vein quartz in both the epizone and anchizone;
- ✓ inter-grain, trail-bound inclusions; W1 trails crosscut G1 trails;
- ✓ aqueous (H_2O - NaCl) fluid inclusions; this type of fluid inclusions is frequently described in the Devonian and Carboniferous sequences in the entire Variscan foreland fold-and-thrust belt exposed in the Ardennes (Darimont et al. 1988, Kenis et al. 2000, Muchez et al. 1997, Schroyen 2000).

The first (A1) and second (A2) type of fluid inclusions are considered primary inclusions that reflect the earliest phase of vein-quartz growth. The timing of these primary inclusions is correlated with the final stages of the burial history of the Lower Devonian metasediments.

The third (G1) and fourth (W1) type of inclusions are closely related with microcracks that formed after vein formation and can most probably be linked with the deformation of the veins during the Variscan orogeny. Type 3 fluid inclusions are interpreted to have formed prior to the formation of the latest type of fluid inclusions (type 4 – W1).

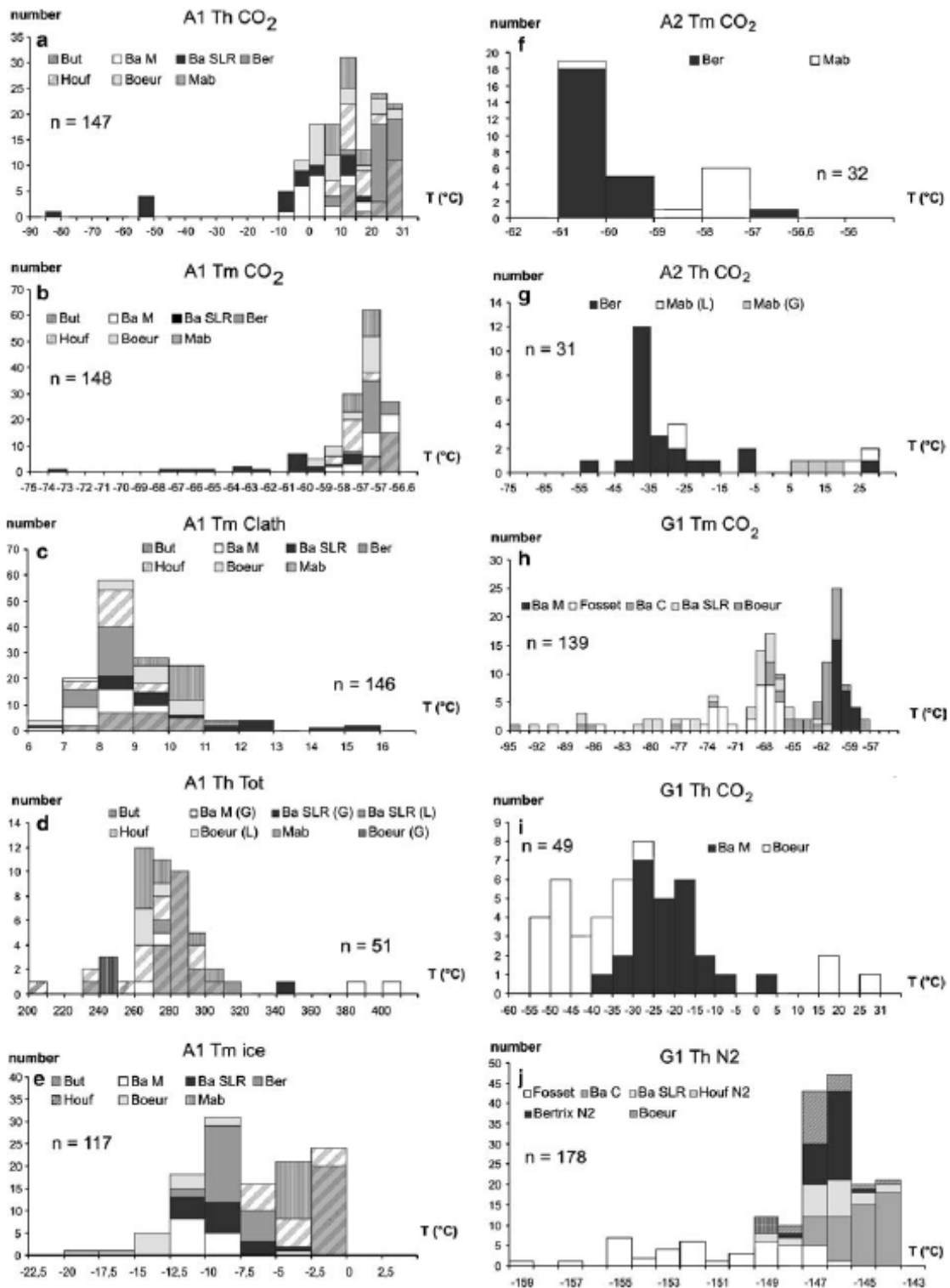


Figure A10 – Histograms for Th CO₂, Tm CO₂, Tm Clath, Tm ice and Th Tot values of the early mixed aqueous/gaseous (A1) and gaseous (A2) fluid inclusions and of the later gaseous (G1) fluid inclusions. But: Bütgenbach; Ba M: Bastogne Mardasson; Ba SLR: Bastogne Sur les Roches; Ber: Bertrix; Houf: Houffalize; Mab: Mabompré; G: homogenisation to the gaseous phase; L: homogenisation to the liquid phase; Th: homogenisation temperature; Tm: melting temperature (Kenis et al. 2005a).

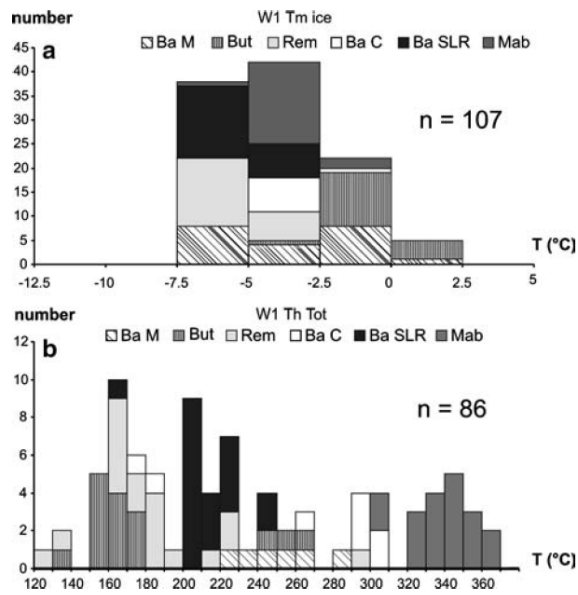


Figure A11 – Histograms for Tm ice (a) and Th Tot (b) values of the secondary aqueous (W1) fluid inclusions. But: Bütgenbach; Ba M: Bastogne Mardasson; Ba C: Bastogne Collignon; Ba SLR: Bastogne Sur les Roches; Mab: Mabompré; Rem: Remagne; Th: homogenisation temperature; Tm: melting temperature (Kenis et al. 2005a).

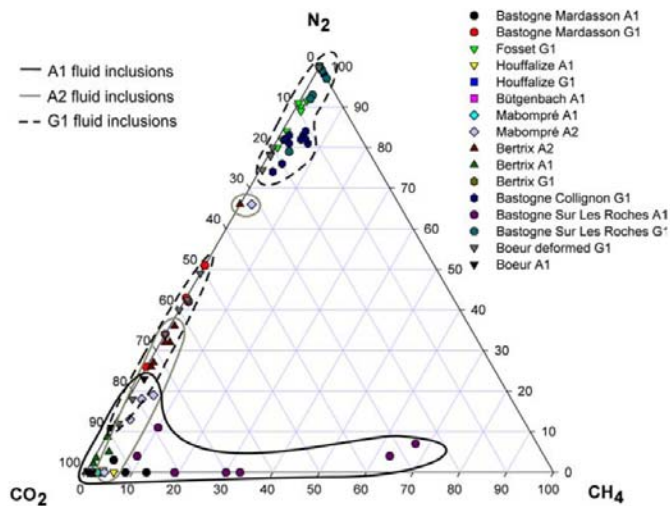


Figure A12 – Raman analysis of the different types of fluid inclusions with non-polar components (Kenis et al. 2005a).

Veins – chemical variation of the fluids

The primary aqueous/gaseous fluid inclusions are common in the metamorphic zone of the High-Ardenne slate belt (Darimont 1986, Schroyen & Muchez 2000). Their compositional range is compatible with metamorphic fluids produced by intense dehydration and decarbonisation under low-grade metamorphic conditions in sedimentary sequences. The presence of a large amount of non-polar species (e.g. CO₂, N₂, CH₄) in the primary inclusions is indicative of an intense fluid-rock interaction during metamorphism. CO₂ likely originated from decarbonisation of sedimentary sequences or oxidation of organic material, while CH₄ is thought to be produced by the maturation of organic matter. The origin of N₂ could be attributed to two main sources: (1) N₂ could be released during maturation of NH₄-bearing minerals in the host rock (e.g. bastonite) due to prograde metamorphism; (2) N₂ can be bound on organic matter.

The A1 inclusions occur in both the epizonal and anchizonal domain, while the A2 inclusions only occur in the epizonal domain (figure A13). In general, the proportion of non-polar species with respect to water decreases from the epizonal domain to the anchizonal domain. In addition, the portion of non-polar species other than CO₂ also

decreases from the epizonal towards the anchizonal domain. The salinity of the primary fluid in the anchizonal domain is rather low (between 0 and 3.5 eq.wt% NaCl), while in the epizonal domain the salinity ranges up to 17 eq.wt% NaCl. Salinity decreases from the epizonal towards the anchizonal domain. The increase of salinity with increasing metamorphism in the closed fluid flow system of the Ardenne-Eifel basin may be attributed to the hydrolysis of Cl-bearing silicates.

The aqueous/gaseous fluid inclusions (A1) in the anchizonal domain all show a limited variation in composition, bulk molar volume and phase-transition temperature. This suggests a homogeneous trapping of a single fluid above the immiscibility surface for mixed aqueous/gaseous fluids. In contrast, the inclusions in the epizonal domain show a wide range in bulk composition, a large spread of phase-transition temperatures within the same fluid inclusion assemblage and variable phase proportions at a wide range of temperatures. Total homogenisation is both to the liquid and gaseous state. Two possible explanations are suggested: (1) the mechanical mixing of immiscible fluids heterogeneously trapped in the two-phase region; the phase separation could have been triggered by strong pressure fluctuations during veining or could be induced by the higher salinity; or (2) mixing of fluids of different composition and possibly different origin.

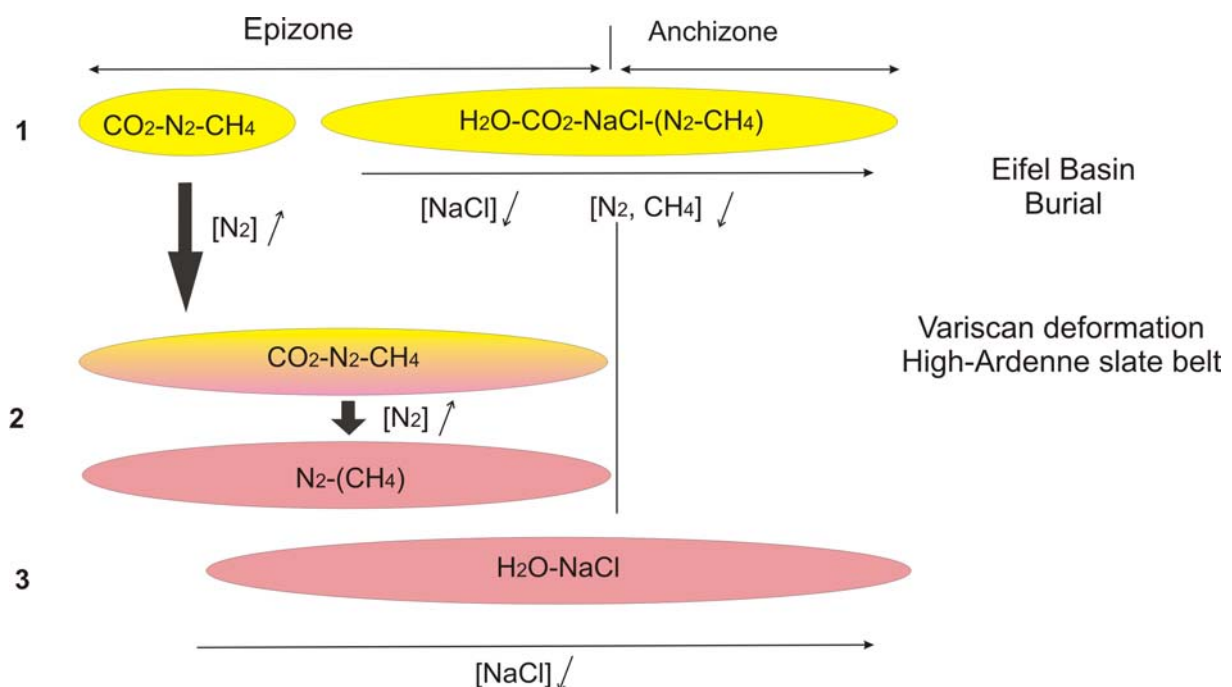


Figure A13 – Temporal and spatial evolution of the chemical composition of the fluid inclusions within the metamorphic area of the High-Ardenne slate belt (Kenis et al. 2005a).

In the secondary gaseous fluid inclusions (G1) different compositions can be recognised, ranging from $\text{CO}_2\text{-N}_2\text{-CH}_4$ to pure $\text{N}_2\text{-(CH}_4)$ (figure A13). Since all three-gas components are miscible at almost all conditions, it is fair to assume different origins for the gases. CO_2 likely originated from the decarbonisation under low-grade metamorphic conditions. CH_4 is thought to have been produced by the maturation of organic matter. N_2 can be released during the maturation of NH_4 -bearing minerals or released from organic matter. The circulation of gaseous Variscan fluids is restricted to the epizonal domain. The proportion of N_2 increases towards the centre of the metamorphic area.

The latest aqueous fluid type (W1) shows a decrease in salinity from the epizonal towards the anchizonal domain (figure A13). Here, chemical processes, described as acting during retrograde metamorphism (e.g. water loss by hydration reactions) could have caused the increase in fluid salinity of the secondary fluids.

Veins – fluid transport

The presence of non-polar species in the primary inclusions indicates an intense fluid-rock interaction. To define the nature of the mass-transport process (open or closed fluid flow system), a stable oxygen isotope analysis has been performed on vein-quartz and their immediate host rock (sandstone and pelite).

The similarity of $\delta^{18}\text{O}$ values between vein and host rock suggests a rock-buffered fluid system, resulting in isotopic equilibrium at peak metamorphic conditions between vein and host rock. Moreover, the differences in isotopic composition of the vein-host rock couple at different localities demonstrates that the isotopic equilibrium existed on a very small scale.

Diffusion is considered the dominant transport mechanism during the formation of the veins. This is supported by the presence of bedding-parallel dissolution seams within the sandstones. Because some of these dissolution seams also crosscut the veins, vein formation and dissolution are considered to have occurred simultaneously. The dissolution in the sandstone is considered the main source of the vein-filling material. A diffusive closed fluid flow system as the main driving mechanism implies that lateral and temporal chemical variation observed in the fluid inclusions can only be attributed to fluid-rock reactions occurring in the direct vicinity of the veins and can thus directly be linked with the metamorphic grade of the host rock. The latter complies with the chemical evolution of the fluids across the metamorphic area of the High-Ardenne slate belt, with more mature fluids in the epizonal central domain in comparison with the anchizonal peripheral domain of the Ardenne-Eifel rift basin.

The closed fluid system is, moreover, supported by the presence of near-lithostatic fluid pressures that are most probably responsible for the fracturing and vein development (Kenis 2004, Kenis et al. 2002).

Veins – P-T conditions at time of veining

For the determination of the P-T conditions at the time of veining, the isochores of the fluid inclusions that occur in growth zones and thus certainly having a primary origin are used. In the anchizonal domain (Bütchenbach) the isochores of the aqueous/gaseous inclusions are used. A homogeneous trapping of a single fluid is suggested. In the epizonal domain (Bertrix) the mixed aqueous/gaseous primary fluid inclusions often decriptitate before total homogenisation. Variable total homogenisation temperatures, moreover, suggest post-entrapment deformation of these inclusions, so that they can not provide sufficient reliability for constraining the P-T conditions. Therefore, in the epizonal domain the isochores of the gaseous (A2)

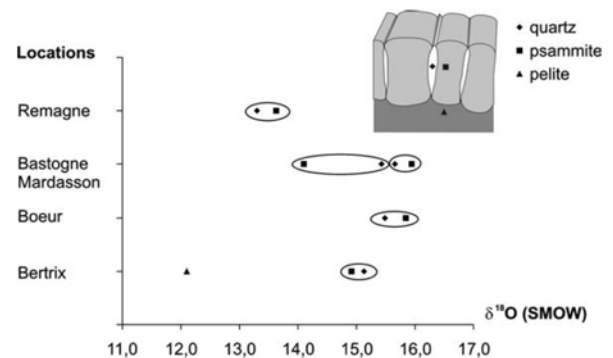


Figure A14 – $\delta^{18}\text{O}$ (SMOW) of the quartz veins and their host rock at different localities (Kenis et al. 2005a).

inclusions are used. The original P-T conditions of entrapment can, however, not be reconstructed from isochore evidence alone. The pressure and total homogenisation temperature serve only as the minimum constraint of entrapment condition. An independent geobarometer or geothermometer is required to determine the exact condition by intersection with the isochores.

In the case of the quartz veins in the High-Ardenne slate belt chlorite geothermometry has been used on chlorites within the veins. Microscopy suggests a syngenetic origin of both quartz and chlorite. At Bertrix (epizonal domain) the analysis shows that chlorites formed at a temperature of $\sim 390^{\circ}\text{C}$ (figure A16). This temperature corresponds to the maximum temperature of metamorphism, constrained from mineral assemblages (Fielitz & Mansy 1999). It also complies with the temperature obtained from chlorites in the host rock, again suggesting a close association between vein filling and metamorphism and a thermal equilibrium of the fluids with the host rock. The latter association infers that the metamorphic temperatures may be used to constrain temperature conditions in the entire metamorphic zone (see Bütchenbach) (figure A15).

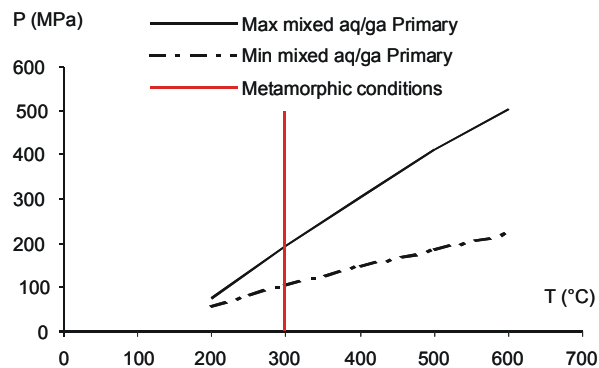


Figure A15 – Isochores of primary mixed aqueous/gaseous inclusions (A1) in the anchizonal domain (Bütchenbach) (Kenis 2004, Kenis et al. 2002). The temperature conditions are derived from the metamorphic temperatures (Fielitz & Mansy 1999).

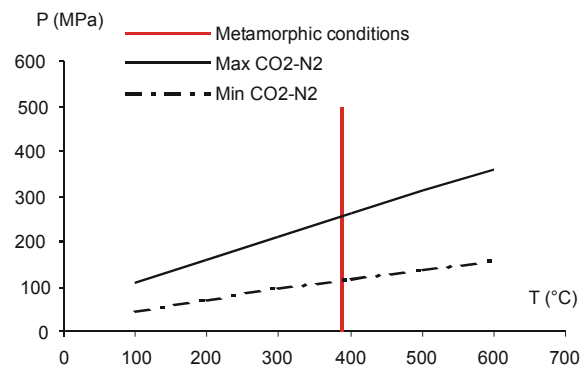


Figure A16 – Isochores of primary gaseous inclusions (A2) in the epizonal domain (Bertrix) (Kenis 2004, Kenis et al. 2002). The temperature conditions are determined by chlorite geothermometry.

In both cases a variation in position of the maximum and minimum isochores is observed (figures A15 & A16). This variation can be indicative of pressure variations or can be due to post-entrapment deformation. Microthermometric evidence (Kenis 2004) allow us to fairly assume that the different position of the isochores reflect a difference in pressure at the time of trapping. The data can thus be applied to estimate pressure variations in the mineralising fluids.

The maximum and minimum fluid pressure in the anchizonal domain (Bütchenbach) correspond to values of ~ 190 MPa and ~ 100 MPa respectively (figure A15). The maximum and minimum fluid pressure in the epizonal domain (Bertrix) corresponds to ~ 255 MPa and ~ 115 MPa respectively (figure A16). The difference in pressure indicates a maximum pressure fluctuation of ~ 140 MPa during veining. Considering a geothermal gradient of $\sim 40^{\circ}\text{C}/\text{km}$ (Helsen 1995, Schroyen & Muchez 2000), veining occurred at a depth ranging between ~ 7 and ~ 10 km. The maximum fluid pressure thus approximates lithostatic confining pressure. The minimum fluid pressure suggests that fluid pressure during veining varied between near-lithostatic and near-hydrostatic.

Both the near-lithostatic maximum fluid pressure and the pressure fluctuation between near-lithostatic and near-hydrostatic, suggests that hydraulic fracturing is the responsible mechanisms for the formation of the veins.

Veins – a Mohr-circle reconstruction

Mineralogical, microthermometrical and geochemical evidence demonstrate that veining occurred at peak metamorphic conditions in a closed fluid flow system in thermal equilibrium with the host rock. Veining occurred at the latest stages of the burial history of the Palaeozoic Ardenne-Eifel rift basin. Veining occurred at near-lithostatic fluid pressures by hydraulic fracturing and generated a regionally consistent, NNE-SSW trending, fracture/vein array.

The geometry of the vein array indicate that veining took place by tensile failure (extension veins) in a stress state, characterised by the differential stress that is relatively high (consistent array of parallel veins) (Cosgrove 1997) and a vertically oriented maximum principal stress (σ_1), caused by the overburden.

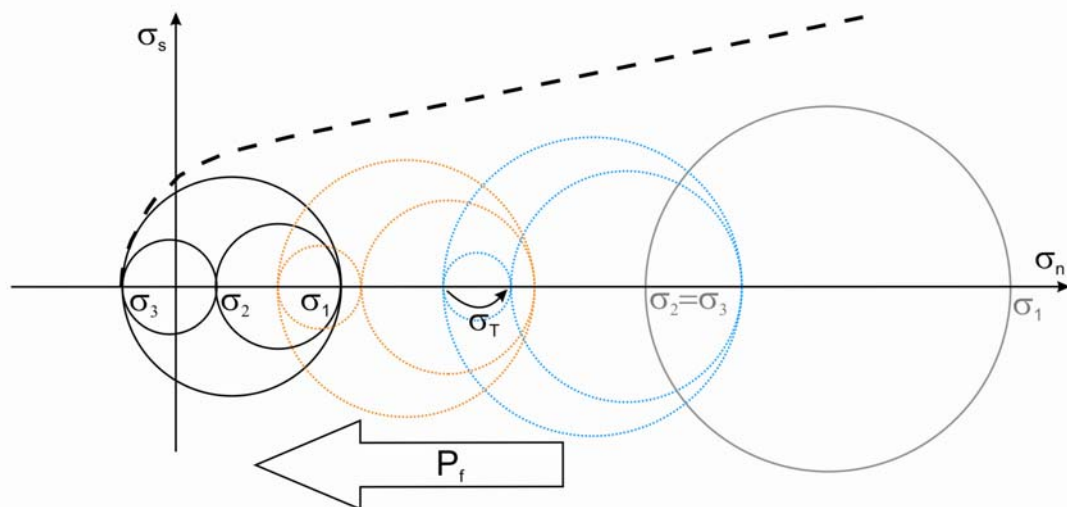


Figure A17 – Mohr-circle reconstruction of the assumed evolution of the state of stress: (1) state of stress in a tectonically relaxed basin; (2) reduction of differential stress by imposing an extra compressive horizontal – tectonic – stress (σ_T); (3) simultaneous increase of fluid pressure (P_f), forcing the stress state to the conditions of tensile failure (Kenis 2004).

By means of a simplified Mohr-circle reconstruction, we attempted to reconstruct the evolution of the stress state that caused vein formation. The starting point is a tectonically relaxed Ardenne-Eifel rift basin ($\sigma_2=\sigma_3$; $\sigma_T=0$). Considering the limited compressibility of the rocks at depth (i.e. Poisson's ratio), the stress state at a depth of ~10 km would be such that the differential stress would be too large (> 4 times the tensile strength of the rock)(Cosgrove 1997) to cause tensile failure. Therefore, to satisfy boundary conditions for tensile failure, a reduction of the differential stress (to less than 4 times the tensile strength of the rock) is required. Because an uplift (and reduction of the maximum principal stress (σ_1)) is excluded, an increase of the horizontal principal stresses is inferred. The latter can

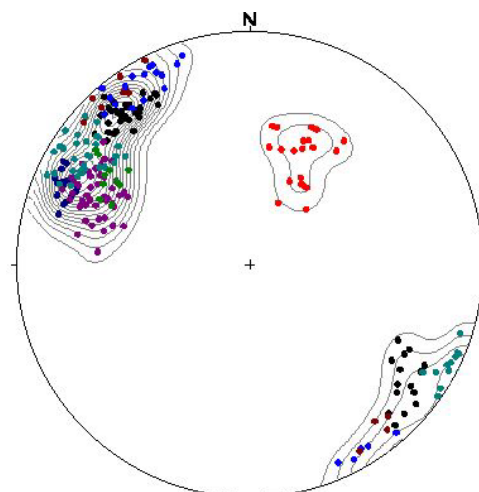


Figure 16 – Orientation of veins prior to folding. Bütchenbach (dark blue); Houffalize (purple); Boeur (black); Mabompré (brown); Bastogne Mardasson (green-blue); Bastogne Collignon (green); Remagne (red); Bertrix (light blue). Lower-hemisphere equal area projection (Kenis 2004).

be realised by adding a positive horizontal – tectonic (σ_T) – stress to the intermediate principal stress (σ_2), and thus indirectly to the minimum principal stress (σ_3) (figure A17). A simultaneous increase in fluid pressure (P_f) will eventually force the stress state into a condition of tensile failure (figure A17).

To estimate the direction of the tectonic paleostress (σ_T), all veins were backrotated to their original position (i.e. before folding). With the exception of the veins at Remagne, all veins were originally oriented NNE-SSW to NE-SW (figure A18). A NNE-SSW to NE-SW directed tectonic regional paleostress (σ_T) can thus be assumed.

Veins – a proxy for high-pressure compartments

Vein quartz originated from fluids that were linked to the regional low-grade burial metamorphism ($\sim 400^\circ\text{C}$) in the deepest part (~ 10 km depth) of the Palaeozoic Ardenne-Eifel sedimentary basin (Kenis 2004, Kenis et al. 2005a). Veining occurred at near-lithostatic fluid pressures by hydraulic fracturing (Kenis et al. 2002) and generated a regionally consistent, NNE-SSW trending, fracture/vein array. At this depth, in the brittle-ductile transition zone, this hydraulic fracturing event is considered to be related to a change in tectonic regime (Sibson 2001) at the onset of Variscan orogeny. Transient co-seismic stress fluctuations (Nüchter & Stöckhert 2006, 2007) may eventually have caused the hydraulic fracturing.

Quartz veins serve as a proxy for high fluid pressures, enabling to outline high-pressure compartments in the metasedimentary sequence of the Palaeozoic Ardenne-Eifel basin. In this respect the Ardenne-Eifel region exposes an analogue of a ~ 340 Ma old, fractured reservoir (Hilgers et al. 2000).

Cusate-lobate morphology – the geometrical characteristics



Figure A19 – Divergent cleavage fan pattern in the pelitic parts of a multilayer structure (Boeur) (Kenis 2004).

The second feature of the brittle-ductile structures is the cusate-lobate geometry of the interface between materials of different composition/competency (figures A4 & A6). The layer-parallel dissolution seams, which crosscut the veins, follow this cusate-lobate morphology, clearly indicating that the cusate-lobate buckling occurred after veining and should be considered a separate – ductile – event. In addition, internal cleavage fanning inside pelitic layers of multilayer structures (figure A19) demonstrates that the cusate-lobate morphology is a consequence of layer-parallel shortening, occurring at the onset of the Variscan orogeny.

The development of this cusate-lobate morphology of the interface between sandstones and pelites due to layer-parallel shortening complies with the kinematic definition of mullions as nowadays acknowledged by the geological community.

The presence of the mullions is, however, entirely constrained by the presence of the veins, although both structures are the result of separate events. Without the presence of the veins, no cusped-lobate geometry will occur at the interfaces. The formation of the mullions is caused by a strong rheological difference between the vein quartz (deforming by dislocation creep) and the sandstones (deforming by solution-precipitation creep). Without this rheological difference no mullions would have formed. Mineralogical and microstructural evidence show that mullion formation occurred at very similar conditions as the vein formation (i.e. 350-400°C, ~260 MPa). The formation of the mullions at the sandstone-pelite interface is pinned by the pre-existing quartz veins.

**Cusped-lobate morphology
– the numerical modeling**

The simple geometry of the mullions provides an unusually well-constrained set of initial geometries and boundary conditions. A simplified analytical model (Urai et al. 2001) suggests that the morphology of the mullions is a strong function of the stress exponent of the power-law creep equation of the sandstone. A more representative plane-strain geomechanical model using finite element techniques has been developed (Kenis et al. 2004) (figure A20). A viscoplastic formulation in which the strain-rate potential can be written as a function of equivalent stress, as implemented in the ABAQUS software package, has been used.

A parameter sensitivity analysis (Kenis et al. 2004) shows that the shape of the individual mullions is controlled by four parameters (figure A21): (1) total layer-parallel shortening; (2) initial aspect ratio of sandstone/psammite segments before shortening; (3) stress exponent of the sandstone; and (4) the competence difference between vein quartz and sandstone. The curvature of the interface is primarily a function of the stress exponent.

The structural observations of a mullion in the field provide the opportunity to construct models specific to each mullion, using a suitably chosen set of parameters. The sensitivity analysis suggests that there might exist a unique set of parameters, which makes the model match all the observations related

Mullion

The term mullion is used to describe the particular cusped-lobate morphology of a folded interface between two materials with a contrasting viscosity due to layer-parallel shortening (van der Pluijm & Marshak 2004).

The textbook example of mullions is located at Dedenborn in the Eifel region (Kenis 2004, Pilgers & Schmidt 1957). These mullions show the same characteristics as the brittle-ductile structures in the Bastogne area (e.g. veins, cusped-lobate morphology, cleavage-bedding intersection).

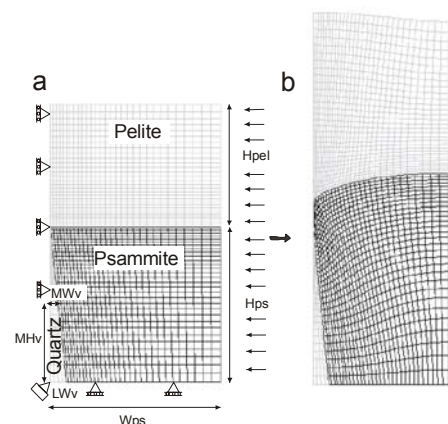


Figure A20 – Mesh of the deformable vein model (Kenis et al. 2004). The triangles give a representation of the boundary conditions imposed on the model. Hpel, Height pelite; Hps, Height psammite; Wps, Width psammite; Hps, Height psammite; MHv, Mid-Height vein; MWv, Mid-Width vein; LWv, Lower-Width vein.

to specific mullions. This provides a tool to solve the inverse problem and determine the rheology of the sandstones.

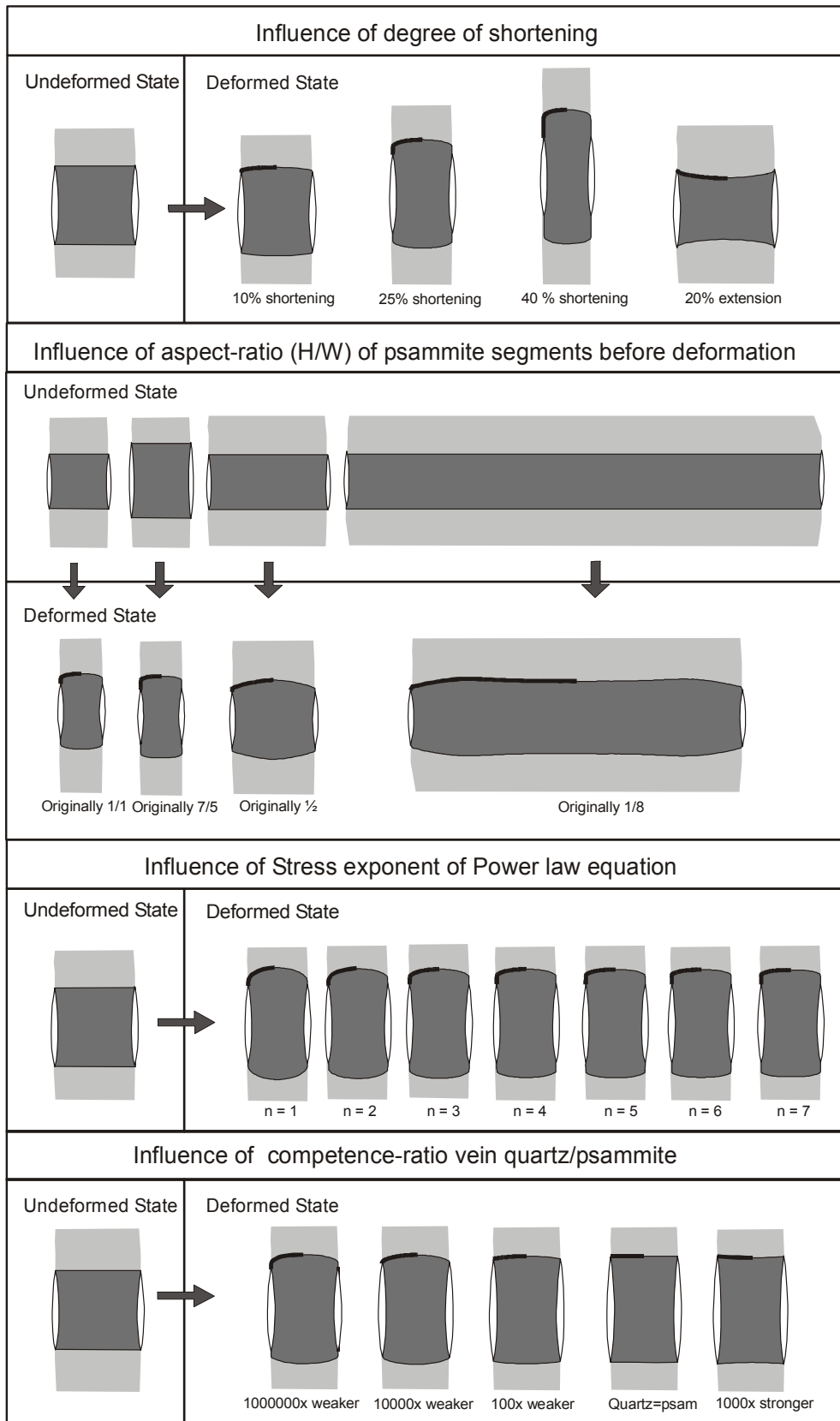


Figure A21 – Schematic overview showing the influence of the four main controlling parameters on the shape of the mullions. All mullions are drawn on a scale of 1/1 (Kenis et al. 2004).

Cusped-lobate morphology – a palaeorheology gauge

To date, we have performed seven case studies of mullions observed in various outcrops (figure A22). Using the numerical parameter estimation method, in all cases the model converges to a single set of parameters, which define the flow law of fine-grained siliciclastic rocks, such as sandstone, at low-grade metamorphic conditions (350-400°C) and geological strain rates (Kenis 2004, Kenis et al. 2005b). We consistently find an approximately ten-fold contrast in strength between the sandstone and vein quartz (wet quartz) (figure A23), together with a stress exponent of 1.

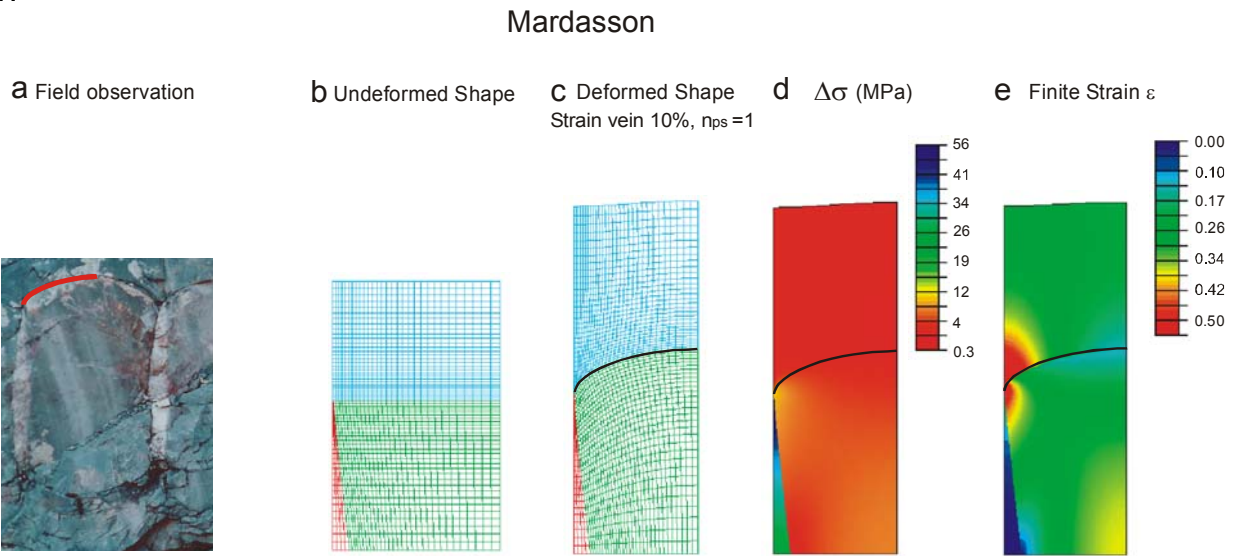


Figure A22 – Best-fit solution of the case study of a mullion at Bastogne Mardasson (Kenis 2004), showing the field observation (a), undeformed (b) and deformed mesh (c) of the numerical model and contour plots of the differential stress (d) and finite strain (e) of the mullion. The result of the numeric solution fits well with observations of the mullion shape.

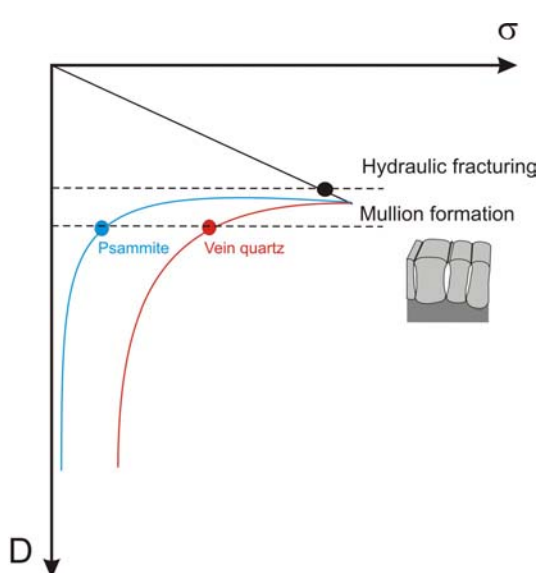


Figure A23 – Crustal strength curve with indication of the strength of the sandstone/psammite with respect to the hydraulic fracturing event and to the mullion development. In the latter case the sandstone/psammite is much weaker than the vein quartz.

This indicates that sandstone at low-grade metamorphic conditions deforms in a linear or Newtonian way. A Newtonian constitutive equation for the deformation behaviour of fine-grained siliciclastic rocks in the middle crust is in agreement with microstructural observations in the sandstone, indicating that solution-precipitation creep was probably enhanced by the presence of phyllosilicates within the fine-grained rocks. The absence of notable deformation by dislocation creep of quartz in the sandstone indicates that the differential stress remained too low for the deformation mechanism to be competitive with solution-precipitation creep. In contrast, the vein quartz is dominantly deformed by dislocation creep indicating high flow stress in these parts and causing an inhomogeneous stress field in the different lithologies, leading to the process

of mullion formation at the onset of Variscan shortening (Kenis et al. 2005b).

As a consequence, the strength of polyphase quartz-rich rocks located in the middle crust is much lower than predicted by conventional models based on flow laws from dislocation creep (figure A23). Because fine-grained siliciclastic rocks control the rheology of the middle crust in many sedimentary basins, these results provide new quantitative parameters for geodynamic modelling in which a flow law for solution-precipitation creep is essential. Moreover, mullions occur worldwide in deformed sediments, and the method is therefore applicable to quantify rock rheology in other areas and geological settings offering further perspective for the quantification of rheological flow laws.

A KINEMATIC MODEL

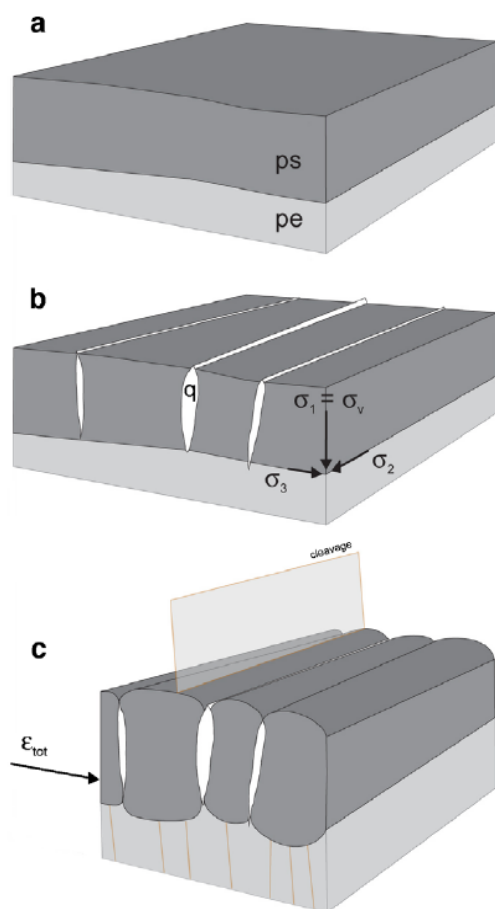


Figure A24 – Schematic model of the development of the brittle-ductile structures in the High-Ardenne slate belt (Kenis et al. 2005b).

This scheme summarises the development of the brittle-ductile structures in the High-Ardenne slate belt.

(a) Layers of pelite (pe) and sandstone/psammite (ps) are deposited in the early Palaeozoic Ardenne-Eifel rift basin, and subsequently compacted during burial in the subsiding basin.

(b) During the latest stages of the basin development and burial (~340 Ma ago), a fracturing/veining event occurred at low-grade metamorphic mid-crustal conditions (350-400°C; ~260 MPa) due to hydraulic fracturing in high fluid-pressure compartments. This hydraulic fracturing event seems related to a change in tectonic regime, heralding the Variscan orogeny. Transient co-seismic loading (Nüchter & Stöckhert 2006, 2007) may eventually have triggered brittle fracturing below the regional brittle-ductile transition.

(c) At the onset of the Variscan orogeny (~330 Ma), layer-parallel shortening resulted in the formation of the cusped lobate morphology of the pelite-sandstone interface, i.e. mullion formation. The strength contrast between the vein quartz and sandstone controlled

the shape of the mullion, which allows us to use the mullions as a palaeorheological gauge. The ongoing Variscan deformation (~320 Ma – Sudetic stage) resulted in the folding and cleavage development, giving rise to the High-Ardenne slate belt.

CLOSING REMARKS

Nearly a century after the terms 'boudin' and 'boudinage' have been coined in the Bastogne area, the 'original' structures in the Ardenne-Eifel region turn out to be very particular, expressing a polyphase deformation history in brittle-ductile deformation conditions at the onset of the Variscan orogeny. Brittle deformation resulted from high fluid pressures causing hydraulic fracturing of the overpressured sandstone layers. Once formed, the quartz veins acted as 'rigid' bodies, causing buckling of the sandstone-pelite interfaces between the veins due to layer-parallel shortening, creating textbook examples of 'mullions'. In this respect, the Ardenne-Eifel region may be considered an interesting natural laboratory to study the brittle-ductile deformation behaviour of siliciclastic metasediments in mid-crustal tectonometamorphic conditions. Notwithstanding the fact that these particular structures are not related to the process of boudinage, historical justice has to be done to the original 'boudins' in the Ardenne-Eifel region by aspiration to create a geological heritage site at Bastogne.

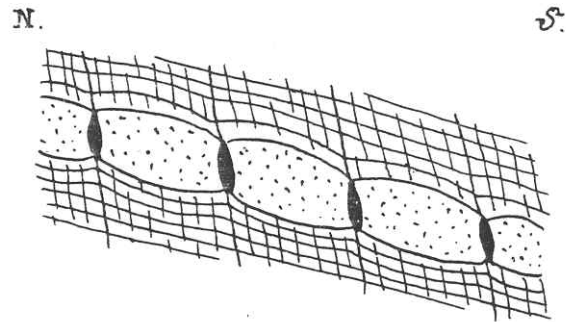


Figure A25 – An original drawing of the brittle-ductile structures in the High-Ardenne slate belt by Stainier (1907).

STOP B – Wellin – Fond des Vaulx quarry:
“Brittle structures in a fold context. Relation between brittle tectonics and karst dynamics”

by Sara Vandycke in collaboration with Yves Quinif & Cécile Havron

INTRODUCTION

The brittle structures of four limestone massifs around Han-sur-Lesse (Ardenne, Belgium) are studied with the aim of understanding the relationship between tectonic and karstologic histories (Havron et al. 2007). A detailed structural analysis has been done in view to correlate tectonic events and karstic development. The quarry offers the opportunity to correlate Variscan folding dynamics and brittle structures scaling due to recent tectonics. Special attention is paid to the relation between brittle structures and karstic features.

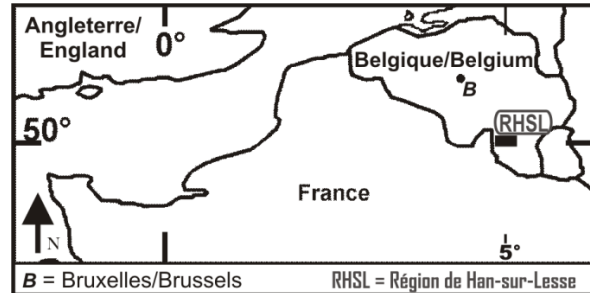


Figure B1 – Location of the Han-sur-Lesse region (RHSL). B: Brussels.

Logistics – Terrain



The Fond des Vaulx quarry (Société Cimescaut) is situated in the Wellin massif. The quarry is near the E411 motorway (exit 23) and is at the banks of the Ry d’Ave river.

This is a quarry in exploitation. Hard hats compulsory! Please approach exploitation front with caution!

Map: 1:25.000 sheet 59/5-6 Wellin-Pondrôme

Contact: Les Carrières du Fond des Vaulx s.a., rue du Fond des Vaulx, 60, B-6920 Wellin, tel.: +32 (0)84 38 86 28; fax: +32 (0)84 38 95 60; e-mail: info@cfv.be; URL: www.cfv.be.

Aims

The purpose of this visit is:

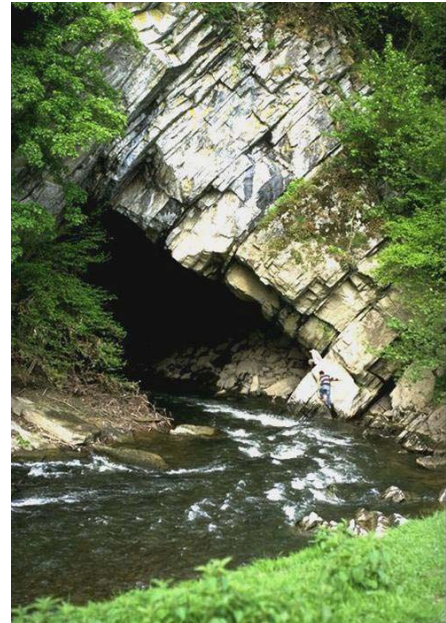
1. to observe the typical cylindrical folds of the Givetian rocks in the southern part of the Dinant fold-and-thrust belt (Dinant Synclinorium);
2. to examine brittle structures in limestones in a fold context (joints, faults, tension gashes);
3. to contrast structures that are karstified and not karstified.

Points to debate:

1. What is the relationship between brittle structures and folds in term of timing and deformation?
2. What type of tension gashes occur? What is their relationship with folding and shearing?
3. What structure can be related to Variscan and post-Variscan dynamics (e.g. extensional Meso- and Cenozoic brittle tectonics)?
4. What is the relationship between karstic dynamics and extensional tectonics? Are the structures inherited or newly formed with respect to Variscan structures?

Grottes de Han-sur-Lesse

The caves of Han-sur-Lesse are a major Belgian tourist attraction with around half a million visitors per year. The Lesse river rushes into the cave system through the "Goufre de Belvaux" with resurgence at the "Trou de Han", on the other side of the "Boine Hill". It is one of the bigger karstic networks in Belgium and it is supposed that some parts are still to be discovered.



The "Goufre de Belvaux".

GEOLOGICAL SETTING OF THE HAN-SUR-LESSE REGION

The Han-sur-Lesse area is located in the southern part of the Dinant fold-and-thrust belt (*Dinant synclinorium*), part of the Variscan Ardenne allochthon. This zone is mainly structured in hectometric and kilometric cylindrical E-W folds (Delvaux de Fenffe 1985, 1990). This area is also close to a virgation zone of the Palaeozoic beds (Lacquement 2001). If the bedding plane is almost E-W in the Han-sur-Lesse area, NE-SW direction is the most common bedding planes strike on the East (Delvaux de Fenffe 1985, Forir 1897, 1900, Lacquement 2001). Two major Variscan compression events are established: N-S compression and NW-SE compression. Brittle structures due to the Meso-Cenozoic extensional events are not evidenced in literature.

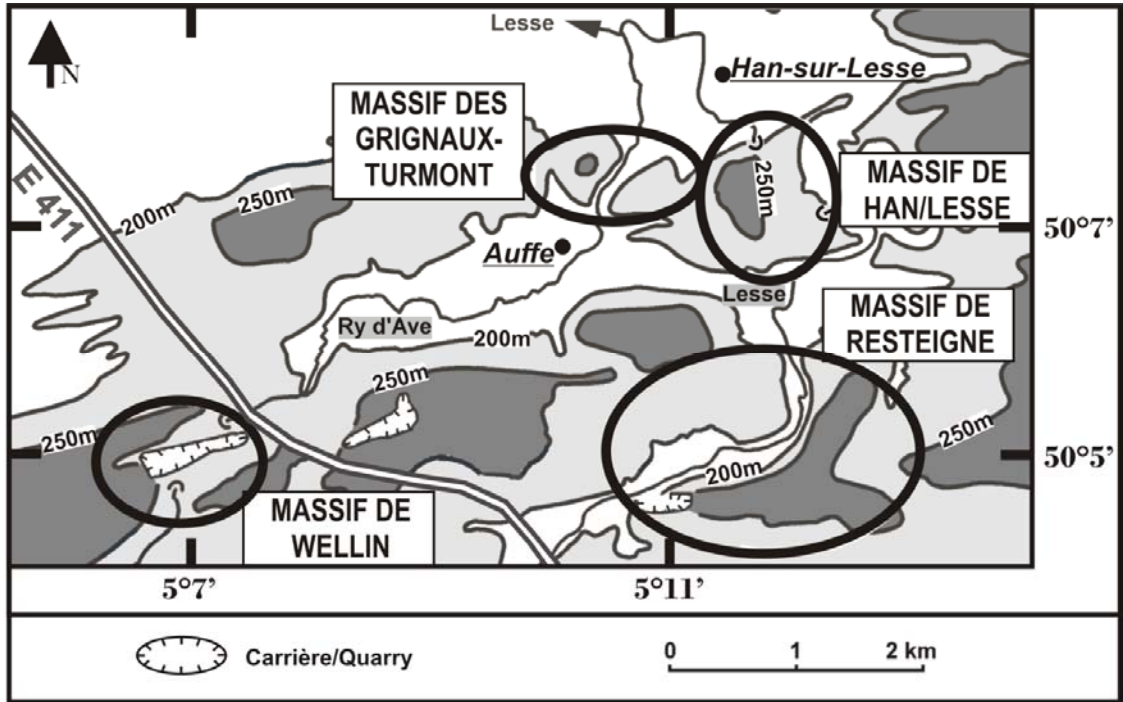


Figure B2 – Localisation of studied massifs: karstified massifs of Han-sur-Lesse and Wellin and unkarstified massifs of Grignaux-Turmont and Resteigne. Hills constituted by limestone are well defined by 250 m levels curves. The regional rivers – “Ry d’Ave” and “Lesse” - are epigenetic.

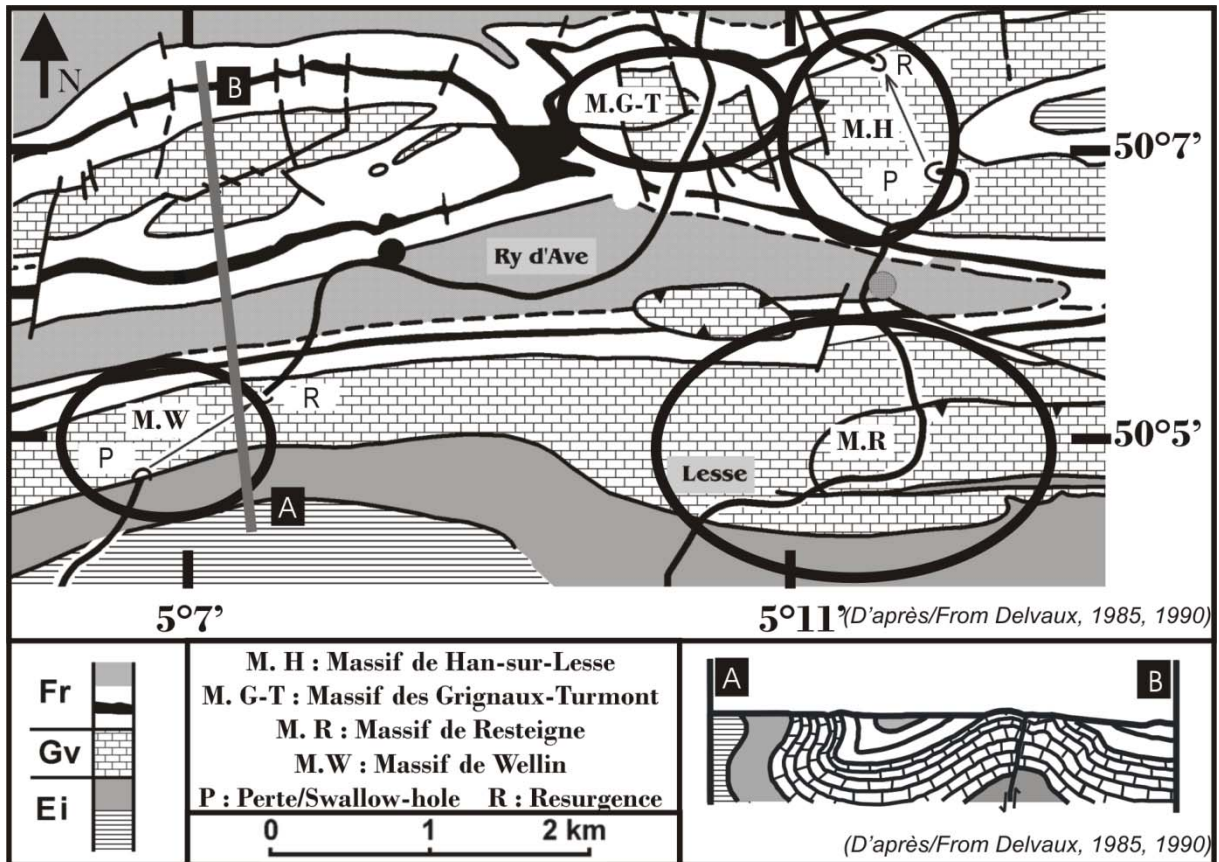


Figure B3 – Simplified geological map and cross-section of the Han-sur-Lesse region (modified after Delvaux de Fenffe 1985, 1990). The four studied massifs are constituted by Eifelien and Givetian limestones. N-S geological section is representative of the Variscan structures in the studied area.

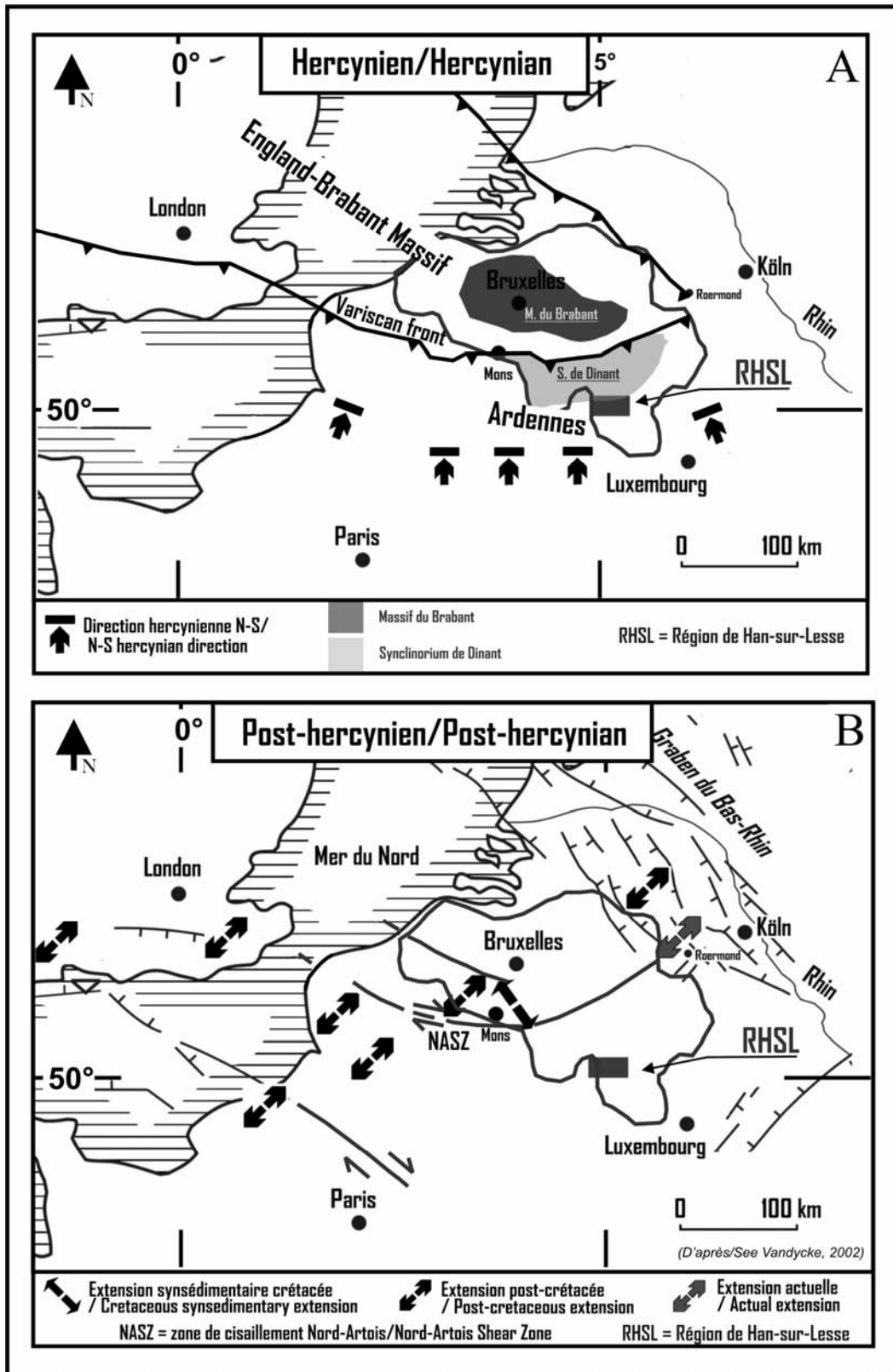


Figure B4 – Structural synthesis of the kinematics in NW Europe (modified after Vandycke 2002). A. Variscan (Hercynian) context (Delvaux de Fenffe 1985, Lacquement 2001). B. Post-Variscan (post-hercynian) context in proximal regions (Quinif et al. 1997, Vandycke 2002).

Fond des Vaultx

The limestones exploited in the Fond des Vaultx quarry are Middle Devonian, mainly Eifelian and Givetian in age. At Wellin, the Hanonet, Trois-Fontaines, Terre d'Hours, Mont d'hours and Fromelennes formations can be observed. The **Hanonet formation** is characterized in the lower part by blackish, argillaceous, pyritic nodular thin limestones, with also silty and micaceous limestones. The upper part is mainly constituted by two massive biostromal units with stromatoporoids, rugose and tabulate corals. The limestones of the **Trois-Fontaines formation** are micritic with occasionally laminated limestones, quite massive with crinoides, coquinoid beds with stringocephalids. The **Terres d'Haur formation** consists of alternating argillaceous, crinoidal, bedded or nodular limestones and mostly with corals, brachiopods and trilobites. The **Mont'hours limestones** are quite similar to the previous one, but more massive. The **Fromelennes formation** closes the calcareous sequence with a dominantly argillaceous formation (Bultynck & Dejonghe 2001, Coen-Aubert et al. 1991, Coen-Aubert et al. 1986).

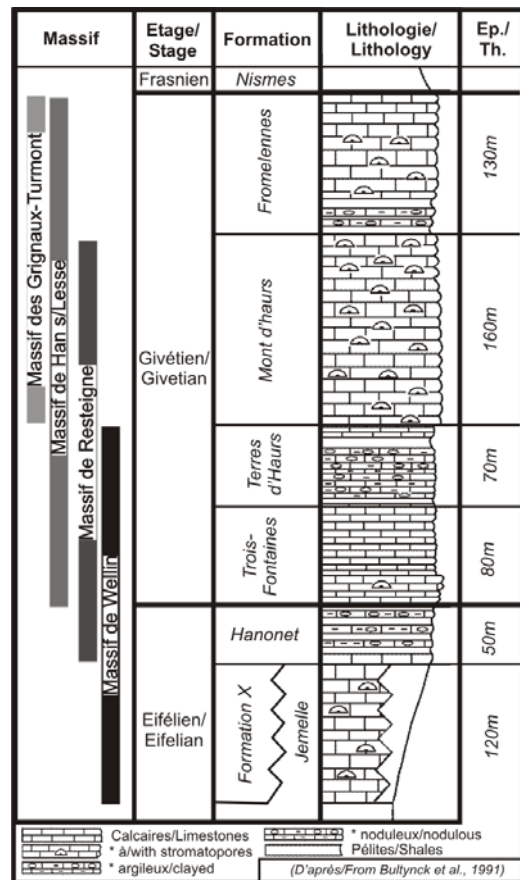


Figure B5 – Lithostratigraphy of the studied massifs in the Han-sur-Lesse area (Havron et al. 2007).

BRITTLE TECTONIC ANALYSIS

Massifs	Failles/Faults	Fentes d/tension /Tension gashes	Joints	Joints de strati. /Bedding planes
Massif de Han-sur-Lesse	43	81	25 + 766	26
Massif des Grignaux-Turmont	6	1	91	37
Massif de Resteigne (Carrière/Quarry)	96	33	70	29
Massif de Wellin (Carrière/Quarry)	105	66	62	25
Total	250	181	232 + 766	117

Table B1 – Number of brittle tectonic structures measured in each limestone massif (karstified or not karstified) in the Han-sur-Lesse area.

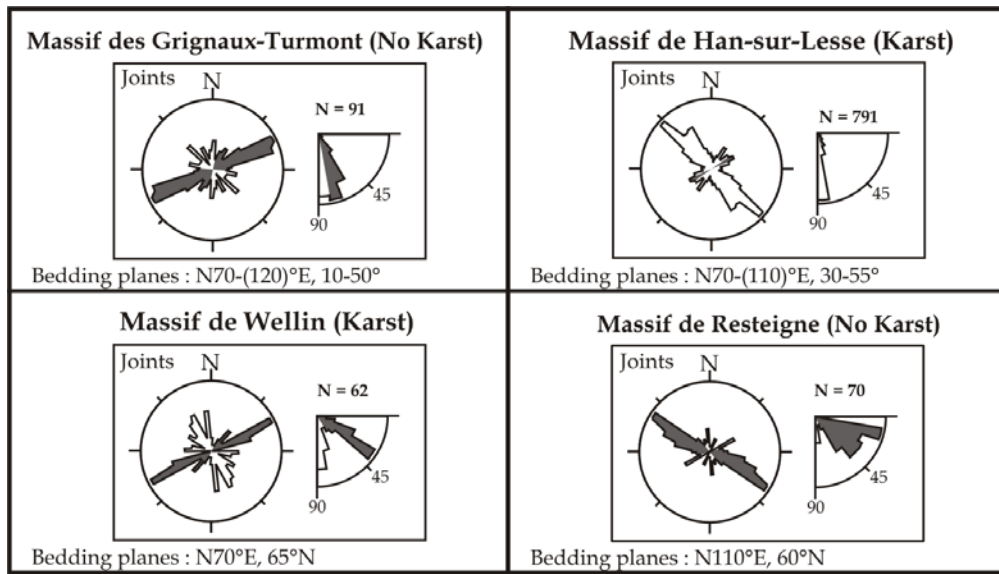


Figure B6 – Geometry of joints measured in the Han-sur-Lesse region. Joints are fractures of rock without displacement of the two parts. Three families of joints are defined: bedding planes, diaclases (in grey in the figure) and joints (in white in the figure). Diaclases are observed in every massif; one group of N140°E-N150°E joints are observed only in the Han-sur-Lesse and Wellin massifs.

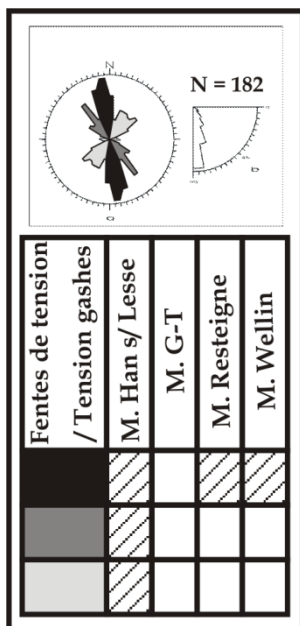


Figure B7 – Geometry of tension gashes in the Han-sur-Lesse region, measured in the Eifelian and Givetian formations; a. strike, b. dip. Three groups of homogeneous tension gashes are measured. All groups are not observed in all massifs. The group of North-South tension gashes is present in every massif; the two other groups all only present in the Han-sur-Lesse massif.

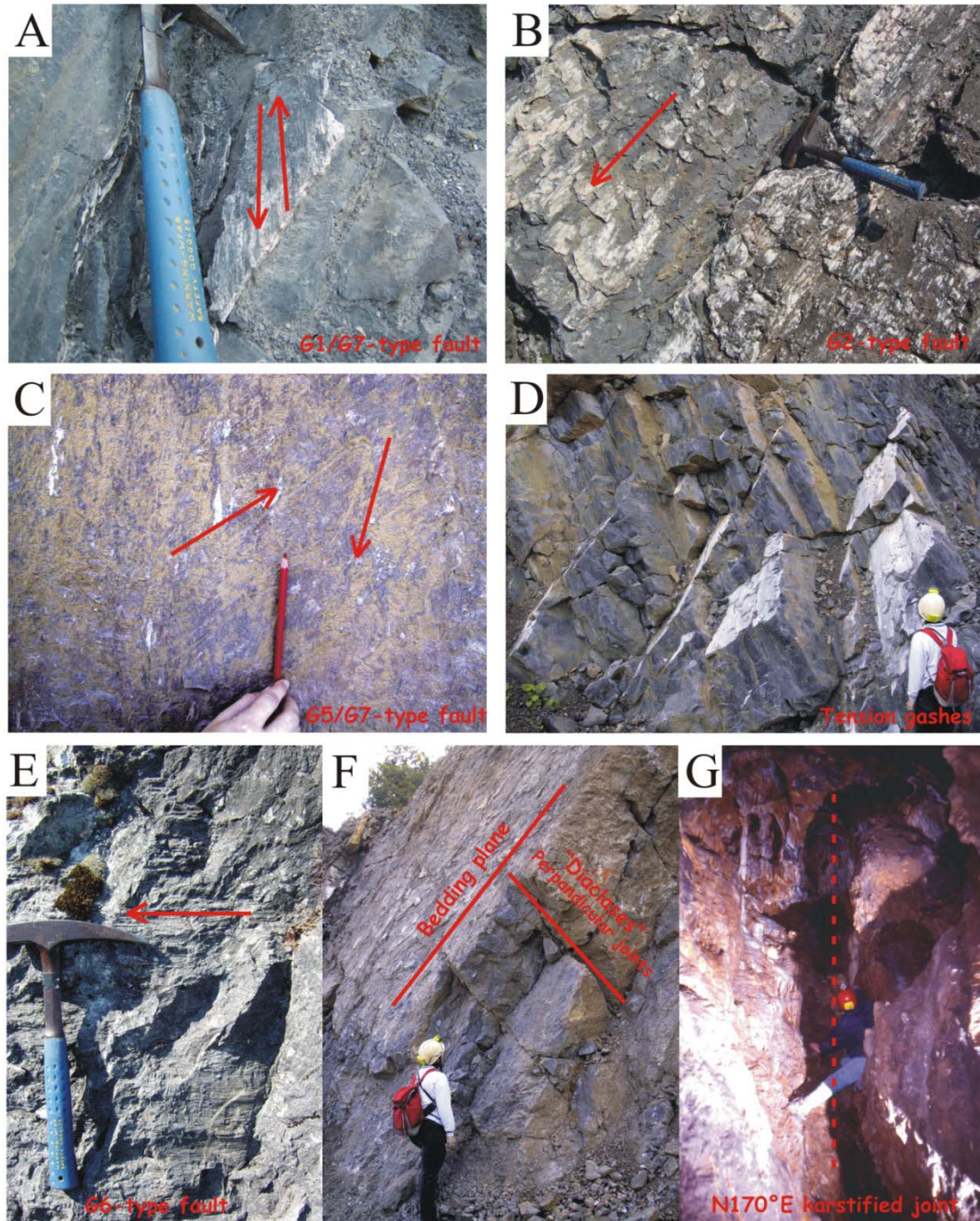


Figure B8 – Brittle structures observed in the massifs of Han-sur-Lesse region. A. Slickenside lineation of reverse fault of group 1 and of normal fault of group 7 on one bedding plane (Massif of Resteigne). B. Oblique fault of group 2 (Massif of Resteigne). C. Normal fault of group 7 surimposed on sinistral strike-slip fault of group 5 (Massif of Wellin). D. Tension gashes (Massif of Wellin). E. Dextral strike-slip fault of group 6 (Massif of Resteigne). F. General view of bedding planes with perpendicular joints or “diaclasses” (Massif of Wellin). G. Vertical N170°E karstified joint (Massif of Wellin). The arrows on faults symbolise the movement of the missing part of fault.

PALEOSTRESS ANALYSIS

The analysis of faults by “Direct Inversion Method” (Angelier 1990, 1994) shows four paleostress tensors that have been active in the Han-sur-Lesse area. They are interpreted as Variscan tectonic settings: N-S compression, NE-SW compression, NE-SW strike-slip and N-S extension. The study of joints shows the existence of numerous, vertical, equidistant N140°E-N150°E joints in the Han-sur-Lesse region. They cross indistinctly all Variscan structures. These NW-SE joints express that extensive Meso-cenozoic tectonics have well affected the Palaeozoic formations of Belgium. Meanwhile, it is important to note that these particular joints are only present in two of the four studied massifs: only in the karstified massifs of Han-sur-Lesse and Wellin. An undetermined site effect probably controlled this. Meso-cenozoic tectonics would have initiated the development of karstic systems of Han-sur-Lesse and Wellin. So, it is observed that karstic networks are structured along some particular orientations related to recent tectonics, with an extensional component. The NE-SW extension event, with NW-SE joints is the most developed brittle system. This system in NE-SW extension is related to the opening of the Rhin Graben and is present in the whole domain studied. It is still active today.

Active tectonics in the Grotte de Lorette at Rochefort

Recent faulting activity has been observed in the Rochefort Cave situated in the Han-sur-Lesse area. Recent tectonic features affect karstic features with fresh scaling, argilleous slickenside, extensional, fallen blocks and displacement of karstic tube. Geophysic instruments have been installed in view to establish the origin of these recent tectonics features: crustal stress, local destalinization or movements due to regional tectonic, etc (Vandycke & Quinif 2001).



A karstic tube displaced by a recent active fault.

N° stress tensor	N	σ_1	σ_2	σ_3	Φ	α	RUP(%)	T.setting	COH(%)
T a	82	359°/09°	089°/09°	192°/81°	0,4	16°	29	C N-S	96
T b (G1 + G2)	89	009°/18°	109°/29°	251°/55°	0,3	16°	37	C N-S	100
T b (G3)	06	303°/08°	213°/01°	117°/82°	0,6	07°	31	C NW-SE	100
T c	12	054°/00°	324°/03°	151°/87°	0,5	08°	24	C NE-SW	100
T d	43	243°/05°	150°/34°	340°/46°	0,1	25°	54	X NE-SW	77
T e	31	221°/78°	072°/10°	340°/06°	0,4	14°	28	E N-S	100

Table B2 – Recapitulative table of calculated stress tensors from measured faults in the Han-sur-Lesse Region (Eifelian and Givetian formations). N° stress tensor = identification of stress tensor, N = computation, σ_1 = trend and plunge of major principal stress axis, σ_2 = trend and plunge of medium principal stress axis, σ_3 = trend and plunge of minor principal stress axis, ϕ = ratio $(\sigma_2 - \sigma_3) / (\sigma_1 - \sigma_3)$, α = the average angle between computed shear stress and observed slickenside lineation, RUP = ratio RUP (between 0% and 200%) of the INVDIR method (Angelier 1990, 1994), T setting = tectonic regimes : compression (C), strike-slip (X), extension (E), COH = coherence ratio between measures and calculus.


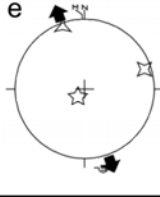
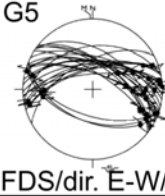

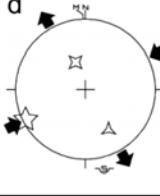

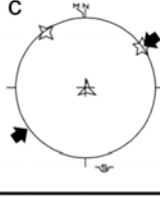

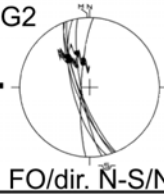

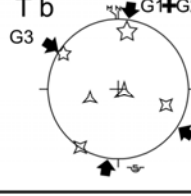

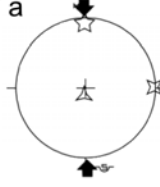
Han-sur-Lesse			M. Han/Lesse	M. G-T	M. Resteigne	M. Wellin		
Analyse en Paléocontraintes /Paleostress analysis								
Régimes tectoniques/ Tectonic settings	Géométrie des failles / Faults geometry		Tenseur de contraintes / Stress tensor					
Extension N-S	 G7 FN/dir. E-W/H		 T e					
Décrochement/ Strike-slip NE-SW	 G5 FDS/dir. E-W/H	 G6 FDD/dir. NE-SW/N	 T d					
Compression NE-SW	 G4 FI/dir. NW-SE/N		 T c					
Compression N-S	 G1 FI/dir. E-W/H	 G2 FO/dir. N-S/N	 G3 FI/dir. NE-SW/N	 T b G1+G2+G3				
	 G1 FI/dir. E-W/H		 T a					

Figure B9 – Geometry of measured faults and calculated stress tensors. The measured faults have been divided into seven homogeneous groups of faults. Stress tensors have been calculated with all the faults in front. FI = reverse fault , FO = oblique fault, FDS = sinistral strike-slip fault, FDD = dextral strike-slip fault , FN = normal fault, H = inherited, N = neoformed. Four tectonic settings have been observed: N-S compression (older than all the others), NE-SW compression, strike-slip event with compression NE-SW and N-S extension. N=number of fault used in the calculus of the tensor (Havron & al., 2007).

RELATIONSHIP BETWEEN BRITTLE TECTONICS AND KARSTIC DYNAMICS

The study of karstified joints indicates that karstic systems in Han-sur-Lesse are structured on two privileged directions: the particular N140°E-N150°E family of joints and N50°E-N70°E family of joints. The karstification along N50°E-N70°E joints would be an indirect record of the action of an older NW-SE extension, probably Cretaceous in age. It forces too to formulate a new hypothesis for the formation of karstic systems of the Han-sur-Lesse region, related to an emptying of older alteration. The karstic system in the Han-sur-Lesse region would be older than expected. They would be formed in at least two stages: one Meso-cenozoic and another purely Cenozoic.

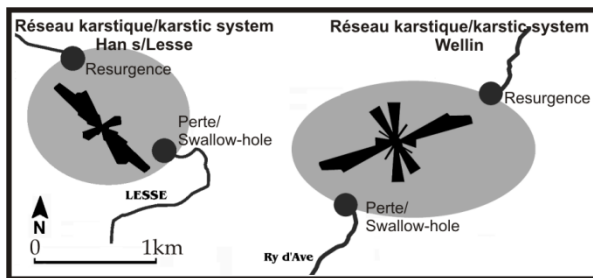


Figure B10 – Geometry of karstified joints i.e. joints from which galleries of caves have been formed in Han-sur-Lesse and Wellin massifs. Two directional groups of joints are karstified: group of N140°E-N150°E joints and group of N50°E-N70°E joints. This last group is formed by vertical joints in Han-sur-Lesse massif and by bedding planes and diaclases in Wellin massif.

DISCUSSION

	TECTONIQUE ET STRUCTURES / TECTONICS AND STRUCTURES	mgh?	KARSTOGENESE ET GEOMETRIE DES RESEAUX / KARSTOGENESIS AND KARSTIC GEOMETRY
Cénozoïque/c	<p>Extension NE-SW</p> <p>Han/Lesse Wellin</p> <p>Restéigne Grignaux-Turmont</p> <p>Extension NE-SW</p>	<p>Gradient hydraulique / YES</p>	<p>Joints NW-SE exprimés/expressed : Karstification</p> <p>Joints NW-SE non exprimés/ unexpressed : Pas de karstification/No karstification</p>
Mésozoïque/c	<p>Extension NW-SE ?</p> <p>Etablie dans les régions voisines / Proved in neighbouring regions</p> <p>Té</p>	<p>Pas de gradient hydraulique / NO</p>	<p>Joints NE-SW : ouverture & altération / opening & alteration</p>
Paléozoïque/c	<p>Hercynien/Hercynian</p> <p>Ta Tc Td</p> <p>Compressions</p> <p>Décrochement/ Strike-slip</p> <p>Plis - Failles/ Folds - Faults</p> <p>Fentes de tension /Tension gashes</p>		<p>Pas de karstification/ No karstification</p>

Figure B11 – Tectonic and karstologic evolution of limestone massifs of Han-sur-Lesse region. Variscan (Hercynian) tectonics have not initiated karstic phenomena. During the Mesozoic, particular karstic alteration would have affected opened N50°E-N70°E joints (“fantômisation” phenomena) (Quinif 1999). Cenozoic NE-SW extension definitively provokes the massive “classic” karstification of the Han-sur-Lesse and Wellin massifs. N140°E-N150°E joints formed by this tectonic activity cut all the other structures independently.

STOP C – Namur Citadel – Chemin de Ronde: “Variscan soft-sediment deformation”

by Manuel Sintubin in collaboration with Ilse Kenis & Noël Vandenberghe

INTRODUCTION

Distinguishing early, soft-sediment deformation features is not always obvious (Maltman 1994). Water-saturated sediments often show a rheological behaviour very similar to that rocks deforming at high P-T conditions by means of crystal-plastic deformation.

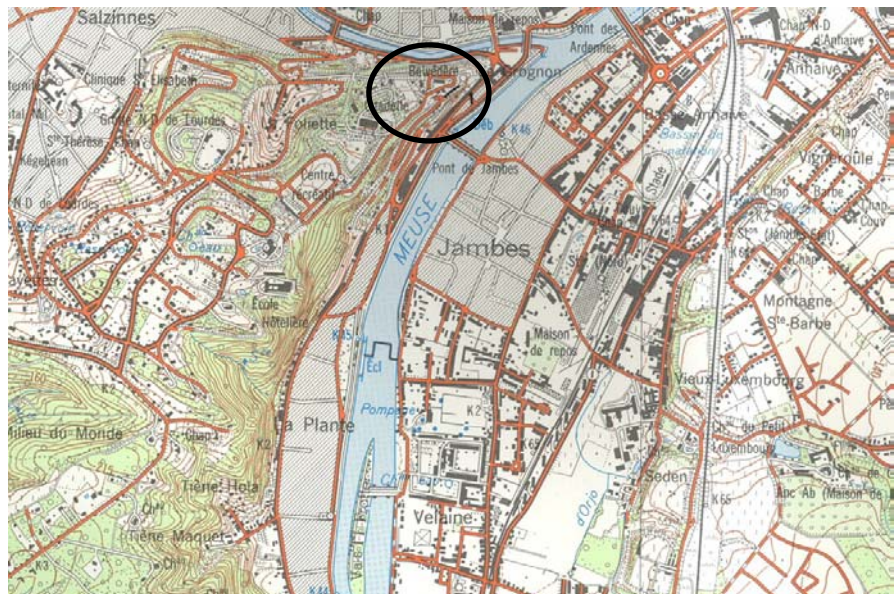
Soft-sediment deformation features commonly originate shortly after deposition and prior to lithification, and are therefore often referred to as penecontemporaneous deformation features (Maltman 1994).

At the Namur Citadel, the Namurian strata (Serpukhovian age, ~320 Ma) offer a unique opportunity to observe a number of synsedimentary and penecontemporaneous soft-sediment deformation features, reflecting a progressive accumulation of deformation at different stages of the Variscan orogeny affecting its foreland, from the time the sediments are deposited (~320 Ma) to the time they are incorporated in the Variscan fold-and-thrust belt (~300 Ma – Asturian stage).



Logistics – Terrain

The outcrops are situated within the scenic setting of the Citadel at the centre of Namur. The Namur Citadel is built on the promontory at the junction of the Meuse and Sambre rivers.



Map: 1:25.000 sheet 47/3-4 Namur-Champion

Aims

The purpose of this visit is:

1. to visit the northern frontal areas of the Variscan orogen;
2. to examine the different types of deformation structures;

Points to debate:

1. how to distinguish soft-sediment deformation features from hard-rock deformation features?

GEOLOGICAL SETTING OF THE NAMUR CITADEL

The outcrops of the Namur Citadel are located within the **Brabant parautochthon**, some 5 km north of the surface trace of the Variscan front thrust at the base of the Ardenne allochthon. This front thrust is commonly known as the *Midi-Condroz thrust* (figure C1). The outcropping rocks are Namurian coal-bearing shales and sandstones deposited in the foreland basin of the northwards prograding Variscan orogen. These rocks have a Serpukhovian age (~320 Ma) (see also Bouckaert 1961). The structure of the Brabant parautochthon consist of (1) the weakly deformed Devono-Carboniferous cover of the Lower-Palaeozoic Brabant basement, (2) the parautochthonous thrust

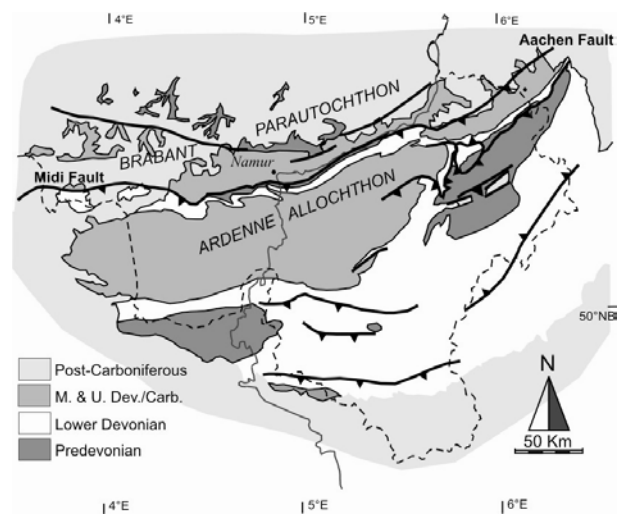


Figure C1 – Schematic geological map of the Ardenne-Eifel area (Belgium, Germany) with indication of the main tectonostratigraphical domains. Namur is situated north of the Variscan front thrust in the Brabant parautochthonous domain.

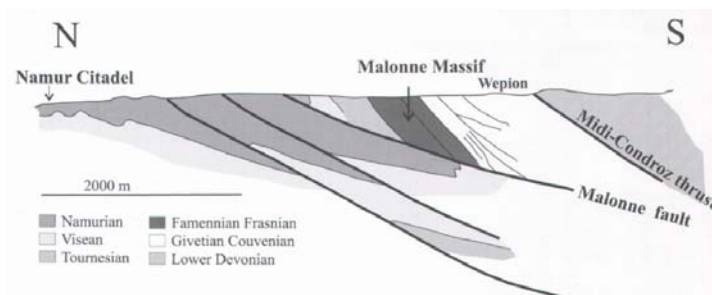


Figure C2 – Simplified cross-section along the Meuse river valley south of the Namur Citadel, displaying the structure of the Brabant parautochthon in the footwall of the Variscan front thrust (Midi-Condroz fault). The Malonne massif is the out-of-sequence thrust sheet, characterised by completely inverted strata.

imbricates, mainly consisting of Upper Carboniferous coal-bearing shales, and (3) an out-of-sequence thrust sheet in the direct footwall of the Variscan thrust front, consisting of Devono-Carboniferous rocks (figure C2). The Namur Citadel is situated in the northernmost domain. The overall attitude of the weakly deformed strata is 20° south-dipping.

The Variscan deformation (~300 Ma – Asturian stage) has clearly affected the rocks exposed at the Citadel. It is believed that rocks were buried 3 to 4 km at the time of deformation (Adams & Vandenberghe 1999). A lot of structures evidence this Variscan folding and thrusting. Also on microscopic scale evidence has been found for local cleavage development (den Brok et al. 1997).

The overall structure of the Variscan front zone is strongly debated. Classically – primarily based on the outcropping rocks – the overall structure is interpreted as a North-verging, slightly overturned syncline, the *Namur syncline* or *Namur synclinorium* (figure C3). In recent years, different other models to explain the structure of the Variscan front has been proposed (e.g. Adams & Vandenberghe 1999, Lacquement et al. 1999, Mansy & Lacquement 2003, Raout & Meilliez 1986). These new models are to a large extent based on the integration of the classical outcrop data along the Meuse river profile and different seismic sections across the Ardennes (figure C4).

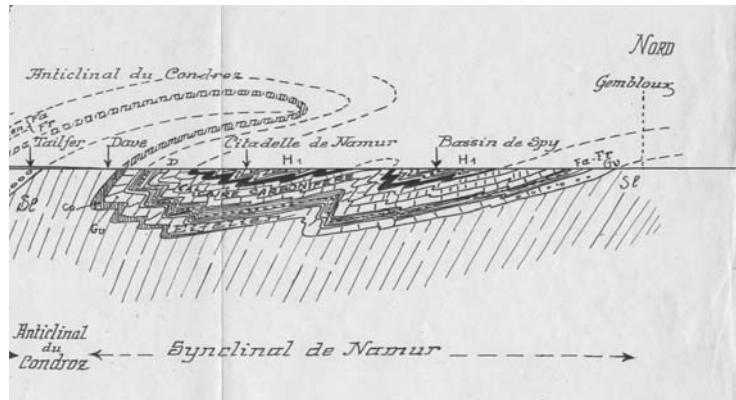


Figure C3 – A classical interpretation of the Variscan frontzone as a syncline, the “synclinal de Namur”. Notice the absence of the Midi-Condroz thrust. In stead an anticline, the “anticlinal du Condroz” is drawn (Kaisin 1935).

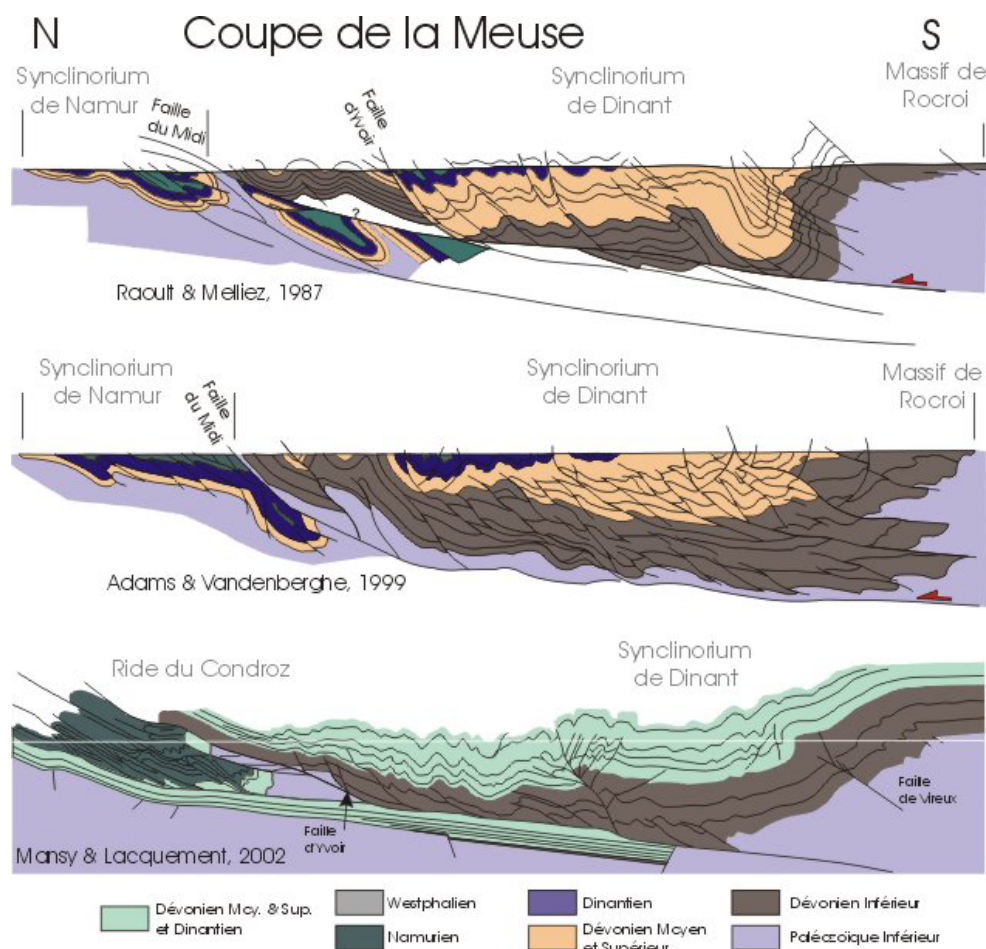


Figure C4 – A number of models of the structure of the northern front of the Variscan fold-and-thrust belt (synthetic figure made by Frédéric Boulvain, *Une introduction à la géologie de la Wallonie*, www.ulg.ac.be/geolsed/geolwal/geolwal.htm).

SOFT-SEDIMENT DEFORMATION FEATURES

According to Vandenberghe & Bouckaert (1984) the following deformation features point to penecontemporaneous deformation and gravity sliding in very soft sediments:

- ✓ the isolated nature of folds;
- ✓ the relationship between intense folding and sandstone occurrence;
- ✓ the occurrence of chaotic sandstone blocks in shales;
- ✓ flat-lying folds in alternating sandstone-shale strata;
- ✓ shale antiforms;
- ✓ chaotic shale masses;
- ✓ convoluted bedding near fault planes (figure C5);
- ✓ honeycomb structures;
- ✓ laminae in shale at angle with the bedding.

These penecontemporaneous deformation features are considered to be induced by the differential and inverse loading of easily deformable shales by overriding sand bars (Vandenberghe & Bouckaert 1984). According to Vandenberghe & Bouckaert



Figure C5 – An example of a penecontemporaneous soft-sediment deformation: sandy layers overlying shales. Note the intense deformation and overturning of the shale top (Vandenberghe & Bouckaert 1984).

(1984) the Variscan deformation, overprinting all earlier deformation structures, is more limited than generally believed.

The penecontemporaneous deformation occurred in the foreland basin north of the prograding Variscan orogen. At that time the main deformation occurred some 100 km to the south within the High-Ardenne slate belt (see STOP A). Variscan deformation could, however, already have affected the foreland, e.g. by steepening the seafloor and inducing massive gravitational instabilities (Vandenberghe & Bouckaert 1984).

THE CHEMIN DE RONDE SECTION

The Chemin de Ronde section (figure C6) exposes strongly deformed series of sandstones and shales. By means of a detailed geometrical study of the section, an attempt has been made to reconstruct the original sedimentary configuration and the subsequent deformation history (Kenis et al. 2003). In one single outcrop three types of deformation features (i.e. synsedimentary seismites, penecontemporaneous slumping, and hard-rock folding) reflects the

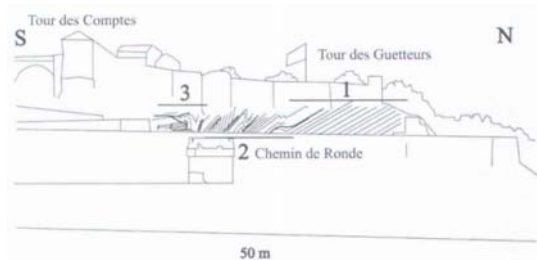


Figure C6 – Simplified cross-section of the Chemin de Ronde section (Kenis et al. 2003).

progressive accumulation of deformation of these sediments in the foreland of the prograding Variscan orogen. From their deposition onwards (~320 Ma) until their final incorporation into the Variscan fold-and-thrust belt (~300 Ma), these Namurian sediments were repeatedly affected by the Variscan orogeny.

The section can be subdivided in three entities, separated by two, subhorizontal to slightly south-dipping, anormal interfaces (I and II on figure C7):

- (1) Unit 1 consists of undisturbed, subhorizontal, finely-laminated shaly series;
- (2) Interface I: it can not be concluded whether interface I is an erosional or tectonic contact;
- (3) Unit 3 is composed of finely-laminated sandy shales; overturned beds underlie interface II (figure C5); these finely-laminated shales can be followed to the north and appear subvertically north of the vertical limb of the folded sandstone layer;
- (4) Interface II has clearly a tectonic origin; its folded nature indicates that thrusting occurred prior to Variscan folding, generating the V-shape synform;
- (5) Unit 2A is composed of regularly, weakly south-dipping shales and sandstones; a sandstone layer becomes discontinuous to the north, displaying contorted ball-type sandstone bodies surrounded by contorted shales; the sediment above this sand-ball horizon are again undisturbed; two steeply south-dipping normal faults (fault IV and V) can be identified under the sand-ball horizon;
- (6) Fault III is truncated by both interface I and II, thus predating the development of both interfaces;
- (7) Unit 2B is dominated by the presence of a thick sandstone layer, which wedges out at the top of the unit; the structure is truncated by interface I; to the north the sandstone layer forms an asymmetric antiform followed by a V-shaped synform; the sandstone layer is truncated by interface II, which itself has been folded in the V-shaped synform.

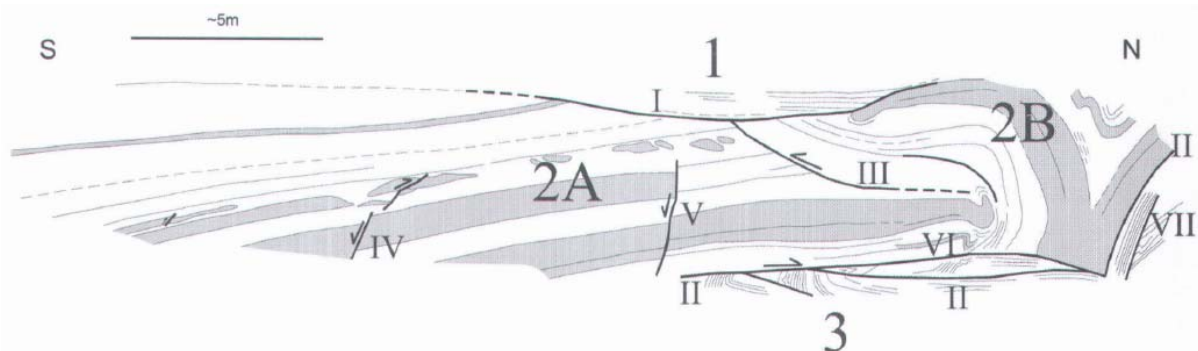


Figure C7 – Schematic drawing of the Chemin de Ronde section. The darker layers represent the more sandy parts of the sedimentary sequence (Kenis et al. 2003).

Faults IV and V end in the same sandstone layer that is highly disturbed (i.e. sand-ball horizon) and covered by undisturbed shales. These deformation features seem all kinematically linked and developed in water-saturated sediments before the deposition of the overlying shales. We consider these features as seismites, caused by shacking of the Namurian seabed. The earthquake-triggered shacking may have induced liquefaction, resulting in an upward squeezing of mud underlying sandy sediments and the loss of strength in the layer, giving rise to the sand balls. Similar fluidized horizons in the same stratigraphical interval demonstrate that at the time of deposition of these sediments (some 320 Ma ago) the basin was regularly affected by seismic events, clearly suggesting its tectonic instability.

Overtured, wavy laminae can be observed in the footwall of faults II, VI and VII. These faults represent different segments of the same, folded fault. The asymmetry of the overturned laminae suggests a top-to-the-north movement. This thrust is interpreted to have been caused by hydroplastic behaviour of unconsolidated layers a few metres to a few tens of meters below the seabed (Vandenberghé & Bouckaert 1984).

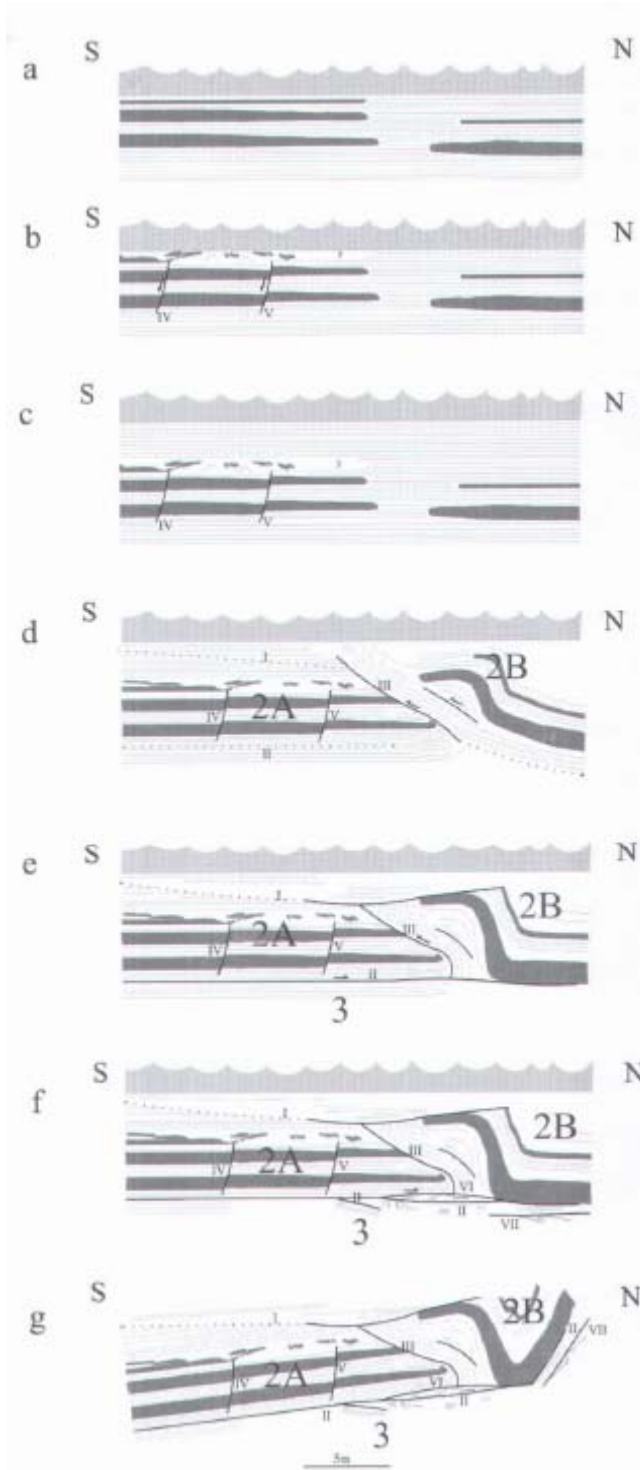


Figure C8 – Restored section and evolution model of the deformation structures. The darker layers represent the more sandy parts of the sedimentary sequence (Kenis et al. 2003).

The lateral wedging out of the sandstone bodies at different levels in the central part of the section suggests that they were originally already discontinuous. This heterogeneous sediment disposition may have played a crucial role in the subsequent deformation.

An attempt is made to reconstruct the deformation history (Figure C8). Originally discontinuous sand bars were deposited on a muddy, shallow seabed. During sedimentation, earthquake-induced shacking of the seabed caused liquefaction of the sediments and resulted in seismites, the two normal faults (IV and V) and an isolated, sand-ball horizon just above the faults (b on figure C8). After further burial (some tens of meters below sea level) (c on figure C8) hydroplastic soft-sediment deformation was triggered. This penecontemporaneous deformation event caused a northwards movement of a part of the sedimentary pile. The relative movement was determined by the heterogeneous sediment disposition (d on figure C8). The absence of sand bodies in the central part of the reconstructed section caused a structural weakness where mud has been squeezed upwards so that the southern sand bodies slid underneath the northern bodies, leading to the back-folding of the wedge tips (d on figure C8). The fold accentuation eventually caused the blocking of the northwards movement on top of interface II (e on figure C8). The nature of interface I remains enigmatic. A thrust contact similar to interface II can be considered. An

erosional gully can, however, not be excluded (f on figure C8). Finally, the Asturian hard-rock deformation was responsible for the sharp synform at the northern end of the section (g on figure C8).

The question remains what triggered the gravitational sliding responsible for the penecontemporaneous deformation. Does the northwards movement infer a northerly dipping palaeoslope? This is doubtful taking into account the palaeogeographical setting along the northern margin of the foreland basin. Or does the penecontemporaneous deformation reflect the northwards push on a south-dipping slope at the tip of a developing accretionary complex in front of the prograding Variscan fold-and-thrust belt?

References

- Adams, R. & Vandenberghe, N. 1999. The Meuse valley section across the Condroz-Ardenne (Belgium) based on a predeformational sediment wedge. In: *Palaeozoic to Recent tectonics in the NW European Variscan Front Zone* (edited by Sintubin, M., Vandycke, S. & Camelbeeck, T.). *Tectonophysics* **309**, 179-195.
- Angelier, J. 1990. Tectonique cassante et néotectonique. *Annales de la Société géologique de Belgique* **112**(2), 293-307.
- Angelier, J. 1994. Fault slip analysis and paleostress reconstruction. In: *Continental Deformation* (edited by Hancock, P. L.). Pergamon, Oxford, 53-100.
- Beugnies, A. 1986. Le métamorphisme de l'aire anticlinale de l'Ardenne. *Hercynica* **2**(1), 17-33.
- Bos, A., De Haas, G. J. L. M., Voncken, J. H. L., Van der Eerden, A. M. J. & Jansen, J. B. H. 1987. Hydrothermal synthesis of ammonium-phlogopite. *Geologie en Mijnbouw* **66**, 251-258.
- Bouckaert, J. 1961. Le Namurine à Namur. *Bulletin de la Société belge de Géologie* **120**(3), 358-375.
- Brühl, H. 1969. Boudinage in den Ardennen und in der Nordeifel als Ergebnis der inneren Deformation. *Geologische Mitteilungen* **8**, 263-308.
- Bultynck, P. & Dejonghe, L. 2001. Devonian lithostratigraphic units (Belgium). *Geologica Belgica* **4**(1-2), 39-69.
- Cloos, E. 1947. Boudinage. *Transactions of the American Geophysical Union* **28**(4), 626-632.
- Coen-Aubert, M., Mamet, B., Preat, A. & Tourneur, F. 1991. Sédimentologie, paléocéologie et paléontologie des calcaires crinoïdiques au voisinage de la limite Couvinien-Givétien à Wellin (bord sud du Synclinorium de Dinant, Belgique). *Mémoires pour servir à l'explication des Cartes géologiques et minières de la Belgique* **31**.
- Coen-Aubert, M., Preat, A. & Tourneur, F. 1986. Compte rendu de l'excursion de la Société belge de géologie du 6 novembre 1985 consacrée à l'étude du sommet du Couvinien et du Givétien au bord sud du Bassin de Dinant, de Resteigne à Beauraing. *Bulletin de la Société belge de Géologie* **95**(4), 247-256.
- Corin, F. 1932. A propos du boudinage en Ardenne. *Bulletin de la Société belge de Géologie* **42**, 101-117.
- Cosgrove, J. W. 1997. Hydraulic fractures and their implications regarding the state of stress in a sedimentary sequence during burial. In: *Evolution of Geological Structures in Micro- to Macro-scales* (edited by Sengupta, S.). Chapman & Hall, London, 11-25.
- Darimont, A. 1986. Les inclusions fluides de quartz filoniens d'Ardenne. *Annales de la Société géologique de Belgique* **109**, 587-601.
- Darimont, A., Burke, E. A. J. & Touret, J. L. R. 1988. Nitrogen-rich metamorphic fluids in devonian metasediments from Bastogne, Belgium. *Bulletin de Minéralogie* **111**, 321-330.
- Debacker, T. N. 2001. Palaeozoic deformation of the Brabant Massif within eastern Avalonia: how, when and why? Unpublished Ph. D. thesis, Universiteit Gent.
- Debacker, T. N., Dewaele, S., Sintubin, M., Verniers, J., Muecher, P. & Boven, A. 2005. Timing and duration of the progressive deformation of the Brabant Massif, Belgium. *Geologica Belgica* **8**(4), 20-34.
- Delvaux de Fenffe, D. 1985. Géologie et tectonique du Parc de Lesse et Lomme au bord sud du bassin de Dinant (Rochefort, Belgique). *Bulletin de la Société belge de Géologie* **94**(1), 81-95.
- Delvaux de Fenffe, D. 1990. Structures tardi- et post-hercyniennes dans le bord sud du Synclinorium de Dinant, entre Han-sur-Lesse et Beauraing (Belgique). *Annales de la Société géologique de Belgique* **112**(2), 317-325.
- Delvaux de Fenffe, D. & Laduron, D. 1991. Caledonian and Variscan structures in the Rocroi-Ardenne Lower Paleozoic basement (Belgium and adjacent countries). *Annales de la Société géologique de Belgique* **114**, 141-162.
- den Brok, S. W. J., Sintubin, M. & Vandenberghe, N. 1997. Early "soft-sediment" and late "hard-rock" Variscan deformation features in the Namurian strata at the Namur Citadelle (Belgium). *Aardkundige Mededelingen* **8**, 69-72.
- Fielitz, W. & Mansy, J.-L. 1999. Pre- and synorogenic burial metamorphism in the Ardenne and neighbouring areas (Rhenohercynian zone, central European Variscides). In: *Palaeozoic to Recent tectonics in the NW European Variscan Front Zone* (edited by Sintubin, M., Vandycke, S. & Camelbeeck, T.). *Tectonophysics* **309**, 227-256.
- Forir, H. 1897. Carte géologique de Belgique: Houyet-Han-sur-Lesse (185). Commission géologique de Belgique.
- Forir, H. 1900. Carte géologique de Belgique: Pondrôme-Wellin (194). Commission géologique de Belgique.
- Franke, W. 2000. The mid-European segment of the Variscides: tectonostratigraphic units, terrane boundaries and plate tectonic evolution. In: *Orogenic Processes: Quantification and Modelling in the Variscan Belt* (edited by Franke, W., Haak, V., Oncken, O. & Tanner, D.). *Special Publications* **179**. Geological Society, London, 35-61.
- Goscombe, B. D., Passchier, C. W. & Hand, M. 2004. Boudinage classification: end-member boudin types and modified boudin structures. *Journal of Structural Geology* **26**(4), 739-763.
- Gosselet, J. 1888. L'Ardenne. *Mém. Expl. Carte géol. France*, 1-889.
- Harker, A. 1889. On local thickening of dykes and beds by folding. *Geological Magazine* **6**(69-70).
- Hatert, F., Deliens, M., Houssa, M. & Coune, F. 2000. Native gold, native silver, and secondary minerals in the quartz veins from Bastogne, Belgium. *Bulletin de l'Institut Royal des Sciences Naturelles de Belgique, Sciences de la Terre* **70**, 223-229.
- Havron, C., Vandycke, S. & Quinif, Y. 2007. Interactivité entre tectonique méso-cénozoïque et dynamique karstique au sein des calcaires dévoniens de la région de Han-sur-Lesse (Ardennes, Belgique). *Geologica Belgica* **10**(1-2), 93-108.
- Helsen, S. 1995. Burial history of Palaeozoic strata in Belgium as revealed by conodont colour alteration data and thickness distributions. *Geologische Rundschau* **84**, 738-747.
- Hilgers, C., Büker, C., Urai, J. L., Littke, R., Post, A., van der Zee, W. & Kraus, J. 2000. Field study of an exhumed lower Devonian high pressure reservoir. *Geophysical Research Abstracts* **2**(SE34), 47.
- Holmquist, P. J. 1931. On the relations of the "boudinage-structure". *Geol. Fären. Färhandl.* **53**, 193-208.
- Hugon, H. 1983. Structures et déformation du Massif de Rocroi (Ardennes). *Bulletin de la Société géologique et minéralogique de Bretagne* **15**, 109-143.
- Hugon, H. & Le Corre, C. 1979. Mise en évidence d'une déformation hercynienne en régime cisailant progressif dans le Massif de Rocroi (Ardenne). *Comptes Rendus de l'Académie des Sciences, Paris* **289**, 615-618.
- Jongmans, D. & Cosgrove, J. W. 1993. Observations structurales dans la région de Bastogne. *Annales de la Société géologique de Belgique* **116**, 129-136.
- Kaisin, F. 1935. Le style tectonique et la genèse mécanique de l'Ardenne. *Bulletin de la Société belge de Géologie* **45**, 191-205.
- Kenis, I. 2004. *Brittle-Ductile Deformation Behaviour in the Middle Crust as Exemplified by Mullions (Former "Boudins") in the High-Ardenne Slate Belt, Belgium*. University Press, Leuven.

- Kenis, I., Muechez, P., Sintubin, M., Mansy, J.-L. & Lacquement, F. 2000. The use of a combined structural, stable isotopic and fluid inclusion study to constrain the kinematic history at the northern Variscan front zone (Bettrechies, France). *Journal of Structural Geology* **22**(5), 598-602.
- Kenis, I., Muechez, P., Verhaert, G., Boyce, A. J. & Sintubin, M. 2005a. Fluid evolution during burial and Variscan deformation in the Lower Devonian rocks of the High-Ardenne slate belt (Belgium): sources and causes of high-salinity and C-O-H-N fluids. *Contribution to Mineralogy and Petrology* **150**, 102-118.
- Kenis, I. & Sintubin, M. 2007. About boudins and mullions in the Ardenne-Eifel area (Belgium, Germany). *Geologica Belgica* **10**(1-2), 79-91.
- Kenis, I., Sintubin, M., Muechez, P. & Burke, E. A. J. 2002. The "boudinage" question in the High-Ardenne slate belt (Belgium): a combined structural and fluid inclusions approach. In: *Tectonophysics* (edited by Labaume, P., Craw, D., Lespinasse, M. & Muechez, P.). *Tectonophysics* **348**, 93-110.
- Kenis, I., Urai, J. L., van der Zee, W., Hilgers, C. & Sintubin, M. 2005b. Rheology of fine-grained siliciclastic rocks in the middle crust - evidence from structural and numerical analysis. *Earth and Planetary Science Letters* **233**, 351-360.
- Kenis, I., Urai, J. L., van der Zee, W. & Sintubin, M. 2004. Mullions in the High-Ardenne Slate Belt (Belgium). Numerical model and Parameter Sensitivity Analysis. *Journal of Structural Geology* **26**(9), 1677-1692.
- Kenis, I., Vandenberghe, N. & Sintubin, M. 2003. Early Variscan, soft-sediment deformation features in the Chemin de Ronde section at the Namur Citadel (Belgium). *Geologica Belgica* **6**(3-4), 161-169.
- Klement, C. 1888. Analyse chimique de quelques minéraux et roches de Belgique et de l'Ardenne française. *Bulletin du Musée royal de l'Histoire naturelle de Belgique* **5**, 159.
- Lacquement, F. 2001. *L'Ardenne Varisque. Déformation progressive d'un prisme sédimentaire pré-structuré, de l'affleurement au modèle de chaîne*. Société Géologique du Nord, Lille.
- Lacquement, F., Mansy, J.-L., Hanot, F. & Meilliez, F. 1999. Retraitement et interprétation d'un profil sismique pétrolier méridien au travers du Massif paléozoïque ardennais (Nord de la France). *Comptes Rendus de l'Académie des Sciences, Paris* **329**, 471-477.
- Lambert, A. & Bellière, J. 1976. Caractères structuraux de l'éodévonien aux environs de Bastogne. *Annales de la Société géologique de Belgique* **99**, 283-297.
- Le Gall, B. 1992. The deep structure of the Ardennes Variscan thrust belt from structural and ECORS seismic data. *Journal of Structural Geology* **14**(5), 531-546.
- Lohest, M., Stainier, X. & Fourmarier, P. 1908. Compte rendu de la session extraordinaire de la Société Géologique de Belgique, tenue à Eupen et à Bastogne les 29, 30 et 31 août et le 1, 2 et 3 septembre 1908. *Annales de la Société géologique de Belgique* **35**, B351-B434.
- Maltman, A. J. 1994. *The Geological Deformation of Sediments*. Chapman & Hall, London, 362.
- Mansy, J.-L. & Lacquement, F. 2003. Le Paléozoïque du Nord de la France et de la Belgique. *Géologues* **133-134**, 7-24.
- McKerrow, W. S., Mac Niocaill, C., Ahlberg, P. E., Clayton, G., Cleal, C. J. & Eagar, R. M. C. 2000. The Late Palaeozoic relations between Gondwana and Laurussia. In: *Orogenic Processes: Quantification and Modelling in the Variscan Belt* (edited by Franke, W., Haak, V., Oncken, O. & Tanner, D.). *Special Publications* **179**. Geological Society, London, 9-20.
- Meilliez, F., André, L., Blicke, A., Fielitz, W., Goffette, O., Hance, L., Khatir, A., Mansy, J.-L., Overlau, P. & Verniers, J. 1991. Ardenne - Brabant. *Sciences Géologiques, Bulletin* **44**(1-2), 3-29.
- Meilliez, F. & Mansy, J.-L. 1990. Déformation pelliculaire différenciée dans une série lithologique hétérogène: le Dévon-Carbonifère de l'Ardenne. *Bulletin de la Société géologique de France* (**8**), **6**(1), 177-188.
- Michot, P. 1980. Le segment tectogénique calédonien belge. *Mémoire de l'Académie royal de Belgique, classe des Sciences. Collection in 8°, 2ème série* **43**, 1-61.
- Muechez, P., Slobodnik, M., Sintubin, M., Viaene, W. & Keppens, E. 1997. Origin and migration of palaeofluids in the Lower Carboniferous of Southern and Eastern Belgium. *Zentralblatt für Geologie und Paläontologie, Teil I* **1995** **11/12**, 1107-1112.
- Mukhopadhyay, D. 1972. A note on the mullion structures from the Ardennes and North Eifel. *Geologische Rundschau* **61**, 1037-1049.
- Nüchter, J.-A. & Stöckhert, B. 2006. Fracturing and transformation into veins beneath the crustal scale brittle ductile transition - a record of co-seismic loading and post-seismic relaxation. *Geophysical Research Abstracts* **8**, 05890.
- Nüchter, J.-A. & Stöckhert, B. 2007. Vein quartz microfabrics indicating progressive evolution of fractures into cavities during postseismic creep in the middle crust. *Journal of Structural Geology* **29**(9), 1445-1462.
- Oncken, O., Plesch, A., Weber, J., Ricken, W. & Schrader, S. 2000. Passive margin detachment during arc-continent collision (Central European Variscides). In: *Orogenic Processes: Quantification and Modelling in the Variscan Belt* (edited by Franke, W., Haak, V., Oncken, O. & Tanner, D.). *Special Publications* **179**. Geological Society, London, 199-216.
- Oncken, O., von Winterfeld, C. & Dittmar, U. 1999. Accretion of a rifted passive margin: The Late Paleozoic Rhenohercynian fold and thrust belt (Middle European Variscides). *Tectonics* **18**(1), 75-91.
- Pilgers, A. & Schmidt, W. 1957. Die Mullion-Strukturen in der Nord-Eifel. *Abh. Hess. Landesamtes Bodenforsch.* **20**, 1-53.
- Piqué, A., Huon, S. & Clauer, N. 1984. La schistosité hercynienne et le métamorphisme associé dans la vallée de la Meuse, entre Charleville-Mézières et Namur (Ardennes franco-belges). *Bulletin de la Société belge de Géologie* **93**(1-2), 55-70.
- Plesch, A. & Oncken, O. 1999. Orogenic wedge growth during collision - constraints on mechanics of a fossil wedge from its kinematic record (Rhenohercynian FTB, Central Europe). In: *Palaeozoic to Recent tectonics in the NW European Variscan Front Zone* (edited by Sintubin, M., Vandycke, S. & Camelbeeck, T.). *Tectonophysics* **309**, 117-139.
- Quinif, Y. 1999. Fantômisation, cryptoaltération et altération sur roche nue - La tryptique de la karstification. Université de Provence. Etudes de géographie physique - Travaux 1999, 159-164.
- Quinif, Y., Vandycke, S. & Vergari, A. 1997. Chronologie et causalité entre tectonique et karstification. L'exemple des paléokarst crétaqués du Hainaut (Belgique). *Bulletin de la Société géologique de France* **168**(4), 463-472.
- Quirke, T. T. 1923. Boudinage, an unusual structural phenomenon. *Geological Society of America Bulletin* **34**, 649-660.
- Ramsay, A. C. 1866. The Geology of North Wales. *Memoirs of the Geological Survey of Great Britain* **3**, 1-75.
- Raoult, J.-F. & Meilliez, F. 1986. Commentaires sur une coupe structurale de l'Ardenne selon le méridien de Dinant. *Annales de la Société géologique du Nord* **105**, 97-109.
- Rondeel, H. E. & Voermans, F. M. 1975. Data pertinent to the phenomenon of boudinage at Bastogne in the Ardennes. *Geologische Rundschau* **64**, 807-818.

- Schroyen, K. 2000. Caledonische en Varistische Fluïda en de metamorfe evolutie van het Stavelot-Vennmassief. Unpublished Ph. D. thesis, Katholieke Universiteit Leuven.
- Schroyen, K. & Muechez, P. 2000. Evolution of metamorphic fluids at the Variscan fold-and-thrust belt in eastern Belgium. *Sedimentary Geology* **131**, 163-180.
- Sibson, R. H. 2001. Seismogenic Framework for Hydrothermal Transport and Ore Deposition. In: *Structural Controls on Ore Genesis. Reviews in Economic Geology* **14**. Society of Economic Geology, Boulder, 25-50.
- Spaeth, G. 1986. Boudins and Mullions in devonischen Schichtfolgen der Nordeifel und Ardennen - Erscheinungsbild, Entstehung und Umformung. *Nachrichten Deutsche Geologische Gesellschaft* **35**, 74-75.
- Stainier, X. 1907. Sur le mode de gisement et l'origine des roches métamorphiques de la région de Bastogne. *Mémoire de l'Académie royal de Belgique, classe des Sciences. Collection in 4°, 2ème série*.
- Stipp, M., Holger, S., Heilbronner, R. & Schmid, S. M. 2002. Dynamic recrystallization of quartz: correlation between natural and experimental conditions. In: *Deformation mechanisms, rheology and tectonics: current status and future perspectives* (edited by de Meer, S., Drury, M. R., de Bresser, J. H. P. & Pennock, G. M.). *Special Publications* **200**. Geological Society, London, 171-190.
- Urai, J. L., Spaeth, G., van der Zee, W. & Hilgers, C. 2001. Evolution of mullion (formerly boudin) structures in the Variscan of the Ardennes and Eifel. *Journal of the Virtual Explorer* **3**, 1-15.
- Van Baelen, H. & Sintubin, M. 2008. Kinematic consequences of an angular unconformity in simple shear. An example from the southern border of the Lower Palaeozoic Rocroi inlier (Naux, France). *Bulletin de la Société géologique de France* **179**(1), 73-87.
- van der Pluijm, B. A. & Marshak, S. 2004. *Earth Structure. An introduction to structural geology and tectonics*. W.W. Norton & Company, New York.
- Vanbrabant, Y. & Dejonghe, L. 2006. Structural analysis of narrow reworked boudins and influence of sedimentary successions during a two-stage deformation sequence (Ardenne-Eifel region, Belgium-Germany). *Memoirs of the Geological Survey of Belgium* **53**, 1-43.
- Vandenberghe, N. & Bouckaert, J. 1984. On the origin of the folding in the Namurian strata at the Namur Citadelle, Belgium. *Sedimentary Geology* **37**, 163-183.
- Vandycke, S. 2002. Palaeostress records in Cretaceous formations in NW Europe: extensional and strike-slip events in relationships with Cretaceous-Tertiary inversion tectonics. *Tectonophysics* **357**, 119-136.
- Vandycke, S. & Quinif, Y. 2001. Recent active faults in Belgian Ardenne revealed in Rochefort karstic network (Namur province, Belgium). *Netherlands Journal of Geosciences* **80**(3-4), 297-304.
- Verniers, J., Pharaoh, T. C., André, L., Debacker, T. N., De Vos, W., Everaerts, M., Herbosch, A., Samuelsson, J., Sintubin, M. & Vecoli, M. 2002. The Cambrian to mid Devonian basin development and deformation history of eastern Avalonia, east of the Midlands Microcraton: new data and a review. In: *Palaeozoic Amalgamation of Central Europe* (edited by Winchester, J. A., Pharaoh, T. C. & Verniers, J.). *Special Publications* **201**. Geological Society, London, 49-93.
- Walls, R. 1937. A new record of boudinage-structure from Scotland. *Geological Magazine* **74**, 325-332.
- Wegmann, C. E. 1932. Note sur le boudinage. *Bulletin de la Société géologique de France* **52**, 477-491.
- Winchester, J. A. & Team, T. P. T. N. 2002. Palaeozoic Amalgamation of Central Europe: new results from recent geological and geophysical investigations. *Tectonophysics* **360**, 5-21.



Tectonic Studies Group

Annual Meeting 2008

La Roche-en-Ardenne, Belgium

8 - 10 January 2008

Acknowledgements

The organisation of the Tectonic Studies Group Annual Meeting in La Roche-en-Ardenne (Belgium) was only possible by joining forces in the good Belgian tradition of “*l’union fait la force*”. The teams of Leuven, Gent and Mons worked perfectly together to make this meeting a success.

We want to acknowledge the *Fonds voor Wetenschappelijk Onderzoek – Vlaanderen (FWO)* and the *Fonds de la Recherche Scientifique (FNRS)* for their financial support.

We want to thank all the people at the *Floréal Conference Centre* not only for their professional approach, but in particular for their hospitality. We want to thank in particular Monique Magonette and Christel Bultot, who guaranteed the smooth organisation. Finally, we acknowledge the *Service de la diffusion et de l’animation culturelles de la Province de Luxembourg* to place the poster panels at our disposal.

